NASA Conference Publication 2282

Aircraft Electric Secondary Power

Proceedings of a conference
held at NASA Lewis Research Center
Cleveland, Ohio
September 14–15, 1982

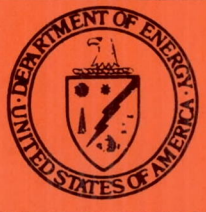

NASA Conference Publication 2282

Aircraft Electric Secondary Power

Proceedings of a conference
held at NASA Lewis Research Center
Cleveland, Ohio
September 14–15, 1982

NASA
National Aeronautics
and Space Administration

**Scientific and Technical
Information Branch**

1983

PREFACE

A workshop on aircraft electric secondary power was held at the Lewis Research Center of the National Aeronautics and Space Administration on September 14 and 15, 1982. The purpose of this workshop was to discuss the technologies related to aircraft power systems with a view toward aircraft in which all secondary power is supplied electrically. Fifteen talks were given in the areas of power systems, machine technology, components, and controllers by both industry and government personnel. Group discussions were then held to obtain input from all of the attendees on technology status and direction. The general topics to be covered in the workshop were selected by Lewis personnel and the speakers were invited by Lewis to participate. Approximately 80 people from government and industry attended the workshop.

The papers included in this proceeding were obtained by taping each speaker's presentation, transcribing the tape, heavily editing the transcription to change it from a spoken to a written format, and including the speaker's Vu-graphs as figures. The final section is a summary of the results from the discussion groups.

Anthony C. Hoffman
Workshop Coordinator

CONTENTS

400-Hz AIRCRAFT POWER-GENERATING SYSTEMS - ADVANCING THE BASELINE

Timothy Glennon
Sundstrand Corp.
Rockford, Illinois 61128

The weight evolution of the 400-Hz hydromechanical aircraft power-generating system (fig. 1) began in 1945 when the specific weight was of the order of 8 lb/kVA. This weight has steadily decreased with various advancements in particular technologies. Current hydromechanical systems typically weigh 1.3 to 1.4 lb/kVA. A 60-kVA system, including the generator and hydromechanical drive as an integrated package, at present weighs about 71 lb. The controls weigh about 9 lb and are getting to be a substantial part of the power system weight. Also over the years the reliability of hydromechanical systems has improved, the logical result of many millions of hours of experience.

This paper covers two areas: today's benchmark system for the 757/767/A310 airplanes and future trends. The 757/767/A310 system represents the commercial state of the art and the direction in which Sundstrand is headed, particularly in regard to weight reduction. Sundstrand introduced microprocessor control in an in-service system in the Boeing 767 and was the first to use databus communications between the controls. This paper briefly discusses Sundstrand's plans to develop this technology. Much of the rest of this conference is devoted to discussions of alternative ways to produce and use power in aircraft. Sundstrand has a few ideas to share with you about that and about the integrated starter drive.

757/767/A310 Systems - Today's Benchmark

The 757 and 767 are two-engine airplanes. They have an integrated drive generator (IDG) at each engine and an auxiliary power unit (APU) generator (fig. 2). All three generators are rated at 90 kVA.

Figure 3, a one-line diagram of the 757/767 bus arrangement, shows the number of components. There are three identical generator control units (GCU) and one bus protection control unit (BPCU). All of these control units use the microprocessor technology and communicate over the databus. A complete control system that is used in current aircraft is shown in figure 4, including a number of current transformers (CT's). Boeing chose to have a completely protected bus system, including the tie bus, and so there are some additional CT's.

Because of the microprocess system a new differential protection scheme was implemented wherein the bus connections could be adjusted in real time if there was enough CT information and enough communication between units. It was made possible by the microprocessor and the databus control.

Sundstrand introduced the microprocessor to aircraft power-generating system control. Figure 5 is a block diagram of the generator control unit. In this particular unit the voltage is regulated with analog circuits, but breaker control, protection, and built-in testing is controlled by an eight-bit microprocessor. Sundstrand uses the 8085 Intel system in a standard configuration with read-only memory, random access memory, independent watch-dog control for the microprocessor, and some nonvolatile memory, which is essential to the built-in test system. The built-in test system (BITE) for this particular airplane is a revolutionary system and the first of its kind.

Historically speaking, built-in testing has been an afterthought. It has not worked very well because it simply has not been very accurate. With the advent of the microprocessor Sundstrand has been able to incorporate active testing on a continuous and specific basis in order to address faults in the system and to isolate them on the basis of tests, not probabilities. The microprocessor processes almost all of the system information on a continuous basis anyway. Sundstrand took advantage of that and used it for the built-in test features. Any particular system malfunction is detected immediately, and an isolation routine is included in the fault-clearing operation. The non-volatile memory is used to store the information. (For example, for the first time we can seriously address problems such as intermittence.) This particular system contains a bus protection control unit and an alphanumeric display, which tells the flight-line mechanic in plain language exactly what is wrong, what the fault is, and what the line-replaceable unit (LRU) is. Boeing has found this to be very helpful in introducing the 767. Figure 6 shows, in a bar-chart form, that historically many parts have been removed that turned out not to be the problem. The common assumption is that systems consist only of an IDG and a GCU. This fails to take into account the 15 or 20 other significant parts that can also fail (e.g., wiring connectors and coolers). A BITE system that does not address those parts is inadequate. Therefore Sundstrand tried to address many of those parts in this new system. As a result the system should achieve a 95-percent confidence level in LRU identification - based on testing and not probability.

Future Trends

A typical assumption is that hydromechanical power-generating systems constitute a mature technology with little improvement possible. Nothing could be further from the truth. The technology is changing and being applied in the same way as the technologies for other approaches. By 1987 the weight of a typical system should be down to 0.8 lb/kVA. That is almost a 50-percent reduction from 1977 levels (fig. 7).

Weight reduction should come from the following technological advancements:

(1) Improved materials. Sundstrand is examining improved materials usage, particularly in the constant-speed drive area. We are testing a 24 000-rpm generator. Present generators run at 12 000 rpm, and therefore the increased speed should result in some generator weight reduction.

Figure 8 is a sketch of a 24 000-rpm two-pole generator that Sundstrand is building. It gives some idea of the rotor construction. There is nothing revolutionary about a two-pole machine: the idea certainly has been around for a long time. Several other people are building them. We are trying to build an extremely reliable one and we are spending some time to do that.

(2) Improved electromagnetic power density. Again, Sundstrand has been a pioneer in improving the power density of the electromagnetics in aircraft through spray-oil cooling and other means by integration into the system. This activity is continuing. Recall from figure 1 that the generator control unit is a significant part (more than 10 percent) of the power system weight. We think there is substantial room for improvement by using large-scale integration and increasing the role of the microprocessor in the power-generating system.

(3) Large-scale integration and expanded microprocessor role. In the generator control unit and the bus protection control unit, one of the obvious improvements is to include all of the system controls in the microprocessor. Sundstrand has an active program to do that. The kinds of controls that are

intended to be included are, for example, voltage regulation of the generator, frequency control, all of the parallel-system controls that might be used for those aircraft that require a parallel system, load management, and configuration management. In the 757/767 system Sundstrand began with load management, through the bus protection and control unit. We actually do remove loads based on the system configuration. Some studies show that management of more of the load system is desirable, and this can also be accomplished. In configuration management you can observe what is happening and configure the system for your particular mission arrangement. Any standard databus that is used on an aircraft can be used to interface and communicate between the units. Also remote display is probably an inevitable development since a central display is preferred over individual displays for each piece of equipment.

Figure 9 shows the architecture of a breadboard GCU that Sundstrand is presently working with. It uses two 16-bit 8086 Intel microprocessors and is an extremely powerful combination of equipment. However, it has fewer parts than, for example, the KC-135 re-engine GCU's. This decrease in parts with an increase in complexity is an expected result of a digital approach. The input-output conditioning is probably conventional. The two units are completely independent but can communicate back and forth and have their own local memories, watch-dog timers, and so forth. If one unit fails, the GCU can still operate to some extent with the other unit or use the other unit for other purposes.

(4) Alternative power. Presently most systems have 400-Hz power with some 28-V dc power. In 1978, Sundstrand suggested that 2000-Hz constant-frequency power be used as a possible approach for weight reduction. A number of aircraft have already been configured with double-voltage systems to reduce distribution system weight. More and different kinds of direct-current power, perhaps 270 V, 100 V, or just more 28 V, or maybe a mixture, could be used.

(5) Integrated starter drive. Sundstrand has been a pioneer in the field of integrated starter drives. In the early 1960's we introduced electric starting for aircraft on the 727. At that time the engine was in the design stage. As the required thrust increased, the engine outgrew the capability of the starter. Since that time we have been constantly studying this system and we feel that, with a simple change in the arrangement of the constant-speed drive components, an integrated starter drive can start the toughest engines.

Figure 10 is a block diagram of one arrangement of a 150-kVA integrated starter drive. In the start mode, alternating-current power is applied to the motor-generator, which would accelerate as an induction motor by using a patented static switch arrangement for the rotor. At that point the hydraulic drive is feathered (i.e., no torque is being transmitted through the transmission). So the motor is completely unloaded. Once it is at speed, it is converted to a synchronous motor, which has very high efficiency and certainly does not disturb the quality of power on the bus. The unit is then brought into stroke and the system can be started easily with working pressures not exceeding 5000 psid, less than, for example, the two-per-unit pressures in the hydraulic units and hence very conservative.

Figure 11 shows how the 150-kVA integrated starter drive system would work with a JT9D engine, a tough-to-start engine. The drag-torque curves are shown for 59° and -69° F. As you can see, the engine can be started hot or cold, under any condition, in 25 seconds with a very reliable torque margin.

Figure 12 is a diagram of the integrated starter drive system. Although the number of CT loops could be reduced, the basic point of this diagram is

that, with the exception of pressure, which is fed back from the hydraulic units, and the real power limit, all of the control variables are normally found in a parallel generating system. The system includes electronic control of frequency (servovalve into the constant-speed drive area). This will be more prevalent and allow for presynchronized paralleling even in split-bus systems.

In summary, then, I have attempted to share with you the state of the art of the 757/767/A310 hydromechanical aircraft power-generating systems: that Sundstrand has 1.3- to 1.4-lb/kVA systems in service, has introduced databus communications, and has introduced the microprocessor. Further substantial weight reductions are possible, to 0.8 lb/kVA in the foreseeable future. The microprocessor control is a powerful, flexible, dual 16-bit system that can handle any parallel-generating-system or starting arrangements that are envisioned. And, of course, the BITE is a landmark system and will continue to be so. Alternative forms of power are not excluded by considering this approach. Higher frequency, higher voltage, and mixed direct-current power can be used if needed. Finally, this system provides an extremely high torque margin for reliable engine starting.

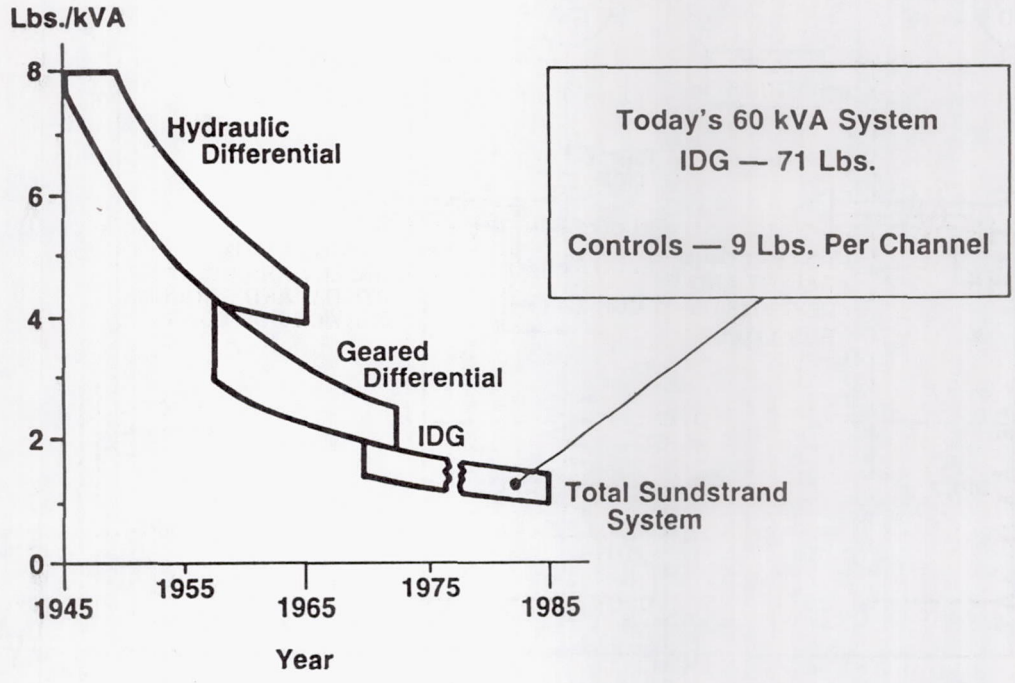

Figure 1. - Integrated-drive generator weight evolution.

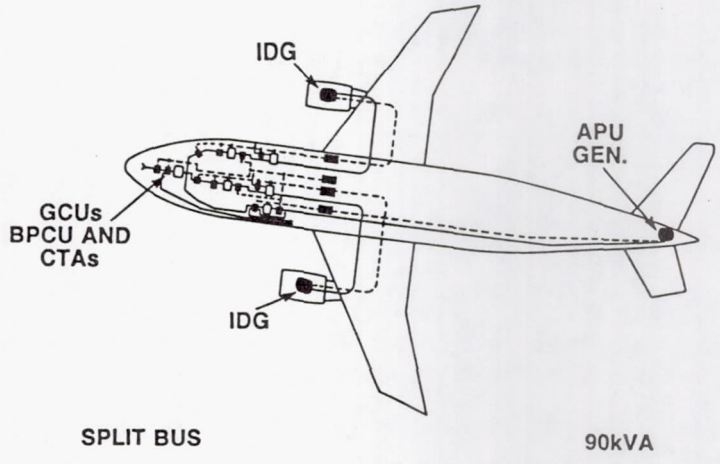

Figure 2. - 757/767 generating system.

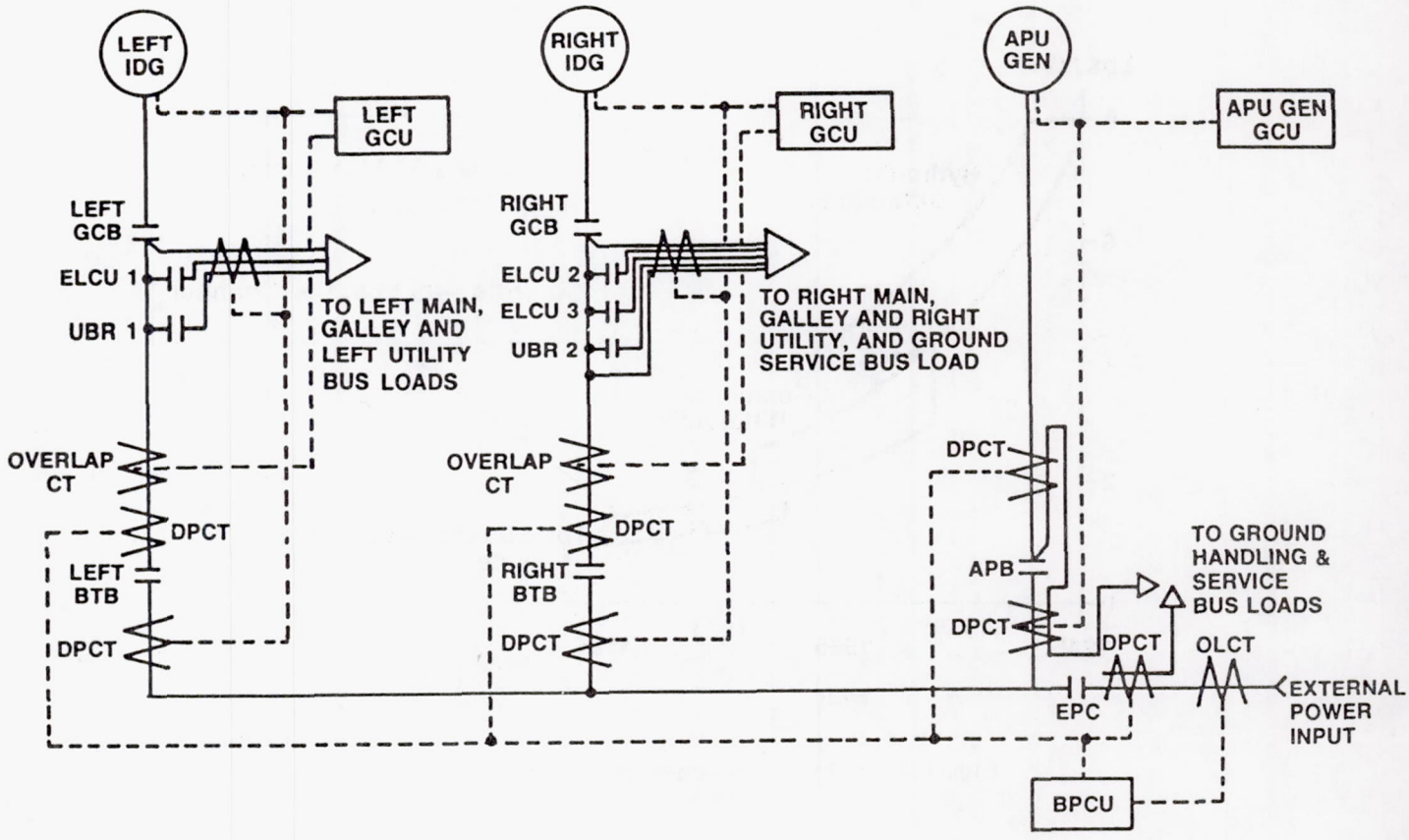

Figure 3. - Schematic of 757/767 EPGS.

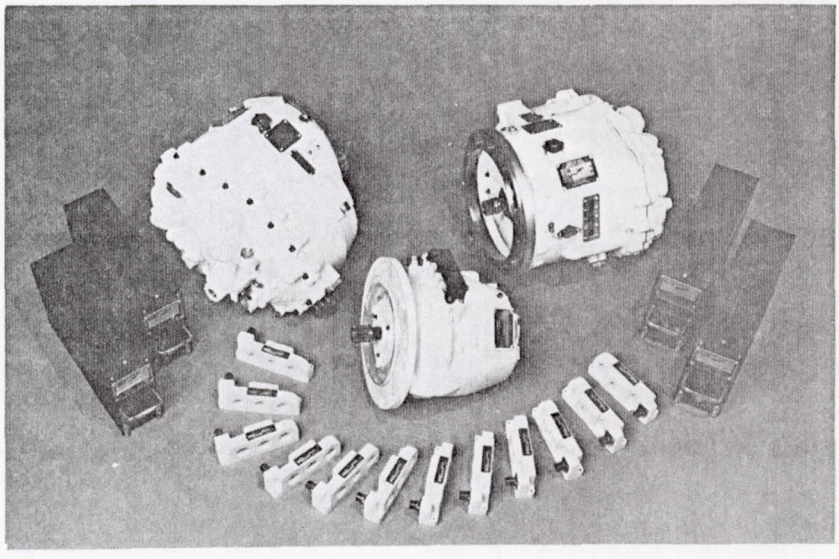

Figure 4. - Complete control system used in current aircraft.

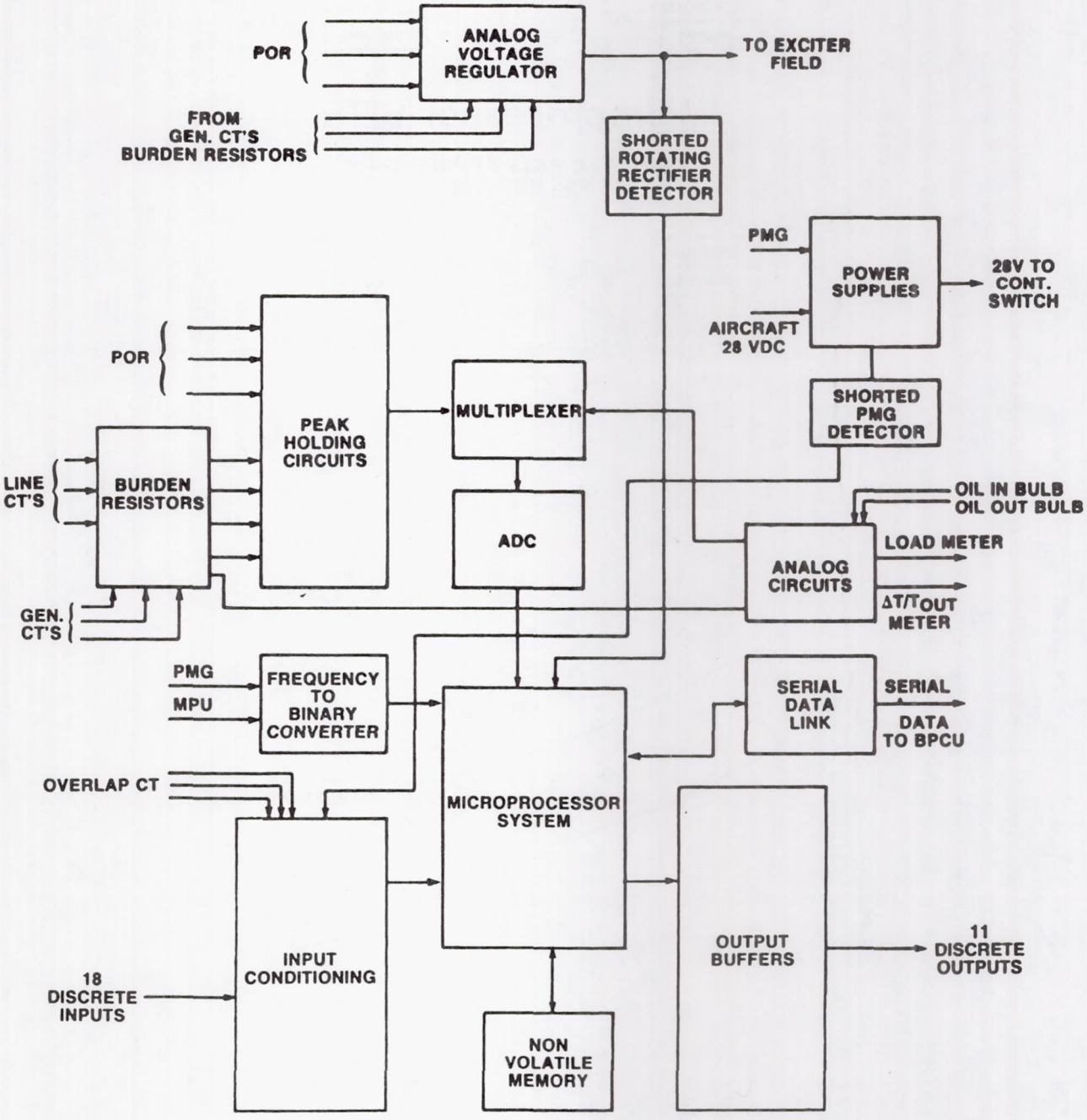

Figure 5. - Block diagram of 757/767 generating system.

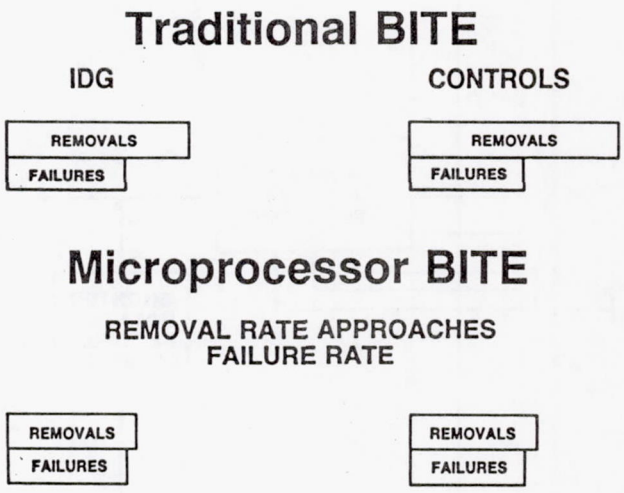

Figure 6. - Tranditional and microprocessor BITE'S.

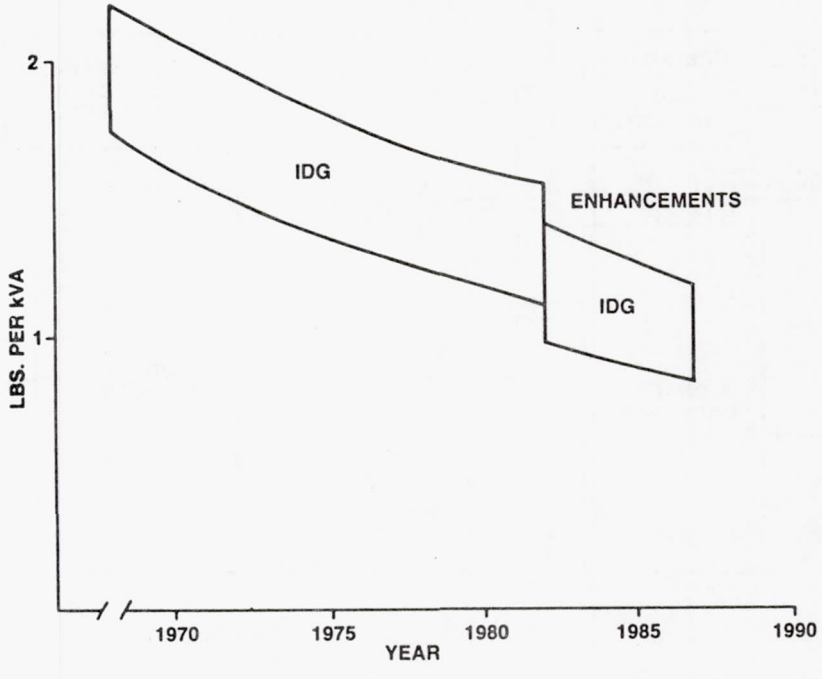

Figure 7. - Future IDG weight trends.

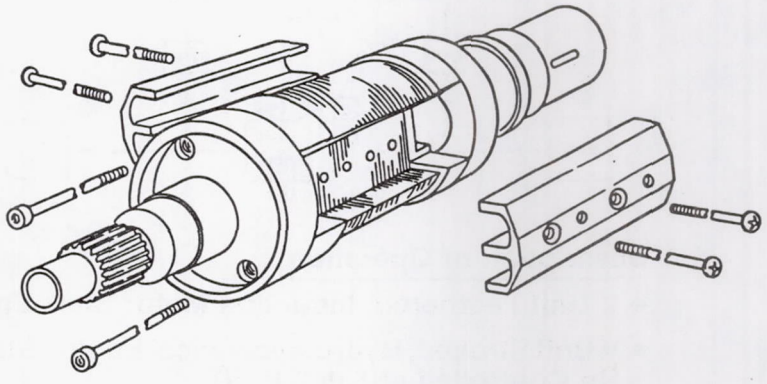

Figure 8. - Two-pole, 24 000-rpm generator rotor.

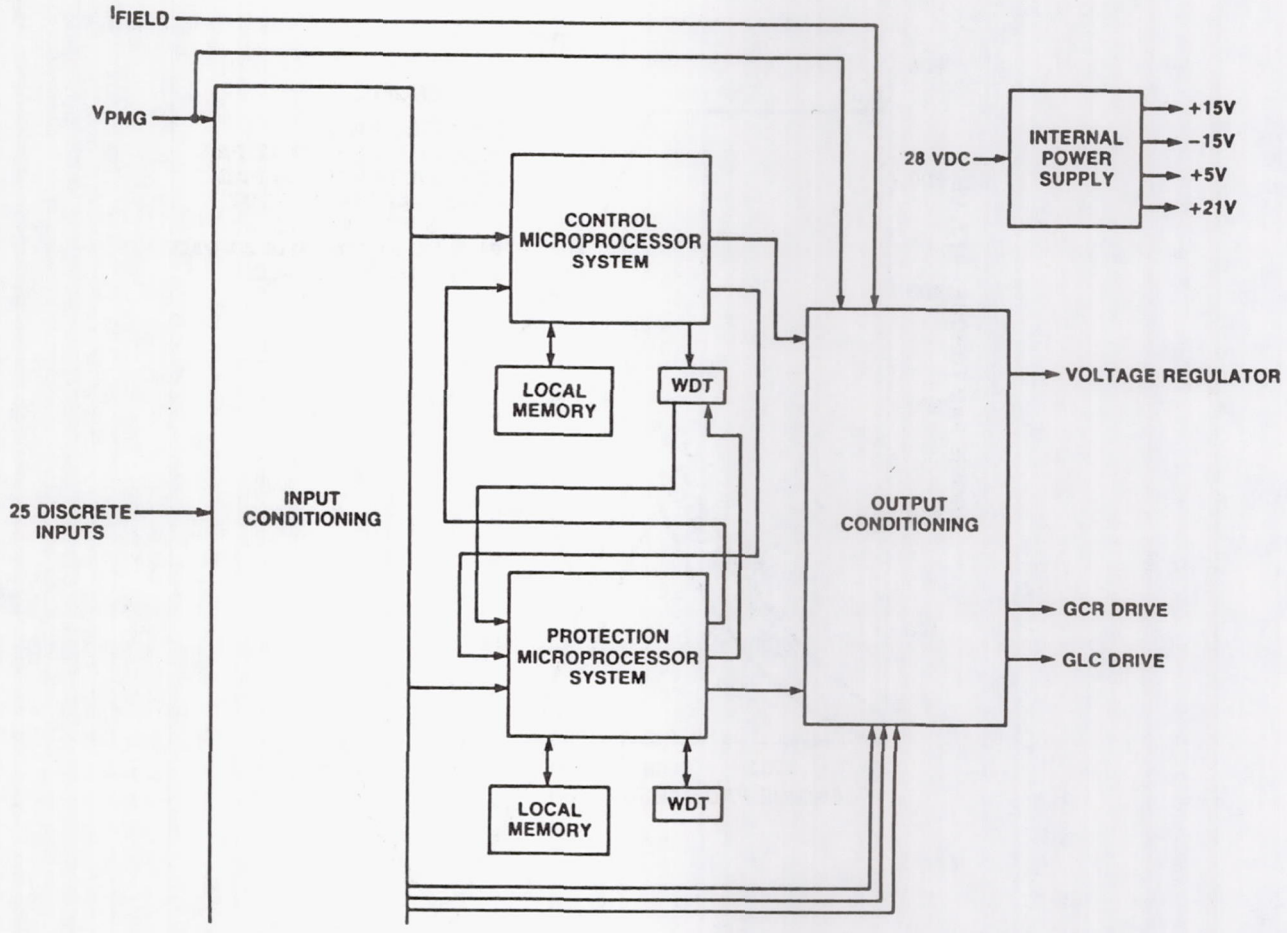

Figure 9. - Block diagram of advanced-architecture generator control unit.

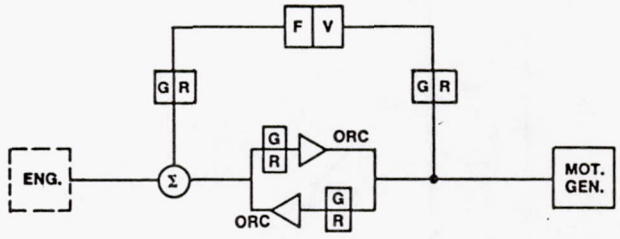

Description of Operation

- V Unit Feathered, Induction Motor Start Up
- V Unit Stroked, Hydromechanical Engine Start Up Controlled at 5,000 PSID
- Working Pressure Decreases With Increasing Input Speed When in CSD Mode

Figure 10. - 150-kVa integrated starter drive.

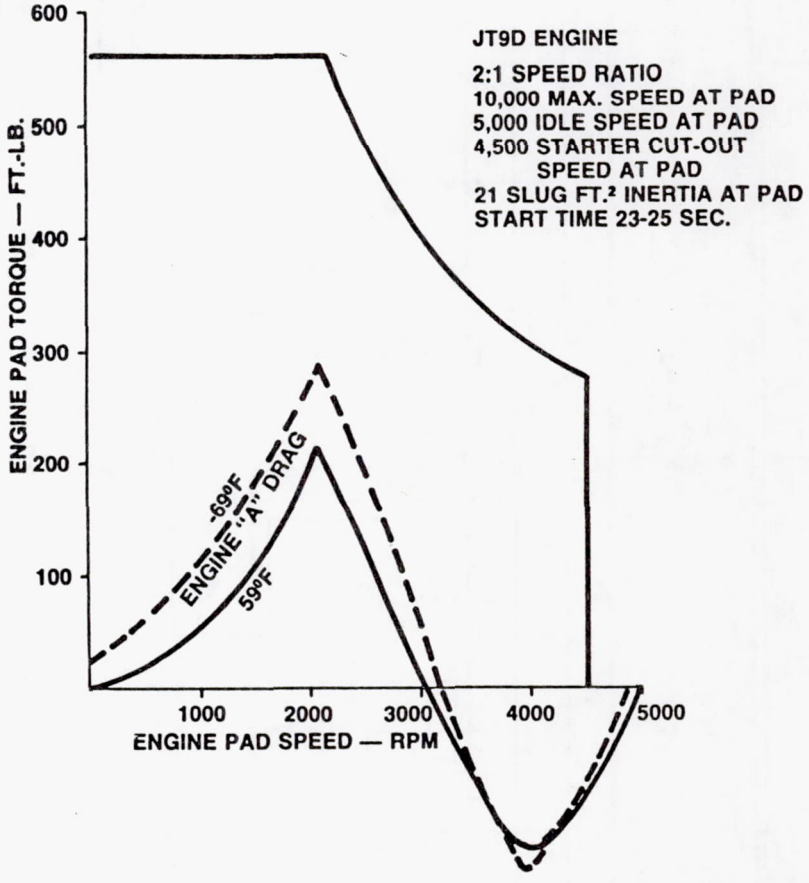

Figure 11. - Torque as a function of speed for 150-kVa integrated starter drive on JT9D engine.

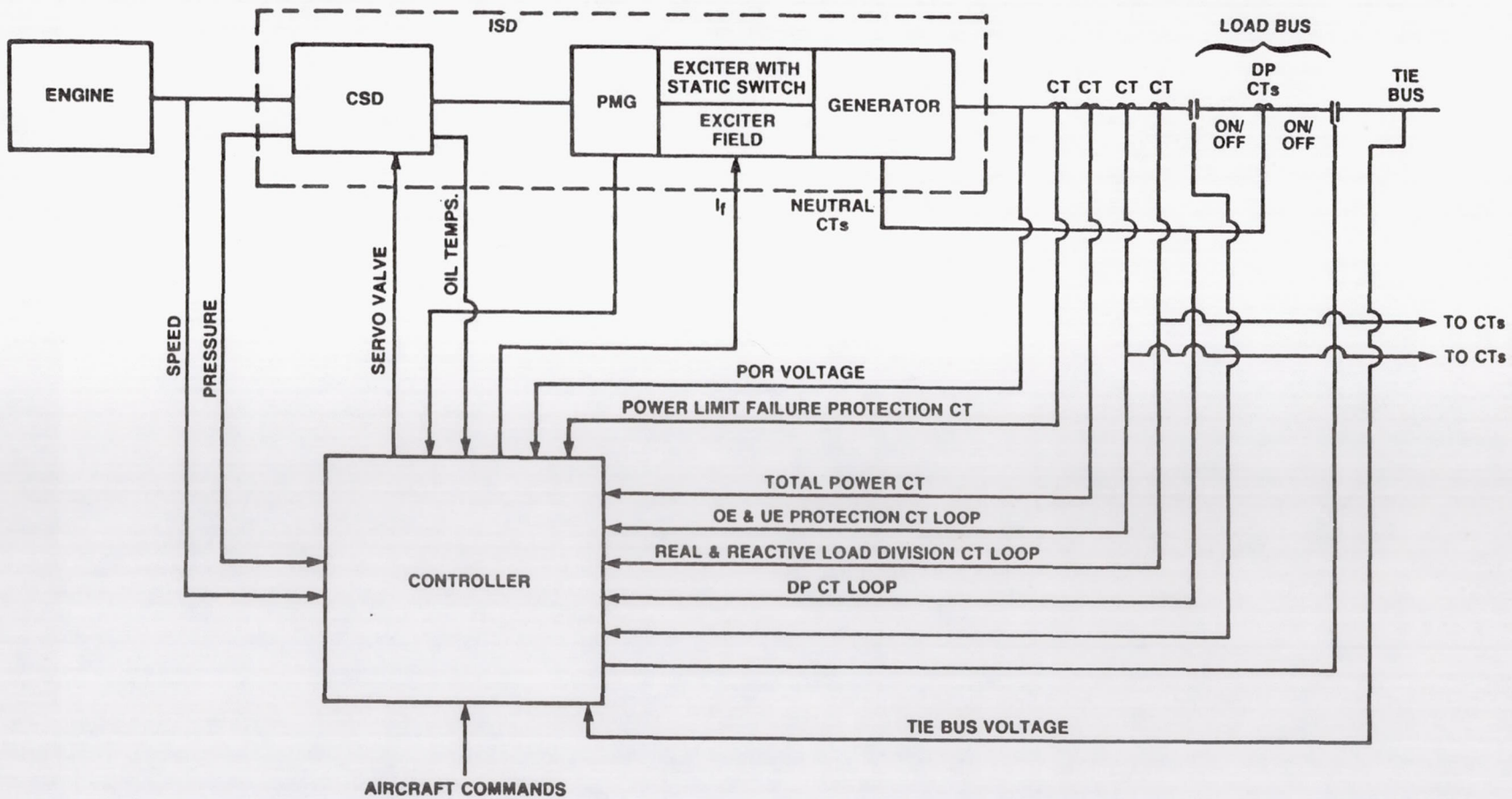

Figure 12. - Block diagram of integrated starter drive system.

HIGH-VOLTAGE (270 V) DC POWER-GENERATING SYSTEM FOR FIGHTER AIRCRAFT

Kevin M. McGinley
Naval Air Development Center
Warminster, Pennsylvania 18974

The Naval Air Development Center's high-voltage, direct-current advanced power-generating system will be used to retrofit current and future military aircraft.

Some of the reasons for choosing high-voltage direct current are the following:

(1) Reduced weight in power-generating systems. Weight is reduced mainly by eliminating the constant-speed drive through direct coupling. Also, the use of more-efficient direct-current generators allows the peripherals, especially coolers, to be smaller and therefore lighter. Also, use of a flat-cable conductor, rather than the conventional round conductor, increases current density by increasing the busing area, and therefore reduces the amount of copper, saving weight. The weight of avionic power supplies is reduced mainly by using high-frequency switching regulators.

(2) Increased efficiency. Efficiency has been increased to 85 to 90 percent by eliminating the constant-speed drive.

(3) Elimination of power interruptions with direct current. Load relays can make contact with a second bus before breaking connection with the first.

(4) No speed restrictions. The main power generators operate between 9000 and 18 000 rpm.

(5) No powerline constraints.

(6) Increased personnel safety by eliminating the hold-on frequency, present in ac systems, which causes muscle contractions.

By using 270 V dc most aircraft loads can be kept below 2 A. This reduces conductor size. The Naval Air Development Center (NADC) has 2-A power controllers, which can be used for almost all of the aircraft loads.

The NADC advanced aircraft electrical system (fig. 1) comprises three subsystems:

(1) Power-generating subsystem. A 270-V, 43-kVA generator will be used, either a solid-rotor generator (new technology) or a wound rotor. The choice will depend on the results of in-house testing. The generator control unit (GCU), which acts as a normal regulator for the generator, also supplies fault interruption signals to the bus contactor. This isolates the generator from any downstream faults. The bus contactor presently used has arc suppression by means of a semiconductor switch. The semiconductor switches on to suppress the initial arc and then an electromechanical relay takes over. Power-conditioning devices are used in retrofit aircraft to convert the 270 V to existing 400-Hz, 115-V power or to 28-V power.

(2) Solid-state electrical logic system (SOSTEL). This system is used for power management. It comprises the main and redundant processors (Navy AYK14 computer), solid-state switches or transducers, a multiplex system, power controllers (used instead of electromechanical devices and circuit breakers to save weight), and a demultiplex system. The system built-in test unit (BITE) monitors the condition of the power controllers and the solid-state switches, either the on-off condition or the fault condition. Under fault condition the processors provide either a redundant source of power or fault isolation.

(3)General-purpose multiplex system. The 1553B databus is used as a datalink between the aircraft avionic systems and the SOSTEL system.

Table I shows the status of hardware development. Most of the material is at NADC under advanced development or scheduled to be delivered. Some of these due dates, especially the August 1982 dates, have been delayed 6 to 8 months because of funding constraints.

The NADC will be testing the solid-rotor generator within the next month or so. The 500-W bidirectional power converter and the ground power monitor have been delivered. The flat power cable is under development. Again, 28-V power controllers have been delivered and tested. The alternating-current controllers have not been delivered. A 270-V, 1-hp brushless motor will be tested shortly.

Figure 2 shows the 270-V dc solid-rotor generator. The regulator is large because it was developed under funding that required few size constraints. The generator weighs about 65 lb.

Table II shows the power distribution. Under full-load conditions efficiency is 85 to 90 percent.

Figure 3 shows changes to be proposed in the power characteristic curves for military standard 704. The low limit will be raised from the standard 125 V to 175 V, and the high limit will be lowered from approximately 425 V to 350 V. Data for preliminary testing on a solid-rotor generator are well within those limits both under fulland low-load conditions. Further testing may indicate that those limits can be brought to an even closer tolerance.

Figure 4 shows the hybrid bus contactor. It uses an electromechanical relay, which is current technology, but includes the recent development of arc suppression with semiconductor switches. In the future, complete semiconductor circuit breakers may replace this contactor.

Figure 5 shows the dc-to-dc power converter. Full-load efficiency for a 3-kW unit is approximately 80 percent. The power converter can go either from 270 V dc to 28 V dc or the reverse. It supplies an emergency source of power by allowing the use of shipboard batteries. Its characteristics are given in table III.

Figure 6 shows a ground fault monitor. It integrates ground cart power to prevent getting transient power from the ground cart. When the ground cart power is within the range of military standard 704, the contact supplying ground power to the aircraft closes.

Figure 7 shows a bus fault sensor. It supplies fault signals to the SOSTEL system. It is not a switching unit but merely supplies the signals for switching redundant power sources and fault isolation.

Figure 8 shows the flat conductor cable that will be used. This cable is rated at 140 A. A round conductor containing a similar amount of copper would be rated at about 80 A. So again, both weight saving and increased current are achieved. NADC has found that because of insulation restraints the use of flat conductor cable is only feasible at 10 A and above. Average percent weight savings (table IV and fig. 9) are approximately 24 percent on a metal aircraft and 32 percent on a composite aircraft. The reason for the different values is that the composite aircraft uses the standard two-conductor system, whereas the metal aircraft uses aircraft shielding as the ground return. The weight of a typical military aircraft could probably be reduced by approximately 880 lb.

Figure 10 shows the 270-V dc controllers, which handle most of the aircraft loads that use the 270-V system. The controllers are approximately 2-1/2 in. long, 1-1/2 in. wide, and 3/4 in. thick. They weigh about 8 oz.

Something new NADC is doing with this system is using computer-aided stability analysis. The software (designated EASY) was developed by Boeing for the U.S. Air Force. Boeing has developed a high-voltage direct-current component library for NADC. This library mathematically models different

system components. Therefore different parameters can be input to study the effect of transients on overall system stability.

Figure 11 shows the airframe/system simulator. The power controllers and some of the SOSTEL system are already installed on it. It will be operational, funding permitted, probably in late 1983.

The long-range goals of the NADC program are shown in table V.

TABLE I. - AAES HARDWARE DEVELOPMENT STATUS

ITEM	STATUS & REMARKS
45 KW 270 VDC WOUND ROTOR GEN	ADM SCHEDULED DELIVERY AUG 1982
45 KW 270 VDC SOLID ROTOR GEN	6.2 MODEL UNDER TEST, TRANSITIONS FY-83
90 KW 270 VDC [TBD] GEN	ADM DEV FY-84, ROTOR TYPE TBD
500 W BI-DIRECTIONAL PWR CONV	28 VDC ⟷ 270 VDC ADM UNDER TEST
3 KW PWR CONVERTER	ADM UNDER TEST
10 KVA PWR CONVERTER	6.2 MODEL UNDER TEST, TRANSITION TBD
GROUND PWR MONITOR	ADM UNDER TEST
GROUND PWR CONVERTER	ADM DEV COMPLETED TEST SCHEDULED FY-82
HYBRID BUS CONTACTER (400 A)	UNDER 6.2 DEV, TRANSITIONS FY-83
FLAT PWR CABLE	UNDER 6.2 DEV, TRANSITIONS FY-83
SOSTEL CONTROL GROUP	FTM SCHEDULED DELIVERY AUG 1982
28 VDC PWR CONTROLLERS	ADM INSTALLED IN SIMULATOR
115 VAC PWR CONTROLLERS	ADM SCHEDULED DELIVERY AUG 1982
270 VDC PWR CONTROLLERS	6.2 MODEL UNDER TEST, TRANSITIONS FY-82
TRANSDUCER SWITCHES	ADM TOGGLE, PROXIMITY, & PUSH BUTTON IN TEST
ROTARY TRANSDUCER SWITCHES	ADM UNDER TEST
MIL-STD-1553 DATA MUX	ADM UNDER TEST
SYSTEM LOAD CENTER	INITIATE ADM DEV FY-84
270 VDC EMERGENCY GEN	INITIATE ADM DEV FY-84
BUS FAULT SENSORS	INITIATE ADM DEV FY-85
270 VDC BRUSHLESS MOTORS	6.2 EFFORT TRANSITIONS FY-85

TABLE II. - 270-V dc SOLID-ROTOR GENERATOR (45 kW)
[Efficiency, ~90 percent; MIL-L-23699 oil; current, 166 A.]

Voltage, V	S	Front bearing	Rear bearing	Coolant inlet	Coolant outlet
		Temperature, °F			
270.05	9 076	110	110	68	78
270.03	9 190	150	140	71	81
270.03	9 245	166	156	76	88
270.00	14 300	200	190	75	90
270.00	14 008	220	210	81	97
270.00	17 997	258	242	89	107
270.00	18 100	270	248	87	92

dc voltage, V	dc current, A	Voltage, V			Current, A			Power, W			Efficiency
		A	B	C	A	B	C	A	B	C	
10-kVA inverter											
250	11.5	116	116	116	7.25	7.25	7.25	850	850	850	0.89
250	22	115	115	115	14.5	14.5	14.5	1650	1650	1650	.90
250	32.5	114.5	114.5	114.5	21.75	21.75	21.75	2500	2500	2500	.92
250	44	113.5	113.5	113.5	29	29	29	3300	3300	3300	.90
Test data											
270	10.5	116	116	116	7.25	7.25	7.25	850	850	850	0.90
270	20.5	115	115	115	14.5	14.5	14.5	1675	1675	1675	.91
270	30.5	114.5	114.5	114.5	21.75	21.75	21.75	2500	2500	2500	.91
270	40.5	114	114	114	29	29	29	3250	3250	3250	.89
Efficiency											
280	10.5	115.5	116	116	7.25	7.25	7.25	850	850	850	0.87
280	20	114.5	115	115	14.5	14.5	14.5	1700	1650	1700	.90
280	29.5	114	114.5	114.5	21.75	21.75	21.75	2500	2500	2500	.91
280	39	113.5	114	114	29	29	29	3300	3300	3300	.91

TABLE III. - CHARACTERISTICS OF BIDIRECTIONAL POWER CONVERTER

(a) General characteristics

Inlet voltage, V	Inlet current, A	Outlet voltage, V	Outlet current, A	Efficiency, percent
290	1.20	32.78	0	--
270	1.21	32.56	0	--
240	1.23	31.89	0	--
290	3.73	28.15	25	65
270	3.93	28.01	25	66
240	4.32	27.66	25	66
290	6.36	27.69	50	75
270	6.75	27.62	50	76
240	7.46	27.51	50	77
290	8.98	27.56	75	79
270	9.57	27.49	75	80
240	10.65	27.39	75	80
290	11.63	27.43	100	81
270	12.43	27.36	100	82
240	13.89	27.26	100	82

(b) Upmode characteristics

24 V dc			270 V dc			Efficiency, percent
Voltage, V	Current, A	Power, W	Voltage, V	Current, A	Power, W	
24.0	3.77	90.5	260.5	0.2	52.1	57.6
↓	4.85	116.4	260.8	.3	78.2	67.2
	7.25	174.0	261.0	.5	130.5	75.0
	9.75	234.0	261.5	.7	183.0	78.2
	12.4	297.6	261.8	.9	235.6	79.2
	13.7	329.8	261.9	1.0	261.9	79.4
	16.4	393.6	261.9	1.2	314.3	79.8
	17.8	427.2	261.9	1.3	340.5	79.7
	19.2	460.8	262.0	1.4	366.8	79.6
	20.0	480.0	262.0	1.45	379.9	79.2
	21.0	504.0	262.0	1.5	393.0	78.0

(c) Downmode characteristics

24 V dc			270 V dc			Efficiency, percent
Voltage, V	Current, A	Power, W	Voltage, V	Current, A	Power, W	
28.0	0.5	14.0	270.0	0.10	27.0	51.8
27.9	1.94	54.1	↓	.40	108.0	50.0
27.8	4.25	118.2		.60	162.0	80.0
27.6	7.30	201.5		.90	243.0	82.9
27.4	9.80	268.5		1.20	324.0	82.9
27.3	11.65	318.0		1.40	378.0	84.1
27.2	13.30	361.8		1.60	432.0	83.7
27.2	15.00	408.0		1.80	486.0	83.9
27.1	15.40	417.3		1.85	499.5	83.5

TABLE IV. - WEIGHT ANALYSIS SUMMARY[a]

	Metal aircraft	Composite aircraft
	Flat cable weight saving, percent	
High	+22.0	+33.6
Medium	+26.8	+31.2
Low -1	+ 4.5	-15.6
Low -2	-40.6	-69.0

[a]If all power runs above 10 A in a typical military aircraft were converted to flat cable, this would result in a weight saving of 880 lb.

TABLE V. - LONG-RANGE GOALS OF NADC PROGRAM

FUNCTION	CONVENTIONAL	ADVANCED
POWER GENERATION	115/208 VAC 400 HZ	270 VDC
• POWER CONVERSION	TRANSFORMER/RECTIFIER	DC-AC & DC-DC CONVERTERS
• BUS CONTACTORS	ELECTROMECHANICAL	SOLID STATE
• POWER BUS	STRANDED CABLE	FLAT
• FLEXIBILITY	NONE	PROGRAMMABLE
CONTROL & PROTECTION		
• CONTROL SWITCHES	ELECTROMECHANICAL	SOLID STATE-LOGIC LEVEL
• FEEDER PROTECTION	THERMAL/MAGNETIC CIR BRKR	SOLID STATE POWER CONTROLLER
• POWER TRANSFER	ELECTROMECHANICAL RELAY	
• LOAD MANAGEMENT	MANUAL & FIXED	AUTOMATIC & PROGRAMMABLE
• CONTROL WIRING	DEDICATED	TSP & FIBER OPTICS
• CONTROL DATA TRANS.	POINT-TO-POINT	DIGITAL MULTIPLEXED
BUILT-IN-TEST	NONE	100% TO WRA
REDUNDANCY	LIMITED	UNLIMITED
PACKAGING	BLACK BOX	MODULAR

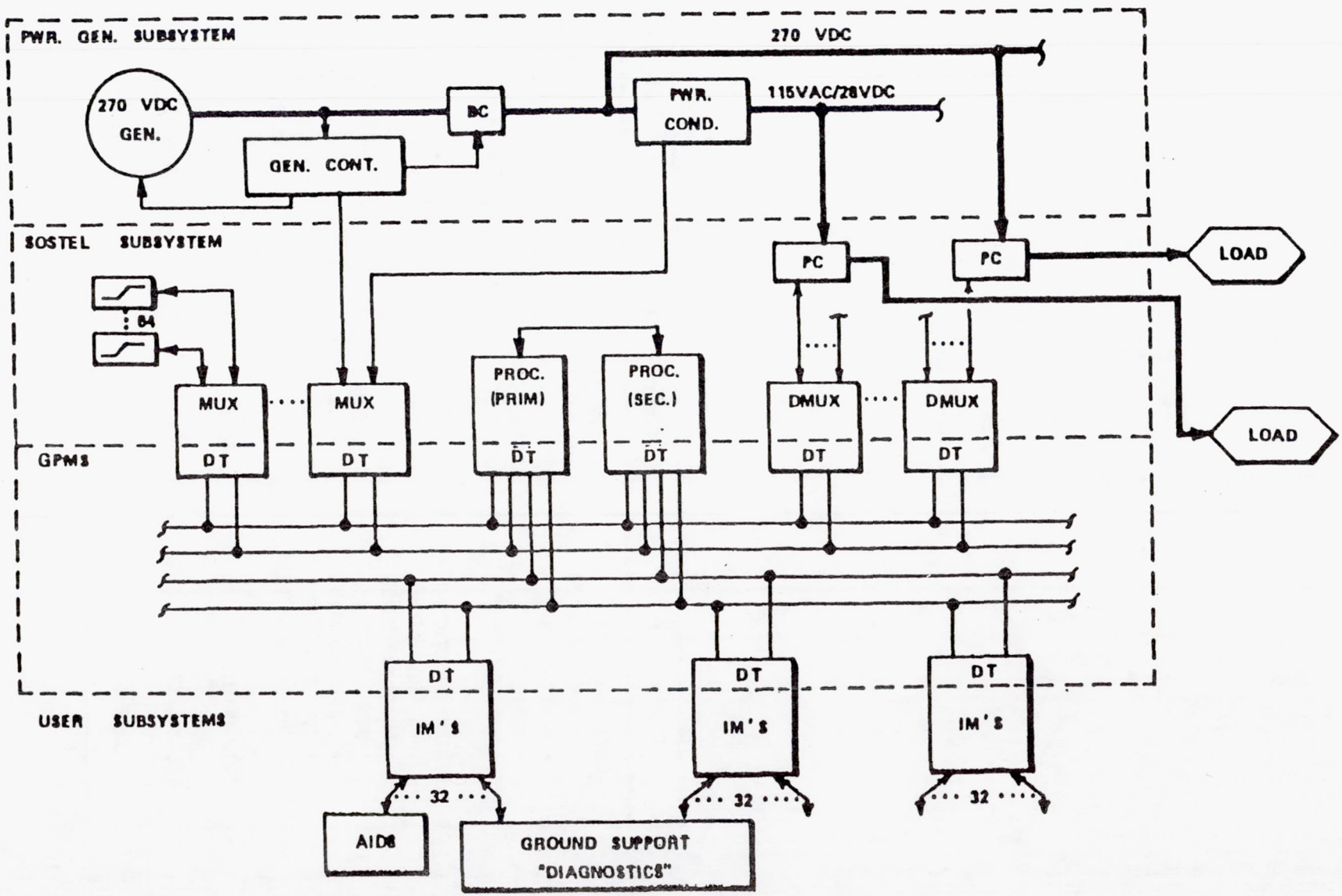

Figure 1. - Advanced aircraft electrical system (AAES).

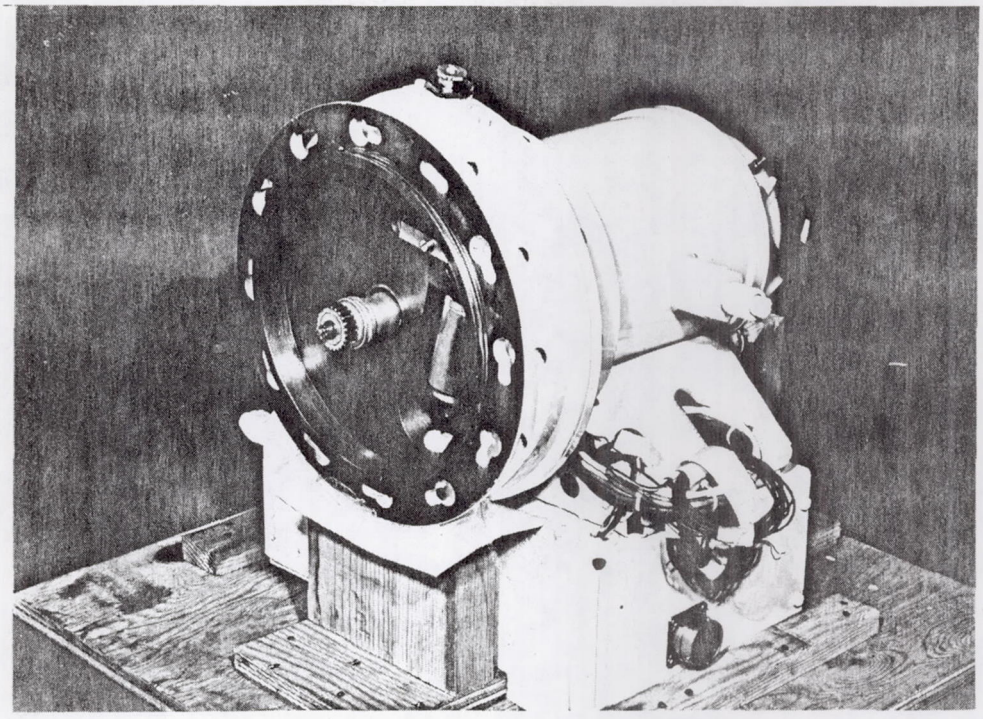

Figure 2. - 270-V dc solid-rotor generator.

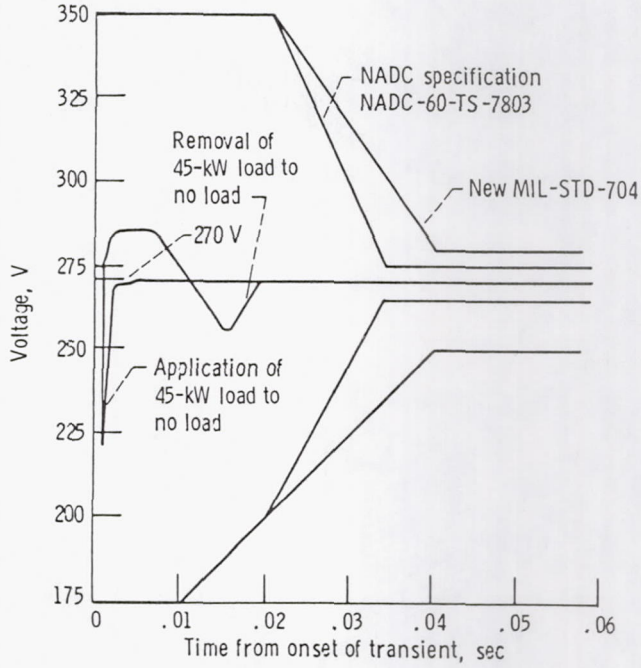

Figure 3. - Transient response of 270-V dc solid-rotor generator system.

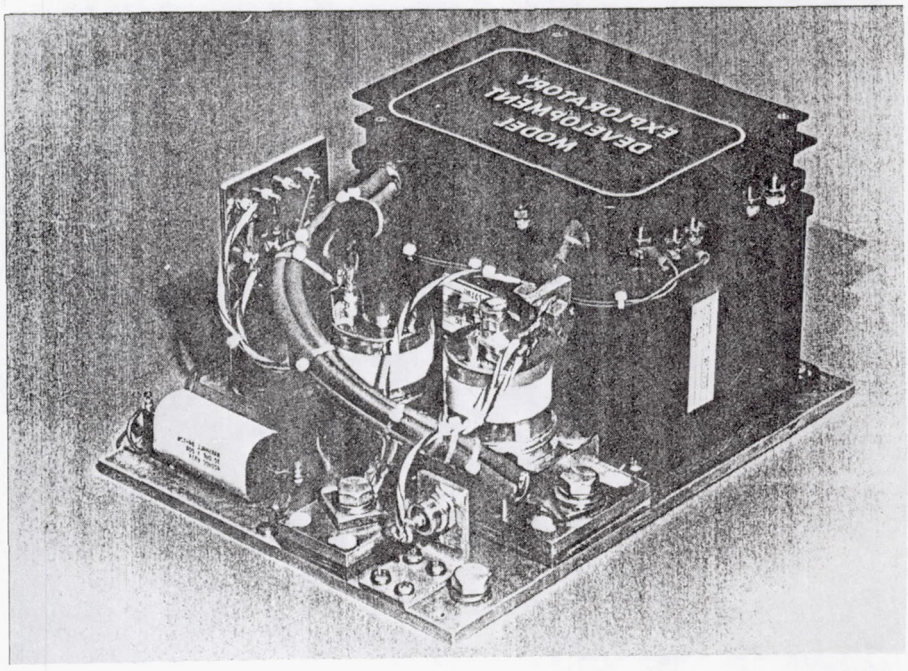

Figure 4. - 250-A, 270-V dc hybrid bus contactor.

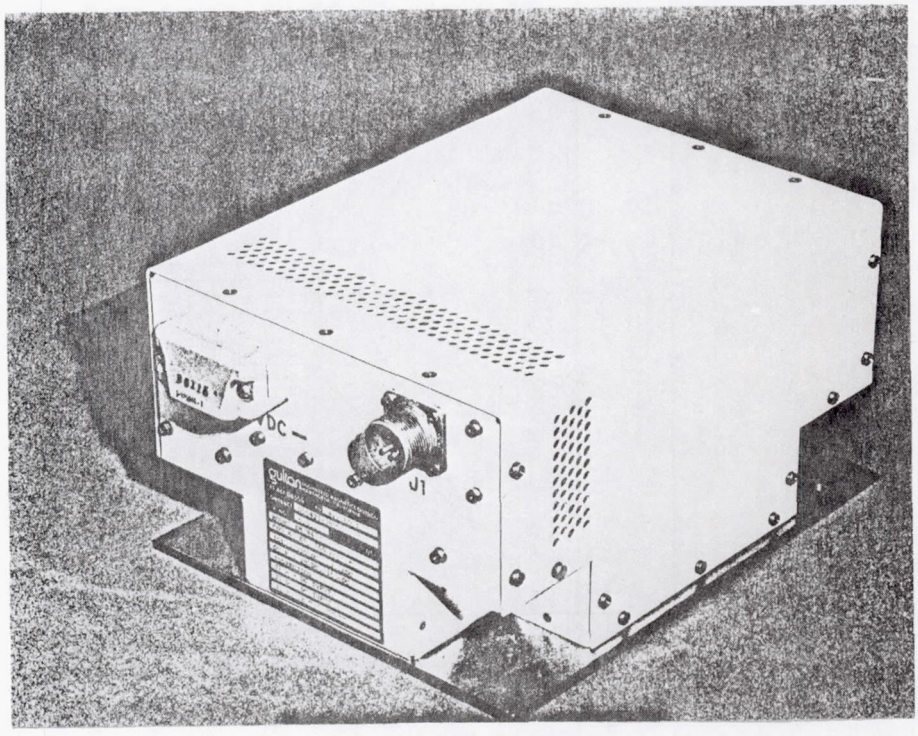

Figure 5. - 270-V-to-28-V, 3-kW power conditioner.

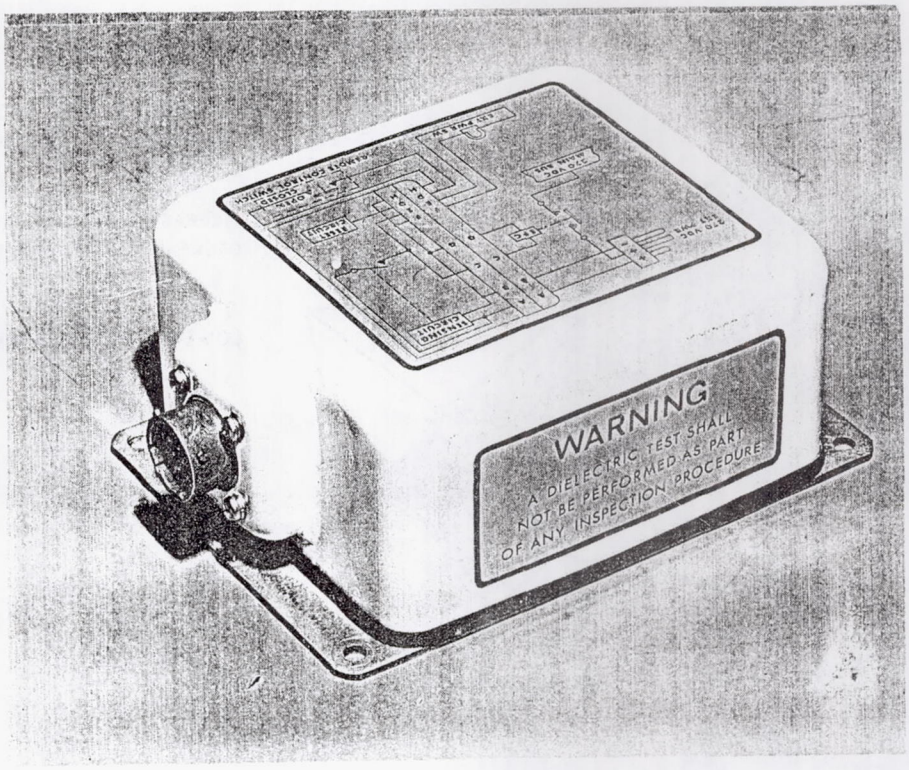

Figure 6. - 270-V dc power monitor.

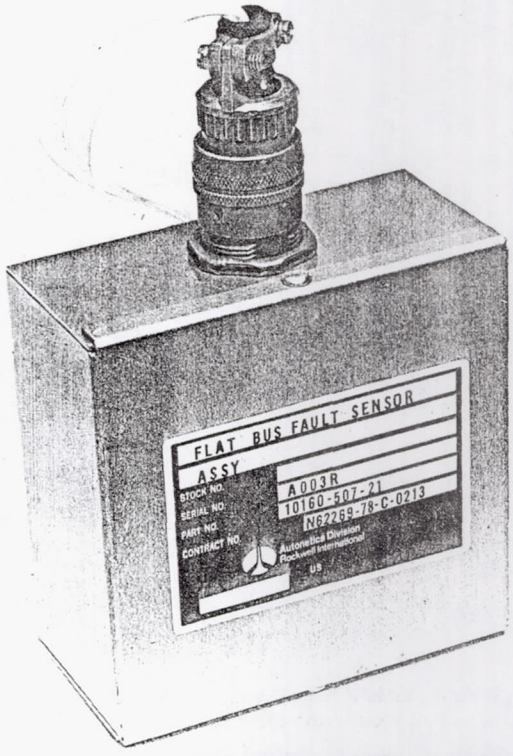

Figure 7. - Flat bus fault sensor assembly.

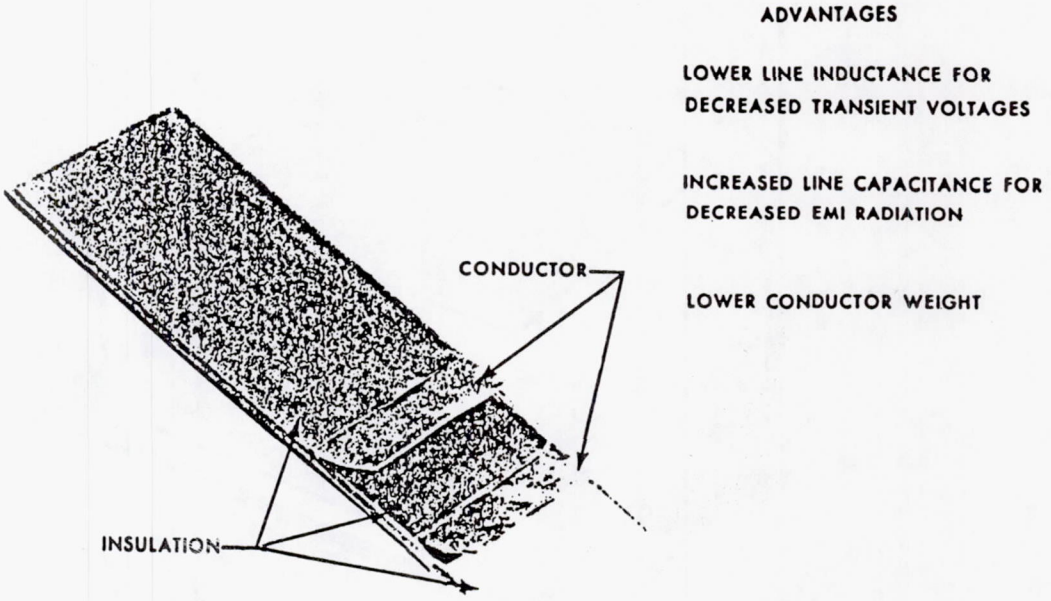

Figure 8. - Flat conductor cable.

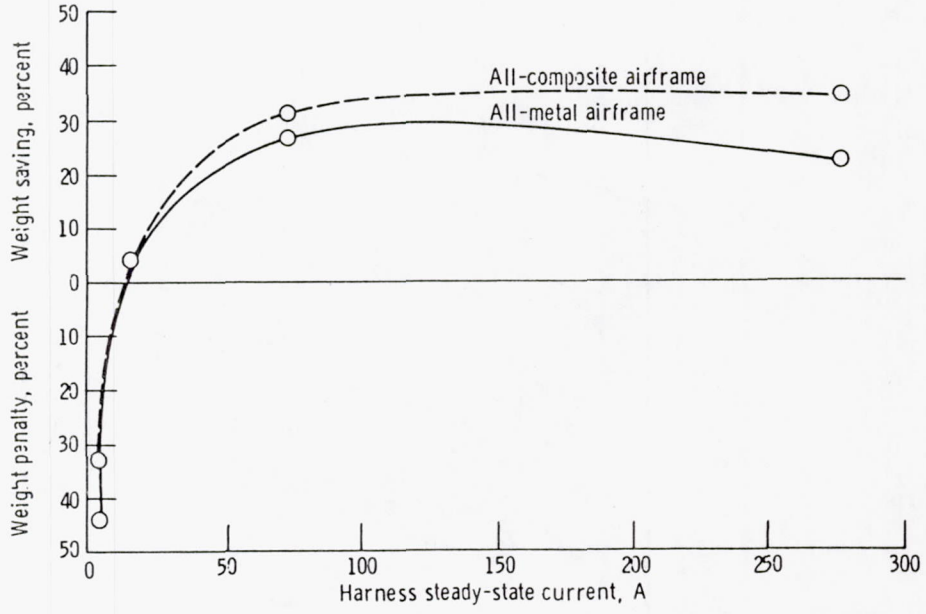

Figure 9. - Weight effects of flat cable versus round cable in 270-V dc power distribution system. (If all power runs above 10 A in the AWACS were converted to flat cable, a weight saving of 880 lb would result.)

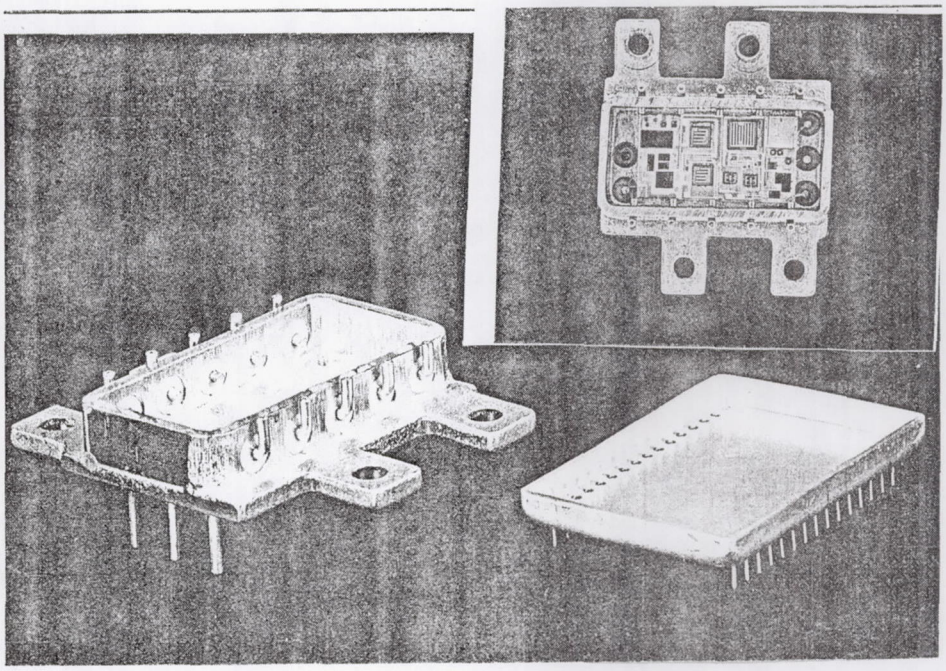

Figure 10. - 270-V dc power controllers.

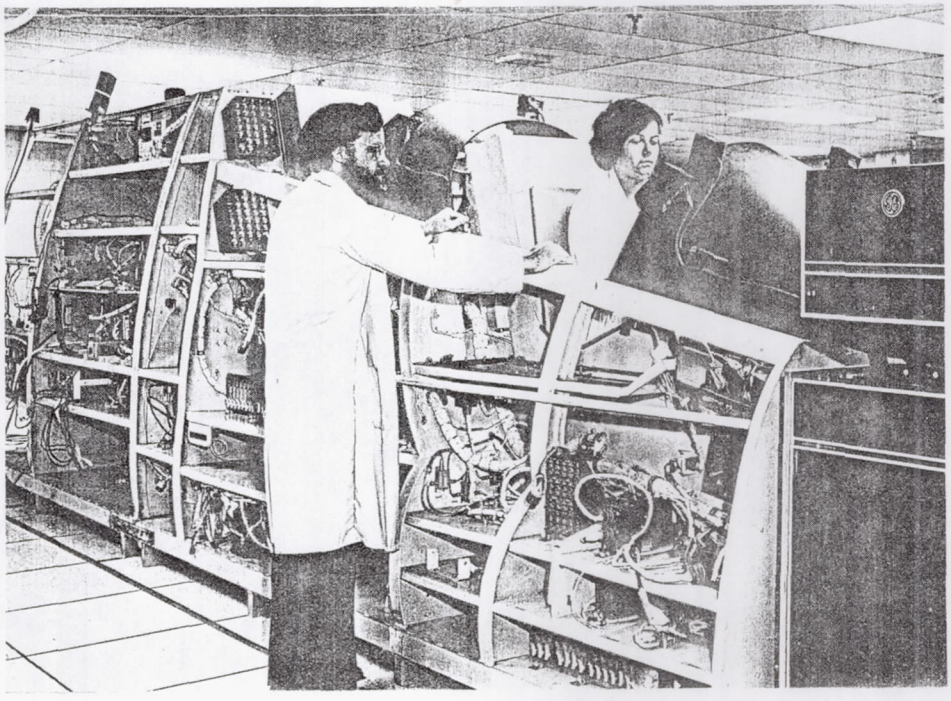

Figure 11. - AAES airframe/system simulator.

THREE-PHASE, HIGH-VOLTAGE, HIGH-FREQUENCY DISTRIBUTED BUS SYSTEM FOR ADVANCED AIRCRAFT

Robert C. Finke
National Aeronautics and Space Administration
Lewis Research Center
Cleveland, Ohio 44135

The NASA Lewis Research Center is developing higher voltage, higher frequency components for spacecraft. The technology is directly applicable to aircraft power-generating systems except that aircraft systems are about an order of magnitude larger than spacecraft systems.

For this paper the following assumptions were used: The system is generic. Everything is powered from the generators. If all the switches were turned on at once, the load would be 500 kVA. The distance from generator to load can be 250 ft. All generators and motors are inherently alternating-current machines. There is no such thing as a brushless direct-current motor. It's an alternating-current motor with electronic commutation. There is also no such thing as a direct-current generator. Alternating-current generators with rectifiers are used. All of the systems are inherently alternating current, and anything else requires hardware to be added to the system.

Figure 1 shows the system model. The model is simple: it has a generator and some level of current and voltage. The current and voltage multiply together to give the total power. All of the diodes, transistors, etc., are represented in the circuit by a forward voltage drop across the diode. There is also resistance of the line, connectors, etc. And finally, the load.

Forward voltage drop in semiconductors is relatively constant. It varies from about 1 to 2 V depending on whether the semiconductor is a silicon-controlled rectifier or a transistor and on what kinds of voltages and currents are going through it. But if there are many diodes in the line, as the system voltage goes down, the wattage lost through forward voltage drop goes up (fig. 2). In a system with a large number of semiconductors the loss curve begins to flatten out around 300 V. That is, the system losses due to all the semiconductors start getting appreciably lower.

For cable with a 2-percent loss, system weight increases significantly (fig. 3). At about 50 V it becomes excessive. For this reason, and because the semiconductor losses are lower there, high voltages would be preferred. To be able to use higher voltages in power systems, semiconductor devices with adequate ratings must be available.

The following components are available for use in aircraft power-generating systems:

(1) High-current power-switching transistor D7ST (fig. 4). The D7ST is the successor to the D60T, which Westinghouse is now producing under a NASA contract. The D7ST features are a voltage of 400 to 500 V at a current up to 150 A, with 400-A peak, and power of 50 kW. Its rise and fall times are 0.75 μsec with a 4-μsec storage time. It can therefore be used in a relatively high-frequency converter to switch high power levels. Although it is a fairly impressive device, it can be improved.

(2) Augmented power transistor. This transistor is in the development stage. The contract specifications are a voltage of 800 to 1000 V, current of 70 to 112 A (gain of 10) with a 400-A peak, power handling of 75 kW, power dissipation of 1.25 kW at 75° C, rise and fall times of 0.5 μsec, and storage time of 2.5 μsec. This device can also be used in power inverters or switches at high voltage and high power.

(3) Fast-recovery, high-voltage power diode. A 1200-V diode with a 50-A forward current (fig. 5) has been developed by Power Transistor Corp. under contract to NASA Lewis. It is a fast diode, with reverse recovery time of 200 nsec. The applications in a system are myriad and include rectification, protection, filters, and clippers.

For higher-voltage systems, up to 1000 V, corona breakdown could be a problem. In a Boeing report done for Wright-Patterson AFB by William Dunbar, corona initiation voltages ranged from 1200 V at 40 000 ft to 400 V at 80 000 ft (fig. 6). With commercial aircraft flying around 40 000 ft, the higher voltages look pretty reasonable for power distribution.

Figure 7, produced by James Triner of NASA Lewis, shows efficiency and weight versus frequency for a 50-kVA transformer with advanced materials. As with voltage, as frequency increases there is a significant drop in weight and around 10 kHz the curve starts to flatten out. However, at that frequency the efficiency has alredy begun to decrease. A little under 10 kHz is a good frequency at which to do inversion and perhaps distribution because the magnetics are maintaining their efficiency but their weight is substantially reduced.

Figure 8 is a comparison of transformers for space and commercial uses. Both are 25-kVA, single-phase transformers. The commercial pole transformer weighs 400 lb, is 97.9 percent efficient, has a voltage of 120/240 V, and has a high voltage of 3850 V. The space transformer has the same power-handling capacity but at a frequency of 20 kHz instead of 60 Hz. That makes a sizeable difference. And it has also been designed extremely carefully from a thermal standpoint. The pie windings are shaped and fastened to aluminum plates for heat removal. Another paper in this conference, by Gene Schwarze of Lewis, describes this transformer technology and its characteristics. The weight difference is also significant - 400 lb at 60 Hz as compared with 7 lb at 20 kHz. The space transformer is also more efficient (99.2 versus 97.9 percent) and has a lower temperature rise.

The type of distribution system selected for an aircraft power system can have a substantial effect on the conductor weight as shown in table I. A two-wire, direct-current system has been selected as the base and allotted a weight of 100 percent. A very substantial weight reduction can be had by going to the three-wire Edison system. The two three-phase, alternating-current systems both exhibit a weight savings over the base. However, the three-phase, four-wire wye shows the largest gain even with a full-size neutral.

NASA Lewis has done research on remote-power-controller technology. The driver for this technology, however, is the semiconductor device, so we first need big enough, fast enough, semiconductors to make and break the circuit. Figure 10 shows early solid-state, remote power controllers (RPC's) developed for use in the space shuttle. These are 28-V RPC's at various sizes, 3 to 5 A up to 15 to 20 A. The next generation of remote power controllers (fig. 11) have voltages up to 120 V dc and currents to 30 A. They were developed by Westinghouse.

Figure 12 shows a Lewis-developed high-voltage, high-power circuit breaker. The figure shows the breadboard and a schematic of the system. The load-switching transistor has been the technology driver. Only recently have 1-kV transistors been developed to go into this circuit. But this circuit breaker has been built and tested. It has been used primarily with the electric propulsion systems. Ion thrusters use a 1-kV screen drive at several amperes. And this circuit breaker has been used as the main bus-interrupt for electrical propulsion systems. So it has been tested in that sort of application and now the technology is ready for other applications.

The following characteristics are recommended for aircraft power-generating systems:

(1) High voltage distribution. High voltage of about 200 to 300 V reduces conductor weight and reduces the effect of semiconductor drops. This provides a lighter and more efficient power system. Corona does not appear to be a problem at these voltages for any aircraft.

(2) Alternating-current distribution. Since all rotating machinery generates or consumes ac power, it appears to be most efficient and simple to distribute the power in that form. In addition, it is much easier to interrupt alternating current than direct current.

(3) High frequency distribution. Frequencies in the range of 10 kHz cause a substantial reduction in the weight of magnetics while still providing a relatively high efficiency.

(4) Multiphase distribution. A three-phase distribution system provides a substantial reduction in conductor weight. It can also be very low in radiation.

TABLE I. - EFFECT OF SYSTEM ARCHITECTURE ON CONDUCTOR WEIGHT

System	Weight, percent of baseline
Two-wire dc (baseline system)	100
Three-wire Edison	37.5
Three-phase delta	75
Three-phase, four-wire wye (neutral, full size)	33.3

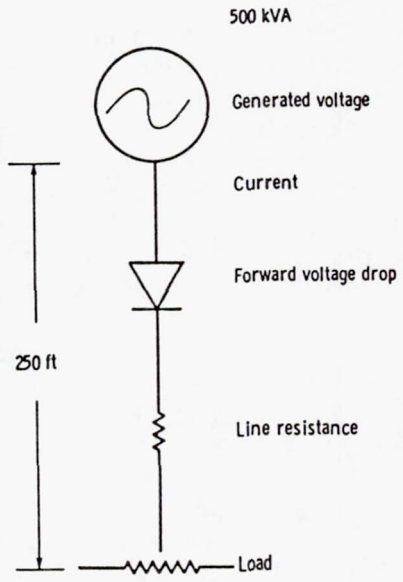

Figure 1. - System model.

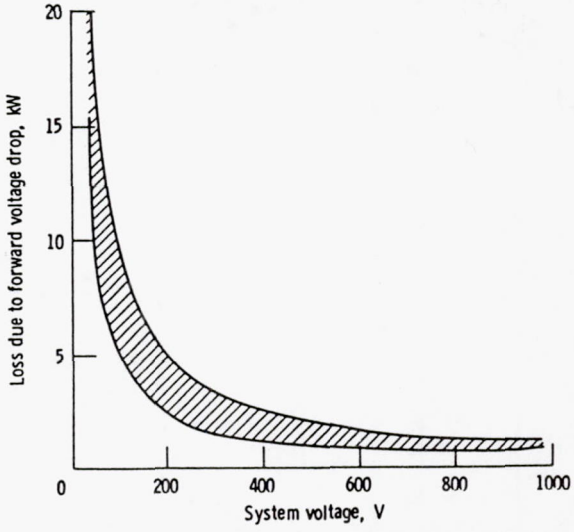

Figure 2. - Loss due to forward voltage drop as a function of system voltage.

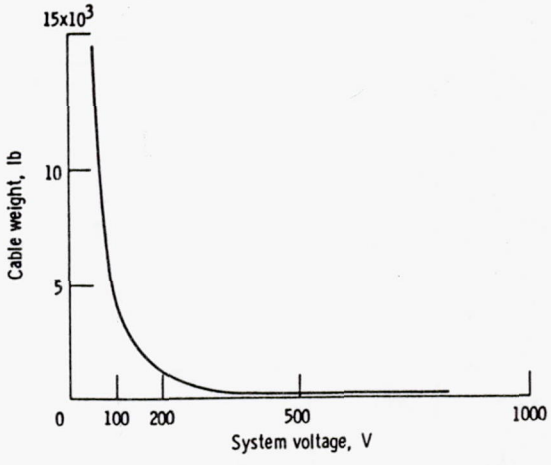

Figure 3. - Cable weight as a function of system voltage.

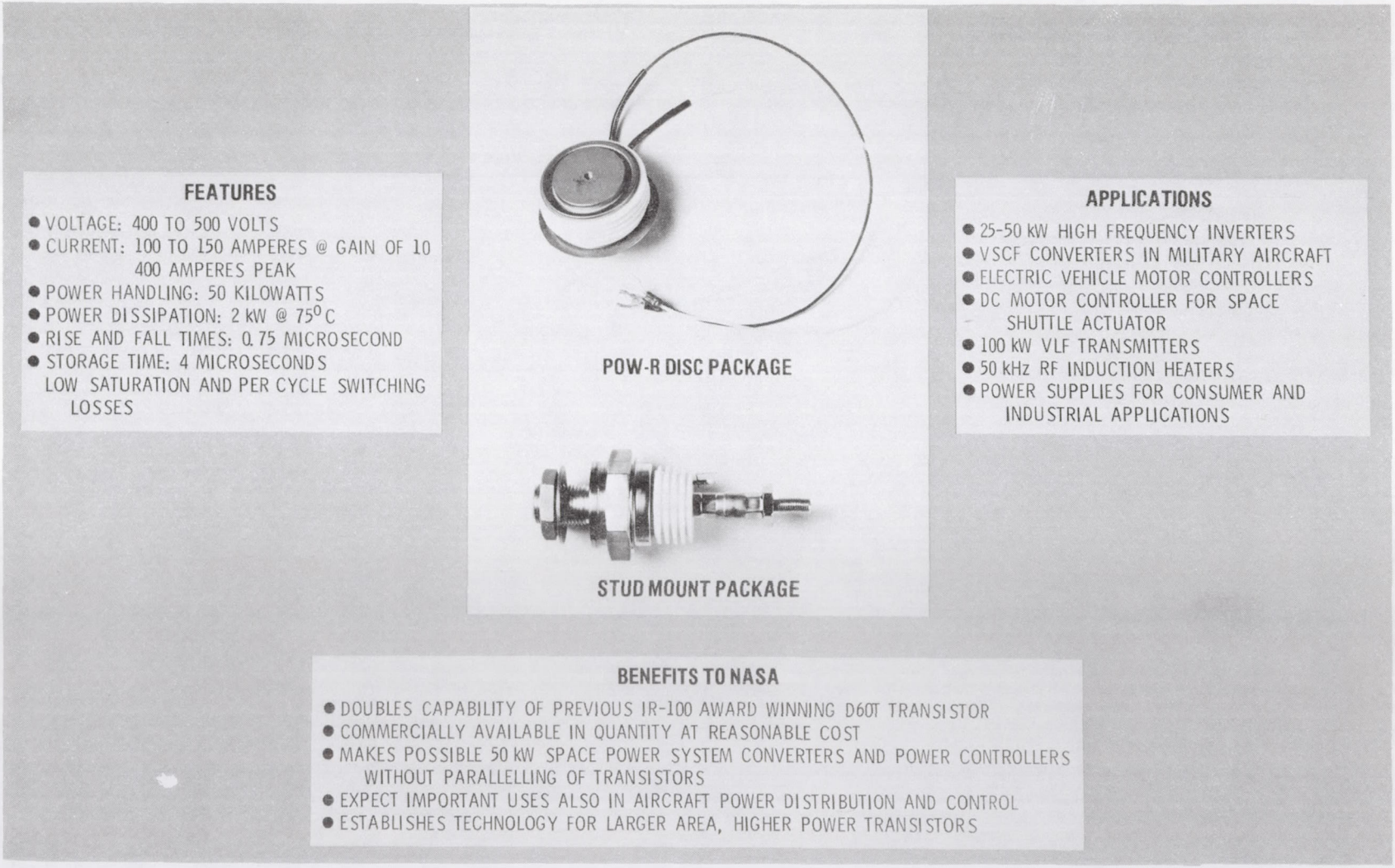

Figure 4. - NASA Lewis high-current power-switching transistor (Westinghouse model D7ST, higher current version of D60T.)

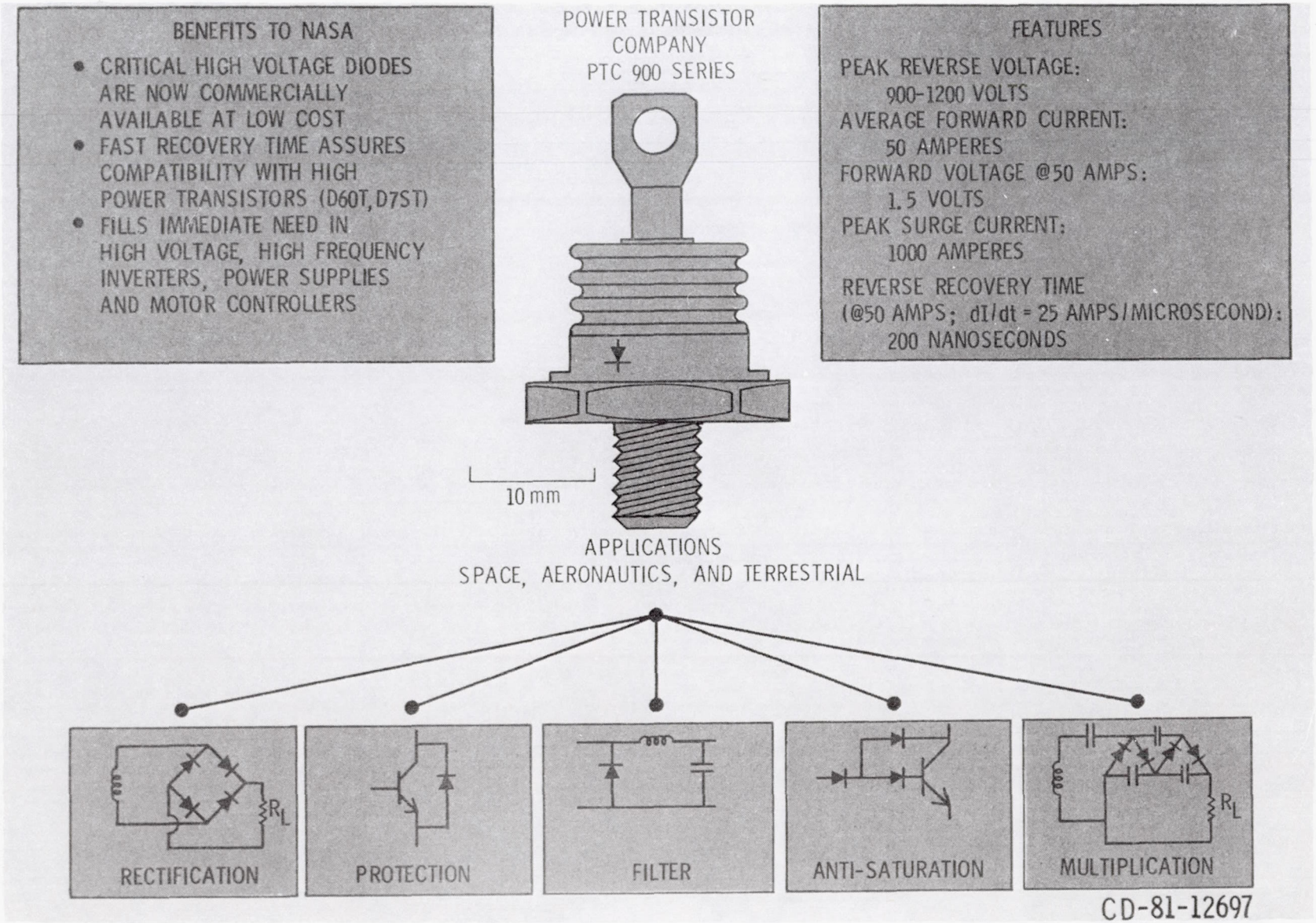

Figure 5. - NASA Lewis fast-recovery, high-voltage power diode.

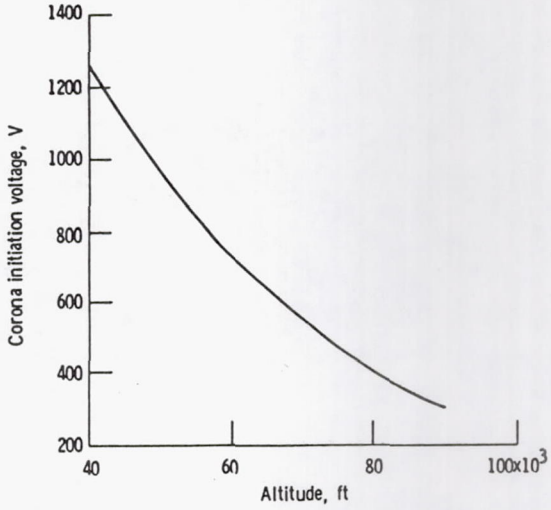

Figure 6. - Corona initiation voltage as a function of altitude.

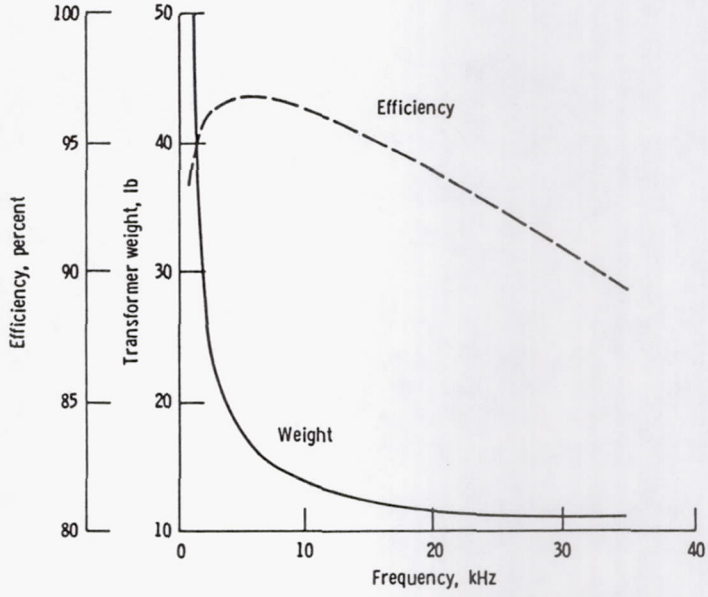

Figure 7. - 50-kVA transformer design for constant flux density. Primary voltage, 440 V; secondary voltage, 1 kV.

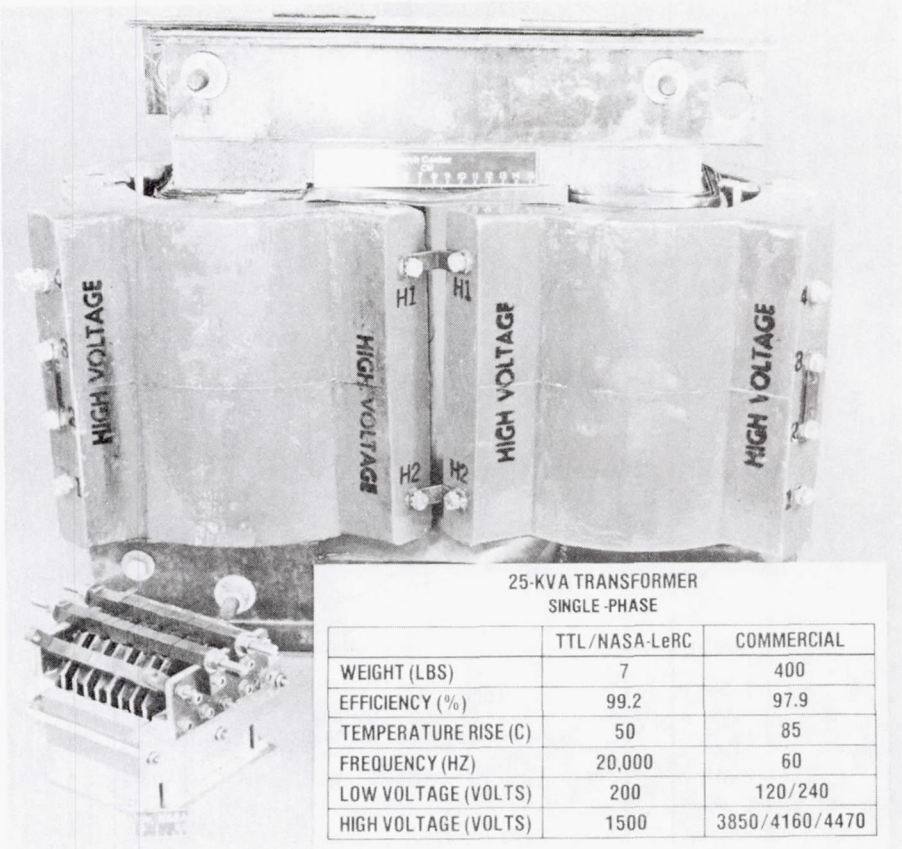

25-KVA TRANSFORMER
SINGLE-PHASE

	TTL/NASA-LeRC	COMMERCIAL
WEIGHT (LBS)	7	400
EFFICIENCY (%)	99.2	97.9
TEMPERATURE RISE (C)	50	85
FREQUENCY (HZ)	20,000	60
LOW VOLTAGE (VOLTS)	200	120/240
HIGH VOLTAGE (VOLTS)	1500	3850/4160/4470

Figure 8. - Comparison of space and commerical transformers.

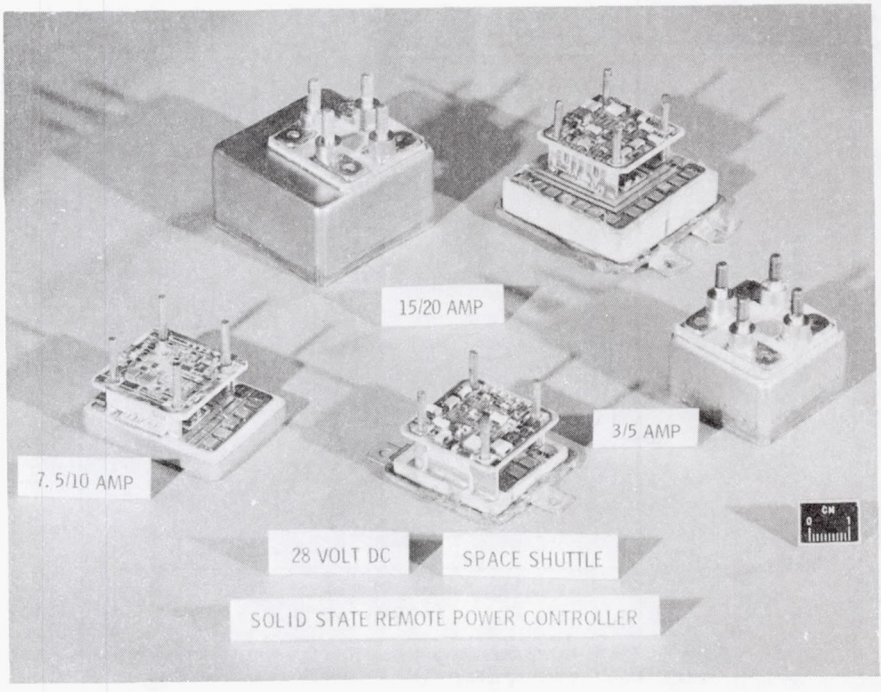

Figure 9. - Solid-state remote power controllers developed for use in space shuttle.

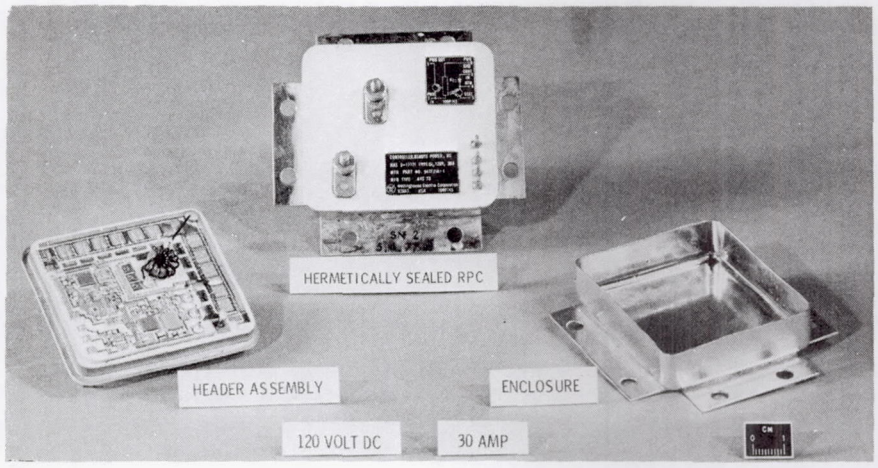

Figure 10. - Next generation of remote power controllers.

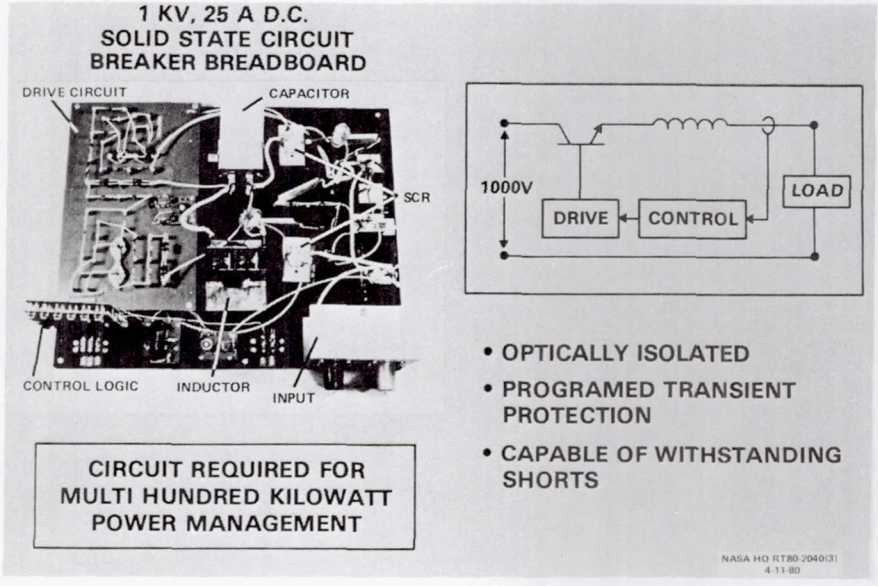

Figure 11. - High-voltage, high-power circuit.

SECONDARY ELECTRIC POWER GENERATION WITH MINIMUM ENGINE BLEED

Gordon E. Tagge
Boeing Commercial Airplane Company
Seattle, Washington 98124

In studies conducted throughout the last 20 years, trade-offs in terms of engine power extraction have been common. What then is different about this study

Probably the most important difference is that today economics is a greater factor than ever before. Also, because of the large cost of development the form and characteristics of the benefits are important. Is less fuel burned Is cost lower Is weight lower Do these things counteract each other An erroneous comparison impacts thousands and millions of dollars, and so the purpose of this study is an overall, comprehensive analysis that answers two questions:

(1) If you had to build a system today, what would be the nature of that system?
(2) What would be the cost, performance, and weight?

The engine probably has the most significant effect on the selection of a secondary power system. Most of the electrical system development in the last few years has been an attempt to make the system better. Another approach is to question the trend to eliminate the use of bleed systems.

New energy-efficient engines will have

(1) Higher turbine inlet temperatures
(2) Higher bypass ratios
(3) Higher pressure ratios
(4) Lower core airflows
(5) Less available bleed air

The main effects of engines, apart from their technical characteristics, are that there is less core flow and less bleed air available. Thus, from a pragmatic standpoint, whether or not you want to change the secondary power system, you may be forced to change it.

Figure 1 shows a comparison of two typical engines and airplane systems. A typical engine for the Boeing 767, with a 12-percent nominal limit provides, for an idle descent condition at 22 000 ft and Mach 0.55, which is also typical of a holding condition, a bleed flow of about 3.6 lb/sec. This is sufficient to provide air for refrigeration and pressurization. If air is also required for cowl and wing anti-icing, the amount of air required would exceed what the engine supplies within its nominal limits. This problem was solved operationally by increasing the thrust during these conditions to provide the necessary pressure and flow. This is basically the current status.

The type of energy-efficient engine that would be used on a 1988 airplane, for a typical 150-passenger baseline, would have a nominal limit of around 9 percent. Because of the small core airflow it would provide much less bleed flow than required for refrigeration, pressurization, and cowl and wing anti-icing. On that particular airplane Boeing has already chosen an alternative for hot-air anti-icing of the wing. For pressurization and cooling and cowl anti-icing there is a wider gap to fill in terms of increasing engine thrust. With an even more advanced energy-efficient engine, to be used on a 150-passenger airplane in 1995, there may even be problems in meeting the

requirement for environmental control alone. Therefore apart from an electrical system development advantage, from a pragmatic standpoint, we may be forced to abandon bleed systems, either in whole or in part.

This then was the motivation for a study (fig. 2) to address the engine, which is the basic source of power, both primary and secondary. First, the three engine manufacturers were asked to what extent they could rematch the engine, that is, make it smaller and more efficient, with no engine bleed at all. Next, an airplane configuration and a secondary power system were selected as a total system that could be built with current technology and would meet not only the basic requirements, but all of the failure conditions. Also, in selecting a two-engine airplane, the problems of system redundancy, failure conditions, and all of the operational requirements were addressed as well. We then put together a study that would provide an initial estimate of weight, performance, and cost, within the scope of secondary power generation. The study will address these issues and concerns:

(1) Engine starting
(2) Electric power generation
(3) Power controllers
(4) Power distribution
(5) Ground power
(6) Auxiliary power unit (APU)
(7) Airconditioning
(8) Cowl and wing anti-icing

In this study, the role of the APU had to be evaluated very carefully. The APU, of course, originally was a flying piece of ground support equipment used to provide independent capability for starting and ground cooling as well as some ground electric power. Later the APU was used to provide in-flight power. So in any cost-performance trade, it was necessary to sort out the role of the APU in terms of its ground functions and its in-flight functions. Throughout this study all of the penalties and benefits related to the APU are based on its in-flight function only.

The purpose of this study was not only to get technical results, but also to indicate direction - where we should be putting our money and where the next logical step for equipment development would be. Those who know the Boeing approach know that we are not only interested in what the right analysis numbers are. For any piece of equipment to be put into inventory, either commercial or military, we need to test the systems on an airplane. Therefore we rely on hardware development, "ironbird" testing, and flight testing on at least a component and subsystem basis. For this we need direction as to where to put our emphasis.

The study involved putting together a task team. We not only had systems experts, but we brought in configuration, system installation, aerodynamics, weight, product assurance, and finance specialists. This study was a model of a very comprehensive analysis not only to identify systems but to evaluate them.

One of the major problems in a customer-client relationship is that the client, in this case the engine manufacturers, will try to satisfy what they perceive as the customer's requirements. Thus it was very important, in our study, to point out that we wanted to know the best answer in terms of power extraction - whether or not to bleed the engine. We also wanted to get a good data base on which to evaluate an advanced-bleed system. That was the purpose of these particular simulations - to get a good engine performance deck that would allow us to bleed air from any port from an optimum standpoint and therefore provide the best possible bleed system and compare it with a good minimum-bleed system.

The next step was to select a good representative airplane. Of course, it makes quite a difference whether it is a two-, three-, or four-engine airplane and whether it is a shortor a long-range airplane. With the preponderance of shortand intermediate-range airplanes today, we selected a two-engine, short-haul airplane as representative for the present and near future. The last objective was to meet all of the dispatch and operational requirements, both from a FAA and a customer standpoint.

Figure 3 shows the general arrangement of the airplane that was used in the study.

Any study that will be accepted by management has to have a very credible data base. The data base used in this study was a two-port bleed baseline (the 767 airplane). Because of the detailed weights and good definition available for that system, the task team used this particular configuration as the data base. This was not necessarily our configuration baseline, but it was our data base. Table I shows the systems that were varied in the study. As a secondary trade-off minimum bleed was figured with and without an APU, but the basic overall study did include an APU.

One of the criticisms of most studies is that an old airplane is used for a particular set of conditions and compared with another airplane under a new set of conditions. In this particular study we took the data base and then put together an advanced bleed system so that in comparing it with the minimum-bleed system we were comparing comparable technology. We did not include in the study advantages that would be applied in one set of conditions and not in the other.

As shown in table I the advanced-bleed system had a conventional constant-speed drive (CSD) and 75-kVA generators. The minimum-bleed system with an APU had one 160-kVA system per engine; without an APU two generators were used on each engine to meet the failure and power-out conditions. The minimum-bleed systems also had an electric starter-generator system. Two factors were held constant in the study: (1) hot-air cowl anti-icing and (2) the hydraulic and flight control system. At present, we do not have confidence in an alternative to cowl anti-icing other than hot air. There are a lot of developments going on and we would be glad to change our position in the near future. But for the sake of this study, we stayed with the hot-air cowl anti-icing system.

Details of the secondary electric power generation system with and without an APU are given in figures 4 and 5. The system with an APU (fig. 4) had one generator on each engine and another generator on the APU. Two electric-driven compressors provided the air for environmental control. The APU was the third air source in case of failure. Power controllers controlled both the starter-generator function and the power of the environmental control system (ECS). Without the APU (fig. 5) another way must be provided to get the third power source. Two generators were used on each engine and a third electric-driven compressor was provided in lieu of the air provided by the APU. This arrangement required an extra set of power controllers.

The system with no APU involved a great many switches. If it were not for the failure conditions, all of those switches could be eliminated. What distinguishes this study from simple weight or energy trade-offs is that it addresses all of the failure conditions.

The advanced-bleed system is compared with the minimum-bleed system in table II. The weight of the starting system decreased from 180 lb for the advanced system to about 10 lb for the minimum-bleed system, and the weight of the pneumatic system, which involves the precooler, the bleed valves, and providing for switchover during engine-out, decreased from 640 lb to 70 lb.

Eliminating the pneumatic engine start and bleed system led to weight savings but adding the starter-generators, of course, increased the weight again. The difference in APU weight had to do with the increased size of the generator for the APU. The net result was a 700-lb weight increase for the minimum-bleed system over the advanced-bleed system.

Table III shows the effect on performance without resizing the airplane. For a basic engine selection the change in the lift-drag ratio is small, but there is a significant reduction in specific fuel consumption for the minimum-bleed systems.

Our environmental control studies kept track of the air required to supply the engine-driven compressors and compared it with the effect of not bleeding the engines. The diagram on the left of figure 6 shows the results of this study as compared with the baseline. The diagram on the right shows the relative effect between the advanced-bleed system and the minimum-bleed system. Both, of course, have extremely low drag; it can hardly be measured. But, for the purists, there is a slight advantage to the advanced-bleed system. Both have less drag than current baseline systems.

An overall performance comparison on a resized airplane is shown in table IV. There is a significant increase percentage-wise in block fuel saving, even though the total numbers do not vary much. The main advantage is that less fuel is burned with the minimum-bleed system than with the advanced-bleed system.

One of the factors that bears on the subject is what a typical block time or block range is. From our 737 experience, the typical block range is a little less than 300 nautical miles. A 727, which is nominally a 2000-nautical-mile-range airplane, has an average block range of less than 400 nautical miles. Between 300 and 500 nautical miles is a typical block range for this size of airplane.

Cost is the most difficult parameter to evaluate from a supplier's, an engine manufacturer's, an airframe contractor's, and an airline's standpoints. The parameters may all be the same, but the significance of the parameters differs. Therefore we chose to evaluate the cost of ownership relative to an airline customer. We have through the years developed a cost model that may not be precise but is fairly accurate in terms of relative comparison. This basically is the model that we used.

The model is based on

(1) Airline fleet service period of 15 yr, 1986 to 2000
(2) Thirty-airplane-fleet nonrecurring cost, prorated to 300-airplane minimum production
(3) 3000 Flight-hours per year, per aircraft
(4) Depreciation schedule, 10 yr
(5) Investment tax credit, 10 percent
(6) Corporate income tax, 48 percent
(7) Annual inflation rate, 7 percent for labor and materials
(8) Current dollars, after taxes
(9) Spares level, 6 percent for equipment, 30 percent for APU

This model (fig. 7) shows that the total cost of ownership consists of investment costs, operating costs, flight operation, and tax adjustments. For this study we included all of the factors that are indicated with solid bullets. The factors indicated with open bullets are in the model but were not included in the study.

Figure 8 shows the difference in cost of ownership between a minimum-bleed system and an advanced-bleed system as compared with the current baseline, namely the 767 two-port bleed system. For the 300- to 500-nautical-mile

range the difference is $3 million to $4 million per year. This is approximately half the saving achieved by the recent decision to go from a three to a two-man crew. The comparison with and without an APU shows benefits that are even larger. The relative comparisons for a 1500-nautical-mile range are much less. However, this particular airplane is not designed to operate at that range most of the time.

Another factor in a cost comparison is increasing fuel price. How do you evaluate the change in fuel price and what effect does it have on the relative comparison between the systems From 1972 to 1982 the increase in fuel price was dramatic; in the last two years the price was more stable. Figure 9 compares an advanced-bleed system with two minimum-bleed systems, both with and without an APU. The left line represents the stable fuel price period of 1980 to 1982; the right line represents the unstable period of 1972 to 1982. Even though the absolute numbers change between the lines, the relative difference between the systems is about the same.

In summary, we took an in-depth conservative approach to the technical data. In all of our weight comparisons and in all of our equipment selections, we did not guess what the potential would be 5 or 10 years from now. We took existing technology and weighed the systems and costed the systems as they exist so as not to inflate the study in favor of the minimum-bleed system. The other technical results are as we have just gone over. Operating weight increased, but block fuel and cost of ownership decreased.

Table V takes these comparisons and addresses our current system in terms of a future developed system. In spite of the 700-lb weight increase, we believe comparable weight between an advanced-bleed system and a minimum-bleed system can be achieved for this type of airplane. The block fuel was less and, as the weight came down, the fuel burned would, of course, be further reduced. From a relative standpoint, we still kept it in the same general category as being less. The significant parameter, however, would be cost. The cost of ownership currently is less, but it would be much less for the developed system, especially the cost of new equipment as well as the fuel and operating costs.

In terms of direction, the switching in the secondary electric power generation system (fig. 5) can be significantly simplified. Subsystem tradeoffs, especially in the environmental control system, be it air-cycle or vapor-cycle, can be significantly improved. The role of the APU is always an interesting one. Although it is a high-cost item, airlines need self-sufficiency. So we are going to conduct some studies relative to APU uses and the better way of integrating the APU into an all-electric system.

Engine selection and optimization turned out to be a very critical factor in our study. Eliminating wing anti-icing resulted in a 7-percent reduction in engine size. Therefore a key factor, both from an airframe and engine standpoint, is that there probably is a greater penalty for mismatching the engine with the airplane than was apparent in the past. And that disparity is even more pertinent today.

In terms of activities, there already has been a fair amount of work done with starter-generators. A program just being completed at the General Electric Co. in Lynn, Mass., has been very successful. We have got quite a bit of development work in power controllers and in electric-driven compressors, and the work being done with alternatives to hot-air anti-icing for both wing and cowl is especially pertinent to Lewis.

Going back to the integration with other systems, needless to say, this study was of limited scope. It only addressed one part of secondary power; a study needs to be done from an overall systems standpoint. We need to include

the power distribution system and all of the synergistic benefits that can be achieved by pulling these systems together. One of the main advantages, over and above the technical results of the study, was that we developed expertise. Our task team arrangement, our ability to put all of the parameters in model form and evaluate different airplane, engine, and system combinations, was successful. We feel that we are in a good position to take the next step.

TABLE I. - STUDY CONFIGURATIONS

SYSTEM	2-PORT BLEED BASELINE	ADVANCED BLEED	MINIMUM BLEED WITH APU	MINIMUM BLEED WITHOUT APU
ENGINE GENERATORS	1-75 kVA GENERATOR/ ENGINE	SAME AS BASELINE	1-160 kVA GENERATOR/ ENGINE	2-120 kVA GENERATOR/ ENGINE
CSD's	1-CSD/ENGINE		–	–
APU GENERATOR	1-75 kVA GENERATOR/APU		1-160 kVA GENERATOR/APU	–
ELECTRIC DISTRIBUTION	400 Hz		HYBRID (400 Hz + WILD FREQUENCY)	HYBRID
AIR SOURCE	2-PORT BLEED	3-PORT BLEED	2 ELECTRIC-DRIVEN COMPRESSORS	3 ELECTRIC DRIVEN COMPRESSORS
COWL ANTI-ICING	HOT AIR	HOT AIR	HOT AIR	HOT AIR
WING ANTI-ICING	HOT AIR	FLUID	FLUID	FLUID
ENGINE STARTING	PNEUMATIC	SAME AS BASELINE	ELECTRIC START	ELECTRIC START
APU	YES WITH AIR SOURCE	SAME AS BASELINE	YES WITH AIR SOURCE	DELETED
HYDRAULICS	STANDARD	SAME AS BASELINE	SAME AS BASELINE	SAME AS BASELINE

TABLE II. - FUNCTIONAL GROUP WEIGHT SUMMARY

Affected functional groups	Baseline bleed (lb)	Advanced bleed (lb)	Minimum bleed with APU (lb)	Minimum bleed without APU (lb)
Vertical tail	850	770	770	770
Body	17,650	17,650	17,650	17,450
Nacelle and strut	2,810	2,660	2,600	2,630
Engine	9,790	9,400	9,400	9,400
Starting system	180	180	10	10
Pneumatics	670	640	70	70
Electrical	1,910	1,910	2,790	3,510
Air-conditioning	1,710	1,710	2,110	2,290
Anti-icing	240	320	320	320
APU	1,150	1,150	1,370	–
OEW (reference)	84,930	84,360	85,060	84,420
Δ OEW	Base	-570	+130	-510
		Base	+700	+60

TABLE III. - RELATIVE PERFORMANCE-DEPENDENT CHARACTERISTICS

		Average cruise		Climb
	Δ OEW	Δ (L/D)	Δ SFC	Δ (T/W)
Baseline bleed	Base	Base	Base	Base
Advanced bleed	-0.79%	+0.18%	-0.17%	-1.91%
Minimum bleed with APU	+0.34%	-0.02%	-0.68%	0%
Minimum bleed without APU	-0.41%	-0.10%	-0.68%	+0.55%

TABLE IV. - PERFORMANCE SUMMARY COMPARISON
[Range, 0530 n mi; altitude, 35 000 to 39 000 ft; step cruise at Mach 0.75; payload, 30 800 lb.]

	Baseline bleed	Advanced bleed	Minimum bleed	
			With APU	Without APU
Taxi weight, lb	142,086	141,242	142,160	141,330
TOGW, lb	141,900	141,056	141,920	141,144
OEW, lb	84,930	84,260	85,220	84,580
Fuel load, lb	26,352	26,182	26,086	25,950
TSLS, lb	24,300	23,300	23,300	23,300
T/W	0.34	0.33	0.33	0.33
Block time (1530 nmi), hr	4.046	4.049	4.042	4.042
Block fuel (1530 nmi), lb	18,673	18,608	18,525	18,420
Block fuel (500 nmi), lb	6,986	6,922	6,857	6,829
Block fuel (300 nmi), lb	4,875	4,821	4,763	4,745
% change block fuel (1530 nmi)	Base	-0.35	-0.79	-1.35
% change block fuel (500 nmi)	Base	-0.92	-1.85	-2.25
% change block fuel (300 nmi)	Base	-1.11	-2.30	-2.67

TABLE V. - CONCLUSIONS AND RECOMMENDATIONS

Results Comparison

	CURRENT	DEVELOPED
WEIGHT	HIGHER	EQUAL
BLOCK FUEL	LESS	LESS
COST OF OWNERSHIP	LESS	MUCH LESS

Direction

STUDIES	ACTIVITIES

• SYSTEM IMPROVEMENTS
  • SIMPLIFICATION
  • SUBSYSTEM TRADES
• APU USE AND ALTERNATIVES
• INTEGRATION WITH OTHER SYSTEMS
• ENGINE SELECTION AND OPTIMIZATION
	• STARTER/GENERATORS
	• POWER CONTROLLERS
	• ELECTRIC DRIVEN ECS
	• COWL AND WING ANTI-ICING

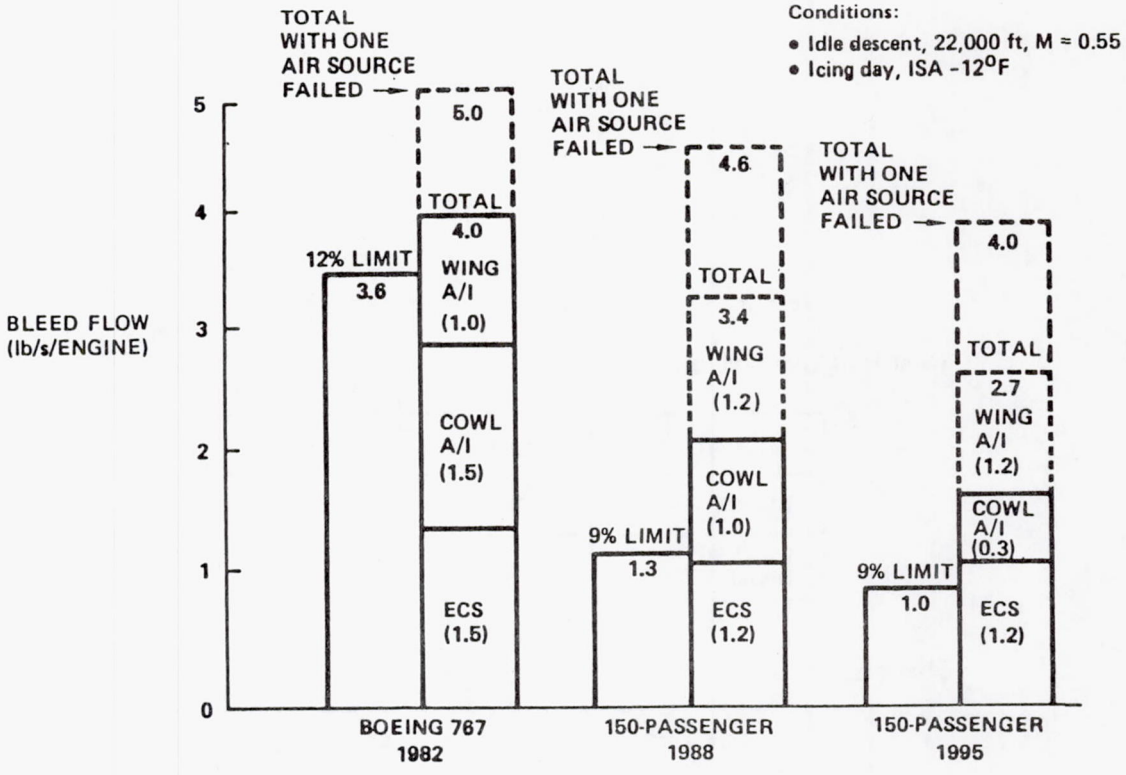

Figure 1. - Bleed availability versus environmental control system and anti-icing requirements.

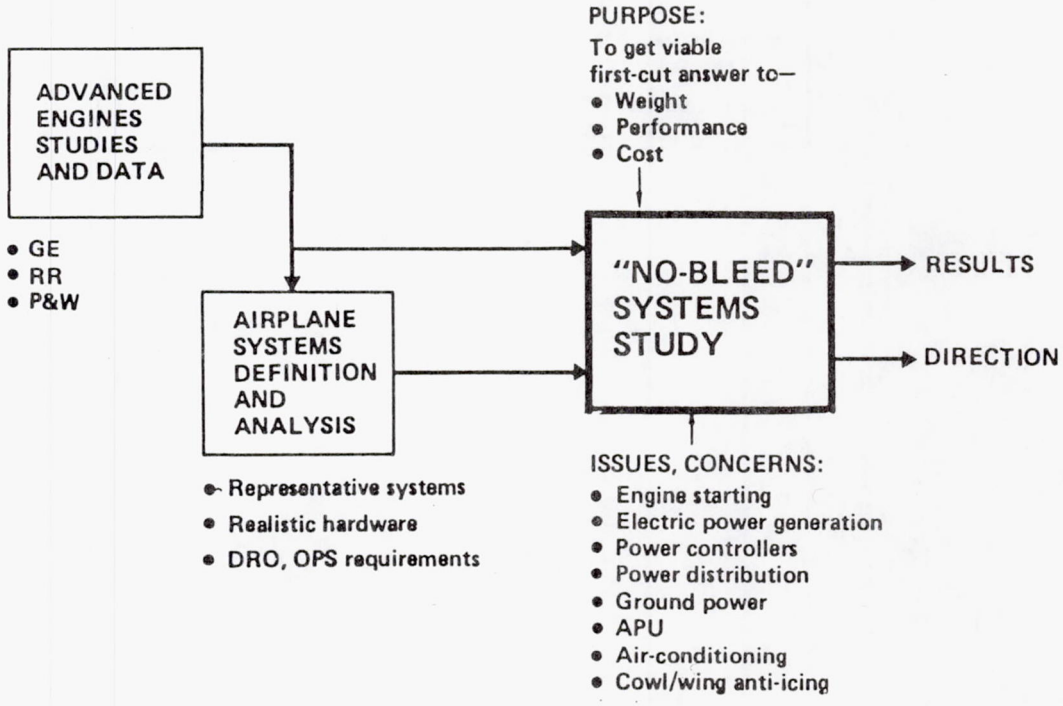

Figure 2. - Study plan.

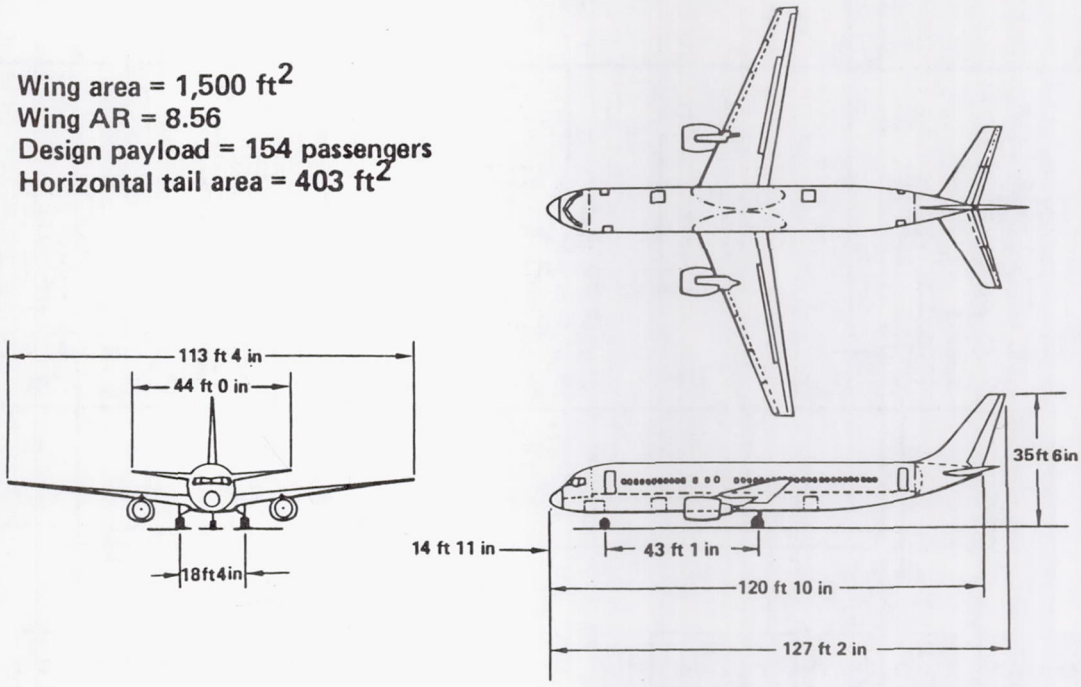

Figure 3. - General arrangement of airplane used in study.

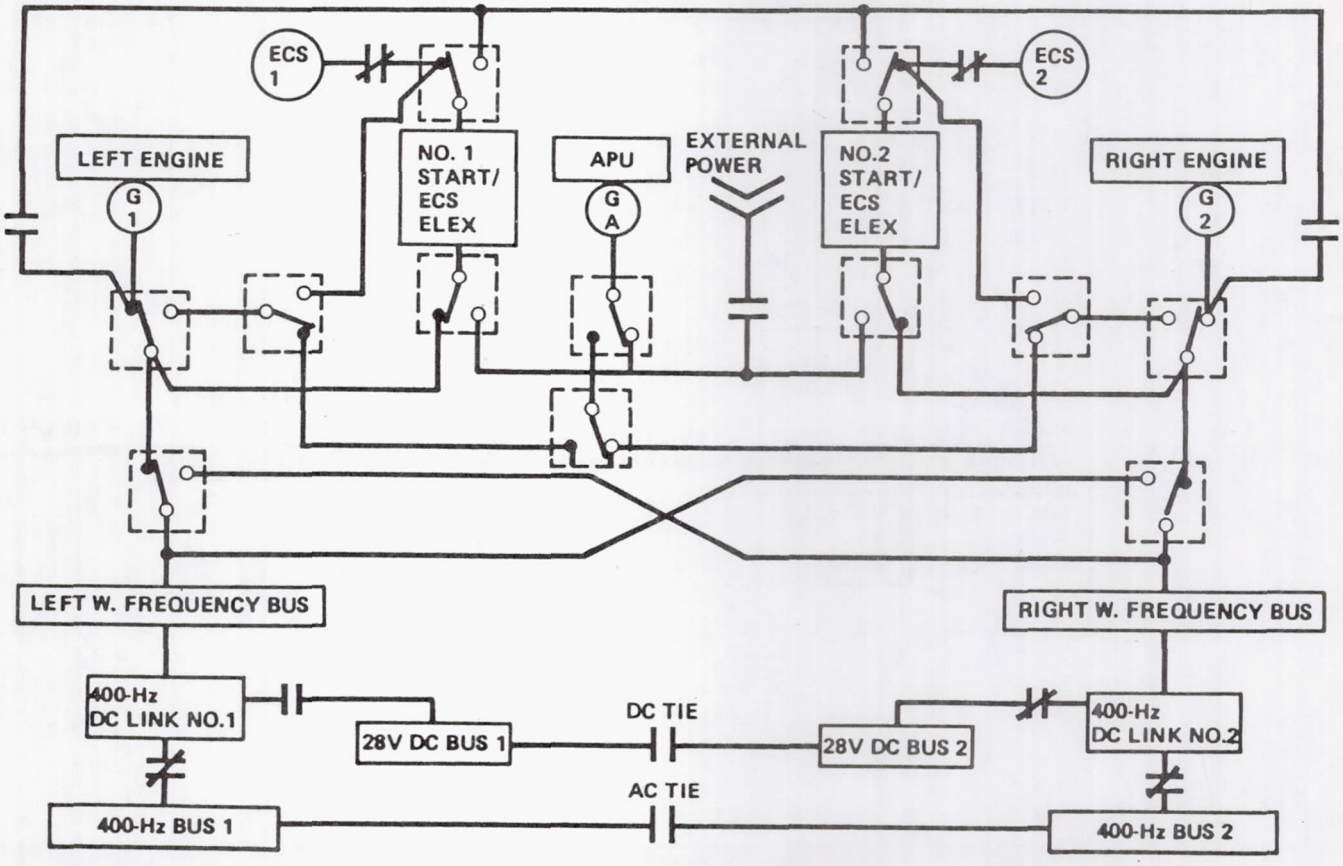

Figure 4. - Electric power system - with APU.

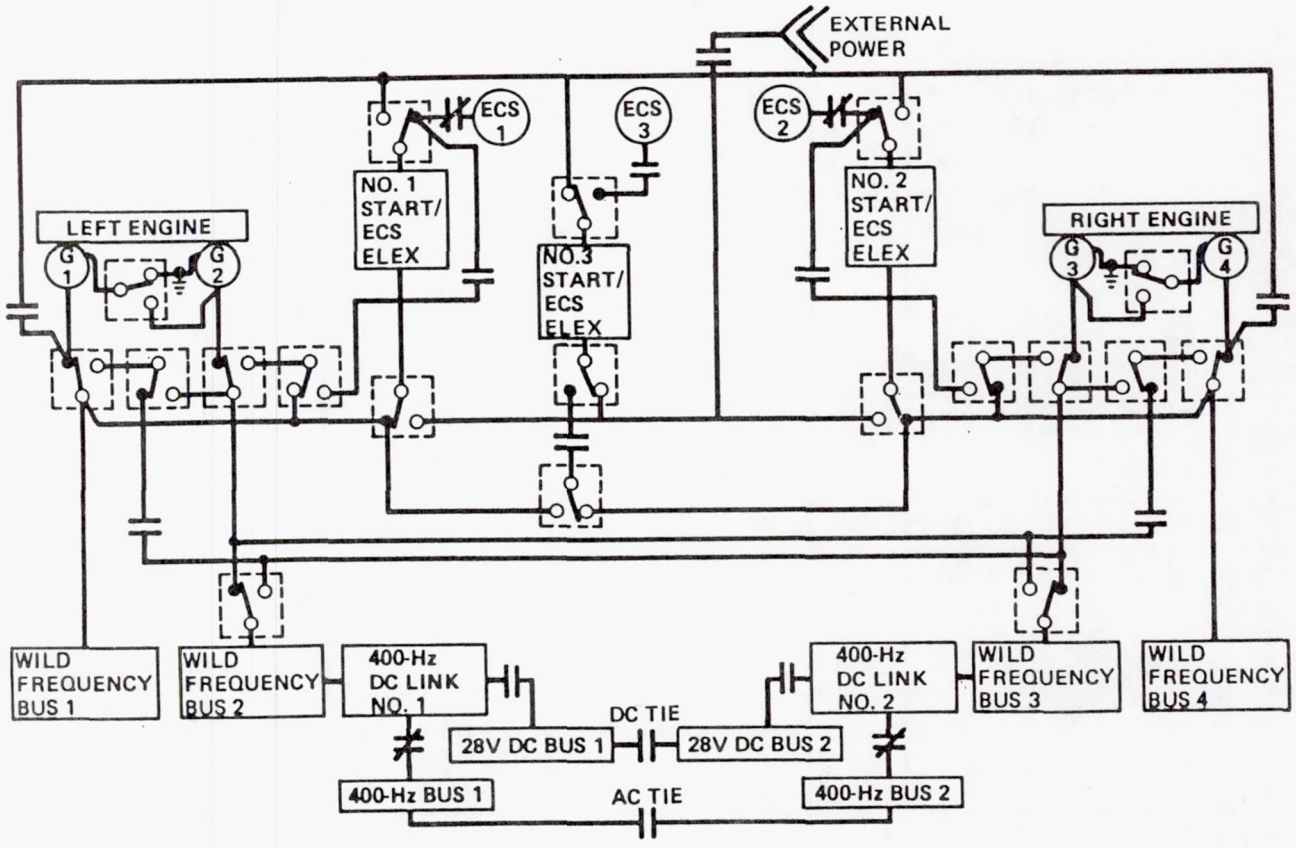

Figure 5. - Electric power system - without APU.

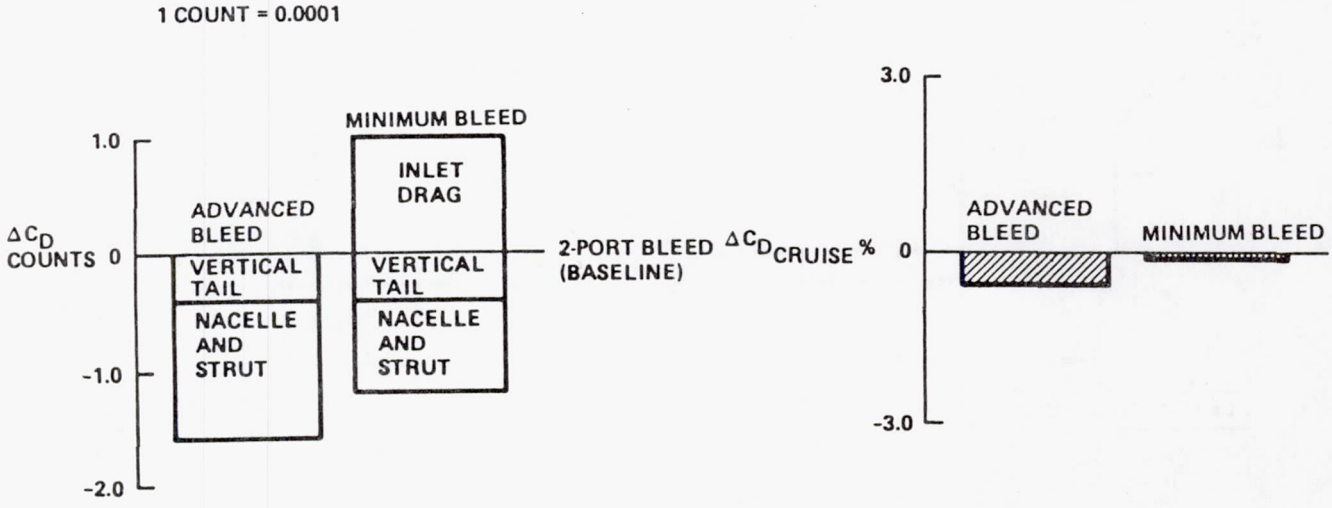

Figure 6. - Drag summary.

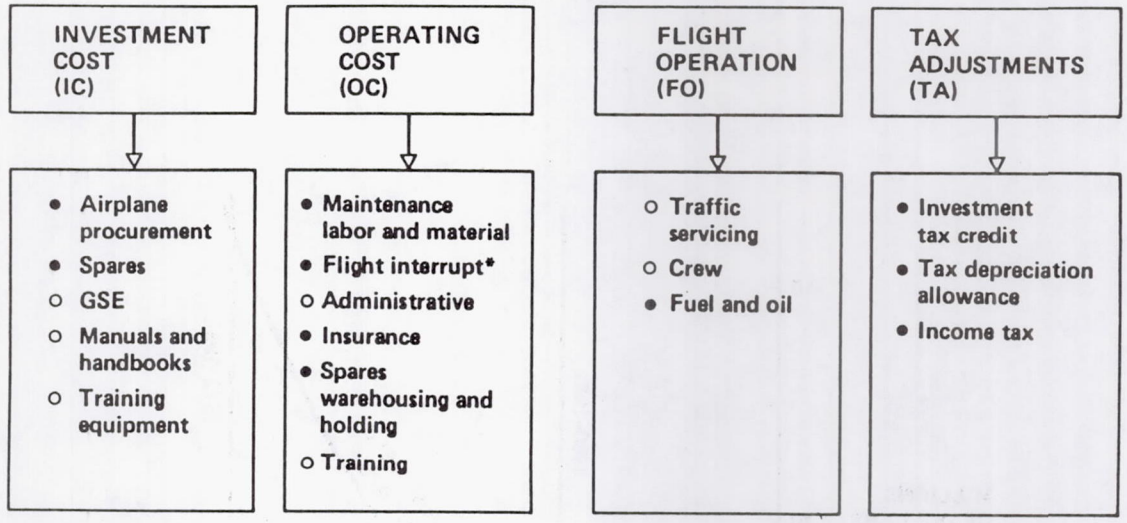

*Partial for delay and cancellation.

Figure 7. - Total cost of ownership.

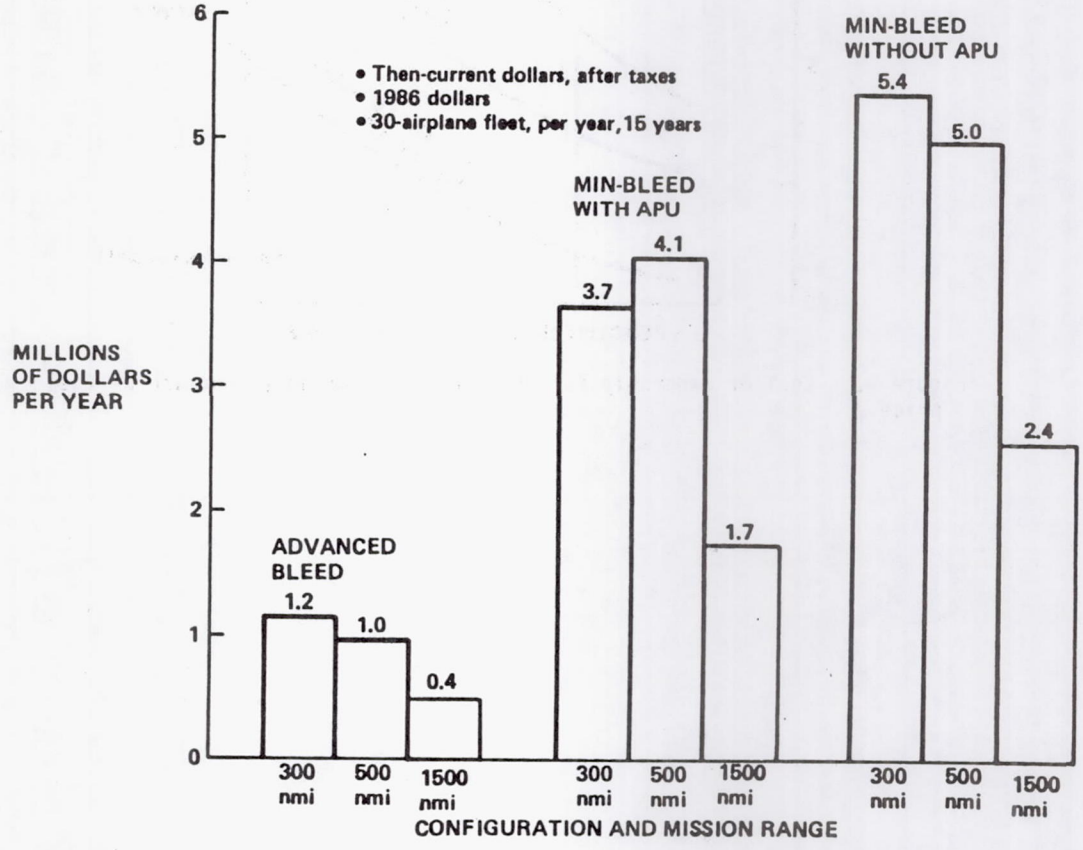

Figure 8. - Difference in cost of ownership between a minimum-bleed system, an advanced-bleed system, and the current baseline.

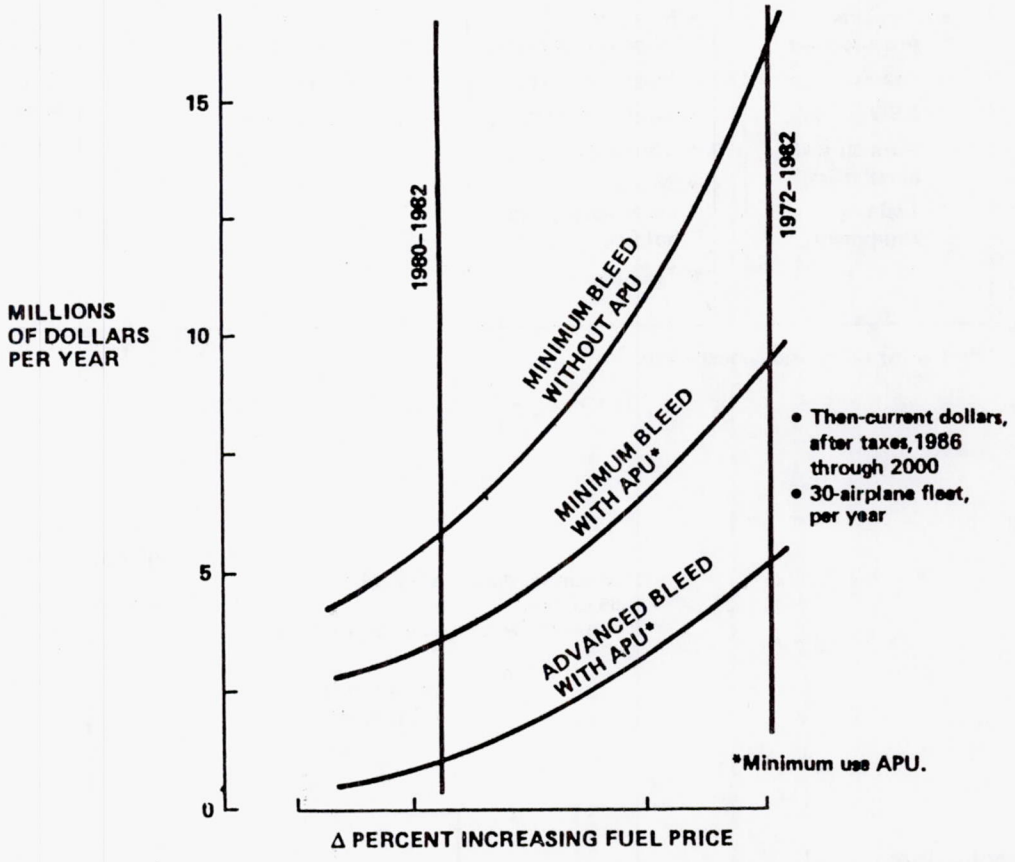

Figure 9. - Cost of ownership for the three systems as a function of fuel price.

PRIMARY ELECTRIC POWER GENERATION SYSTEMS FOR ADVANCED-TECHNOLOGY ENGINES

Michael J. Cronin
Lockheed-California Company
Burbank, California 91503

Although enthusiasm for the all-electric airplane is waning and current projections are that it will not be a reality until the 1990's, I feel that we can have an all-electric airplane by 1985. The variable-frequency, variable-voltage power system is a very efficacious system for an all-electric airplane.

An advanced-technology engine (fig. 1) is exemplified by a high bypass ratio and a high compression ratio resulting in a low core airflow. Taking bleed from the core flow upsets the aerothermodynamic cycle of the engine and is a problem for the engine designer. As the discharge section gets smaller, there is a point at which the physical installation of the same size bleed ducts into that small core section becomes a problem. Then a splitter must be used to bring the hot ducts through the engine case into the pylon. That splitter is in the bypass airflow.

The all-electric engine would not have these problems. Elimination of the bleed-core hardware, the blowout doors, and some of the transverse-thrust loads are further synergistic weight and cost benefits that derive from the all-electric airplane.

Figure 2 shows cruise specific fuel consumption (sfc) as a function of bypass ratio. With no secondary power extraction, specific fuel consumption decreases with increasing bypass ratio. Engines using conventional power extraction are limited in bypass ratio to some lower value. The all-electric can use a higher bypass ratio and thereby gets the benefit of a reduced sfc. Figure 3 shows very simply that bleed air does cost fuel and decrease energy efficiency.

Figure 4 shows that for a Pratt & Whitney energy-efficient engine (E^3) a 2.2-lb/sec bleed increases sfc by 4.7 percent (refer to 70-percent power line). That 2.2-lb/sec bleed is equivalent to about 220 hp. Plotting mechanical power extraction versus Δsfc shows an increase of only 1.3 percent in sfc for 220 hp. (This is a representative horsepower for an electric-driven environmental control system (ECS).) This comparison is the basis for saying that mechanical power extraction is much more efficient than bleed power extraction.

Engine sizing effects for a twin-engine, 150-passenger airplane with a conventional bleed system, a 50-percent recirculation system, an electric ECS with bleed deicing, or an all-electric system are compared in table I. With one engine out during a 22 000-ft hold (table IA), 53 percent of the core flow would be demanded by bleed in the conventional system. Even with 50-percent recirculation, ECS bleed would still constitute 39 percent of the core flow. Of course, with the all-electric system there would be no effect at all on the core flow. For an airplane with advanced ECS bleed and with one engine out during icing at maximum climb power at 20 000 ft and a Mach number of 0.65, there is a 12.8 percent loss of net thrust on the remaining engine, due to bleed. The change in fan diameter to compensate for this thrust loss is about 4.6 in. For the all-electric airplane the net thrust loss is only 2.6 percent, and the fan diameter change to compensate is about 1 in. For the constant-inlet diameter, constant-thrust case the turbine inlet temperature for the bleed system would increase 113 deg F, as compared with 16 deg F for the all-electric system. That is a large increase for the General Electric engine.

The weight increase for the bleed system would be 16.2 percent.

Another aspect is the temperature margin for the engine with one engine out (fig. 5). Clearly the margin between the turbine inlet temperatures for maximum climb and takeoff is much narrower for the E^3 engines than for the CF6 and other current engines. Therefore a 113 deg F rise, as shown on table I really overheats the engine. A 16 deg F rise is well within the lower band in figure 5.

Finally, there is the question of what is done with the bleed air after it is tapped. Because it is at such a high temperature during takeoff, we invariably have to consider a precooler (fig. 6). The precooler needs bypass fan air to pass through it in order to reduce the temperature of the air entering through the pylon. The ducting, valves, precoolers, pneumatic starter, and the ballooning of the nacelle (caused by placing pneumatic starters at, say, the 6 o'clock position) are all eliminated in the all-electric system.

The engine manufacturer must be concerned about the stability margins on the engine; that is, the difference between the steady-state operating line and the surge line. He must preserve this margin for throttle chops and throttle bursts and different altitudes. A typical compressor map is shown in figure 7. The one favorable aspect of bleed is that it tends to raise the surge line and drop the operating line. So bleed does increase the stability margin. Horsepower extraction raises the steady-state operating line and thereby reduces the stability margin. Neither Pratt & Whitney nor General Electric think that this is any problem, particularly when they know what the horsepower extractions will be.

In the all-electric airplane the generator is the sole source of electric power; it powers the primary and secondary flight controls, the environmentals, and the landing gear. It eliminates the need for bleed air, the high-pressure hydraulic system, and the pneumatic system. To accomplish this may require large generators in the 300- to 500-kVA class.

There are five candidates for all-electric power systems: the advanced constant-speed drive (CSD); the variable-speed, constant-frequency (VSCF) system; the VSCF:dc link; the 270-V dc system; and the direct-driven generator system. All of these systems, except the last, have been developed.

Figure 8 shows diagrams of these power generation systems. The conventional CSD system takes the variable input speed of the engine and gives a constant output speed to the generator. The generator can be optimally designed since it is driven at a constant speed. With a constant-voltage, constant-frequency (CVCF) bus some of the generator output can be converted to 270 V dc for flight controls and some can be converted to 28 V dc.

In the VSCF cycloconverter system the CVCF bus is obtained electrically. The generator must be designed to operate over the engine's speed range. Some of the output can be converted to 270 V dc and 28 V dc just as in the previous system. The VSCF:dc link approach is similar to the cycloconverter system except the power is rectified and inverted to obtain the CVCF bus. In the 270-V dc system all of the power is rectified and distributed on a dc bus. To obtain other voltage levels or ac, the power must be inverted. In the direct-drive system, as much of the power as possible is used in the variable-voltage, variable-frequency (VVVF) form. This eliminates the need to condition or regulate the power. The other types of power required, such as 400 Hz, 270 V dc, and 28 V dc are provided on a dedicated basis.

Figure 9 shows the effect of speed on power output. The power output of any rotating piece of machinery is proportional to its speed. Hydraulic and constant-displacement pumps have output proportional to speed; centrifugal pumps have output that is a cubic function of speed. Centrifugal compressors

and positive-displacement compressors like the Heli-rotor have variable-rate output, either a cubic function or linear. Piston engines have always had power output proportional to their speed, and turbine engines have power output that is a much stronger function of speed. Motors and generators are no different. The motor and generator want to produce power that is proportional to their speed. It is an unnatural function for a piston engine to put out, say, its maximum horsepower when it is idling. Everything has a speed function. A motor-generator system can be made to produce constant power as a function of speed. However, when that is done, the machines must be sized for rated power at minimum speed. As a result, the machines are oversized for any other operating speed. Providing constant power as a function of engine speed in an aircraft power system also results in oversized machines as shown in figure 10. The CSD, VSCF, and 270-V dc systems all have twice the power capability required by the mission. The crosshatched areas in those plots represent wasted power-producing capability and as a result, a weight penalty.

The VVVF system is sized for the mission; therefore it has no excess power-producing capability. There are many large loads in flight (e.g., galley and deicing) that are not present on the ground. As a result the power requirements are less and can be made to match the output at the engine's 50-percent idle speed.

Another factor in the comparison of these systems is shown in figure 11. The power flow in the CSD, VSCF, and 270-V dc systems passes through two devices; but in the VVVF system it passes through only one. As a result, the first three systems have added complexity, inefficiency, and weight to contend with. This is in addition to the larger generators required by the VSCF and 270-V dc systems.

In the transmission of power (fig. 12) the conventional system requires the use of larger gages. After transmitting 40 kVA for 75 ft, a gage change is necessary, and this increases weight. For the 200-V dc system there is some improvement and even more for the 230/400-V system and the 400-V dc system. Therefore the use of higher voltage must be considered. In the study done for NASA Johnson Space Center, Lockheed selected a 230/400-V ac system as the primary power system and doubled the frequency.

Figure 13 shows the magnetic weight of a system as a function of frequency. When the British and American advisory staffs were evaluating power systems for world-wide standardization, it took a lot of time to settle on the 400-Hz system. At one point 250-Hz systems were considered. They gave motor speeds of 24 000 rpm, which was thought to be reasonable, and the voltage level was assumed to be reasonable at that time. Now we should look at some higher frequencies. And again in the NASA Johnson study, Lockheed chose 800 Hz. An 800-Hz system would reduce electromagnetic weight about another 30 percent. That looked like a good compromise. It also permitted a 48 000-rpm maximum motor speed.

We must be careful not to denigrate variable-voltage, variable-frequency systems in an off-handed way. They are the electrical engineer's choice for motors and for many loads in the airplane. Use of VVVF systems does not abrogate use of other high-technology systems, such as advanced CSD, VSCF, or dc-link. All are used in the hybrid system. It is only a matter of how much of each of these systems is used. We want to use as much power in the VVVF form as possible. Motors and electronics can operate over a wide range of voltage and frequency with no prospect of damage if the voltage-frequency ratio (V/F) is kept constant. Sixty-Hz power can be used in 400-Hz transformers if the V/F is maintained. Even an 800-Hz system is compatible with a three-phase 200-V, 400-Hz system and existing ground supplies.

Figure 14 shows dedicated power sources derived from the VVVF system. Any type of dedicated power can be used in an airplane with the variable-frequency, variable-voltage power source. The link, for example, already uses the samarium-cobalt generator, which develops variable-voltage, variable-frequency power.

Variable voltage, variable frequency is the inherent form of power from a permanent-magnet (PM) generator. When wound-rotor machines were used, we had to make the regulator produce that type of power. Now the PM machine produces variable-voltage, variable-frequency power, and it is inherently suited to the aircraft load versus the engine speed profile. When an airplane is landing with a heavy deicing load on the wings or the windshield, you don't want all that heat being dissipated after landing. The power will automatically be reduced as the engine is throttled back on touchdown. The VVVF system is also an excellent power source for motors and transformers because of its constant V/F. And here is a critical point - during cruise, jet engines, and turboprop engines particularly, operate almost at constant speeds. This provides, in effect, a constant-voltage, constant-frequency system during most of the flight. We are trying to keep the transmission simple, to make the generator and the installation itself the simplest in the engine, and to improve generator and system reliability. We are going back to some very basic concepts in making the overall system extremely simple. The Navy and the Air Force complain bitterly about the decreasing availability of aircraft, and this is caused by the use of sophisticated electronics. We should take stock of the effect on aircraft availability of the choice of power system.

The features of the VVVF system are (1) kVA is proportional to speed, (2) minimum voltage regulation, (3) no frequency transients, (4) low harmonics, (5) low radiofrequency interference, (6) high transmission efficiency, (7) low weight, (8) low cost, (9) low maintenance support, (10) high reliability, and (11) high aircraft availability.

Figure 15 shows synchronous generator performance as a function of speed for the wound-rotor machine. The 400-Hz generator (120-V phase voltage and 120 kVA) designed for 12 000 rpm would lose almost all of the load very quickly below the threshold of 380 Hz. The reason is the square law effect of the integral excitor. The only way to sustain the power from that generator would be to decrease the voltage in step fashion. Although most system engineers do not realize it, a 400-Hz generator can be operated from 200 to 400 Hz if the voltage is controlled at the 50-percent voltage (60 V). But the power will not increase with speed unless the voltage is raised in step fashion.

How do we design a generator for a VVVF system? First, we recommend a higher per-unit voltage and a higher per-unit frequency. These values will depend on an analysis of the loads. High per-unit speeds are desirable. Second, we recommend a large air-gap generator (16 000, 24 000, or 48 000 rpm). The large air-gap machine would exhibit lower regulation, and we want to avoid the need for a regulator. This will minimize the voltage transients; the x_d, what we call the transient direct-axis reactance, will be lower. The voltage unbalance will be lower. The overload output will be potentially higher. A 75-kVA generator will produce as much as 700 A with this type of design. Third, we recommend moderate electric loading, or current density - about 12 000 A/in^2. Oversize the conductor. There is always a balance between the copper and the iron in the machine. Lower current densities will improve efficiency because there would be lower IR drop, reduced I^2R losses, and reduced unbalance. We might have to accept a slight increase in weight. And, again, let us not make a fetish of weight. The military services and the airlines would like to see a bit more reliability for a change.

Fourth, we recommend replacing high-permeability irons with Cubex, cobalt iron, silicon iron, Supermendur, or Hyperco-50. Here the desire for low weight must be balanced with acceptance of increased costs. For example, Hyperco-50 probably costs about 40 times more than a silicon iron.

Figure 16 illustrates VVVF generator regulation. We want to keep the inherent regulation of the generator small. This regulation is a function of the impedence drop, the air-gap flux density, the cross magnetomotive forces (MMF), and the load factor. We all know, from our basic training and machine design, that the reactance drop is the biggest component. It is most significant at low power factors. In other words, when the current is lagging the voltage by a large degree, IX drop has a significant effect on ΔV. Because the VVVF tends to operate at good power factors, even though the IX may be fairly large, it has a minimal effect. The IR drop is most effective in reducing the voltage. Therefore it is necessary to keep the IR drop down to have good regulation.

Table II shows the motor loads from an airplane. There is a profusion of motor loads in a large bomber, a tactical fighter, or a troop transport, there being probably over 200 motors in an airplane. All of these loads can be operated off the VVVF generator directly by using squirrel-cage induction motors. As shown in table II, almost all of the motor loads can be powered by the variable-voltage, variable-frequency system. One load that does not appear to match the VVVF output is a fan. Normally fans are required to provide a constant airflow and therefore require a constant-frequency power source.

Figure 17 shows induction motor performance. Figure 17(a) shows what would happen if you were to use constant voltage and drop the frequency. The top curve shows the normal condition of a 400-Hz motor at 200 V, a typical torque-speed curve. At 200 Hz the constant-voltage motor is able to provide a much larger torque. But as the motor's load, for instance a compressor, decreases in speed, the torque demand is actually decreasing. A motor operating in this fashion has large amounts of excess torque. On the other hand the variable-voltage, variable-frequency system (fig. 17(b)) provides constant torque capability at any speed. As a result, the torque capability and demand are better matched.

Figure 18 is from one of the studies that AirResearch did for NASA 7 to 10 years ago. It shows the weight of, say, a 25-hp brushless dc motor versus speed. At 20 000-rpm motor speed the specific weight of the motor is about 0.78 lb/hp. This excludes the electronics because the brushless dc motor has to have electronic commutation. An induction motor at the same 20 000 rpm would only weigh 0.48 lb/hp (fig. 19), and it does not require electronic commutation. This comparison indicates a significant weight advantage for the induction motor.

Another comparison that can be made concerns power regeneration in motors under an overhauling load condition. Figure 20 illustrates the circuitry required to get power regeneration in a brushless dc motor. Figure 21 shows that no circuitry is required for regeneration with an induction motor.

In summary, Lockheed is proposing a three-phase, 400-V, 800-Hz, direct drive power system. A samarium-cobalt generator would be the primary source of power. The constant V/F makes it ideal for supplying induction motors. Use of 400 V and 800 Hz provides the following: 100-V, 400-Hz, or 270-V dc ground power at 50-percent engine speed, 48 000-rpm motor speeds, lower feeder weights, lower transformer and machine weights, and lower filter weights. The system design is extremely simple and provides output power proportional to engine speed. Constant-voltage frequency or loads can be supplied by dedicated supplies.

General Electric, working with the Air Force Aeropropulsion Laboratories, developed the 150-kVA samarium-cobalt starter-generator shown in figure 22. There is no question that future generators will be large. This 150-kVA generator has quite nominally good sizes and specific weights. This generator started the RB-211 engine in 25 sec at 59° F (fig. 23). However, at -53° F the start time was longer, coming up to 6000 rpm in 90 sec.

Figure 24 shows the results of the first study Lockheed did for NASA Johnson. It indicates that a fleet of 300 all-electric airplanes, with fuel at $1.80/gallon, operated over a 16-year period would result in a $5.14 billion saving. When the added benefit of operating the airplane with reduced static stability is included, the total saving would be $9 billion. People had difficulty accepting that study. Therefore Lockheed performed another study for NASA Langley that was similar to the Johnson study but added the avionics and air traffic control areas. Some of those results are shown in figure 25. With a far-term flight control system, a far-term secondary power system, and air traffic control, a total of 44 000 lb could be saved on a 350-passenger airplane. This proved that the 23 000-lb saving projected in the previous study (on a 500-passenger airplane) was conservative. With additional innovative technologies, an even bigger saving could be realized. In a 700-passenger airplane that we looked at for NASA, doing the same thing with the breakdown (fig. 26), the weight saving could be 60 000 lb, and possibly 77 000 lb, with all of the advanced technologies. Fuel savings with the 350-passenger airplane (fig. 27) is an attractive 20 percent. The payoffs of that are such that NASA and the military should be encouraged to investigate closely the benefits that are derived from the all-electric airplane in terms of fuel efficiency, as well as all the other benefits (listed in table III).

TABLE I. - ENGINE SIZING EFFECTS - BLEED VERSUS ELECTRIC ECS
[Two-engine, 050-passenger airplane; 25 000-lb E^3 engines.]

A: CONDITION: ONE ENGINE OUT/ICING/22.K FT HOLD

	BLEED – LB/SEC			
	CONVENTIONAL	50% RECIRC	ELECTRIC ECS/ BLEED DE-ICE	ALL ELECTRIC
LB/SEC	5.5	4.3	3.1	0
% CORE FLOW	53%	39%	25%	0%

B: CONDITION: ONE ENGINE OUT/ICING/MAX CLIMB: 20K/0.65M

	ENGINE IMPACT	
CONSTANT T41	ADV ECS (BLEED)	ALL ELECTRIC
$\Delta - F_N$ (LOSS)	-12.8%	-2.6%
ΔD_T	+4.6	+1.0
CONSTANT THRUST		
$\Delta T41$	+113 °F	+16 °F
ΔWT	+16.2%	0

TABLE II. - ABILITY OF VVVF SYSTEM TO HANDLE MOTOR LOADS

	YES	NO	IFFY
• MAIN LANDING GEAR	X		
• NOSE LANDING GEAR	X		
• LG DOORS	X		
• LE SLATS	X		
• TE FLAPS	X		
• INLET DOORS	X		
• FUEL PUMPS (BOOST)	X		
• FUEL PUMPS (TRANS)	X		
• ENGINE FUEL PUMPS	X		
• ENGINE LUBE PUMPS	X		

	YES	NO	IFFY
• THRUST REVERSERS	X		
• VARIABLE WING SWEEP	X		
• TILT TAIL	X		
• CANOPYS	X		
• CARGO DOORS	X		
• PAX DOORS	X		
• FANS		X	
• FCS	X		X
• ECS	X		X
• MECHANICAL ACTS	X		

TABLE III. - BENEFITS OF ALL-ELECTRIC AIRPLANE

AIRLINES/MILITARY	AIRFRAME SUPPLIER	ENGINE SUPPLIER
• LOWER ACQUISITION COSTS	• LOWER OEW/TOGW	• BLEED PROVISIONS ELIMINATED
• LOWER DOC/FUEL COSTS	• IMPROVED PERFORMANCE	• IMPROVED SFC/ PERFORMANCE
• REDUCED MAINTENANCE/ LOGISTICS	• REDUCED ENGINEERING HOURS	• REDUCED WEIGHT
• LOWER CAPITAL INVESTMENT	• REDUCED MANUFACTURING HOURS	• TRANSVERSE THRUST LOADS REDUCED
• HIGHER PRODUCTIVITY/ AVAILABILITY	• SIMPLIFIED AIRCRAFT SYSTEMS	• NO 'CUSTOMIZED' BLEED REQS
• LOWER LIFE CYCLE COSTS	• REDUCED SYSTEMS TESTING	• SIMPLIFIED POWER PLANT
	• LOWER SYSTEM/ COMPONENT COSTS	• REDUCED INSTALLATION/ REMOVAL TIMES

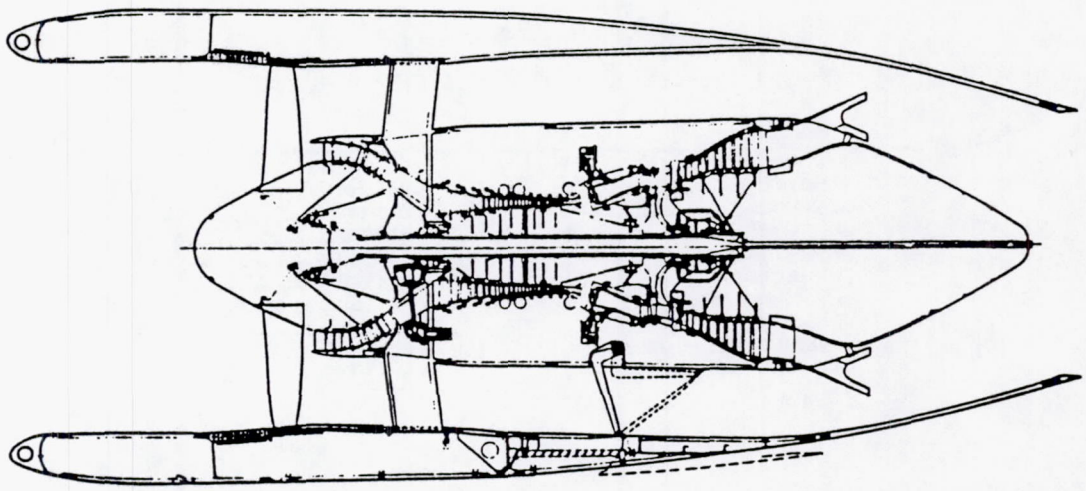

Figure 1. - Cross section of energy-efficient engine and nacelle.

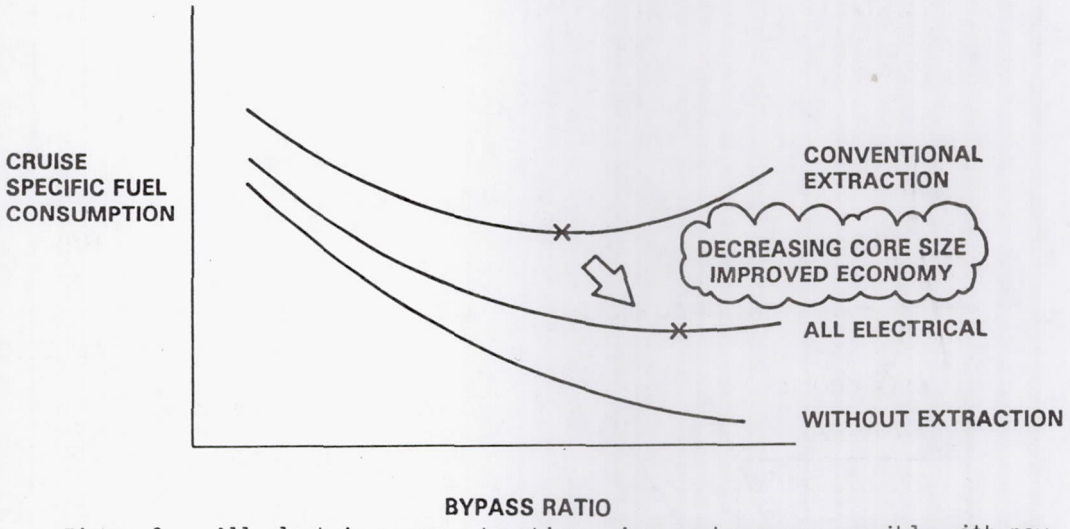

Figure 2. - All-electric power extraction - improved economy possible with new engine design.

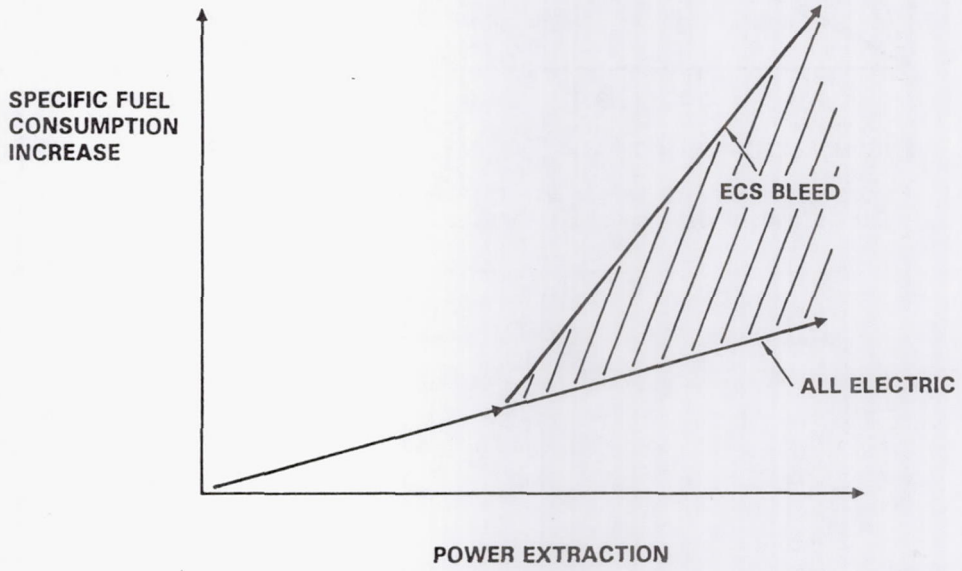

Figure 3. - All-electric power extraction - improved fuel consumption appears significant.

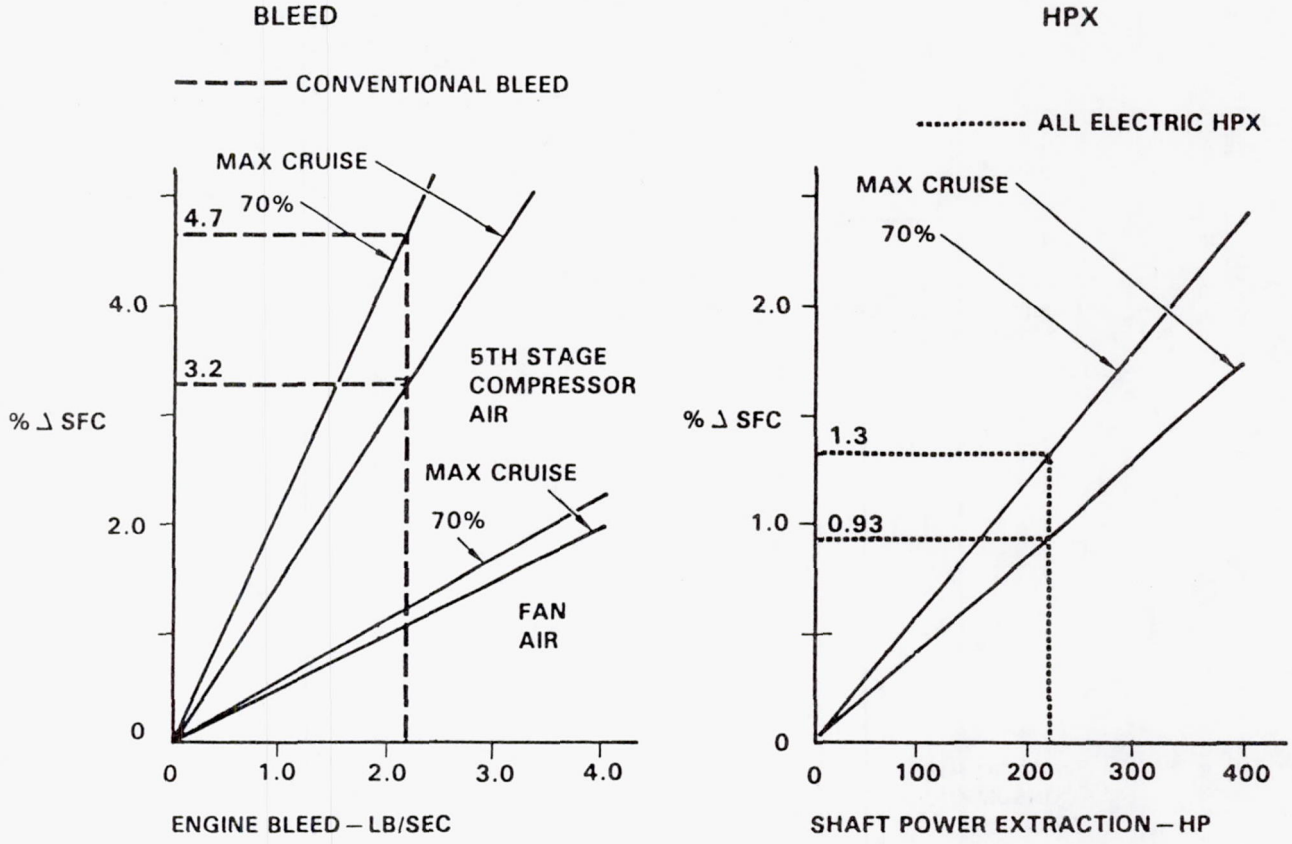

Figure 4. - Increase in sfc with 2.2-lb/sec bleed - altitude, 35 000 ft; Mach 0.8; standard day; constant thrust.

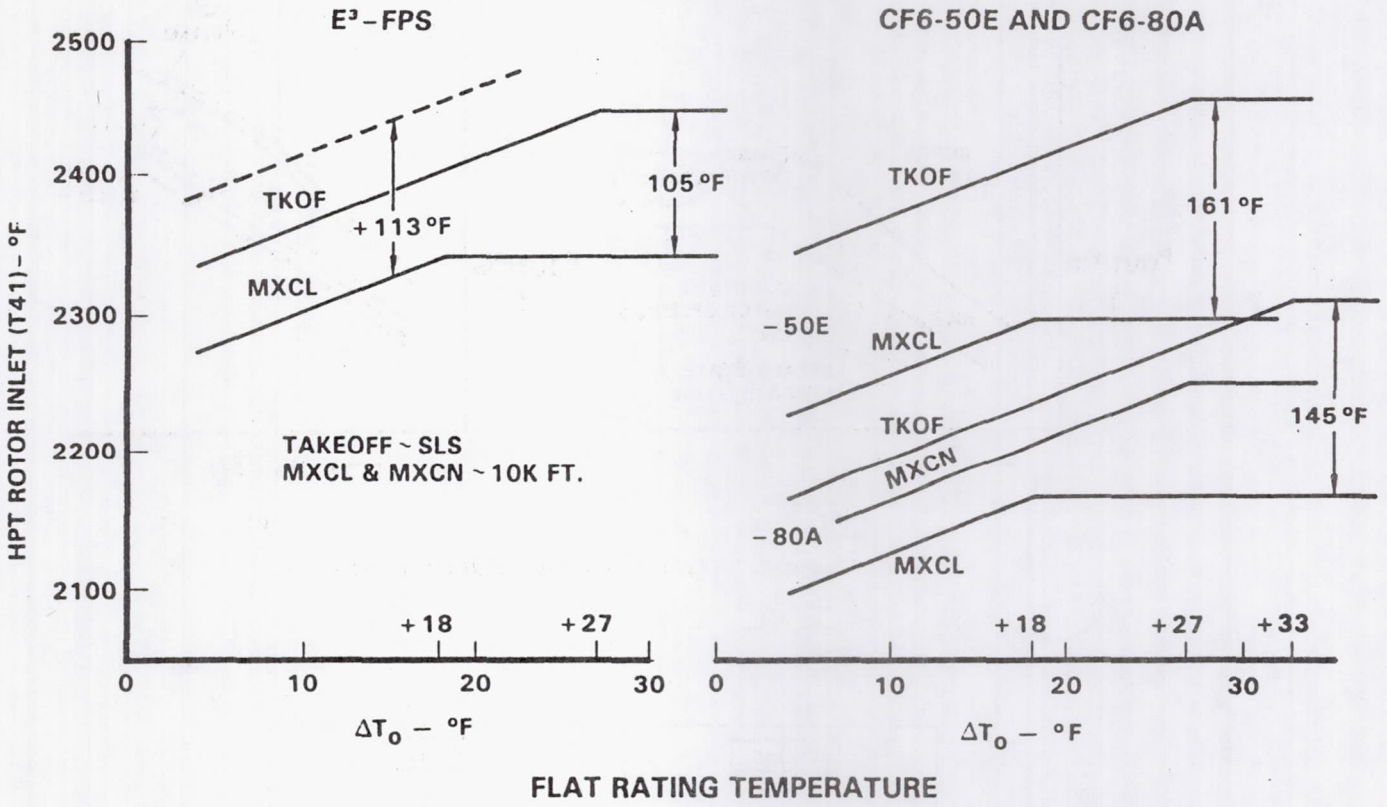

Figure 5. - Temperature margin for engine out - average engine-cycle deck.

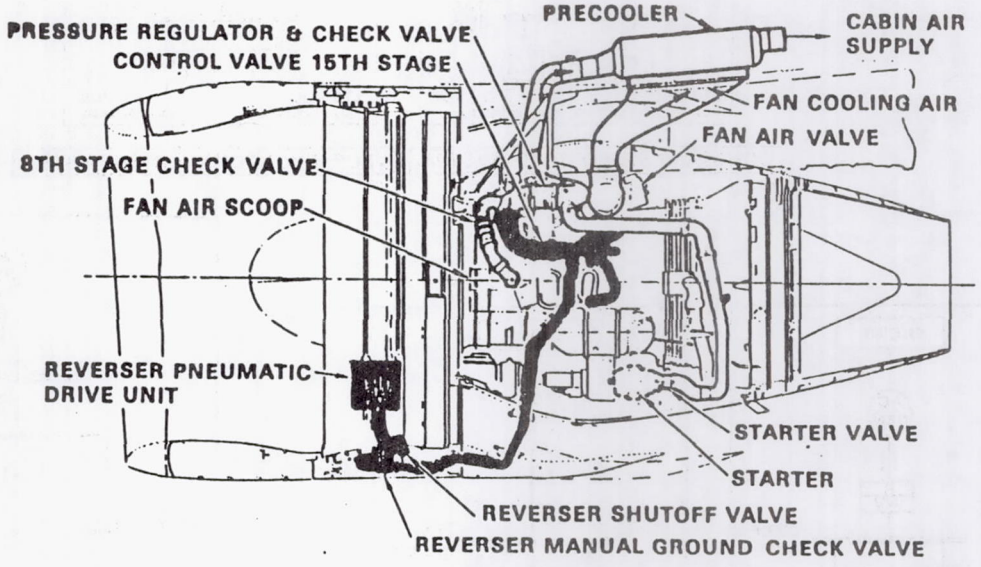

Figure 6. - Powerplant assembly - P&W JT9D-7R4.

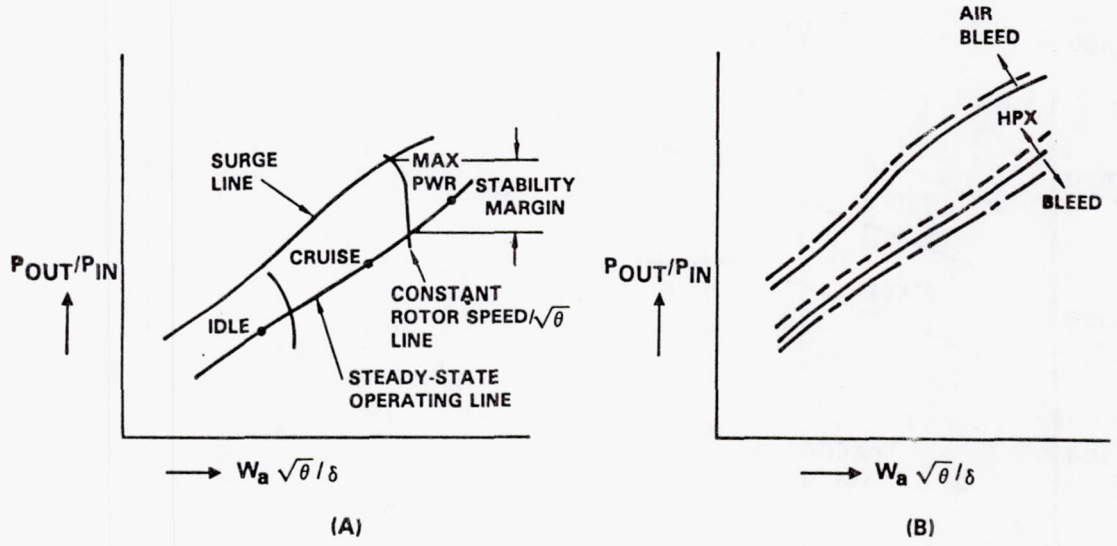

Figure 7. - Typical engine compressor map.

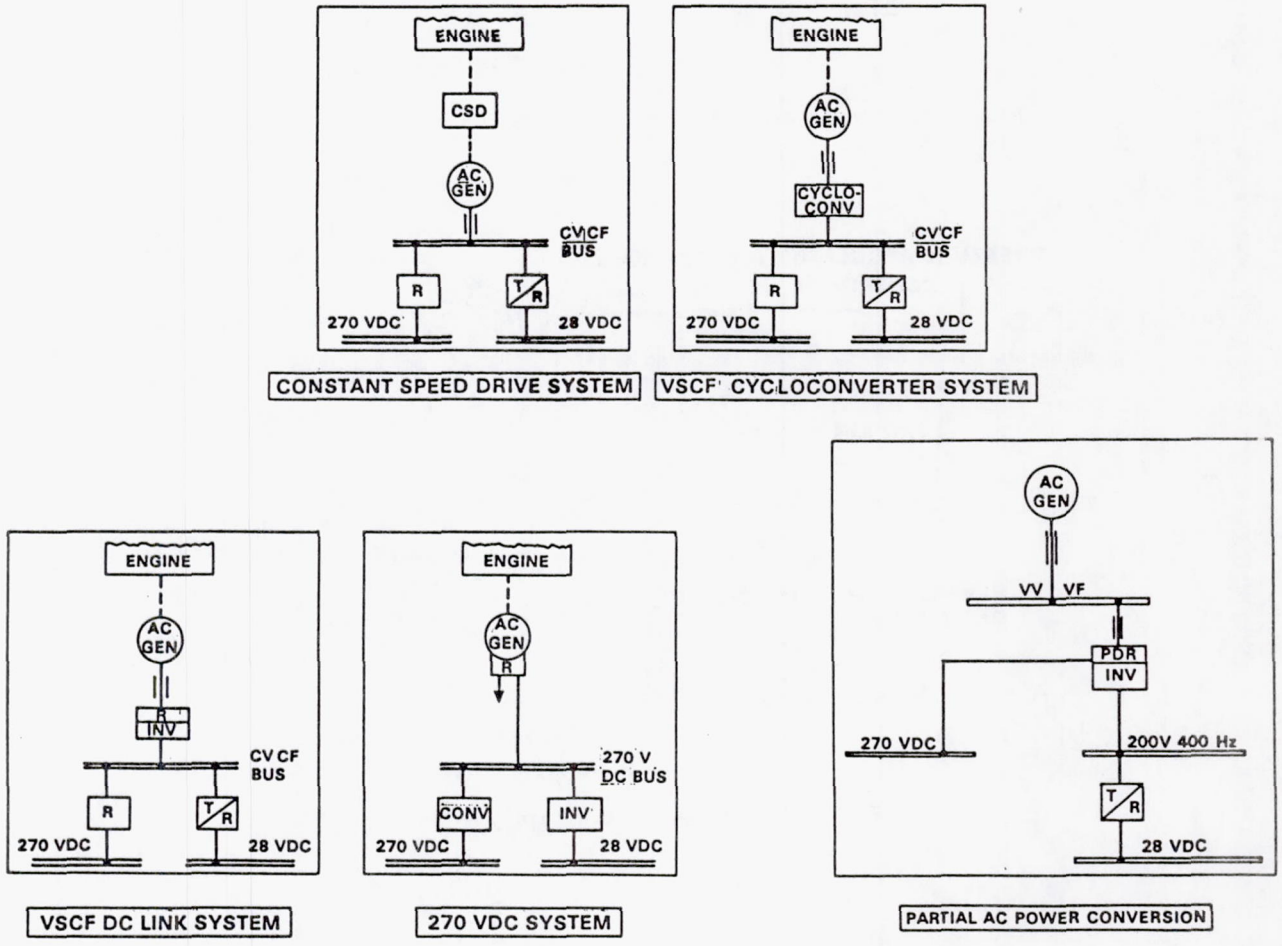

Figure 8. - Power generation systems.

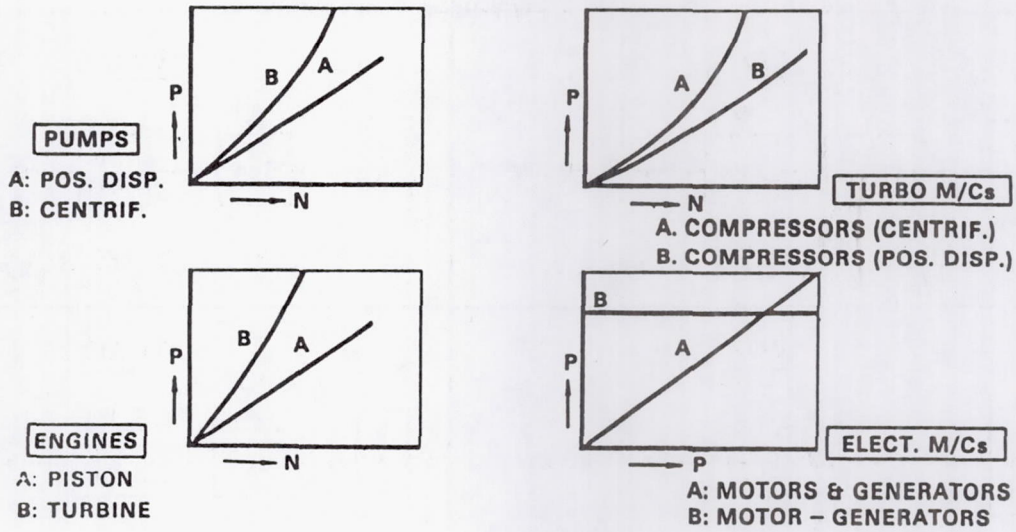

Figure 9. - Power ouput as a function of speed.

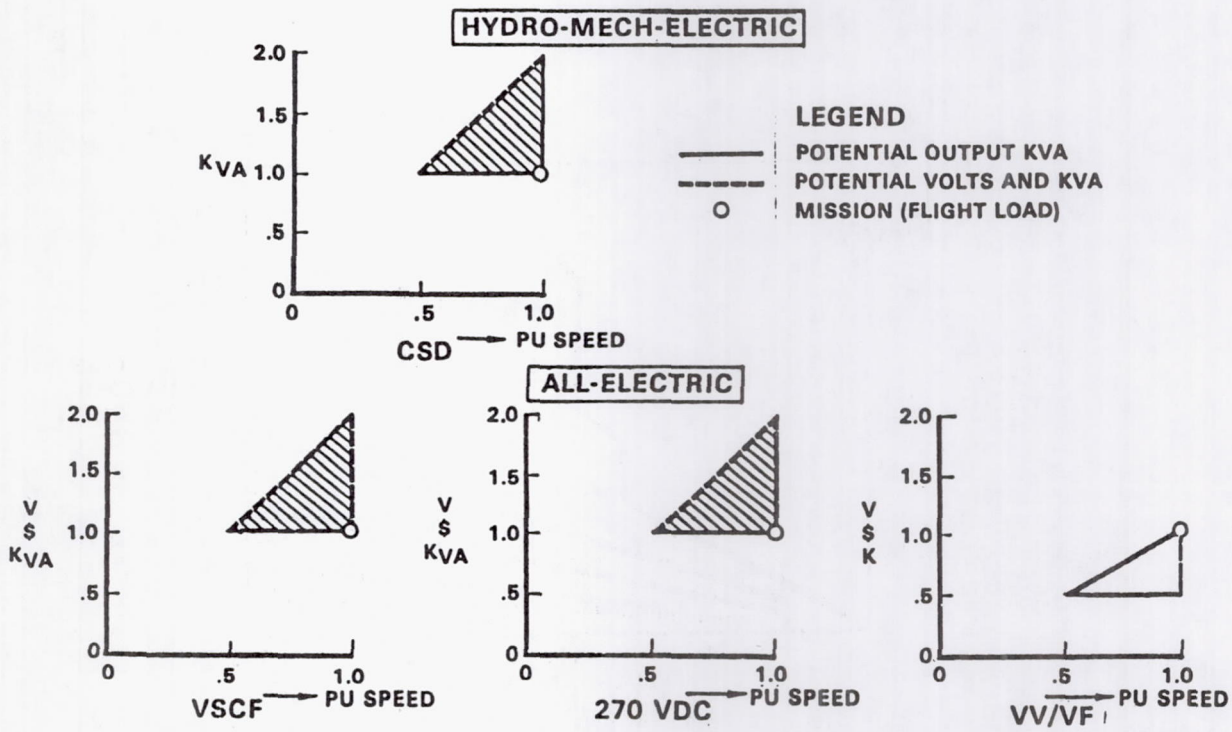

Figure 10. - Specific power system capability.

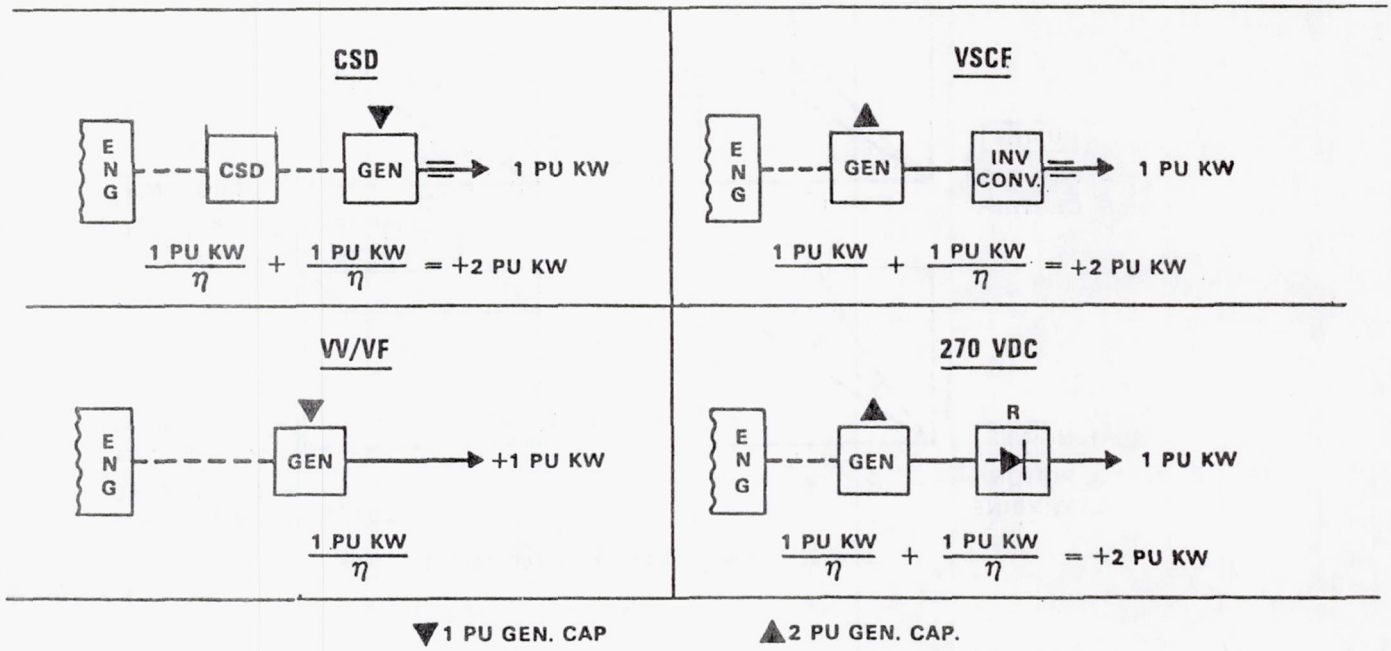

Figure 11. - Effect of speed range - based on 2:0 engine speed range.

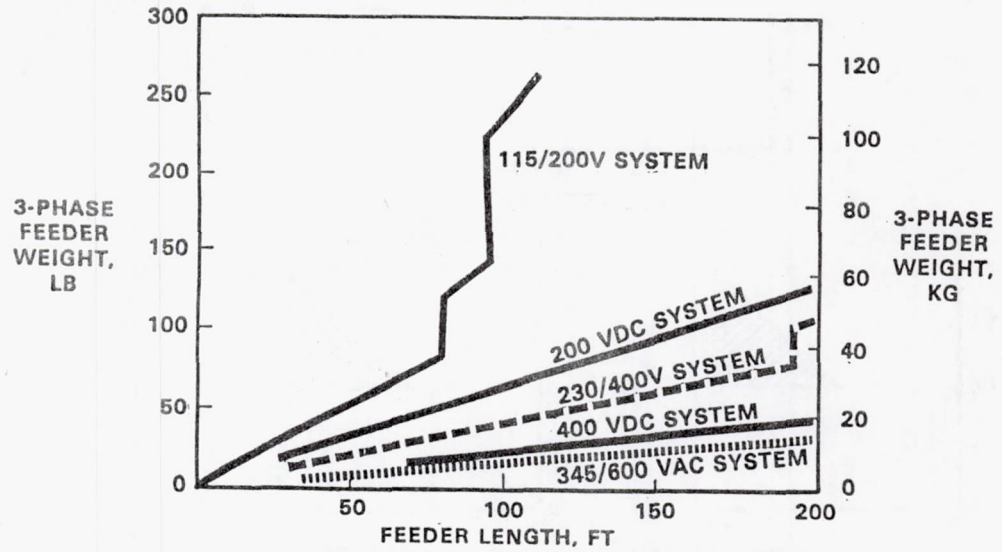

Figure 12. - Electric feeder weight as a function of transmission voltage and distance.

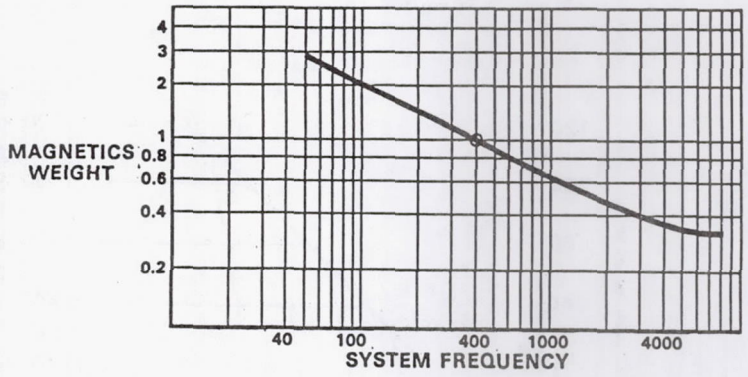

Figure 13. - Magnetics weight as a function of system frequency.

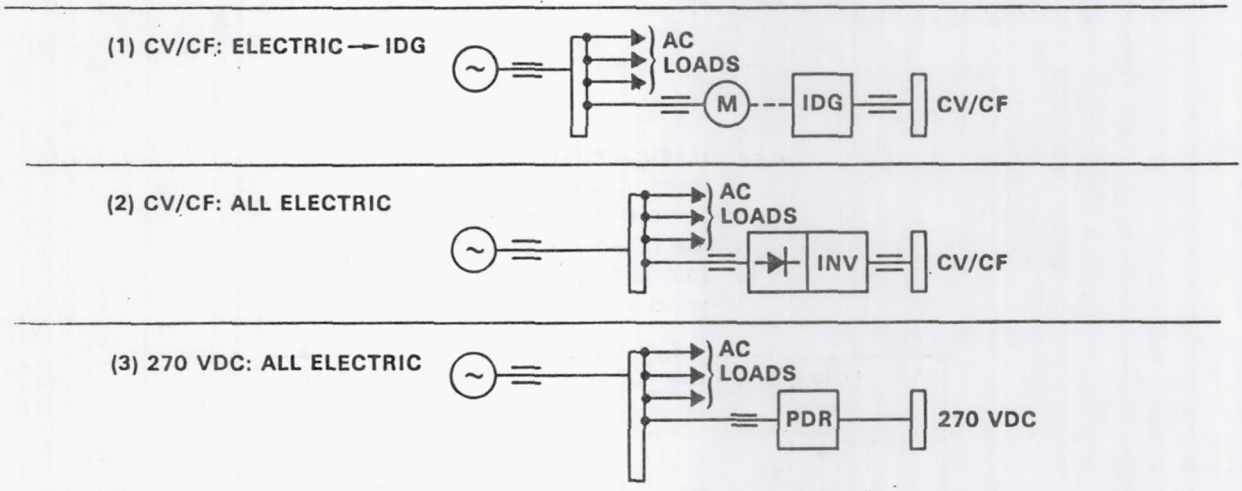

Figure 14. - Dedicated power sources from VVVF system.

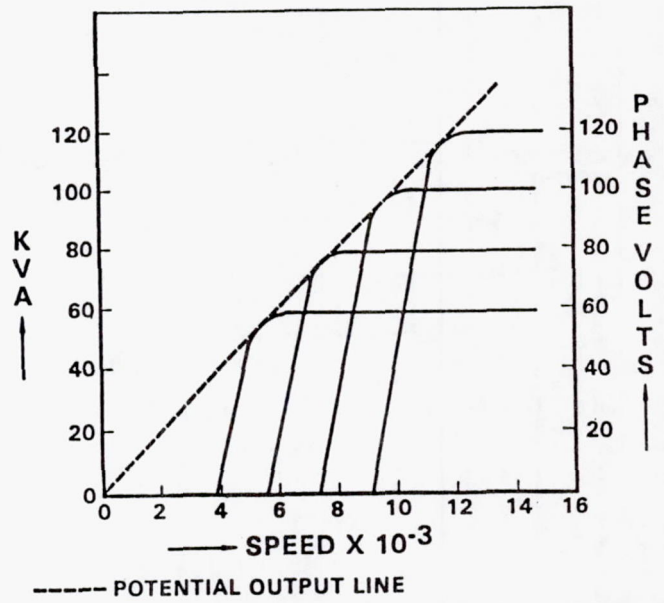

Figure 15. - Synchronous generator performance as a function of speed - brushless wound rotor.

- REGULATION A FUNCTION OF:
  - ✓ IMPEDANCE DROP
  - ✓ SYNCHRONOUS IMPEDANCE Z
  - ✓ AIR GAP FLUX DENSITY
  - ✓ CROSS-MMFs
  - ✓ LOAD POWER FACTOR

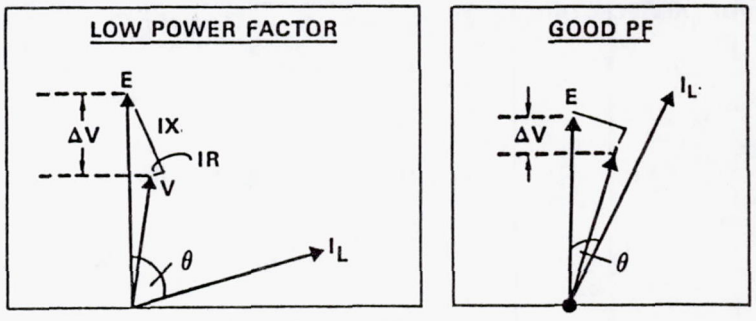

Figure 16. - VVVF generator regulation.

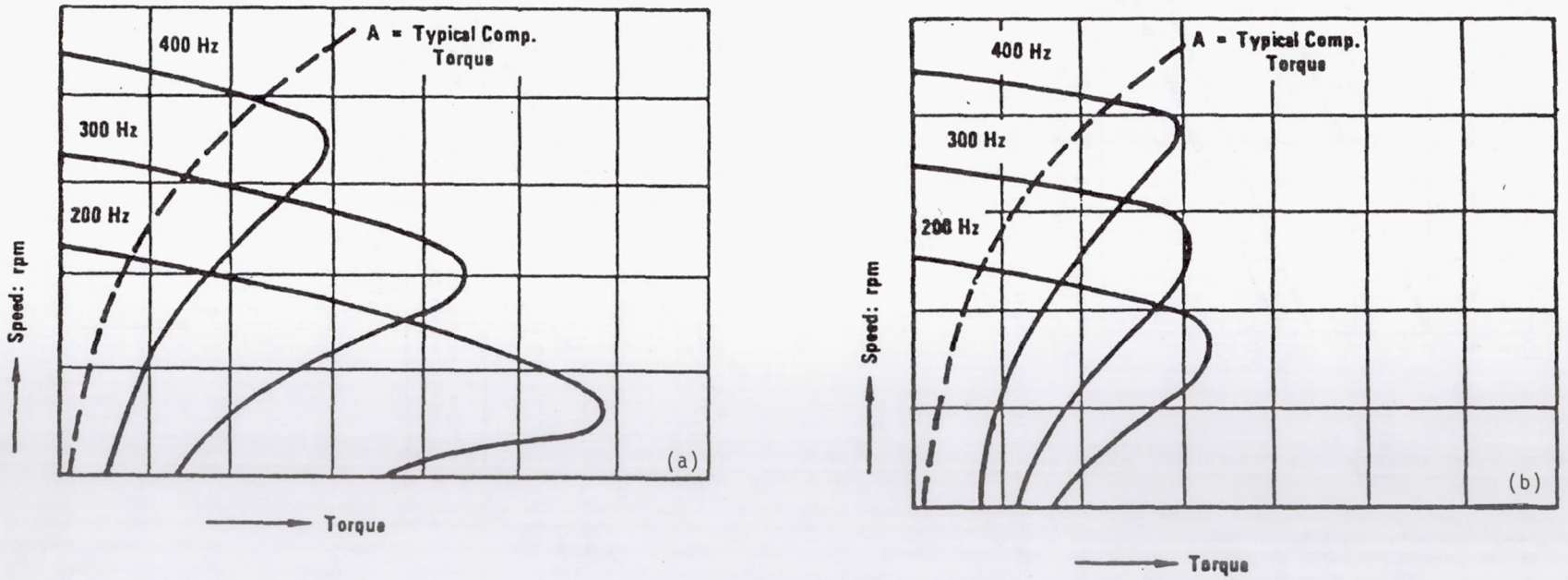

(a) Voltage constant.
(b) Voltage proportional to frequency.

Figure 17. - ac induction motor speed as a function of torque.

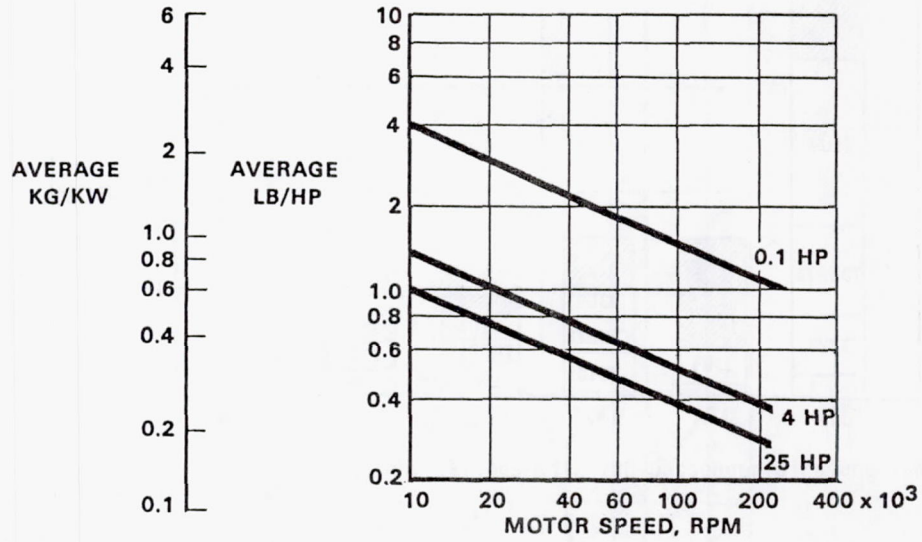

Figure 18. - Brushless dc motor weight as a function of speed - electronics weight excluded.

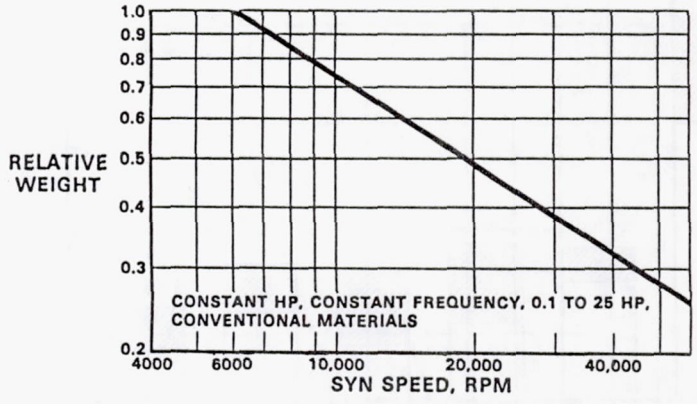

Figure 19. - Induction motor weight as a function of speed.

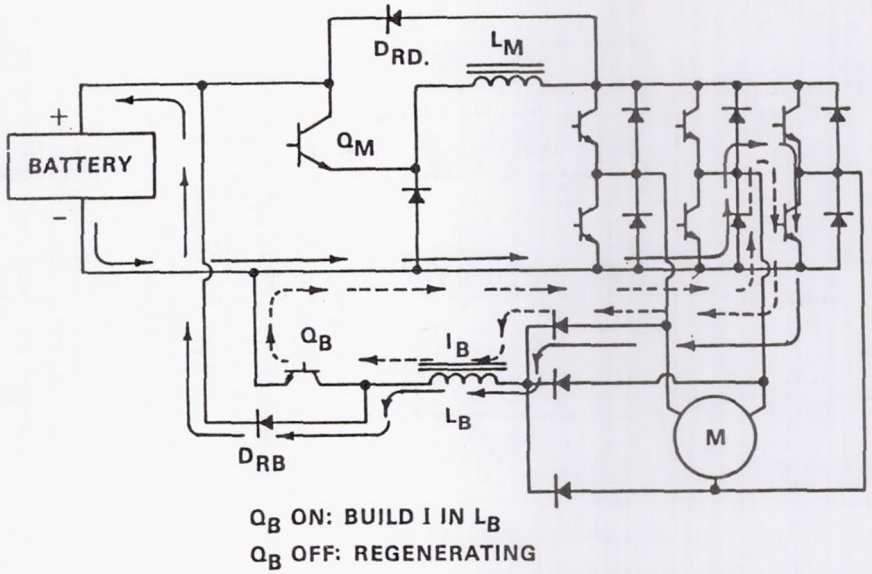

Figure 20. - Regeneration aspects of brushless dc motors.

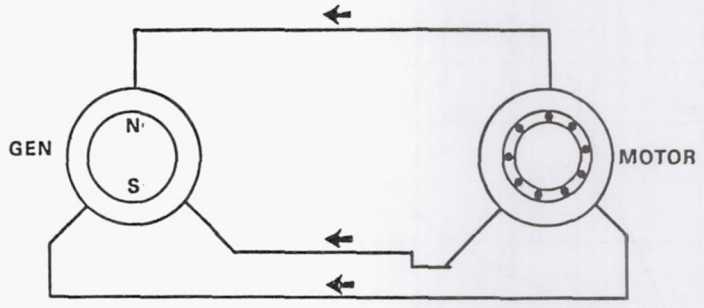

Figure 21. - Regeneration aspects of ac induction motors.

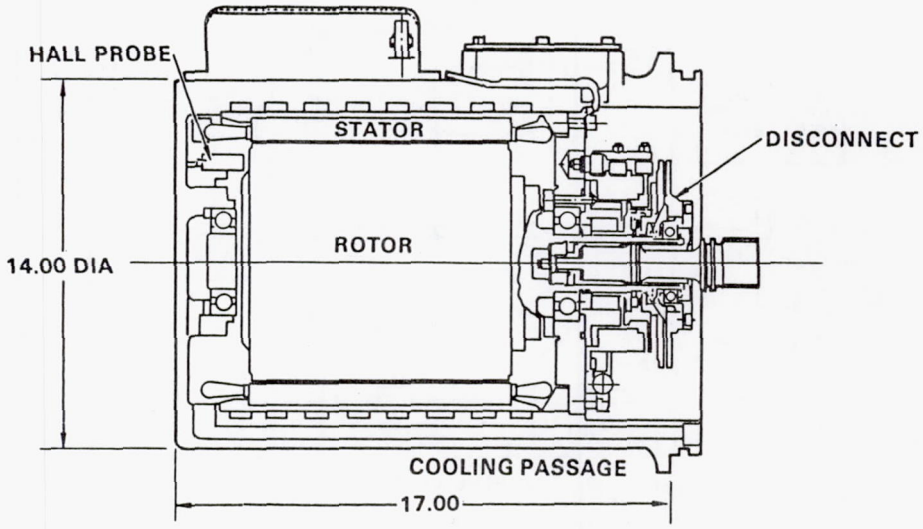

Figure 22. - Cross section of 150-kVA samarium-cobalt starter-generator.

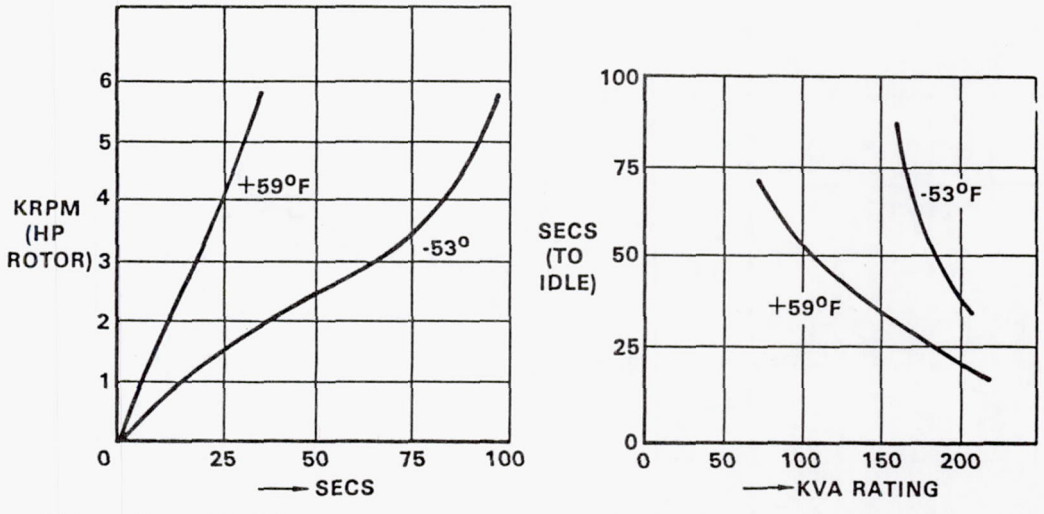

Figure 23. - RB-211 engine start times with samarium-cobalt starter-generator.

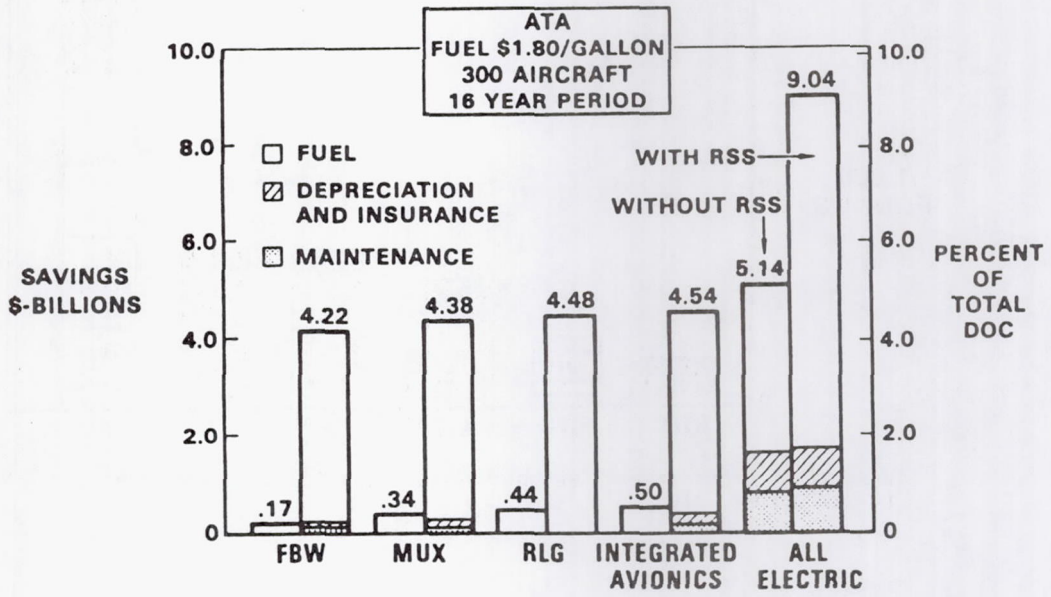

Figure 24. - Technology value of all-electric airplane.

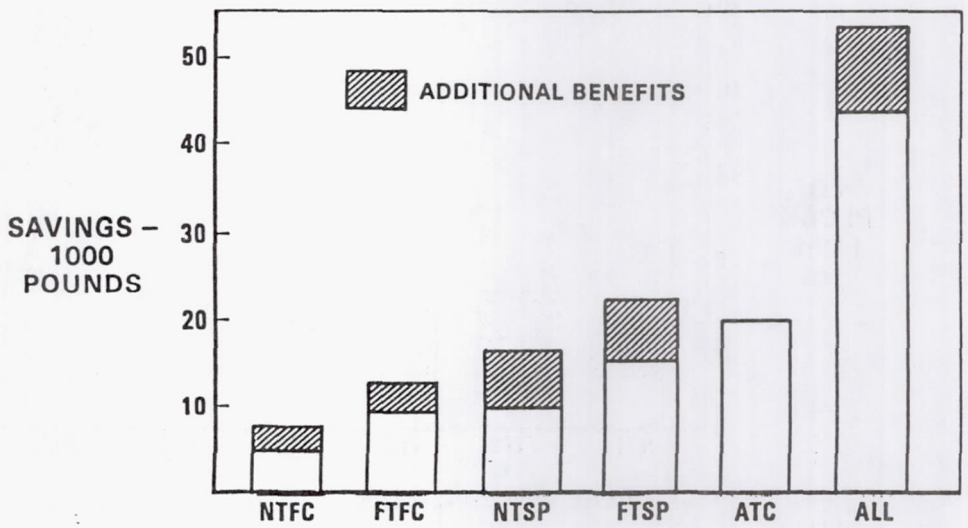

Figure 25. - Gross takeoff weight savings with 350-passenger airplane - NASA Lewis/Lockheed study.

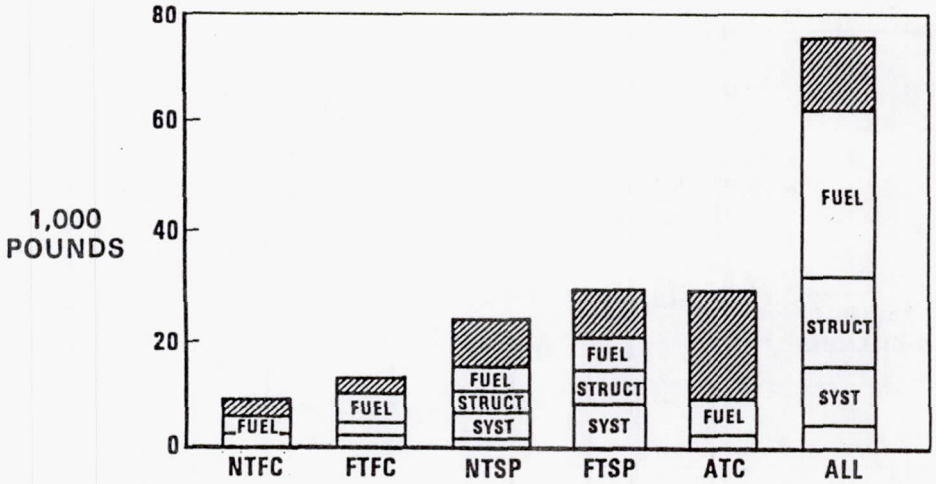

Figure 26. - Gross takeoff weight savings with 700-passenger airplane - NASA Lewis/Lockheed study.

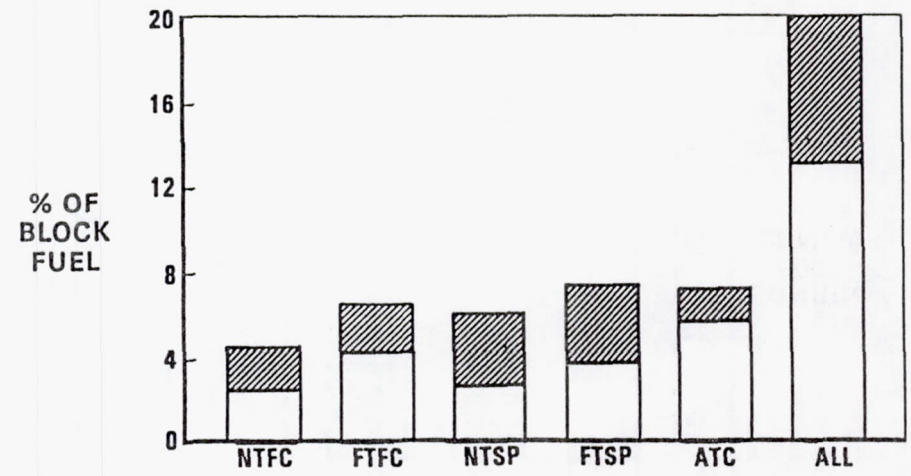

Figure 27. - Fuel savings with 350-passenger airplane - NASA Lewis/Lockheed study.

INSTALLATION OF ELECTRIC GENERATORS ON TURBINE ENGINES

Herbert F. Demel
General Electric Company
Aircraft Engine Group
Cincinnati, Ohio 45215

This discussion of the installation of generators on turbine aircraft is based on studies performed at General Electric, in particular the studies of the samarium-cobalt generator.

Contributing technologies were derived from three contacts: two from the Air Force, and one from the NASA Lewis Research Center. All three programs had two common elements: the samarium-cobalt generator, and variable-speed, constant-frequency (VSCF) solid-state technology. The generator-engine integration study was performed for the Air Force and finished in 1979. The goal was to determine the feasibility of integral generators. A study based on the Energy Efficient Engine (E^3) program was performed for NASA Lewis. It sought to define potential engine improvements that would provide performance increases. The General Electric Aircraft Equipment Division performed a development and hardware study for the Air Force on the 150-kVA permanent-magnet (PM) VSCF starter-generator. The results of this study were applied to the other two programs.

The potential advantages of an electric secondary power system at the engine level are

(1) Improved engine efficiency, by elimination of constant bleed air (electric-driven environmental control system (ECS))

(2) Enhanced reliability because of the solid-rotor PM generator-starter and fewer engine-mounted accessories

(3) Improved maintenance because there is only one type of secondary power

(4) Improved accessibility because the engine periphery is less congested and the line replaceable units (LRU) that remain are more easily replaced.

The secondary power system must be evaluated on the overall aircraft level to determine the net payoff. For example, weight added to the engine could be offset by weight reductions on the aircraft; this is particularly true in the integration of generators with the engine. The applications for the highand low-bypass-ratio engines are quite different. In high-bypass-ratio engines there is much more freedom to locate generators either inside or outside the engine without increasing the engine's frontal area. In low-bypass-ratio engines the location is more difficult because the space in the front end of the engine is smaller and also because we would like to minimize frontal area increase. Existing engines would have to be analyzed for the effect on engine dynamics. Of course, it is much easier to design an engine to incorporate secondary power systems than to incorporate them in an existing engine. A wide spectrum of possible engine configurations would have to be considered. The all-electric secondary power system that has only electric power extraction would have electrically driven accessories. A hybrid power extraction system could still use some mechanical power (e.g., mechanically driven engine accessories).

The parameters for system selection are performance, safety, reliability, maintainability, physical weight, volume, and initial and operational cost. The higher efficiency of electric secondary power systems would reduce the size of heat-exchanging systems, and result in a small improvement in the

specific fuel consumption (sfc) of the engine. Permanent-magnet generators require short-circuit protection such as a rotor disconnect. For high-speed applications the generators would also require rotor burst protection. The effect on engine efficiency in terms of specific fuel consumption would not be as important since the secondary power level is relatively small as compared with the engine power, but has to be considered. Permanent-magnet-rotor generators would have to be safe in terms of electric safety, disconnects, or other means and, in high-speed applications, burst protection. Reliability is one of the highest priorities, especially if the generator is to be integrated with the engine. Maintainability for an externally mounted generator would be similar to that for current aircraft. However, the engine would have to be designed for easy access with an integral generator. The engine physical weight might not decrease. The volume available will depend on the type of engine - high or low bypass ratio - and the power required by the aircraft. Initial and operational costs would be major trade-offs.

Two different design concepts will be discussed: the integrated generator and the externally mounted generator. Each concept has advantages and disadvantages.

Figure 1 shows a cross section of the TF-34 high-bypass-ratio engine with a 120-kVA samarium-cobalt permanent-magnet generator integrated into the front end. The generator, which also works as a starter, is placed on an extension of the high-pressure turbine shaft; the stator is mounted into the frame structure. The generator is cooled by 200° F engine oil circulated through and around the stator. To remove the generator, the engine must be removed from the aircraft and split, which is of course a disadvantage. However, because of the large dimensions and conservative design we expect high reliability, and therefore maintenance would not be required frequently. The reliability of this generator could be increased many times with improved technology. It could then be viably integrated, especially in military aircraft. Military aircraft have low-bypass-ratio engines or pure jet engines, where external placement of the generators would increase the frontal area.

To remove and replace this generator would take 4 to 5 hours. It weighs about 100 lb. Sixty kVA would be necessary to start the engine; the startup procedure would take about 23 sec, which is equal to pneumatic starting as was desired.

The possible implications of engine dynamics have been studied, and in this case it was not too great of a disadvantage to have the generator mounted on the high-pressure shaft, although it resulted in a somewhat shorter bearing life. This machine has about a 0.065-in. geometric radial gap. The side forces induced through eccentricity would be small.

Figure 2 is also a cross section of a high-bypass-ratio engine. This is the E^3 engine, the result of the Energy Efficient Engine program General Electric is conducting for NASA. This design shows two generators mounted separately on an external gearbox located in the core area. Because the core area is aft of the fan frame and between the core and the fan bypass flow duct, cowl doors would have to be opened to get to this area. The two generators are rated at 150 kVA each; the use of two generators is the result of a study for the all-electric aircraft where redundancy was required.

The accessory drive system can be made smaller by eliminating the hydraulic pumps. If electric-driven engine accessories are used, the accessory drive system could be reduced even further. Electric-driven engine accessories could be located in strategic areas around the engine for easy access and maintainability. One advantage of this would be, for example, that a fuel pump could be operated to get the flow desired without any bypass flow and with a decrease in fuel temperature.

Figure 3 is a frontal view of the area shown in figure 2, showing the location of the generators mounted side by side. The generator speed is 24 000 rpm and the high-speed fuel pump speed is 27 000 rpm. Each generator weighs about 100 lb and is 10-1/2 in. in diameter and 14 in. long. The cyclo-converters are mounted external to the engine and are readily accessible.

When the characteristics of the integrated engine-generator are compared, it is always to a base engine design that uses a conventional secondary power system.

The integrated-engine-generator study was really a matrix of three studies on three existing military engines: a large high-bypass-ratio CF6 engine; a smaller high-bypass-ratio engine, the TF-34 used on the A-10 airplane; and a high-performance, low-bypass-ratio engine, the F-404.

The study was conducted to determine the feasibility of an integrated generator-starter. The ground rules were to use existing engines, a samarium-cobalt generator, and VSCF technology. After the study one engine (the TF-34) was chosen to be studied in greater detail. One requirement was the incorporation of a safety disconnect. Since a permanent-magnet generator cannot be deenergized as long as it is rotating, we had to disconnect it either mechanically or electrically in case of a failure. An electric fuse disconnect was chosen as the best solution at that time, but others working on this problem indicate other possible ways to safeguard against a short in the generator.

The results of this study show that the highest payoff of the integrated generator-starter would be in high-performance aircraft, where it would not induce drag and therefore have a negative effect on aircraft design. The application to high-bypass-ratio engines is not as advantageous because electric power can be extracted through other means without affecting the frontal area of the engine. For example, generators could be located in the core area or in the pylon.

The integrated generator-starter would eliminate the accessory gearbox. There would not be a mechanical drive shaft extending to the outside of the engine. Therefore the engine accessories would have to be driven electrically. An all-electric secondary power system has only one source of power, in contrast to conventional systems, which have multiple sources of power. High reliability results from fewer components and conservative design. Low maintenance results from high reliability and the elimination of subsystems. The interface between the engine and the aircraft would also be simplified since only fuel and electricity are transferred between them.

The disadvantages are obvious: the center of the engine is not readily accessible since the engine has to be split and removed from the aircraft. The redundancy question had not been studied at that time, but it seems that it would be difficult to achieve redundancy in the limited space available. Development risk, as on any new system, would be present.

The objective of the study using the E^3 engines was to define the optimal location of the generator system on commercial aircraft. The selection of a twin-engine aircraft resulted in two generators per engine for redundancy. The study showed that the externally mounted generators had more advantages than integrally mounted generators for this application. The benefits of externally mounted generators are as follows: the generators can be optimized since they are not limited to engine speed, redundancy can be easily achieved by mounting two generators on the accessory gearbox, the generators are easily accessible for repair or replacement, and current-technology generators can be used. The major disadvantage of externally mounted generators is that they require a mechanical drive system and an accessory gearbox.

In summary, the integrated generator is best used in turbojet and low-bypass-ratio engines, where there is no easy way of placing generators

externally without influencing frontal areas. This would be the case for high-performance aircraft, especially military, where the adjustment of engine design on existing engines would be feasible.

The hybrid system, which would use generators and mechanically driven engine accessory systems, has advantages for high-bypass-ratio engines. The highest payoff would be on the overall aircraft level, where maximum power can be extracted and used on the aircraft, for example, for all-electric environmental control systems. The primary advantage of using samarium-cobalt generators, either integrated or external, would be their higher reliability as compared with conventional wound-rotor generators. They also require less maintenance and have lower life-cycle costs. The technology of samarium-cobalt generator starters is available now and could be incorporated into any existing engine.

In conclusion, a comprehensive study would be required to show the advantages and disadvantages of all-electric secondary power on the overall system level. This multidimensional matrix would have to include military as well as commercial aircraft. The electric power requirements for engine-out and peak-power conditions would have to be established and matched to the redundancy required. The electric system question of ac versus dc or the hybrid system would have to be addressed, and the development of end-user equipment would have to proceed. Studies at the engine level would include the evaluation of the location and design of secondary power systems, comparing integrated and externally mounted generators. Systems have never been compared on an equal basis: they have been compared with the baseline only, but not against each other with the same ground rules. Advanced engine accessory development would have to continue, since fuel and lubrication pumps are components that actually size the accessory gearbox because of their frontal area and mounting requirements. The use of electric power on the engine level would have to be investigated, including systems for thrust reversal and geometric actuation as well as new methods of electrically anti-icing engine nacelles. New technologies must be pursued to provide protection against stator shorts in permanent-magnet generators. Split machine construction would allow redundant integral generators to be built.

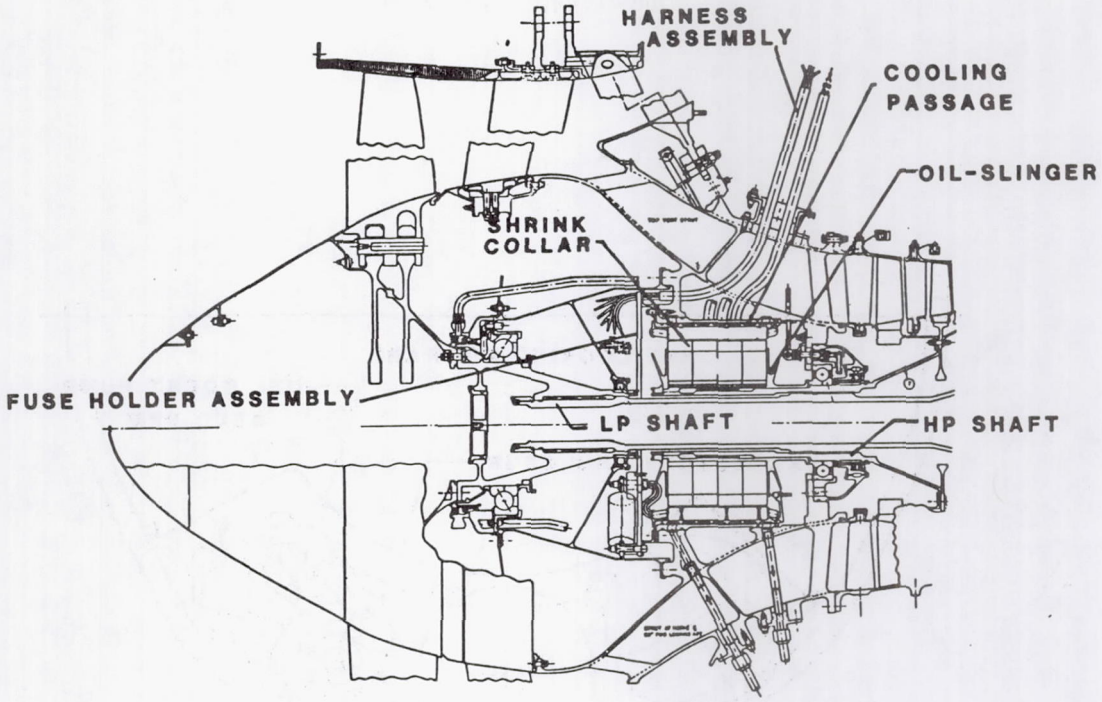

Figure 1. - 120-kVA, permanent-magnet integrated engine starter-generator.

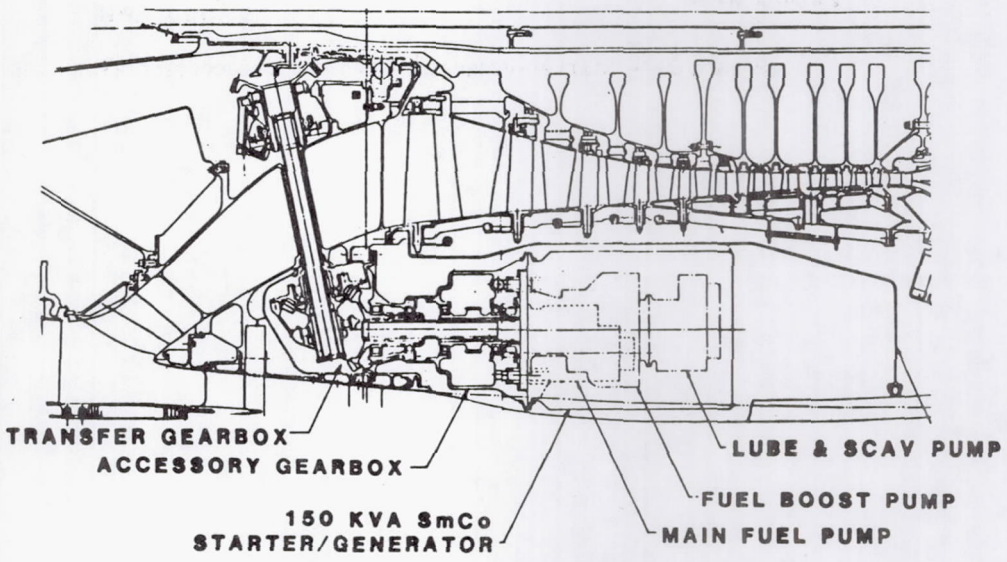

Figure 2. - Gearbox-driven starter-generator.

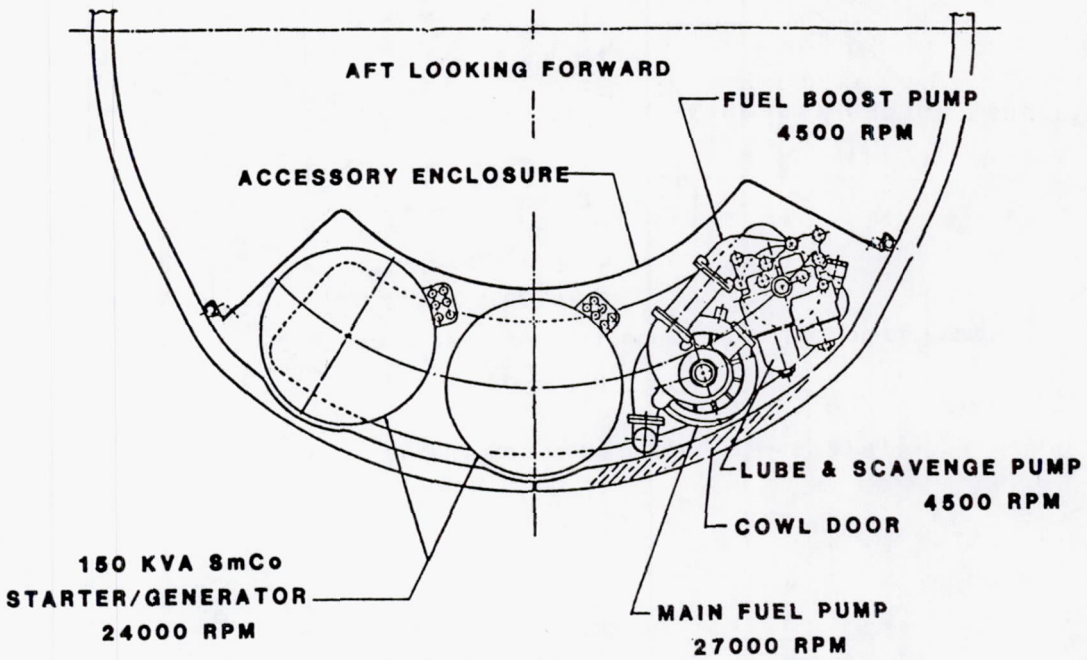

Figure 3. - Starter-generators and engine accessories.

PERMANENT-MAGNET MOTORS AND GENERATORS FOR AIRCRAFT

E. F. Echolds
AiResearch Manufacturing Company
Torrance, California 90509

This presentation covers electric motors and generators that use permanent magnets to develop their flux fields. Most of the discussion is on the rotating machinery, but aspects of control and power conditioning are also considered. The discussion is structured around three basic areas: rotating machine design considerations presents various configuration and material options, generator applications provides insight into utilization areas and shows actual hardware and test results, and motor applications provides the same type of information for drive systems.

ROTATING MACHINE DESIGN CONSIDERATIONS

Permanent magnets can be used in a variety of configurations. Most applications are radial air-gap designs. The high-energy permanent magnets (fig. 1) that are in use today have very low tensile strength. Structural support is typically accomplished through the use of a shrink sleeve, which assures a continuous compression load on the magnets at all rotational speeds and temperature extremes. The sleeves can be of nonmagnetic or bimetallic material. The rotor with the radial magnets is the lowest cost construction method. Construction using tangential magnets allows a larger number of poles and a higher flux density since two magnets feed one pole piece.

The development of permanent-magnet alloys combining rare earths and cobalt, principally samarium cobalt, over the last 10 years has produced materials of more than twice the energy product of earlier magnets like AlNiCo 9. In addition, the coercive strength, or resistance to demagnetization of samarium cobalt, makes it ideal for motor and generator applications. It can work effectively into relatively large air gaps and will not permanently demagnetize when subjected to overload currents. The demagnetization curves are shown in figure 2 for two grades of samarium cobalt and AlNiCo 9 for comparison.

High-speed or high-performance electromagnetic machinery operating with samarium-cobalt magnets will often be limited in design by the ability to cool the stator assembly. Air cooling is the simplest method of stator cooling. Air can be directed through the machine, over the housing, or both. A more sophisticated method is liquid cooling by means of a housing heat exchanger. The maximum effectiveness is reached in a "wet" winding configuration, where the coolant is brought into direct contact with the stator copper. Stator cooling types are shown in figure 3. Fluid cooling is more effective than air cooling, and the liquid-cooled housing is the most reliable of the cooling methods shown.

To optimize a machine for any application, a large number of variables must be assessed. AiResearch Manufacturing Co. has developed a program, called BIGMAG, that is capable of operating in either a motor or generator mode. When given the desired machine power and speed, the program can optimize the design around any desired parameter, such as weight or efficiency, while operating within prescribed design constraints, such as machine reactance or rotor tip speed. The output from the program provides a complete description

of the stator and the rotor as well as the loss distribution and input and output power at a variety of load conditions.

GENERATOR APPLICATIONS

The voltage and frequency of a permanent-magnet generator are directly proportional to speed. Most generator applications require operation over a significant speed range. Since the output is at constant volts per hertz, some of the unconditioned power can be used directly. Where regulated and conditioned power is required, ac, dc, or a combination can be achieved with power semiconductors. The control can be done either at the generator or at the utilizing equipment, depending on the transmission considerations and the environment or space available in the specific situation.

A samarium-cobalt permanent-magnet generator built by AiResearch for the Naval Air Development Center is shown in figure 4. The power-conditioning electronics, in brassboard form, are packaged beneath the rotating machine. Thyristors are used for the control capability over a 9000- to 18 000-rpm generator speed range.

The 8-pole rotor assembly shown in figure 5 displays the significant features of a tangentially oriented magnet configuration. The steel pole pieces have holes for weight reduction. The rotor support sleeve is beryllium copper. Extensions of the nonmagnetic center hub complete the rotor shaft.

One of the key features of the permanent-magnet generator is the transient voltage response to step load changes (fig. 6). There is no electromagnetic field time constant to delay the flux field correction. The inherent regulation of the machine controls the maximum voltage excursion on application or removal of load. The terminal voltage is electronically corrected by changing the control thyristor firing angles to achieve the desired steady-state voltage. The test data taken on the 270-V dc generator show the unit capability in comparison with specification requirements under a full 100-percent step load change.

The dimensions and weights of the 45-kW, 270-V dc generator are shown in figure 7. The generator includes a quick disconnect, which is essential in a permanent-magnet machine. Because the generator excitation cannot be removed in case of an internal fault, it is necessary to disconnect the generator from the drive pad in order to interrupt the fault current. This disconnect has been tested and therefore represents actual sized hardware. The final package size for the control electronics is also represented in the figure. The weights shown in the figure represent a design of 3 or 4 years ago and could be reduced in a new design.

One interesting area of application for the permanent-magnet rotating machine is its dual use as a main engine starter and generator. With more sophistication added to the control logic, the power thyristors can be used to commutate the unit as an engine starter motor and then to switch mode when the engine is up to speed to provide aircraft electric power. AiResearch performed a design study for a 150-kW starter-generator. The higher frequency results in a smaller machine, but for large aircraft transmitting power at high frequency presents voltage drop problems. For smaller (fighter type) aircraft with shorter cable runs, the high-frequency machine might still be attractive. For commercial airliners and large military aircraft, the low-frequency option appears to be preferable. The high- and low-frequency options are compared in table I. It should be noted that the high-frequency, high-speed machine has a significant advantage in electromagnetic weight over the low-frequency, low-speed machine.

Permanent-magnet motors provide considerably more flexibility than conventional 400-Hz motors. Because there is no inherent speed constraint, the motor can be matched to the drive requirement rather than forcing the driven equipment off optimum design. When full-power output from a pump, fan, or compressor is not required, the drive motor speed can easily be reduced by the control electronics to reduce energy consumption. The controller also permits limitation of inrush currents on startup. Even current limited, the starting torque of a permanent-magnet motor tends to exceed that of an induction motor of equivalent size. The disadvantage is that the power is handled through solid-state devices. The ultimate goal is energy savings.

The application of permanent-magnet motors in aircraft systems is quite broad and includes variable-speed compressors, primary and secondary flight controls, variable-speed fuel pumps, variable-speed fans, and other actuation and motor systems. Key areas are those in which the high-speed and variable-speed features are useful. In addition, permanent-magnet motors are ideal for servoapplications in flight control systems. The high torque-to-inertia ratio and control characteristics are ideal for servosystems. General actuation and drive motor uses such as landing gear actuation and valve position drives are also suitable.

Motor converters can use thyristors, transistors, or a combination of the devices in their power-switching circuits. In general, for higher power levels, thyristors become more attractive because a single thyristor can handle more power than a single transistor. Paralleling of devices has been done successfully, but it does affect system complexity and cost. A good example of a thyristor system would be a double-bridge arrangement where the variable-speed generator output would be rectified, voltage would be controlled by the first three-phase thyristor bridge, and the motor-switching commutation would be done in a second thyristor bridge. For power applications of 60 hp or less, transistors can be used with only two transistors per leg. Control and commutation in one bridge circuit would be provided by modulating the six transistors in the system when they were conducting during their commutation function. Transistors, because of their superior control characteristics and growing power-handling capability, will be used in most aircraft converter applications.

AiResearch continuously monitors state-of-the-art power transistors suitable for power-conditioning equipment. Internally funded research programs allow for both testing and evaluation of such devices. As part of the research programs, AiResearch has designed and built a special high-power transistor test console, shown in figure 8. The console provides an effective tool for complete device characterization in both chopper and inverter modes of operation. This is a necessary effort to determine how transistors will operate in the final circuit.

Performance testing has been completed on a 26-kW, 26 000-rpm samarium-cobalt motor driven from a dc line. The control approach uses a series transistor chopper feeding a thyristor bridge. The efficiency of the motor is shown in figure 9 over a 4:1 speed range and a 4:1 shaft torque range. The excellent efficiency characteristics show the potential for energy savings where variable speed is desired.

AiResearch has also developed a primary flight-control actuator under a contract from the Air Force Flight Dynamics Laboratory at Wright-Patterson Air Force Base. This design, shown in figure 10, uses two samarium-cobalt motors, since a completely redundant system was required. The motors are six-pole machines with tangential magnet orientation operating at 9000 rpm at the full 270-V dc input. The performance characteristics of this actuation system are

summarized on the figure. The motor alone is approximately 3.5 in. in diameter and 8 in. long.

High horsepower can be achieved in relatively small machines if high-speed operation is acceptable. However, small motors operating at high speeds introduce significant cooling considerations. In addition, the maximum horsepower that can be achieved at a given speed is limited by the rotor diameter and the rotor length-to-diameter ratio because of critical speeds and other dynamic problems. Figure 11 illustrates a safe operating region for machines designed with radial magnets and shows the general characteristics of the power limitation with respect to speed. The absolute power limit for a given speed is dependent on application details. This curve can be improved by using other design techniques; however, the basic message is that for large horsepower machines, the speed will be limited.

TABLE I. - COMPARISON OF 150-kW GENERATOR-STARTER MOTORS

	HIGH FREQUENCY	LOW FREQUENCY
SPEED	18,990	14,250
POLES	8	4
FREQUENCY	1266	475
DIAMETER	5.81	8.27
LENGTH	9.38	12.88
ELECTROMAGNETIC WEIGHT	50.88	84.50

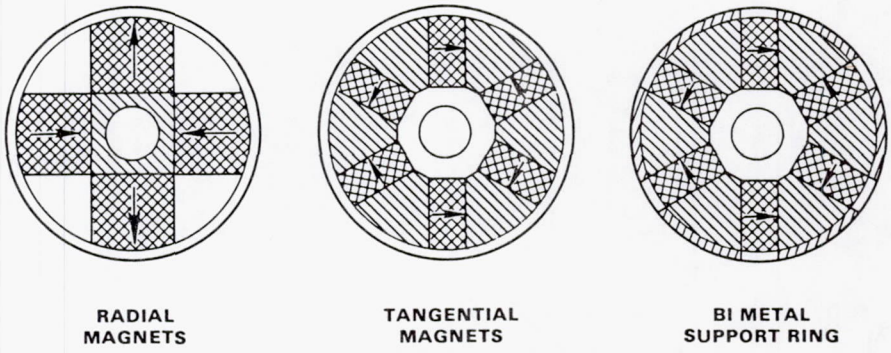

Figure 1. - Permanent-magnet rotor types.

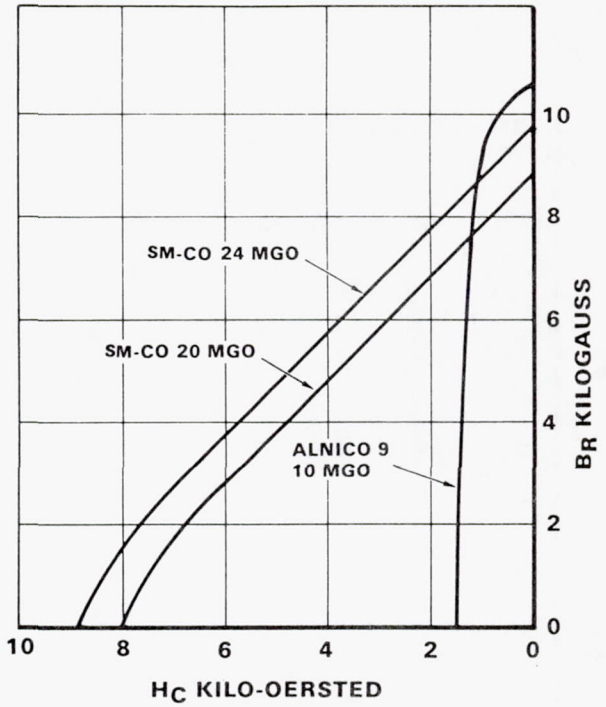

Figure 2. - Permanent-magnet alloy improvements.

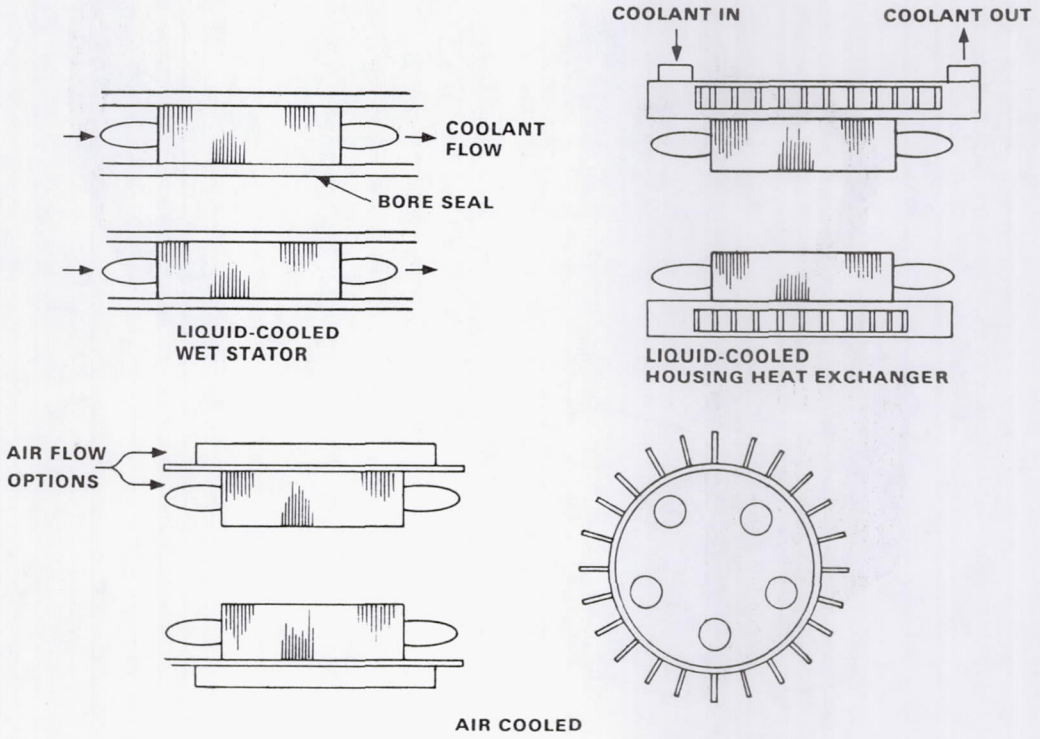

Figure 3. - Stator cooling types.

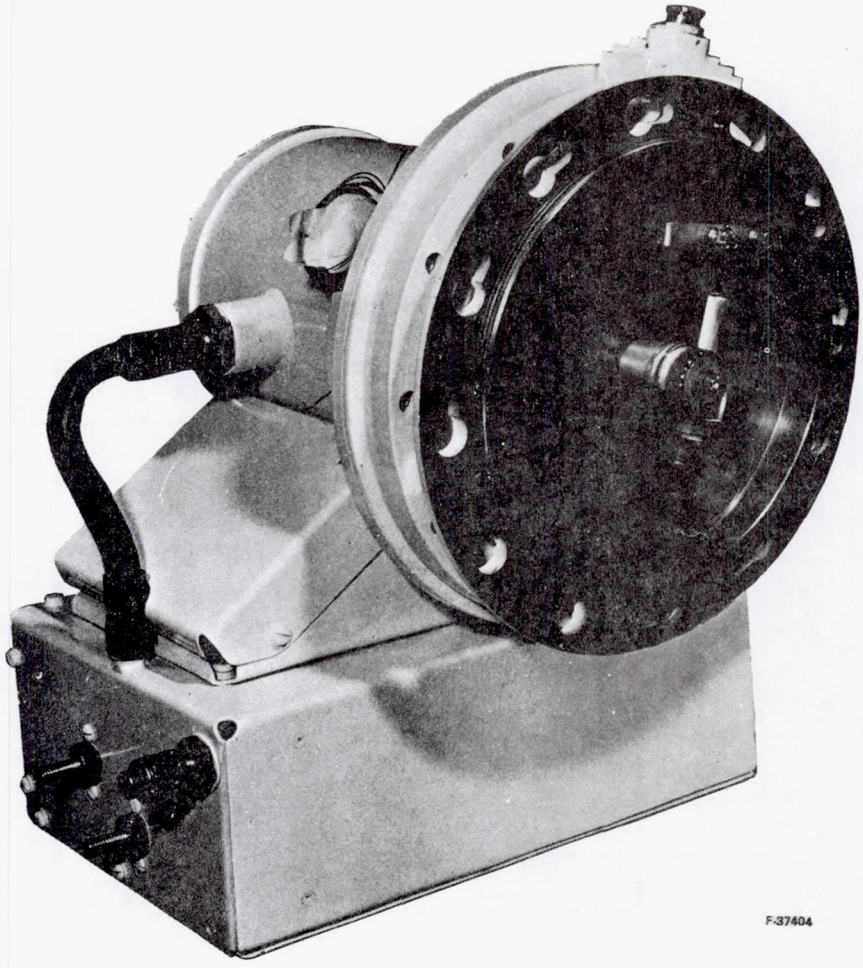

Figure 4. - 270-V dc, 45-kW permanent-magnet generator.

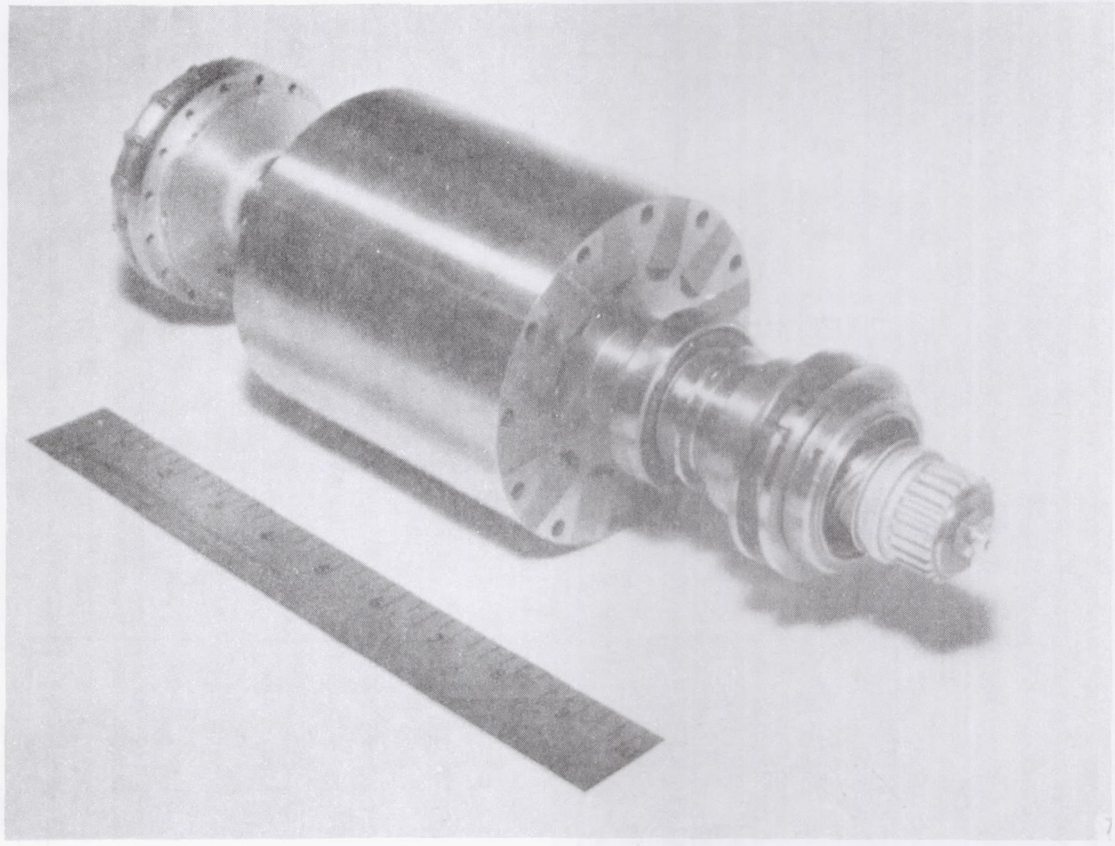

Figure 5. - 270-V dc generator rotor assembly.

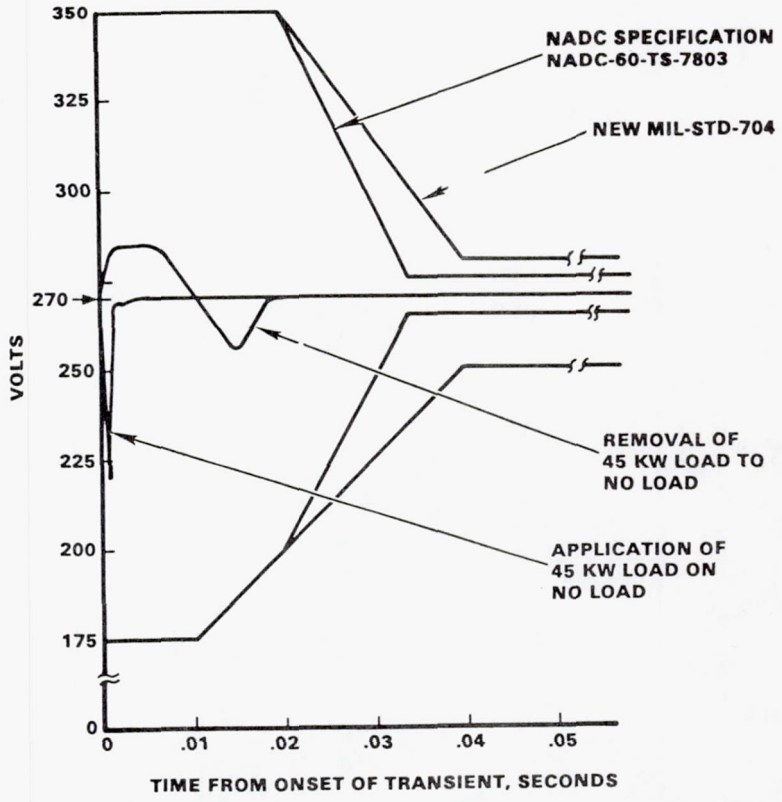

Figure 6. - Transient response of 270-V dc generator system.

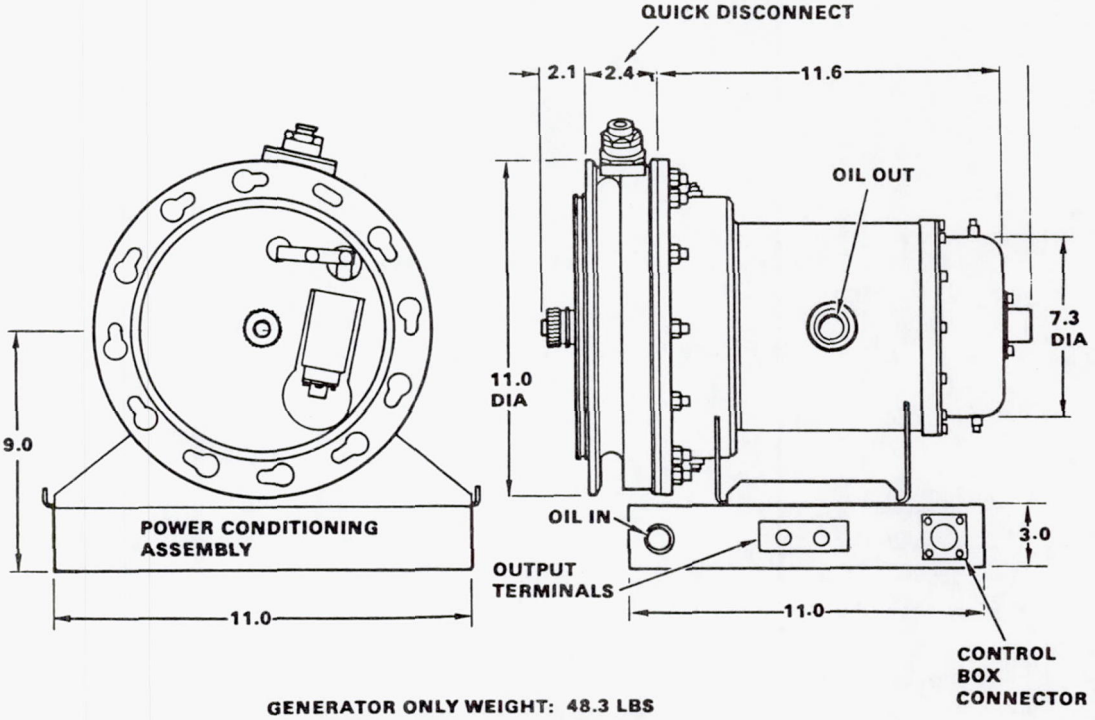

Figure 7. - 270-V dc, 45-kW generator and power conditioner assembly.

- DESIGNED AND BUILT BY AIRESEARCH
- EFFECTIVE DEVELOPMENT TOOL

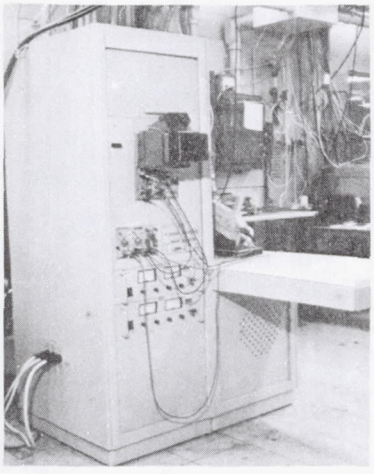

TEST CAPABILITIES

- DEVICE CHARACTERISTICS
- COMPLETE CHOPPER EVALUATION
- COMPLETE INVERTER EVALUATION

RATINGS

- 0-600VDC @ 300A INPUT
- 0-2000ADC LOAD CAPABILITY
- 0-100KHZ FREQ CAPABILITY

Figure 8. - High-power-transistor tester.

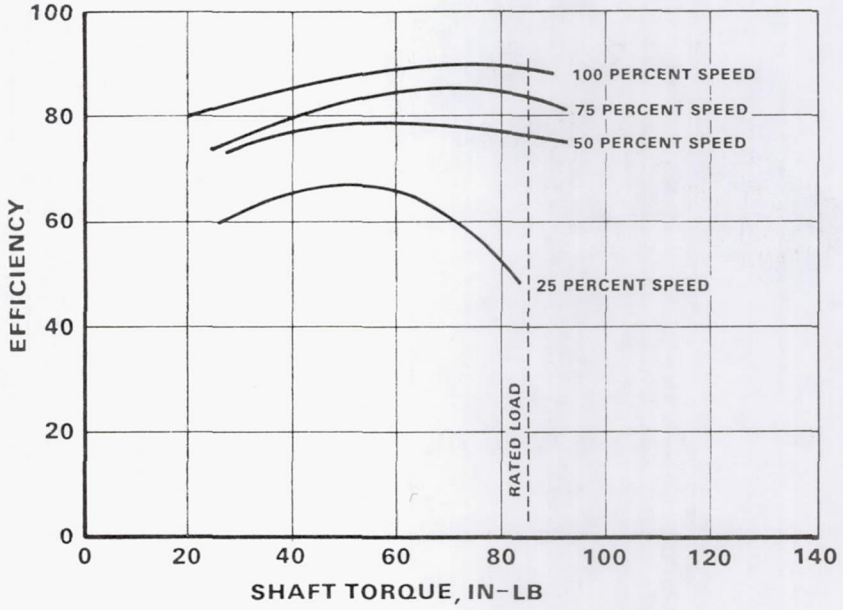

Figure 9. - Typical performance of variable-speed motor.

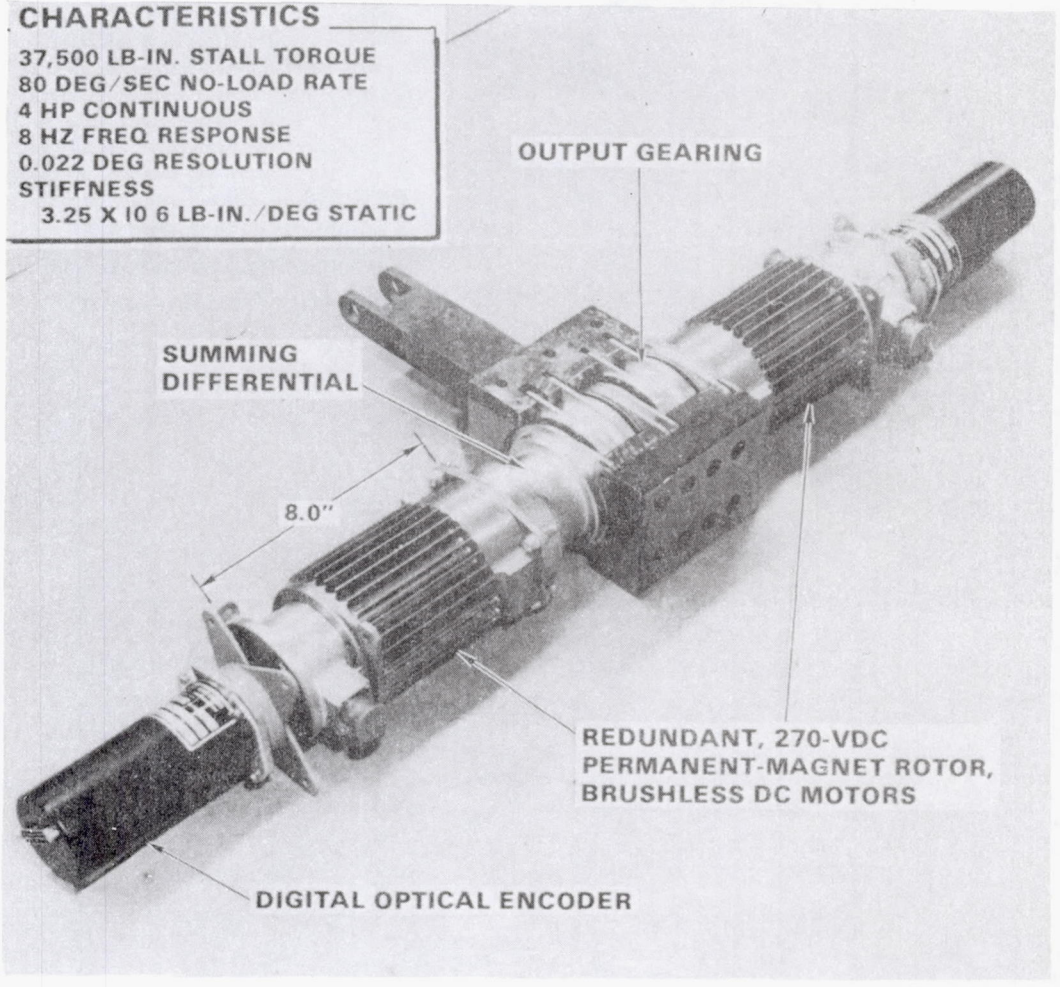

Figure 10. - EMA flight-configured hingeline actuator.

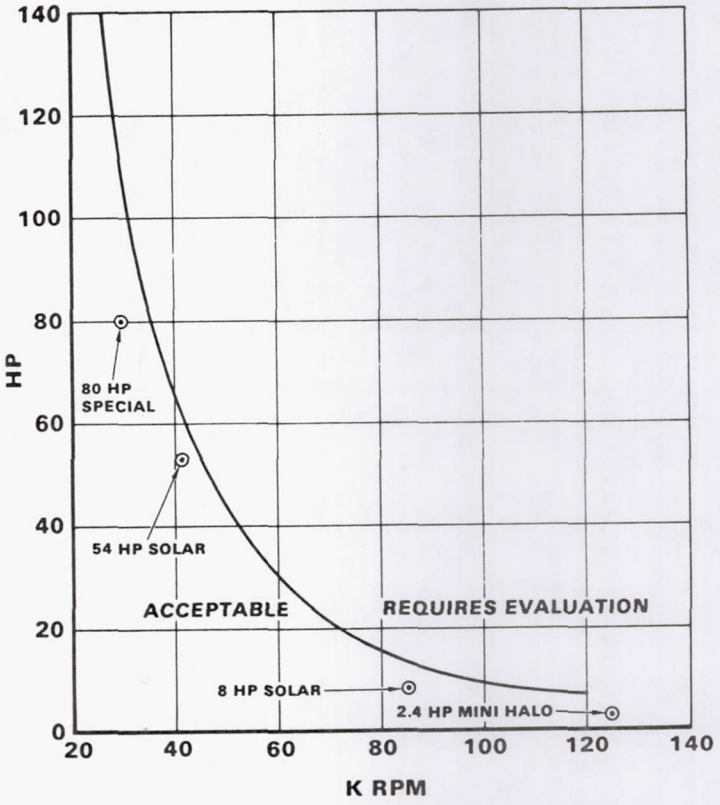

Figure 11. - Horsepower as a function of speed (radial magnet orientation).

APPLICATION OF ADVANCED MATERIALS TO ROTATING MACHINES

James E. Triner
National Aeronautics and Space Administration
Lewis Research Center
Cleveland, Ohio 44135

In discussing the application of advanced materials to rotating machinery, we will cover the following topics: the torque-speed characteristics of ac and dc machines, motor and transformer losses, the factors affecting core loss in motors, advanced magnetic materials and conductors, and design tradeoffs for samarium-cobalt motors.

Figure 1 shows the torque-speed characteristics for various types of motors. The series motor has a high starting torque for very low speeds. The shunt motor and the permanent-magnet motor can be used as control devices for many of the components within the all-electric airplane. Many of the characteristics of the shunt and permanent-magnet motors can be duplicated with a wound-rotor motor by varying the rotor resistance.

Figure 2 compares the losses within a 5-hp, three-phase motor and a 15-kVA transformer. The basic difference is that the motor has friction and windage losses in addition to core (iron) loss and I^2R loss. However, as the load on the transformer increases, the copper loss (the I^2R loss) predominates. Similarly in the motor the I^2R loss is the major loss at higher loads.

Figure 3 shows weight and efficiency as functions of frequency for a 50-kVA transformer. It illustrates the advantage of using higher frequencies. Of course, from 60 Hz to 400 Hz there is a dramatic change. At slightly higher frequencies, around 1000 Hz, there is another significant drop in weight. However, at too high a frequency, the weight gain is not that significant. The peak efficiency for this particular design is at 5 kHz. This contradicts the old adage of copper loss and iron loss being the same. For this particular design the copper and iron losses are the same at 10 kHz, which is not the optimum efficiency point. The figure shows that significant tradeoffs can be made in designing both transformers and motors for advanced all-electric airplanes.

Figure 4 shows some of the factors affecting core loss. For a simple two-segment commutator (on the left), if we look at one phase, it is essentially a pulsating square wave; if we combine a number of elements (lower left), we get a high-frequency voltage ripple. This would translate into a loss within the material. The diagrams on the right show that under the pole faces, without any rotor current, the magnetic field is constant. However, when current is applied in either a generating or a motoring mode, the distribution of flux density tends to increase in one pole face and to decrease in the other pole face as the machine goes through a cycle. This would limit the flux density at which the motor or generator could be operated.

Figure 5 shows this even more significantly. The current flowing in the rotor actually decreases the flux density in the left side of the pole pieces (shown by path 2). Through path 1 the flux density is essentially constant. Through path 3 the current actually enhances the flux density within the machine. Therefore flux density changes linearly across the pole face as current is applied. At higher flux densities magnetic saturation is approached, as shown by the flattened tip of the flux waveform. This would result in additional core loss.

Figure 6 compares three materials with the properties required in rotating machinery. A fairly high flux density is required to get the windings of the machine smaller and reduce the accompanying I^2R loss. Armco M-4 steel is presently being used in most rotating machinery. The new Metglas 2605 significantly reduces core loss to about one-fourth that of M-4. However, this may not be a fair comparison because the M-4 is much thicker than the Metglas - 4 mil as compared to 1 mil. Another material, Supermendur, also has high flux density characteristics, but its losses are greater than those of M-4 even though it is thinner. Thus from a loss standpoint, M-4 is better than Supermendur at this point. However, Metglas may be a formidable contender as a new material for rotating machinery.

Metglas has been applied to some transformer designs with a significant reduction in iron loss (fig. 7). Also because of the reduction in iron loss and the higher flux density characteristics, the copper loss could be reduced. Since this is a phenomenon that increases with the square of the current, the reduction in copper loss is fairly significant.

Lewis is investigating a new material called intercalated graphite. Table I shows that intercalated graphite can achieve the same levels of resistivity as copper and aluminum at one-third of the weight. It also has a much higher strength than copper, so that it could be integrally wound as part of the structure of either the rotor or stator of the machine. This should significantly reduce the weight and increase the strength of the motor.

Samarium-cobalt motor studies have been performed for electric vehicle research. Figure 8 shows the percentage of total weight for the different components for a current and two advanced samarium-cobalt motor designs. The current motor weighs 1.7 lb/hp. Using the Metglas, a lighter material with less loss than the iron presently used for motor designs, significantly reduces the percentage of total weight of iron while keeping the same amount of copper used in the current design. The specific weight decreases to 0.74 lb/hp. Incorporating intercalated graphite fibers changes the weight distribution again. Here intercalated graphite would also be used in the frames. The weight of the machine is again significantly reduced, to 0.57 lb/hp. These machines operate at 8000 to 9000 rpm. Raising the operating speed to 20 000 to 26 000 rpm would decrease specific weight further, to around 0.31 lb/hp. It appears that quite a bit of design work could be done in this area to support an all-electric airplane motor.

In summary, the major motor losses are core (iron) loss and I^2R (copper) loss. With Metglas, core loss can be reduced by a factor of 4, and Metglas is lighter than conventional electrical steels. Intercalated graphite conductors may have resistivity equal to that of copper at one-third of the weight. Also high-speed samarium-cobalt motors have high efficiency and low specific weight. Therefore significant latitude is available in designing rotating machinery for an all-electric airplane.

TABLE I. - CHARACTERISTICS OF INTERCALATED GRAPHITE AS COMPARED WITH COPPER, ALUMINUM, AND GRAPHITE

Material	Density, g/cm^3	Resistivity, Ω-cm	(Figure of merit)$^{-1}$, m	Cost, $¢/cm^3$
Copper	8.9	1.8×10^{-6}	16	19.6
Aluminum	2.7	2.8	7.6	
Graphite	1.7	40	68	
		[a]1.8	4.9	
Intercalated graphite	2.7	[b]2.8	7.6	10.5
		[c]6	16	

Material	Density, g/cm^3	Strength, psi	Ratio of strength to weight	Thermal expansion, $°C^{-1}$
Copper	8.9	32×10^{-3}	3 600 psi	16×10^{-6}
Aluminum	2.7	16×10^{-3}	6 000 psi	14
Steel	7.9	600 000	76 000	7
Intercalated graphite	2.7	$(300 \text{ to } 1000) \times 10^3$	$(180 \text{ to } 600) \times 10^{-3}$	~1

[a]Possible.
[b]Needed to compete with aluminum.
[c]Needed to compete with copper.

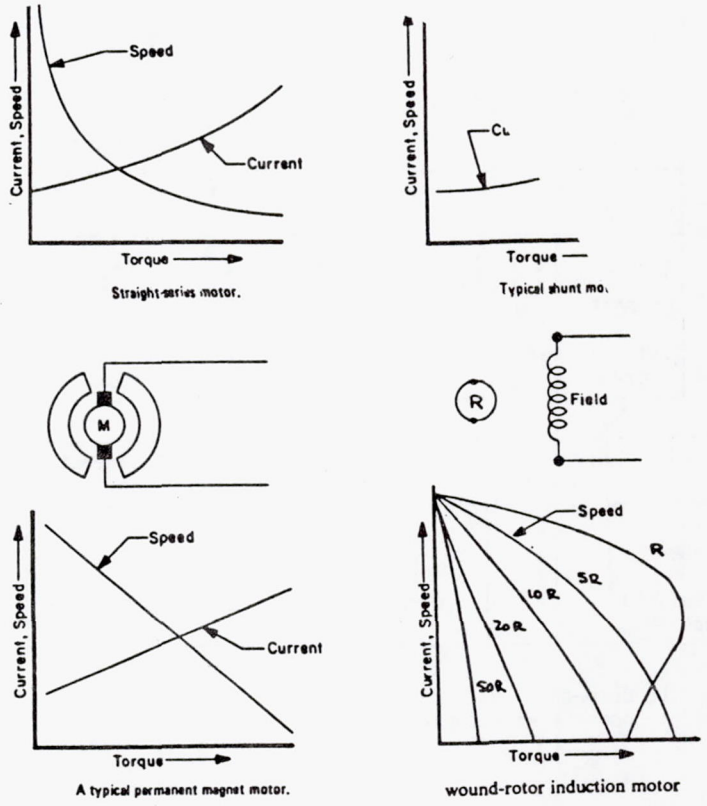

ɴe 1. - Torque-speed characteristics for ...

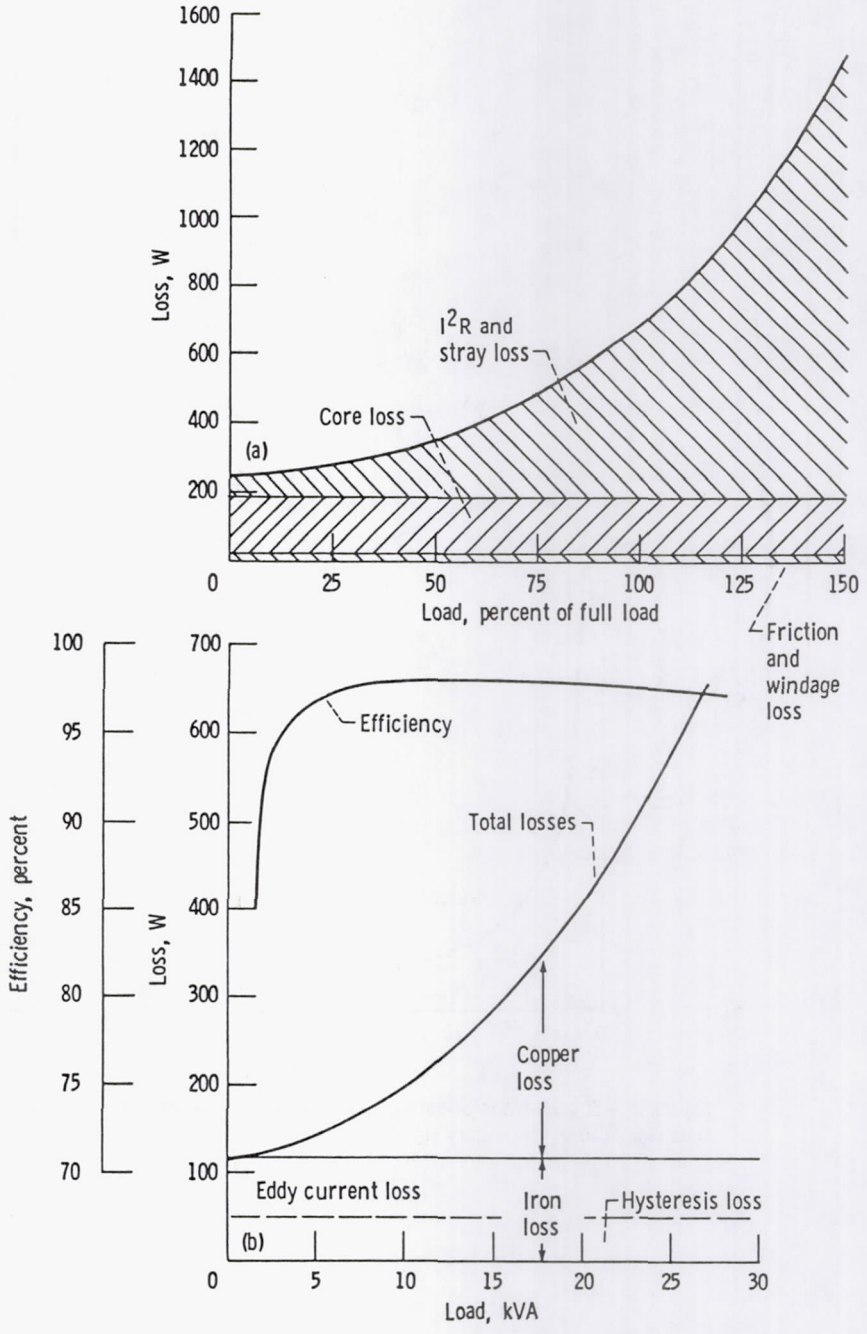

(a) 5-hp, three-phase motor.
(b) 15-kVA transformer.

Figure 2. - Comparison of loss characteristics for 5-hp motor and 15-kVA transformer.

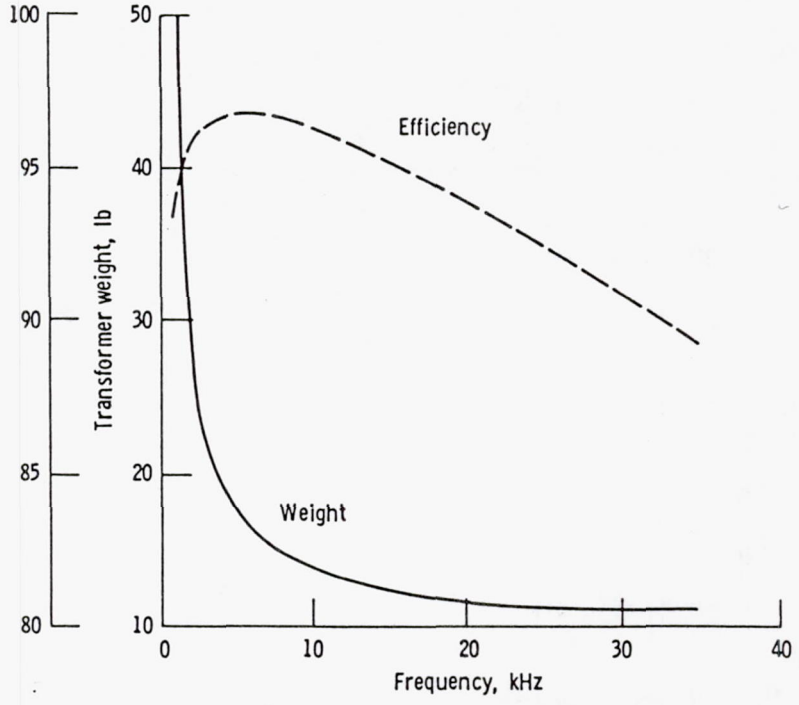

Figure 3. - 50-kVA transformer design for constant flux density. Primary voltage, 440 V; secondary voltage, 1 kV.

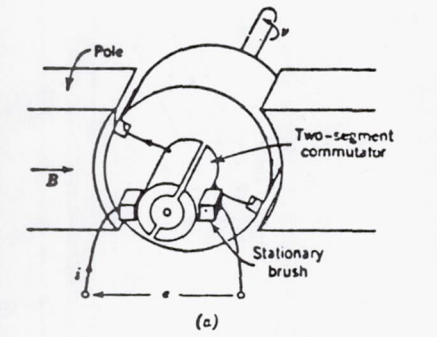

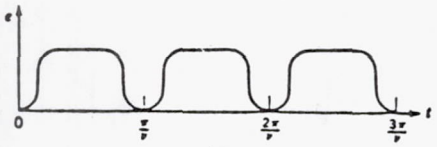

An elementary commutator machine and its generated voltage e.

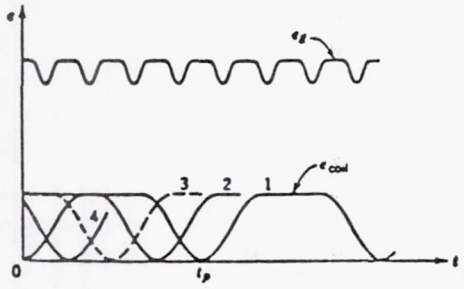

Summation of coil voltages to produce the generated voltage e_g.

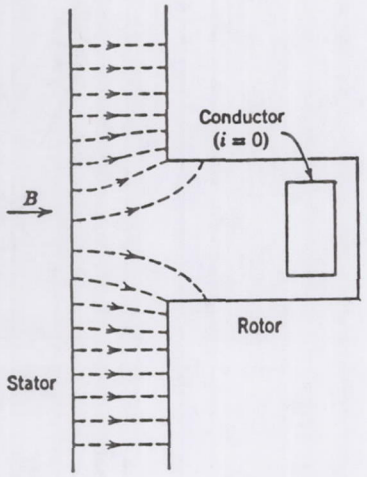

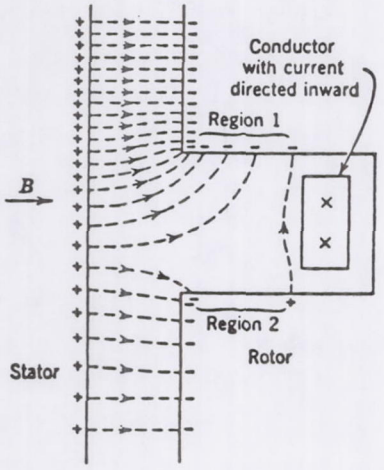

Figure 4. - Core loss factors.

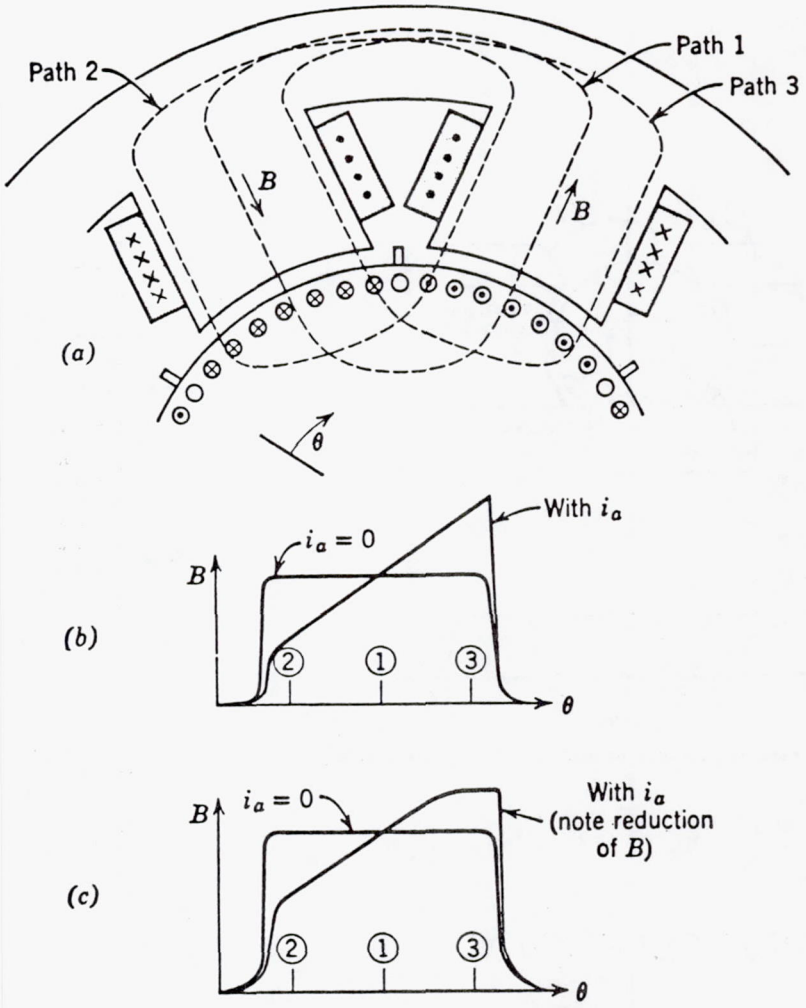

Figure 5. - Effect of armature magnetomotive force.

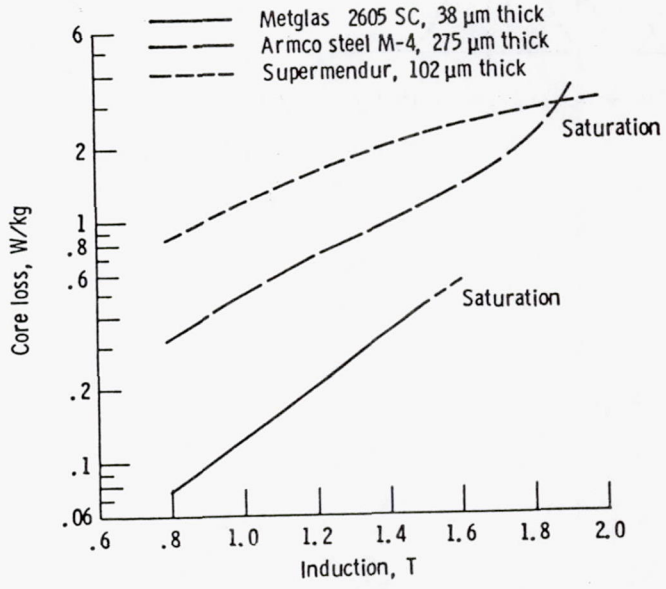

Figure 6. - Core loss as a function of induction for various materials. Frequency, 60 Hz.

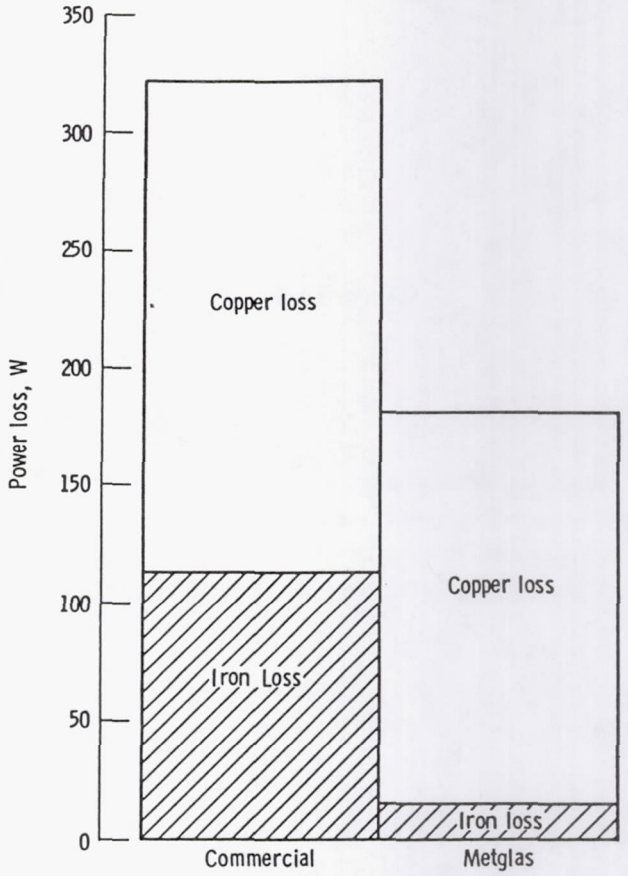

Figure 7. - Improvement on 15-kVA transformer using Metglas.

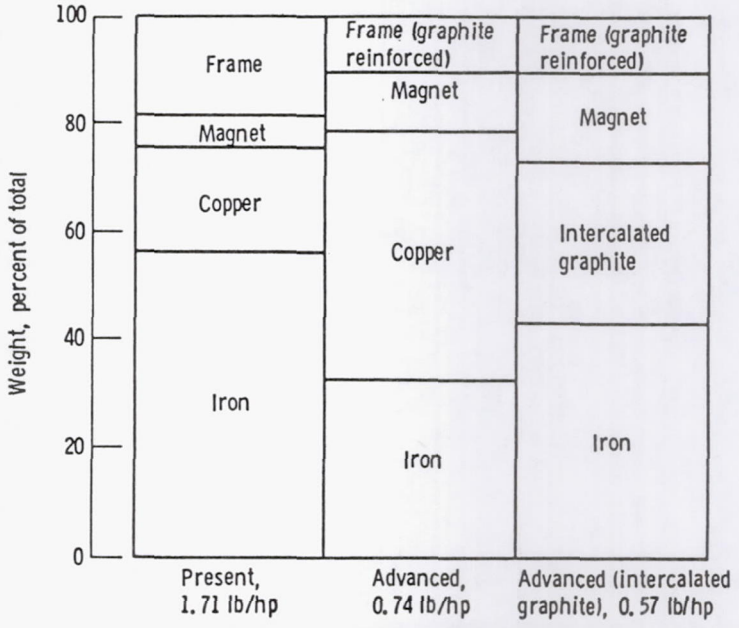

Figure 8. - Weight of samarium-cobalt motors. Efficiency, 93 percent; horsepower, 15 hp.

INTERCALATED GRAPHITE ELECTRICAL CONDUCTORS

Bruce A. Banks
National Aeronautics and Space Administration
Lewis Research Center
Cleveland, Ohio 44135

For years NASA has wanted to reduce the weight of spacecraft and aircraft. It would certainly be advantageous to find a lightweight synthetic metal to replace copper. The subject of this paper, intercalated graphite, is such a material.

As shown in figure 1 intercalated graphite is made by heating petroleum or coal to remove the hydrogen and to form more covalent bonds, thus increasing the molecular weight. The coal or petroleum eventually turns to pitch, which can then be drawn into a fiber. With continued heating the pitch-based fiber releases hydrogen and forms a carbon fiber. The carbon fiber, if heated sufficiently, becomes more organized in parallel layers of hexagonally arranged carbon atoms in the form of graphite. Certain chemicals or dopants are introduced between the layers of this high-temperature-treated, highly oriented graphite fiber. These chemicals, called intercalants, react with the carbon to form a large molecule and are diffused into the graphite between its layers of carbon atoms. The intercalants affect the electron distribution of the carbon in a manner that increases its electrical conductivity. The conductivity in the A direction (in the planes) is substantially increased. In the C direction (perpendicular to the planes) it is not increased at all. A conductor of intercalated graphite is potentially useful for spacecraft or aircraft applications because of its low weight. These intercalated graphite fibers can be coated with various metals so that they can be soldered. With an appropriate fiber cable design, it may be possible to terminate them and treat them much like conventional conductors.

As shown in figure 2 the mass of a wire is equal to the density n times the area A times the length L. Resistance is $\rho L/A$, were ρ is resistivity. For a wire of a definite length that is to have a certain resistance, the resulting mass is proportional to the length squared, because the longer it is, the thicker it must be to have the same resistance. Density and resistivity can be varied in searching for the ideal conductor. Ideally, one wants to reduce the mass of conductor on an aircraft or a spacecraft by keeping its weight and resistance low.

Depending on the specific application, a variety of materials can be used (table I). Although copper is fairly dense compared to other materials, its resistivity is very low. Aluminum is slightly more resistive but substantially lighter, so that its product $n\rho$ is about half that of copper. Although that is good, aluminum suffers from some engineering termination difficulties that have tended to reduce its widespread replacement of copper conductors. Other materials are better than aluminum, such as sodium, which is even farther from being a practical wire material because of its reactivity. Graphite fibers are much lighter than aluminum but have extremely high resistivity (250 $\mu\Omega$-cm). However, if the graphite fibers are heat treated at high temperature, they become highly oriented and possess low resistivities (40 to 60 $\mu\Omega$-cm) and will have densities that approach single-crystal densities of 2.26 g/cm^3. The product $n\rho$ is still higher than that of copper by a factor of 4. However, intercalated highly oriented pyrolytic graphite (HOPG) has an $n\rho$ of 4.3 $\mu\Omega$-cm as compared with 15.1 $\mu\Omega$-cm for copper. The problem is that HOPG is not a fiber but a bulk material and so does not have

the characteristics suitable for fabrication of a wire. Intercalated graphite fibers have a slightly higher $n\rho$ of 8.1 μΩ-cm, which is still better than that of copper. There are practical problems that must be resolved. For example, arsenic pentafloride is a very airreactive intercalant. There are many ways of treating the fibers or of using other intercalants so they will not be air reactive after intercalation.

Intercalation has other potential advantages, as shown in table II. Intercalated graphite fibers are extremely strong (250 000 psi compared with 40 000 psi for copper) and have a high strength-to-weight ratio. The expansion coefficient is much lower than that for copper. This might make them ideal for high-tension lines because they would not droop due to thermal expansion in the summer.

As shown in figure 3 when HOPG is intercalated, its normal resistivity ρ of 40 μΩ-cm is reduced by some constant k depending on the type of intercalant. For arsenic pentafloride, $k = 24.2$. The mass of the conductor then is dependent on n, ρ, k, R, and L. The resistivity is dependent on two components. Resistance is offered in the conductors as a result of phonon interaction with the electrons and defects interacting with the electron transit. Phonon interaction is not changeable, but one can obtain relatively defect-free graphite.

Thus there are several factors that cannot be easily changed: the density of intercalated graphite does not vary much, the phonon term cannot be changed, length and resistance are prescribed. However, to try to minimize the mass of the conductors, we can try to find graphite that is well organized and defect free and then search for the ideal intercalant by focusing on the terms outside the bracket in figure 3.

The orientation and number of defects are directly dependent on the process used to make the fibers (fig. 4(a)). Both the structures and the properties are affected by processing. If oil or coal is heated, it begins to increase in molecular weight and hydrogen is evolved. It goes through a liquid-crystal phase, called mesophase. As the process continues with increasing temperature (1000° to 2500° C), we eventually obtain carbon. Increasing temperature to 3000° C increases organization and graphitization to produce an ideal graphite-like structure.

In the liquid phase, where the pitch becomes a thick fluid, it initially is not very organized, that is, there is an isotropic orientation of hexagonal platelets. Within this sea of randomly organized, or disorganized, platelets, there develop droplets of the mesophase, or liquid-crystal phase. In this phase the platelets link up and gradually change direction, so there is very good organization within these spheres. They also coalesce as the material is heated (fig. 4(b)). Each hexagonal platelet touches the next and there is a gradual, smooth transition to a more complete liquid-crystal phase.

Figure 5 shows pitch coalescing under polarized light. Droplets of the mesophase liquid crystal are immiscible with the surrounding isotropic pitch and thus gradually get bigger as they coalesce. Figure 6 shows a polarized-light photomicrograph and a drawing based on interpretation of the orientation of the platelets in the polarized-light photomicrograph. The lines are drawn parallel to these platelets. The platelets follow each other in a continuous manner just as in a pneumatic liquid crystal in that there is a continual or gradual variation in orientation of these platelets. Extruding the mesophase liquid crystal with some of the globules that have coalesced in this sea of random changes in direction through spinnerettes provides further directional organization to these fibers (fig. 7). This spun mesophase pitch-based carbon fiber (fig. 8) is not necessarily a graphite fiber unless it is heat treated. Generally, spun carbon fibers are of the order of 10 μm in diameter, which is

ideal for a variety of engineering reasons. Figure 9 is an end view of such a fiber; it shows no semblance of graphite organization. It is simply a carbon fiber that has been extruded and is largely amorphous. It is not graphitic. It is a fiber of the type one might use for structural composites. However, by suitable processing and proper heat treatment, the fiber can be organized with an onionskin type of geometry (fig. 10), where the graphitic planes are organized circumferentially just like the skin of an onion. This type of fiber is very difficult to intercalate because intercalation occurs through the edges of the planes. Because there are very few edges present, it is difficult to intercalate radially. However, one can similarly fabricate a different type of fiber (fig. 11) in which the planes are radial. The wedge is caused by further shrinkage of the fiber due to hydrogen release, but this does not occur in all radially oriented fibers.

The radially oriented fiber is the ideal geometry to intercalate. Even with this orientation it is possible not to have an ideal geometry of AB,AB staggered orientation of hexagonal planes, but rather a geometry of parallel but rotated planes with respect to each other. This is called turbostratic graphite (fig. 12). Although it is disorientation of a lower importance, the defects causing poor conductivity must also be eliminated.

Figure 13 shows an internal void. These voids and surface defects all increase the resistivity of a fiber before intercalation and have a direct effect on the ultimate resistivity. Figure 14 shows an included particle, which is another defect to be avoided. Progress has been made by various types of treatment and processing to minimize the occurrence of these defects.

The molded graphite normally found in a machine shop (fig. 15) is polycrystalline and has fairly high resistivity and low density (table III). Extruded graphite is slightly more organized and has a higher density. Pyrolytic graphite exhibits both good organization and anisotropy. There are three orders of magnitude difference in the resistivity in the plane as opposed to through the plane. The highly oriented pyrolytic graphite (HOPG) exhibits the highest degree of organization and anisotropy. The most highly organized fiber, P100, which is commercially available, has a resistivity of 250 $\mu\Omega$-cm. Pyrolytically deposited fibers have been made in which the fibers have been grown through decomposition of organic gases; these have properties that approach those of HOPG. Intercalation of these fibers would result in very high conductivity.

The intercalant used in figure 16 is potassium. Figure 16 shows a first-stage intercalation in that there is one carbon layer between each intercalant layer. The compound is actually C_8K. One can put various intercalant concentrations in materials. For example, you could have a first stage compound where it is between every carbon layer, or a second stage (between every other carbon layer). To obtain the higher conductivity per volume, a second or third stage would generally be optimal, although at least 10 stages have been identified. Stages of intercalation are shown in figure 17.

Some of the many intercalants include K, Br_2, Cl_2, Cs, Li, Na, F, Rb; N_2O_5, SO_3, CrO_2; IBr; ICl, $AlCl_3$, $CuCl_2$, $FeCl_3$, $NiCl_2$, $MnCl_2$, $ZnCl_2$, $SbCl_5$; $PdCl_2$, $MoCl_5$; CrO_2Cl_2; $Ba(NH_3)_2$; H_2SO_4; SbF_5; and AsF_5. Many of the intercalants such as bromine are very air reactive. Some of them such as copper chloride are not air reactive. A reactive material can be introduced first as a wedge to pry apart the molecules so that another material can be introduced later. Figure 18 shows pyrolytic graphite strips that have been intercalated with bromine as well as virgin graphite. The intercalated graphite strips are wider (the outside two pieces). They were intercalated by immersing the graphite in bromine and as a result they became about 30 percent

thicker. They delaminated because this bromine wedge was driven in so fast that stresses exceeded the intralaminar bonding forces.

Figure 19 shows two pieces of pyrolytic graphite held by small C-clamps. The left one is not treated; the right one was intercalated with gaseous bromine and photographed using laser holography double exposures. The exposures were taken 30 seconds apart. The interference fringes indicate the intercalant is leaving from the edge. Thus, intercalation swells the graphite and, as it deintercalates to some residual compound, it actually gets thinner. The process occurs out the edges rather than through the face.

If intercalation is done too quickly, by immersion in liquid bromine, defects will be generated that can increase resistivity. Figure 20 shows pyrolytic graphite that was intercalated by liquid immersion rather than by vapor exposure. The intercalation was so rapid that it disrupted the surface structure of the graphite. Deintercalation occurred all over the surface not just from the edges - indicating structural damage to the surface.

Figure 21 illustrates what happens in real time with respect to resistance of pyrolytic graphite strips upon intercalating with bromine. The resistivity was reduced by a factor of 16.7 in 280 minutes. When the graphite was removed from the vapor, it began to deintercalate, so the resistivity increased again (fig. 22). However, it did not rise to the same level. There was a net reduction in resistivity of 4.3 $\mu\Omega$-cm in this particular experiment. Thus there was a net increase in conductivity.

Many engineering aspects pertinent to the practical application of intercalated graphite conductors need to be looked at. One is coating fibers to make them solderable. Figure 23 shows a fiber that was electroplated with copper. The coating is not uniform. One would like a very thin coating; one would like to be able to solder these fibers so that they could be treated like a conventional wire to at least some extent. One of the problems with the particular process used is shown in figure 24. As can be seen, some of the fibers have coalesced during electroplating and would be less flexible because the plating joins them and they fracture quite easily. NASA Lewis is looking at a variety of intercalants. Many engineering aspects must be considered before they can really compete with copper conductors, but there are many exciting opportunities. A suitable method of terminating a bundle of brittle fibers must be determined. The fibers have to be coated for soldering so that they can be used from a spool just like a conventional wire. A suitable insulation has to be derived for them that is intercalant resistant, with consideration given to limit fiber flexure. If you bend fibers over too small a radius of curvature, they will fracture because they are so thin, but coating with insulation should make them more pliable. At high current, intercalated graphite "wires" may get hot momentarily, which may affect the intercalant: it may deintercalate or it may go to a different stage in intercalation. Thus the residue intercalation compound has to be stable on exposure to air, moisture, salt, or vacuum. It must be stable under steadily applied dc and ac fields. Some of these concerns are not well understood at this point and they are subjects of current research activity.

BIBLIOGRAPHY

1. Singer, L. S.: Carbon Fibers from Mesophase Pitch. Fuel, vol. 60, Sept. 1981.
2. Hooley, J. G.: The Intercalation of Layered Structures. Carbon, vol. 18, 1980, pp. 82-92.

TABLE I. - CHARACTERISTICS OF MATERIALS

Material	Density, n, g/cm^3	Resistivity, ρ, $\mu\Omega$-cm	$n\times\rho$, $\mu\Omega$-g/cm^2
Copper	8.9		15.1
Magnesium	1.74	4.4	7.7
Aluminum	2.7	2.8	7.6
Sodium	.97	4.8	4.6
Calcium	1.55	3.4	5.2
Graphite fibers	2.15	250.0	537.5
Highly oriented pyrolytic graphite (HOPG)	2.26	40.0	90.4
Intercalated graphite fibers (AsF_5)	2.7	3.0	8.1
Intercalated HOPG (AsF_5)	2.7	1.6	4.3

TABLE II. COMPARISON OF INTERCALATED GRAPHITE FIBERS WITH METALS

Material	Tensile strength, psi	Strength to weight ratio, psi cm^3/g	Thermal expansion coefficient, $1/C^\circ$
Copper	40 000	4 490	16×10^{-6}
Aluminum	80 000	29 600	14
Steel	400 000	50 600	7
Intercalated graphite fibers	250 000	147 000	1

TABLE III. - CHARACTERISTICS OF MOLDED GRAPHITE

	Resistivity, $\mu\Omega$	Density, m^3
Bulk carbon		
Molded polycrystalline graphite	1 400	1.75
Extruded polycrystalline graphite	900	1.77
Pyrolytic graphite		
A	250	2.20
C	300 000	
Highly oriented pyrolytic graphite		
A	40	2.26
C	200 000	
Carbon fibers		
Thornel 300 (450 ksi tensile)	1 800	1.75
Thornel 50 (pan)	750	2.02
Thornel P100 (pitch)	250	2.15
Pyrolytically deposited (endo)	59	----

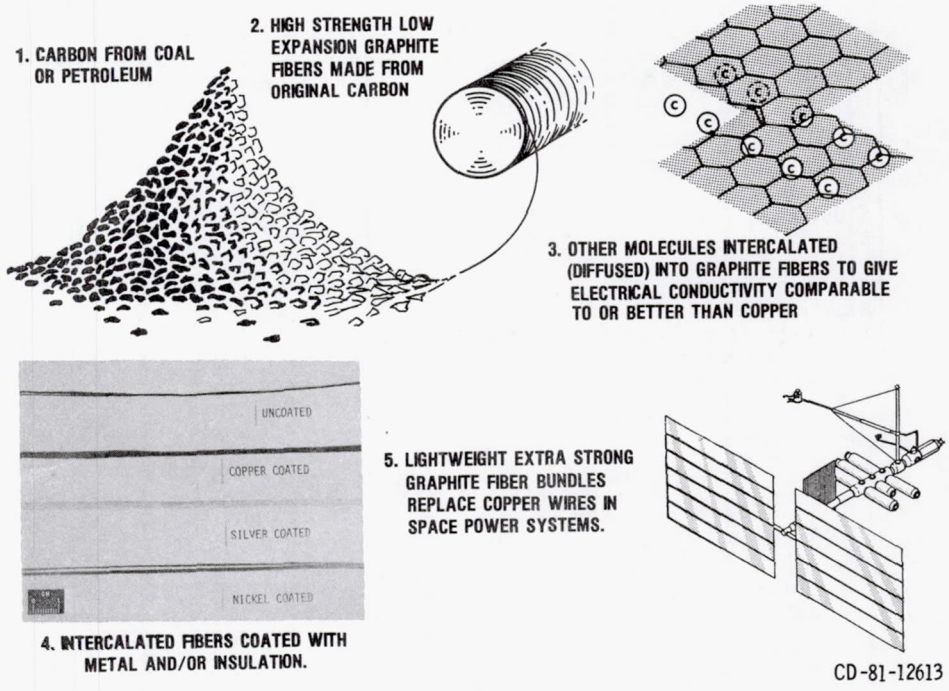

Figure 1. - Graphite intercalated conductor.

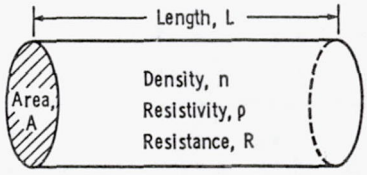

Mass of conductor = nAL

$$R = \frac{\rho L}{A} \quad \text{or} \quad A = \frac{\rho L}{R}$$

$$\text{Mass of conductor} = \frac{n\rho L^2}{R}$$

Figure 2. - Characteristics of conductors.

ρ_I = Resistivity after intercalation

k = Constant for each intercalant $\approx$ 24.2 for AsF_5; 12.7 for HNO_3; 3.5 for Rb

$$\rho_I = \frac{\rho}{k}$$

$$\text{Mass of conductor} = \frac{n\rho L^2}{kR}$$

$$\text{where } \rho = \frac{\rho_{phonon}\,\rho_{defect}}{\rho_{phonon} + \rho_{defect}}$$

$$\text{Mass of conductor} = \frac{\rho_{defect}}{k}\left[\left(\frac{n\rho_{phonon}\,L^2}{\rho_{phonon} + \rho_{defect}}\right)\frac{L^2}{R}\right]$$

Figure 3. - Intercalated graphite conductors.

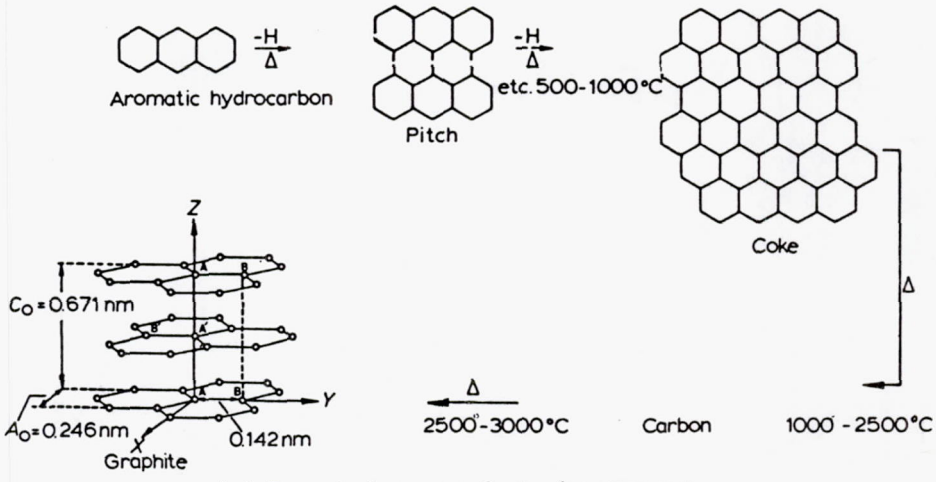

(a) Dependent on manufacturing process.

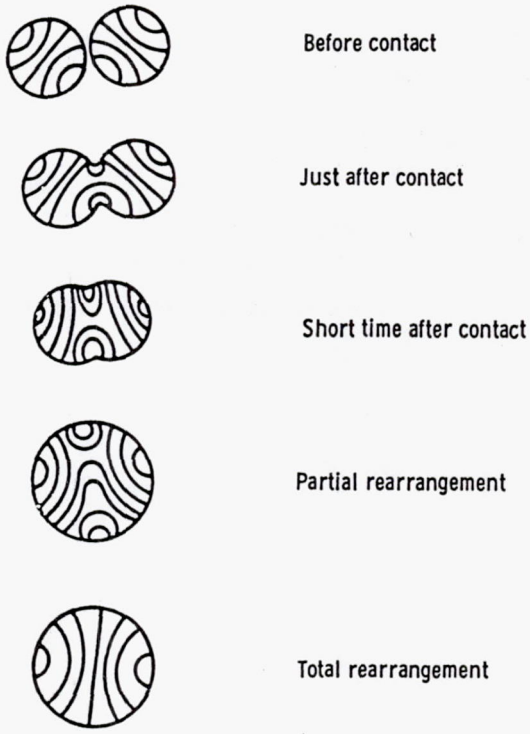

(b) Arrangement of hexagonal platelets.

Figure 4. - Orientation and number of defects.

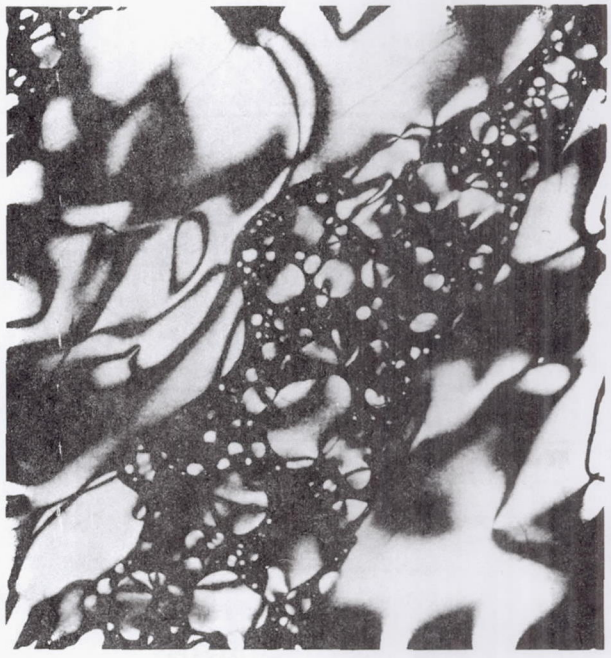

Figure 5. - Polarization of pitch under polarized light.

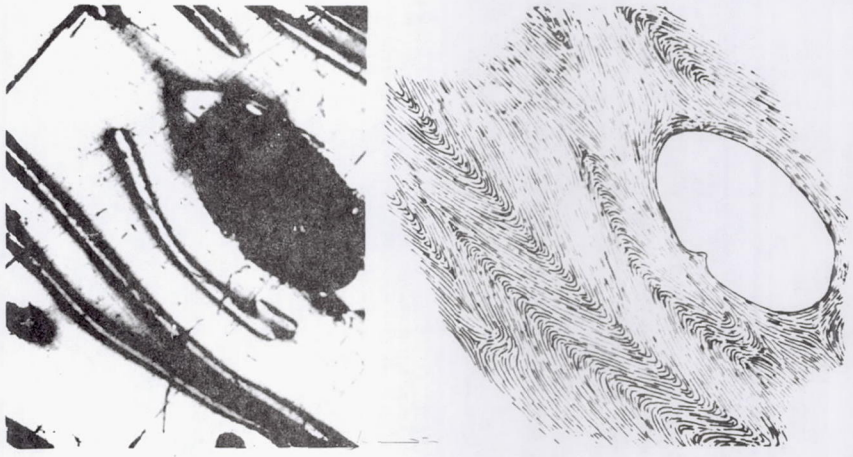

Figure 6. - Polarized-light photomicrograph and drawing based on orientation of platelets in photomicrograph.

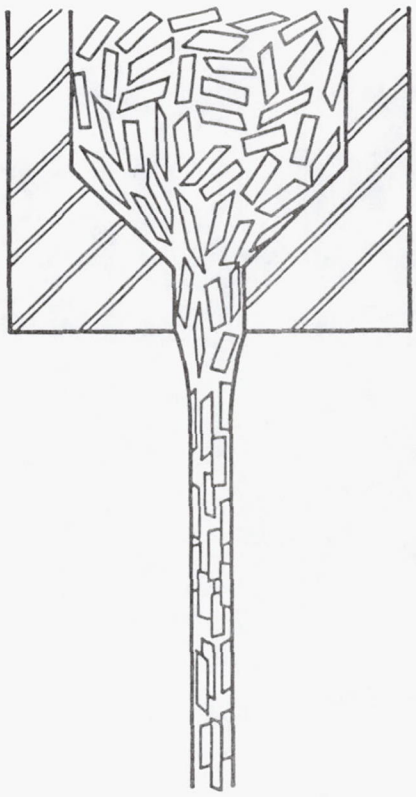

Figure 7. - Extrusion through spinnerette.

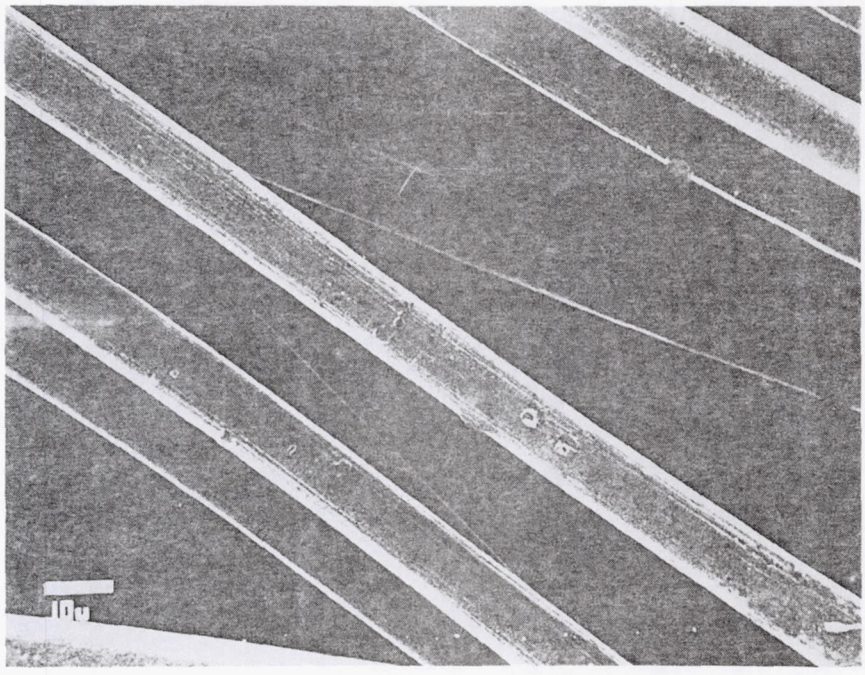

Figure 8. - Spun meso-phase pitch-based carbon fiber.

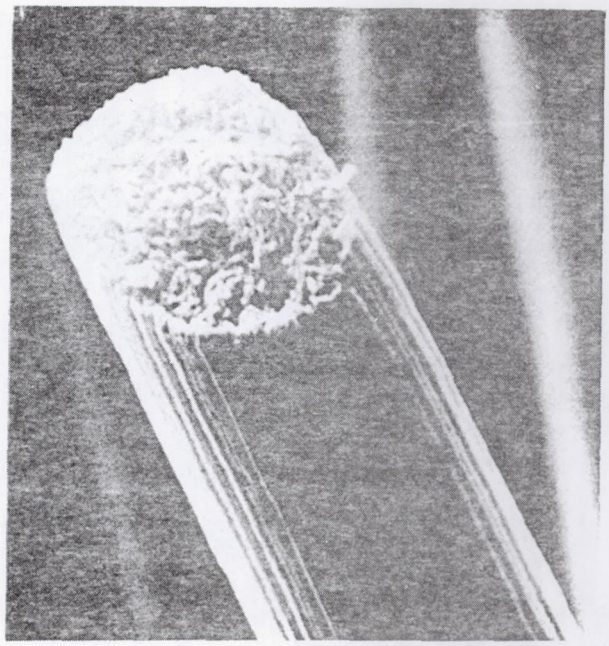

Figure 9. - End view of spun meso-phase pitch-based carbon fiber.

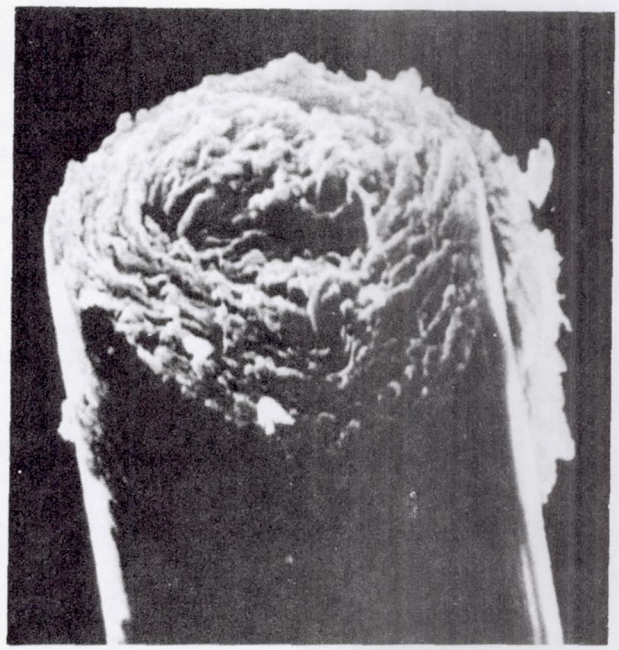

Figure 10. - Onion-skin fiber geometry.

Figure 11. - Radial fiber geometry.

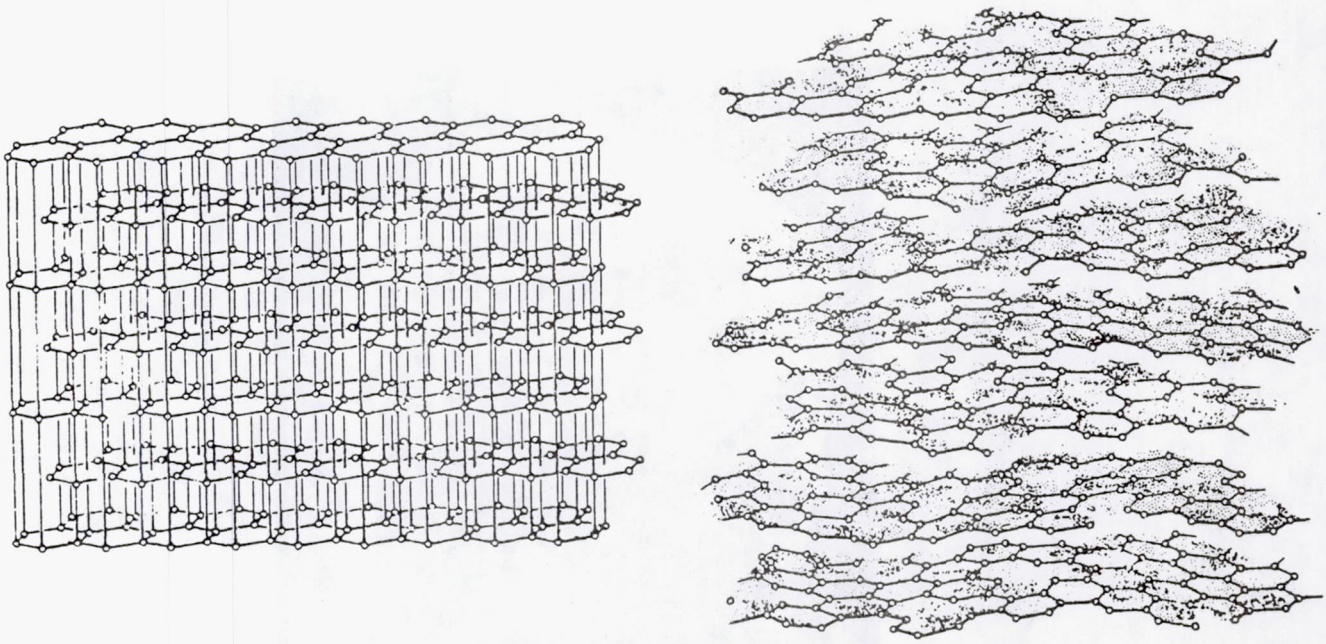

Figure 12. - Orientation of turbostratic graphite.

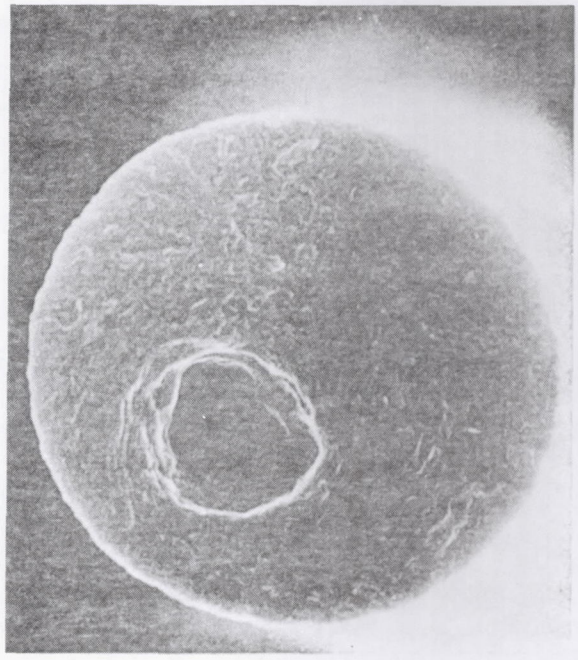

Figure 13. - Internal void.

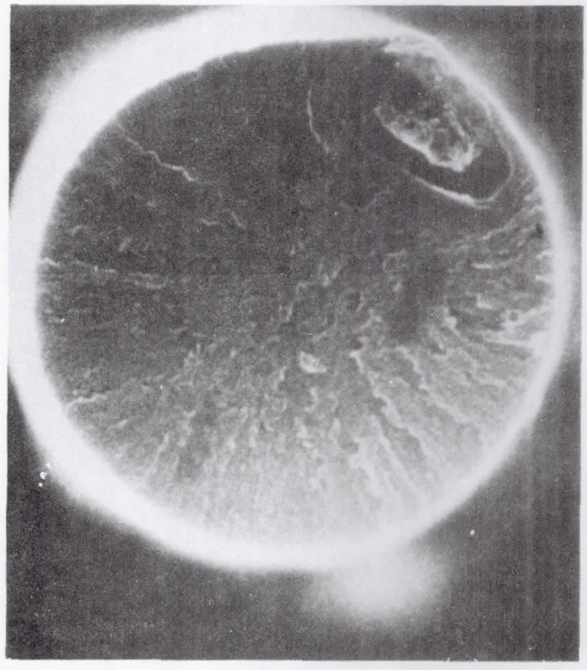

Figure 14. - Included particle.

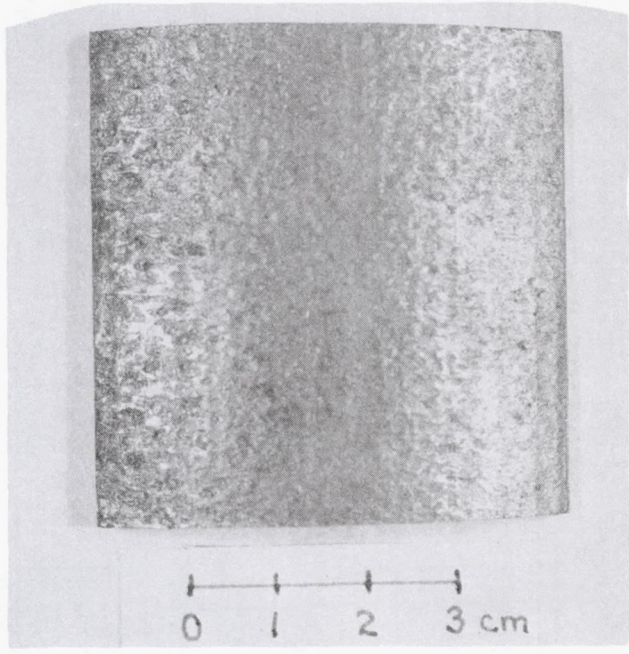

Figure 15. - Polycrystalline graphite.

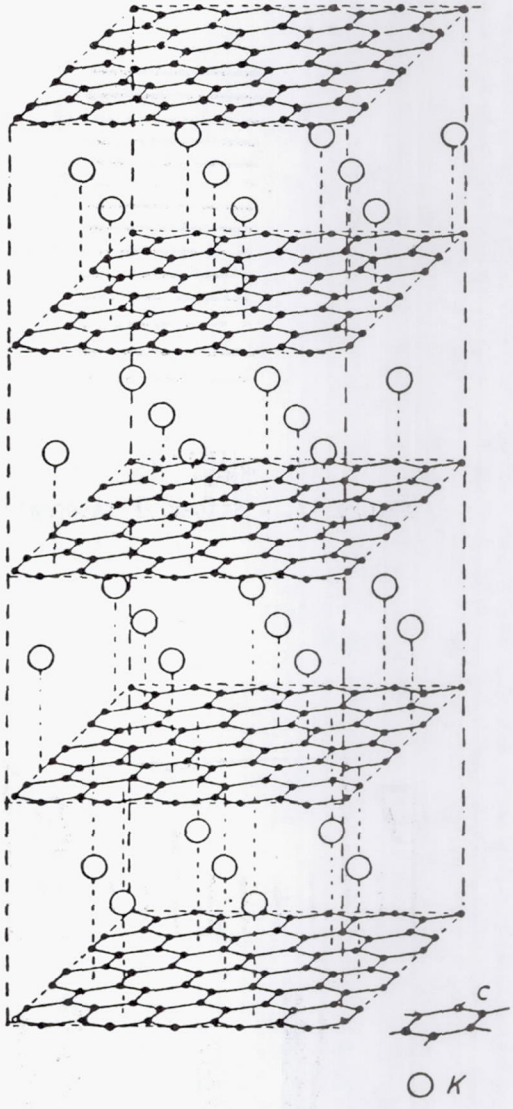

Figure 16. - First-stage intercalation.

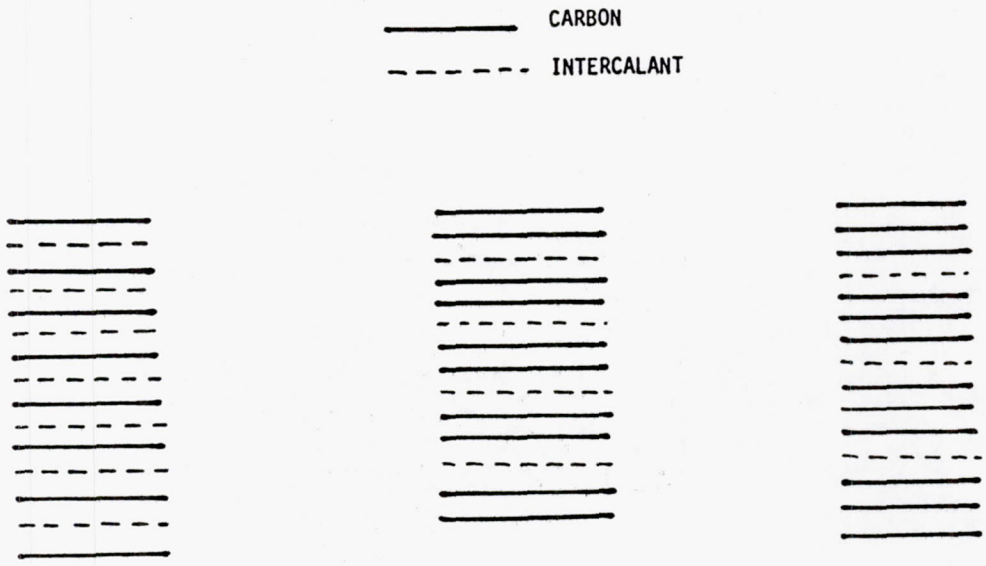

Figure 17. - Stages of intercalation.

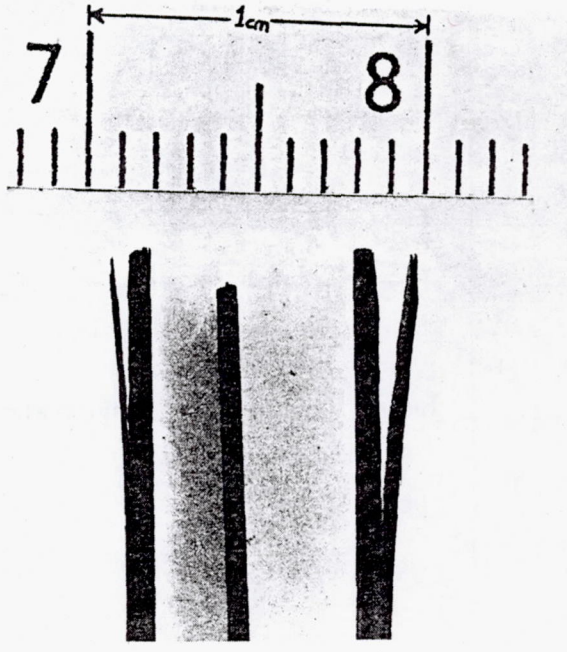

Figure 18. - Graphite strips intercalated with bromine.

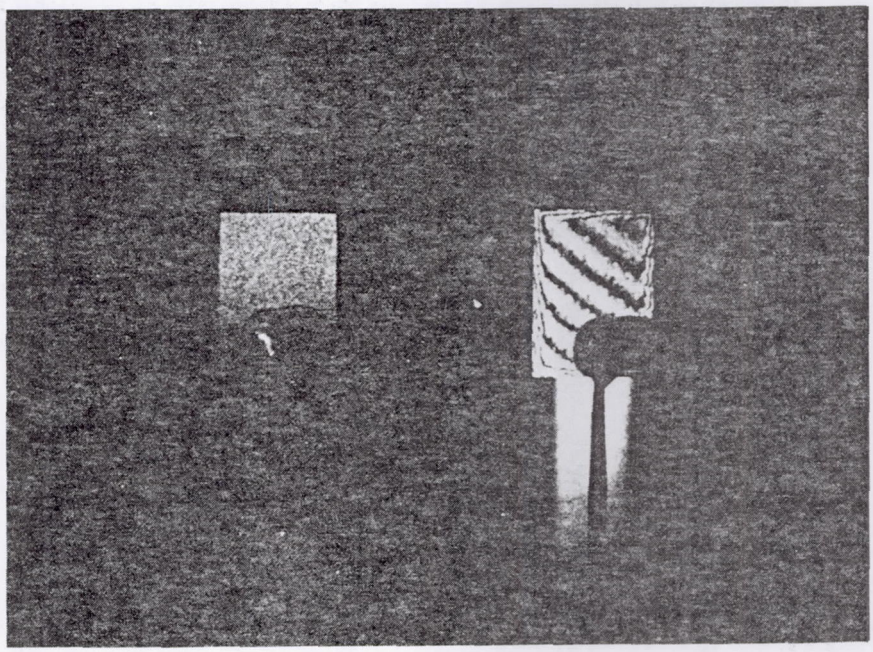

(a) Untreated (b) Intercalated with gaseous bromine.

Figure 19. - Two pieces of pyrolytic graphite.

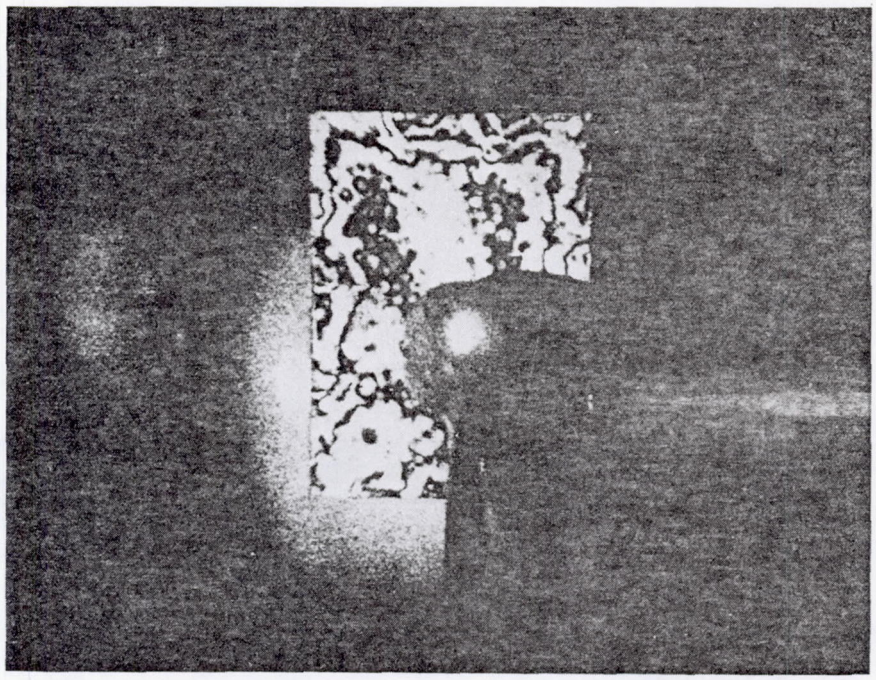

Figure 20. - Pyrolytic graphite intercalated by liquid immersion.

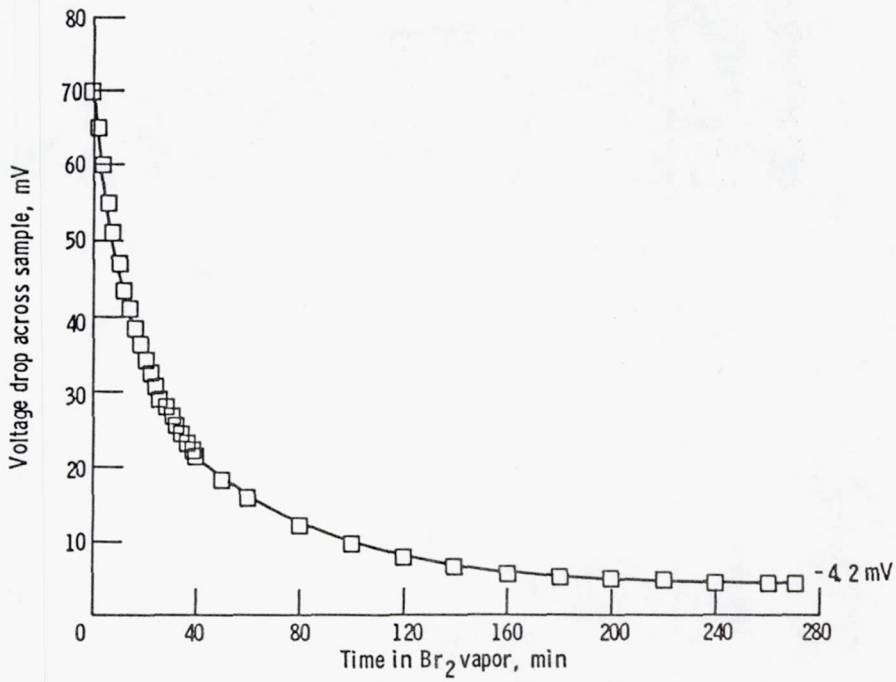

Figure 21. - Voltage drop across sample as a function of time in bromine vapor.

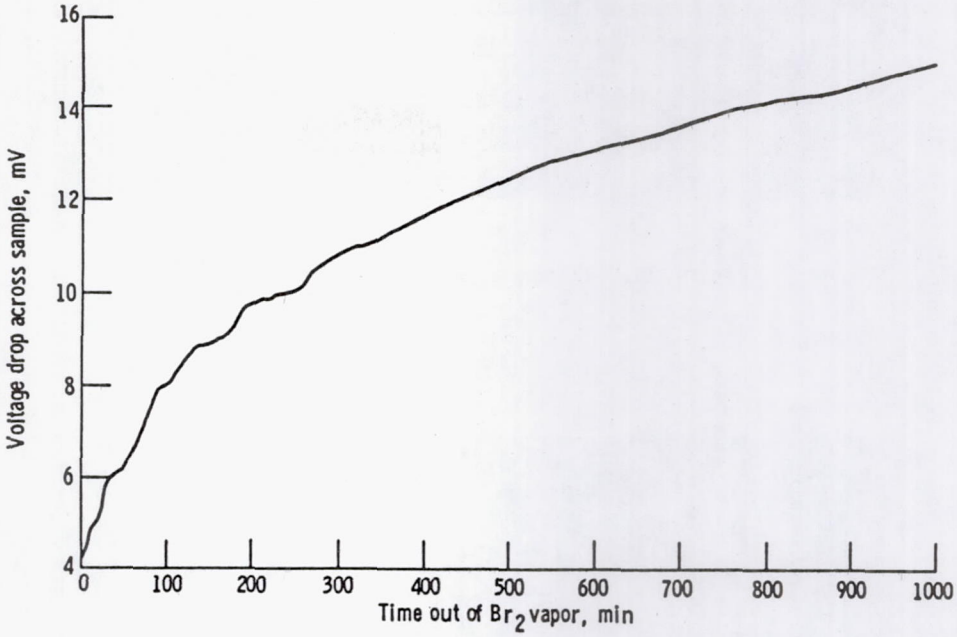

Figure 22. - Voltage drop across sample as a function of time out bromine vapor.

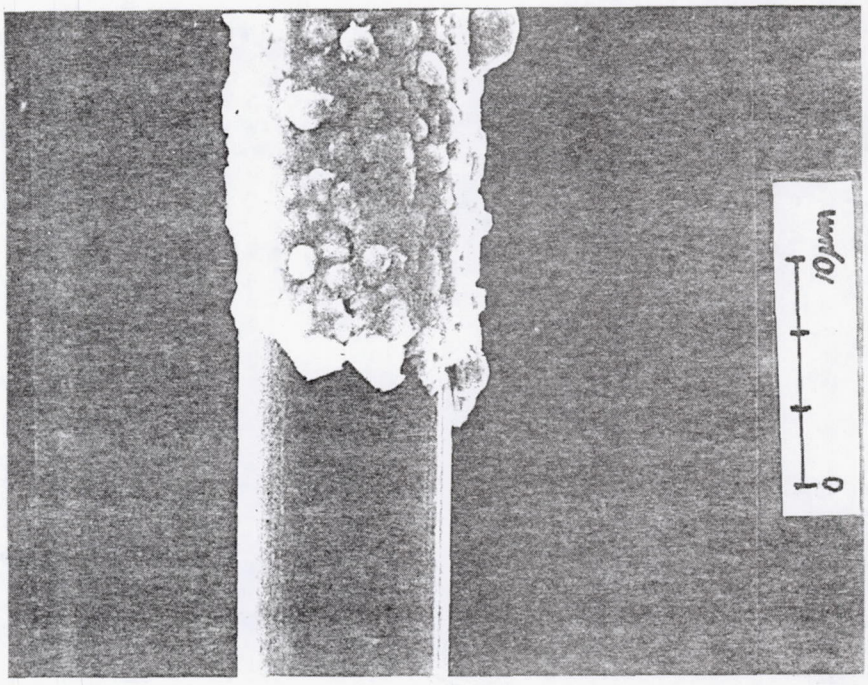

Figure 23. - Fiber electroplated with copper.

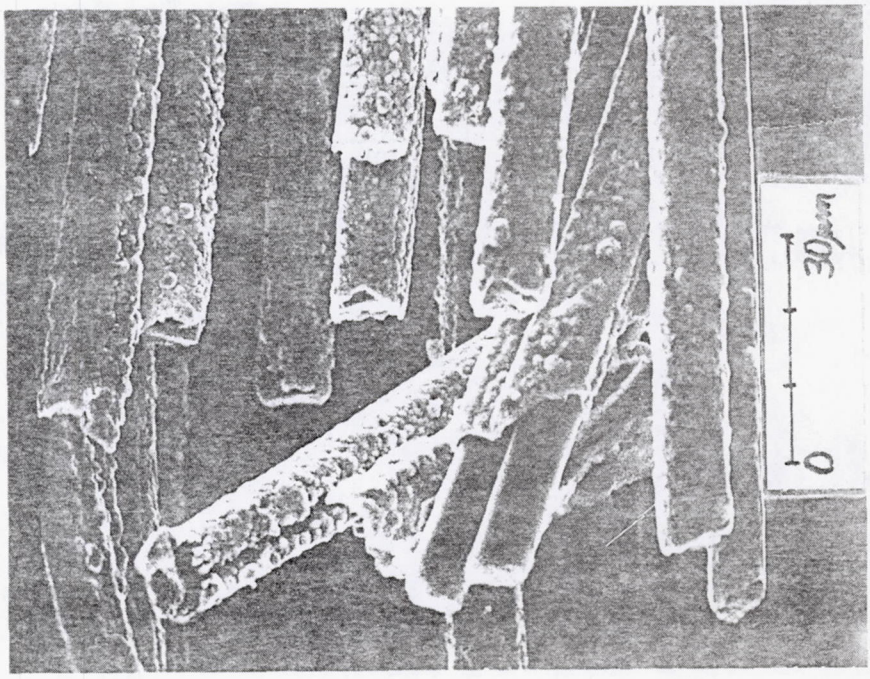

Figure 24. - Fibers coalesced during electroplating.

NEW DEVELOPMENTS IN POWER SEMICONDUCTORS

Gale R. Sundberg
National Aeronautics and Space Administration
Lewis Research Center
Cleveland, Ohio 44135

This paper represents an overview of some recent power semiconductor developments and spotlights new technologies that may have significant impact for aircraft electric secondary power. Primary emphasis will be on NASA-Lewis-supported developments in transistors, diodes, a new family of semiconductors, and solid-state remote power controllers. Several semiconductor companies that are moving into the power arena with devices rated at 400 V and 50 A and above are listed, with a brief look at a few devices.

Advanced power electronic component development for space applications has been going on at NASA Lewis for more than a decade, as shown in figure 1. A wide range of development work has been done, including transformers and inductors, semiconductor devices such as transistors and diodes, remote power controllers, and supporting electrical materials development. Present power component capability for space applications is about 25 kW. Work in the early and middle 1980's should raise this capability to 100 kW and begin to move toward a megawatt capability.

Industrial Research & Development Magazine recognized the D60T high-power switching transistor as one of the 100 outstanding new products introduced in 1978. The D60T - a triple-diffused, NPN silicon transistor - introduces a combination of expanded power ranges, low energy losses, and fast switching speeds. Rated at 400 to 500 V and 100-A continuous (200 A peak) collector currents, these transistors have reduced transistor switching times by a factor of 2 to 5. Therefore they are used in 50-kHz inverter designs. Principal applications are dc-dc inverters, dc motor controllers, and solid-state remote power controllers. Research devices based on this technology have proven feasible to 1200 V, and with larger area silicon wafers, power-handling capability to 100 kW will soon be available.

Against the backdrop of a circuit diagram for a solid-state remote power controller a technician holds a D60T ready for assembly in a stud package (fig. 2). In her right hand the interdigitated silicon wafer can be seen inside the base. The emitter-base contacts are visible in the ceramic-to-metal top held in her left hand. To the left are shown three package types: a special flat-base package (a modification of the stud package), a stud package, and a disk package.

Figure 3 shows the Westinghouse D7ST, which is now being marketed as a direct transfer of technology from a research contract supported and directed by NASA Lewis. The two package types available are shown in the center photograph. Around the photograph are listed the features and applications of the D7ST. The primary benefit of the new transistor to NASA is the extension of the power-handling capability to 50 kW without paralleling of transistors. This opens new areas of application and direction for future space power system design.

The main ratings and characteristics for a 1000- to 1200-V transistor developed by Westinghouse under contract to NASA Lewis are as follows:

Voltage, V	1000 to 1200
Current, A	25 to 40 (gain of 10); 120 peak
Power handling, kW	30
Power dissipation at 75° C, kW	1.25
Rise and fall times, μsec	0.5
Storage time, μsec	3

Westinghouse successfully completed the program by delivering 50 transistors that met the listed specifications. The 33-mm-diameter wafer used the same emitter-base geometry as the D7ST.

The ratings and main characteristics for augmented power transistors to be developed in a research contract now under way at Westinghouse are as follows:

Voltage, V	800 to 1000
Current, A	70 to 112 (gain of 10); 400 peak
Power handling, kW	75
Power dissipation at 75° C, kW	1.25
Rise and fall times, μsec	0.5
Storage time, μsec	2.5

Transistors from this program should be available by the fall of 1982. The two significant developments of this program will be demonstration of glass passivation of the wafer to provide hermetic sealing of the junctions and a new package that isolates the thermal and electrical interfaces.

Figure 4 shows the benefits to NASA, the features, and the general applications of a newly developed 50-A, 1200-V fast-recovery power diode. Power Transistor Company developed the new diode on contract to NASA Lewis. Because of the large commercial demand for such a device in motor controllers, Power Transistor Company is already marketing the product as their PTC 900 series power rectifier.

Figure 5 is a copy of a data sheet showing both bipolar and Darlington transistors rated at 450 V and 100 A. They are encased in an innovative package with separate electrical and thermal interfaces. The transistors can be easily paralleled. Fuji has recently introduced a new 1000-V, 100-A transistor to add to a growing family of power semiconductors.

One of Motorola's new MJ series of Darlington transistors is shown in this partial copy of a data sheet (fig. 6). This is a totally new package with isolated electrical and thermal interfaces. This model is produced in three ratings: 850 V, 50 A; 450 V, 100 A; and 250 V, 200 A.

Figure 7 shows one of several models of bipolar and Darlington transistors available from Power Transistor Company. They are working on a new low-cost package, a 1000-V transistor, and a gate turnoff thyristor for 460-V ac motor control applications. They are also developing a 150-A, 1200-V fast-recovery diode on contract to NASA Lewis. This will be a higher current version in a DO-8 size package of the PTC 900 series described previously.

Table I shows the ratings of three new Darlington transistors under development at the GE Discrete Semiconductor Device Center in Syracuse, N.Y. The three devices (ZJ504E, ZJ604E, and ZJ704E) are compared with an existing device, the ZJ504. These new Darlingtons are being developed as the primary switches for a pulse-width-modulated (PWM) inverter-motor controller in an advanced electric vehicle power train program. This effort, supported by the DOE and managed by NASA Lewis, is under contract to Ford Motor Co. with General Electric as the major subcontractor.

Table II shows the specifications in greater detail for the 604E/704E versions of the new ZJ series under development by General Electric. Also given are specifications for a high-power flyback diode used in the PWM inverter-motor controller. New packaging concepts are also being explored in this work.

Several companies that have, or soon will have, bipolar, Darlington, or metal oxide semiconductor field effect (MOSFETS) transistors in the 400-V, 50-A and above power ranges are listed here.

(1) Fuji Electric Co. Ltd., Dallas, Texas (Japan)
(2) General Electric Co., Auburn, New York
(3) Hitachi Ltd., Japan
(4) International Rectifier, El Segundo, California
(5) Motorola Semiconductors, Phoenix, Arizona
(6) Power Tech, Fairlawn, New Jersey
(7) Power Transistor Company, Torrance, California
(8) Siemens AG, West Germany
(9) Solitron Devices, Riviera Beach, Florida
(10) Thomson CSF, Canoga Park, California (France)
(11) Toshiba Corp., Japan
(12) Westcode Semiconductors, Fairlawn, New Jersey (England)
(13) Westinghouse Semiconductor, Youngwood, Pennsylvania

In the case of foreign companies the city and state of the U.S. distributor is given where known.

Thermal Associates has introduced a new concept in packaging high-power semiconductor chips (fig. 8). This package is lighter than conventional packages, yet it provides compression bonding of electrical leads without soldering or other point-contacting methods. Of primary importance is the separation of the thermal and electrical interfaces of the package.

Figure 9 shows a new invention, the FET-gated transistor (FGT), by Dr. Daniel Chen of Virginia Polytechnic Institute and State University. NASA Lewis is presently supporting a grant to VPI/SU to prove feasibility and to develop the concept. On the figure Q_1 is the main bipolar power transistor, Q_2 and Q_3 are power field effect transistors (FET's), and D is a Zener diode. The Q_2 is in a Darlington, and the Q_3 is an emitter-open configuration with Q_1. Conduction in Q_1 is controlled by signals to the gate terminals of Q_2 and Q_3. Dr. Chen is presenting a paper entitled "FET-Gated High Voltage Bipolar Transistors" at the upcoming IEEE Industrial Applications Society Meeting in San Francisco, October 4-7, 1982.

The primary advantages of the FGT are fast switching, no reverse-bias second breakdown (RBSB), very simple drive requirements, and good use of the semiconductor chip area. The use of emitter-open switching essentially eliminates the bipolar storage time delay and gives very fast switching speeds. It also eliminates RBSB problems and thereby reduces the need for energy-wasting snubber circuits. The FET bipolar combination enables the bipolar to be operated safely at the V_{CEO} sustaining rating. This fact reduces the bipolar chip area required such that the total chip area of the combination will be comparable to that of a bipolar transistor.

A new family of semiconductors, called deep-impurity devices, is being investigated at the University of Cincinnati with NASA Lewis support. In understanding how deep-impurity devices work, we must look at bulk effects in silicon (or some other semiconductor material) rather than typical p-n junction characteristics. We are interested in what happens in silicon doped with

a deep impurity such as gold between charge-injecting electrodes. We are investigating the addition of impurities to silicon that add one or more energy levels at or very near the center of the energy band. The center lies at 0.55 eV from both the conduction and valence bands in silicon. We use shallow impurities to compensate the material (that is, to adjust the Fermi level) but do not form conventional p-n junctions. Three types of gating are possible and have been explored in this work. Switching can be accomplished by light gating, injection gating (the addition of an injection gate in the space between anode and cathode), or MOS-voltage gating (metal-oxide-semiconductor gate).

Switching devices and transducers are the areas in which most of the effort to date has been focused. The primary interest now is in switching devices with gate-controlled threshold voltages (limited only by the breakdown voltage of silicon), controllable holding voltage giving evidence of zero forward voltage drop, thyristor-like switching with both turnon and turnoff capability, logic functions, PWM controllers, discriminators, and optical switches. Of secondary interest has been the demonstration of several very sensitive, miniature transducers: gas flowmeters, magnetic field Hall-type probes, temperature-to-frequency thermometers, and infrared detectors. The gas flowmeter is a hot-wire anemometer type, but only 0.2 mm on a side, with response times of a second and much greater sensitivity than a p-n junction device. The multiple-internal-reflection extrinsic infrared detectors have demonstrated quantum efficiencies greater than 34 percent, a flat detectivity curve out to 160 K, and multiple frequency ranges when using silicon-germanium alloys.

The capabilities of voltage-controlled oscillators and detectors, voltage-controlled pulse width modulators and delay lines, and a temperature-to-frequency thermometer are based on preand postbreakdown oscillations in devices with certain doping characteristics. Because of the possibility of charge storage in the deep levels, an exciting possibility has been predicted for very small, vertically integratable memory devices having an excellent immunity to radiation.

The upper part of figure 10 shows a cross section of a double-injection, deep-impurity device. The bulk material is gold-doped silicon compensated by a shallow donor such as phosphorus. The energy level diagram is shown in the lower part of figure 10 as a reminder. The gold acceptor level at 0.54 eV is the level activated and predominates in the device behavior.

Also shown in the upper part of the figure are the anode and cathode formed by diffusing p^+ and n^+ regions into the bulk material. These regions provide efficient ohmic contacts and the appropriate band bending at the surface to promote high Thus this is called a double-injection device. If only an n^+ region were produced, the device would be a single-injection device with characteristics following Murray Lampert's traps-filled-limit behavior as shown in the next figure.

The upper part of figure 11 shows a double-injection, gold-doped, n-type silicon diode with two gates added. We refer to them as MOS (metal oxide semiconductor) voltage gates. Applying a positive voltage to the cathode gate (or negative to the anode gate) decreases the threshold voltage from V_{TH} to V_{TH}', or it may turn the diode off from a conducting state. We have demonstrated that the cathode gate is more effective in controlling the switching behavior. Therefore, in practice, both gates have been replaced by one gate located near the center of the channel but closer to the cathode. As the gate voltage is increased positively, V_{TH} decreases and vice versa. The holding voltage is not much affected by the gate voltages.

Figure 12 shows two oscilloscope traces of the switching characteristics of the injection-gated device. Both photographs show current on a scale of 10 mA per division versus voltage at 20 V per division. Figure 12(a) shows a threshold voltage of about 155 V and a holding voltage of 16 to 20 V depending on the current level; the gate voltage is zero. The remarkable result of an injection gate is shown in the superposition of several traces in figure 12(b). As the gate-to-cathode voltage V_{GC} is made more negative in increments of -4 V, the holding voltage decreases. In fact, with $V_{GC} = -16$ V, the holding voltage is at or near zero. This presents the very exciting possibility of a device with zero forward voltage drop leading to a very energy-efficient switch. Obviously there is some power loss in the gate, but experimental data have shown these losses to be less than 10 percent of the primary conduction losses. Additional efforts in processing of the bulk silicon have reduced V_H by a factor of 4 or 5.

Now keeping in mind the basic physics of the deep-impurity device and its switching capabilities with the ability to vary both the threshold and holding voltages, we want to look at the voltage limitations in silicon. Figure 13 shows threshold voltage as a function of length in or across a slab of silicon. The breakdown limit is shown as a linear function of length in bulk silicon. The calculated curve for p-n junction devices is quite conservative in that it calculates the breakdown limit across the depletion region by assuming one side of the junction to be very lightly doped. This gives an upper limit in the region of about 10 000 V. Deep-impurity devices also have a square-law breakdown threshold but a smaller coefficient. The calculated curve for the deep-impurity material lies to the right of the p-n junction curve and shows a factor of 10 or more higher breakdown limit. If surface effects and material defects are neglected, there appears to be a very real possibility of devices with threshold voltages from 10 to 100 kV. Recent experimental data confirm the curve up to 800 V.

Another area of work that Lewis is supporting is solid-state remote power controllers. Figure 14 shows a hermetically sealed, fully operational remote power controller (RPC) along with the header assembly and enclosure of the RPC ready for final assembly and hermetic sealing. The hybrid version used semiconductor chips, individual piece parts, optical isolation, and thick-film manufacturing techniques. On the left is the header assembly substrate that contains the power transistor drive circuit, current-limiting resistor, and side rails for support and electrical contact to the upper control substrate shown just to the right. On the right side is the enclosure soldered to the substrates for hermetic sealing. The RPC is about 4.5 cm on a side and weighs 3.5 oz.

Figure 15 shows the 30-A version of the 120-V dc solid-state RPC developed for NASA Lewis by Westinghouse Aerospace Division. This version incorporates I^2t trip characteristics rather than current limiting. This version has a single-layer substrate (6 cm by 7 cm) and weighs about 7 oz.

Figure 16 lists several advantages of solid-state remote power controllers developed by NASA Lewis. With the new high-power transistors now available we have extended the power range to 25 to 50 kW and the voltage to 1000 V. The technology has been developed and is not dependent on a particular component. Actually, 1000-V, 25-A solid-state power controllers have been demonstrated using thyristors, transistors, and an array of FET's. Gate-turnoff thyristors (GTO's) could also be used.

TABLE I. - TRANSISTOR DESIGN TRADE-OFFS

	504	504E	604E/704E
I_C, A	200	133	150
H_{FE}	200 at 2 V	100 at 2 V	100 at 2.5 V
V_{CE}	280 V at 200 A	350 V at 133 A	400 V at 150 A
V_{CE}	500 V at 1 A	500 V at 1 A	550 V at 1 A
Size, cm^2	2.41	2.41	3.04

TABLE II. - CHARACTERISTICS OF POWER DARLINGTON TRANSISTOR AND FLYBACK DIODE

(a) Power Darlington transistor

Continous current rating, A	150
Turnoff state of the art, V:	
V_{CE} at I_C = 150 A, $\pm I_{B1}$ = 1.5 A, $V_{BE1(off)}$ = -5 V, V	400
V_{CE} at I_C = 1 A, $\pm I_{B1}$ = 1.5 A, $V_{BE1(off)}$ = -5 V, V	550
H_{FE} at I_C = 150 A, V_{CE} = 2.5 V, T_J = 100° C	100
$V_{CE(sat)}$ at I_C = 150 A, I_{B1} = 1.5 A, T_J = 100° C, V	2.5
t_s (inductive) at I_C = 150 A, $\pm I_{B1}$ = 1.5 A, μsec	4
t_f (inductive) at I_C = 150 A, $\pm I_{B1}$ = 1.5 A, μsec	2
Maximum chopping frequency, Hz	3000
R_{OSA}, °C/W	0.15
T_A, max, °C	50
Number of transistors in parallel in power module	3

(b) Flyback diode

Average current rating, A	150
Reverse blocking voltage, repetitive, V	550
V_{FM} at I_{FM} = 400 A, T_J = 125° C, V	2.0
t_a = I_F = 400 A, di/dt = 200 A/μsec, T_J = 125° C, nsec	500
t_b = I_F = 400 A, di/dt = 200 A/μsec, T_J = 125° C, nsec	500
R_{OSA}, °C/W	0.15
T_A, max, ° C	50
Number of diodes in power module	1

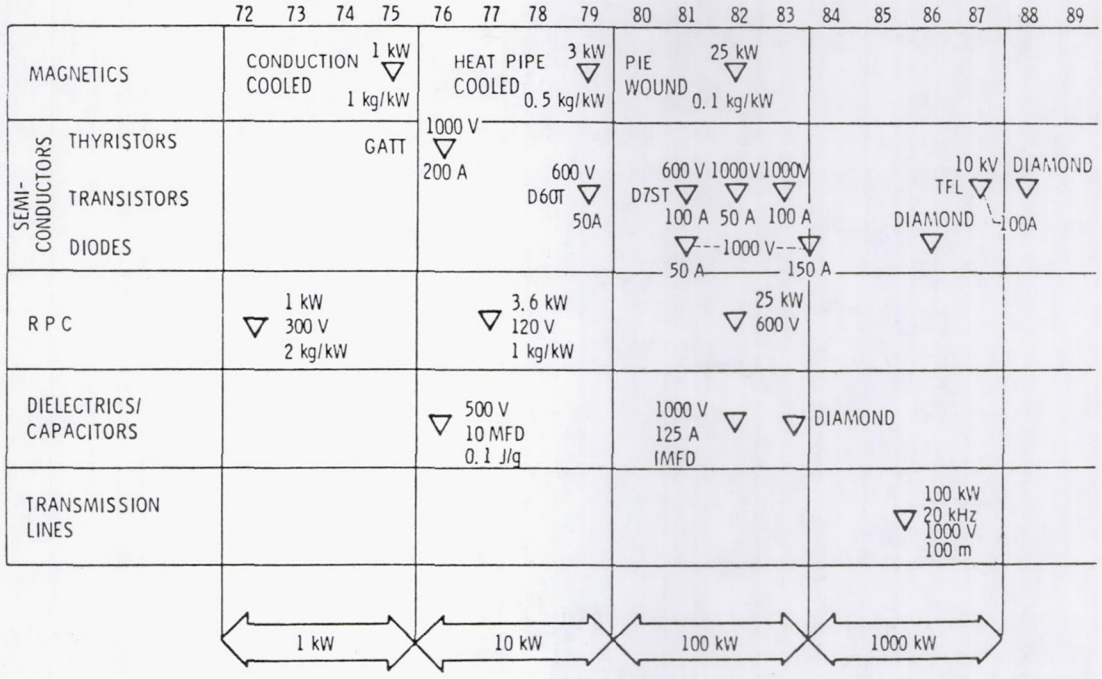

Figure 1. - Power electronics development at Lewis Research Center.

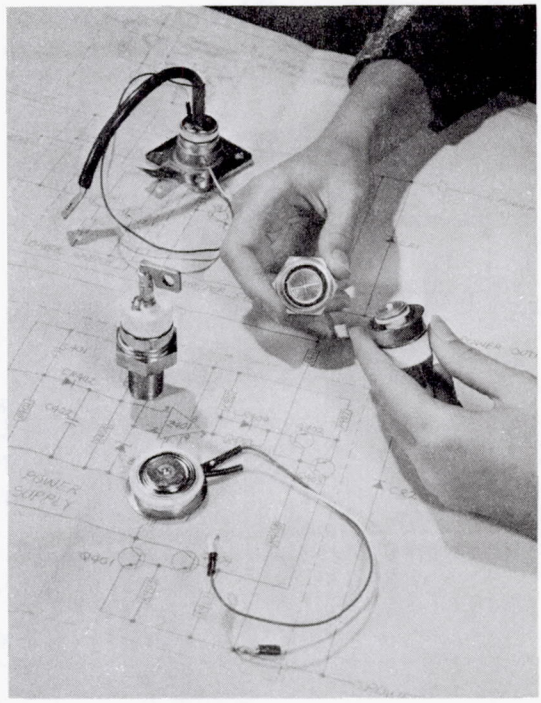

Figure 2. - High-power switching transistor D60T.

FEATURES

- VOLTAGE: 400 TO 500 VOLTS
- CURRENT: 100 TO 150 AMPERES @ GAIN OF 10
  400 AMPERES PEAK
- POWER HANDLING: 50 KILOWATTS
- POWER DISSIPATION: 2 kW @ 75°C
- RISE AND FALL TIMES: 0.75 MICROSECOND
- STORAGE TIME: 4 MICROSECONDS
  LOW SATURATION AND PER CYCLE SWITCHING LOSSES

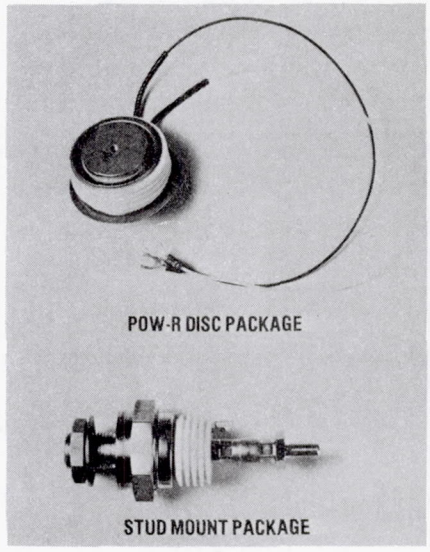

APPLICATIONS

- 25-50 kW HIGH FREQUENCY INVERTERS
- VSCF CONVERTERS IN MILITARY AIRCRAFT
- ELECTRIC VEHICLE MOTOR CONTROLLERS
- DC MOTOR CONTROLLER FOR SPACE SHUTTLE ACTUATOR
- 100 kW VLF TRANSMITTERS
- 50 kHz RF INDUCTION HEATERS
- POWER SUPPLIES FOR CONSUMER AND INDUSTRIAL APPLICATIONS

BENEFITS TO NASA

- DOUBLES CAPABILITY OF PREVIOUS IR-100 AWARD WINNING D60T TRANSISTOR
- COMMERCIALLY AVAILABLE IN QUANTITY AT REASONABLE COST
- MAKES POSSIBLE 50 kW SPACE POWER SYSTEM CONVERTERS AND POWER CONTROLLERS WITHOUT PARALLELLING OF TRANSISTORS
- EXPECT IMPORTANT USES ALSO IN AIRCRAFT POWER DISTRIBUTION AND CONTROL
- ESTABLISHES TECHNOLOGY FOR LARGER AREA, HIGHER POWER TRANSISTORS

Figure 3. - High-power switching transistor D7ST.

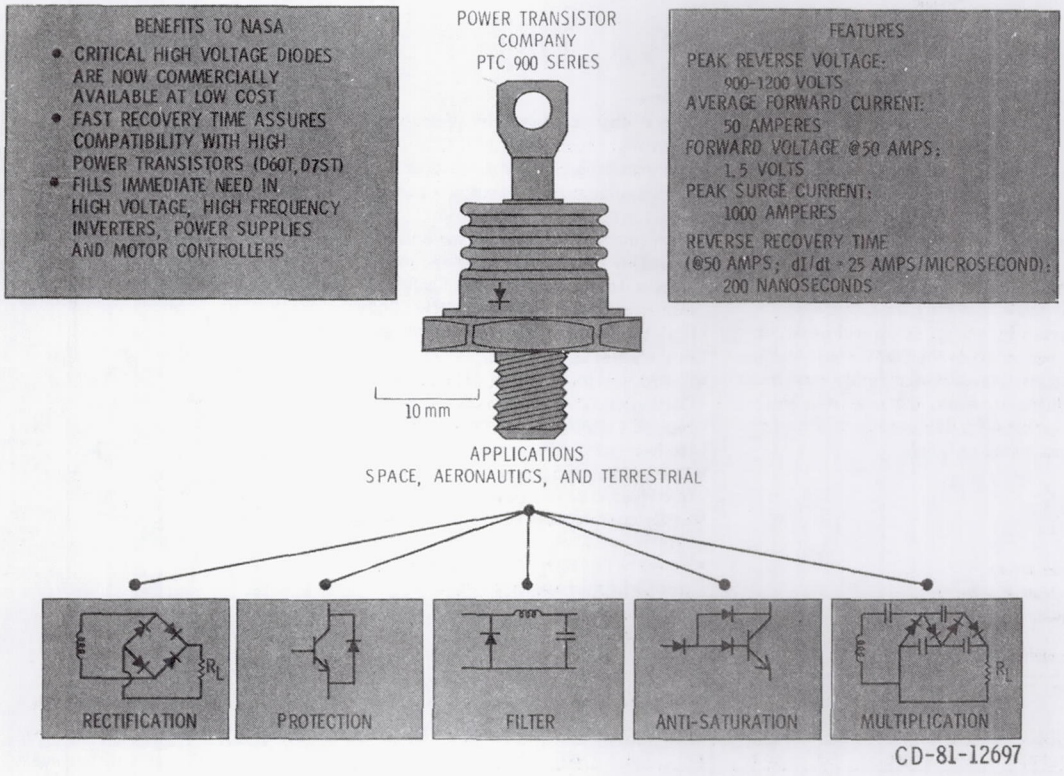

Figure 4. - Fast-recovery, high-voltage power diode.

BBT

Building Block Transistors

REVOLUTIONARY NEW POWER TRANSISTORS

These are the power transistors whose performance have attracted so much attention both in Japan and elsewhere. These have been manufactured using the planar process techniques specially improved by FUJI and can be recommended with confidence.
Only one element is sufficient to carry such a heavy current as 100A (V_{CEO} (sus) 450V) and they are suitable for inverters for the speed control of AC or DC motors up to the 10kW class and for constant voltage power supply equipment. BBTs have uniform characteristics and can be connected in parallel to provide capacities up to 60kW.

Features

- High voltage, large capacity (V_{CEO}(sus): 450 volts, Ic cont: 100 Amps)
- The scattering effect is reduced to a minimum as a result of employing the planar process of manufacture.
- Uniform characteristics allows units to operate in parallel and to be applied to motors drawing 60kW. (The FUJI transistor inverter series FRENIC5000G have already incorporated this element in the series up to 22kW).
- In addition to the single (2SC2770) and Darlington (2SD1066) a compound type (ET102) with a built-in fast recovery diode is also available.
- The molded package protects the unit from humidity and heat.
- Easily connected to heat sinks. (Cooling fin)
- Screw terminals for the emitter and base grouped conveniently together to simplify connection.
- Compactly designed.

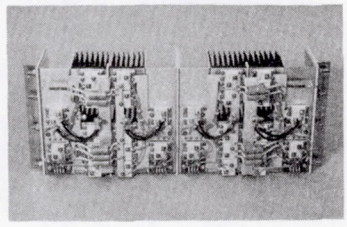

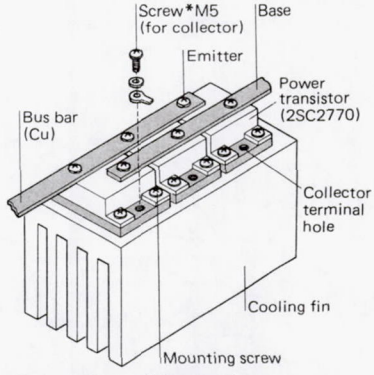

Example for parallel connection
Note: *When the heat sink is isolated from the base use the collector terminal.

Applications

- Industrial inverters
- Power supply equipment

■Specifications

Type	V_{CBO} volts	V_{CEO} volts	V_{CE} (SUS)	Ic amps.	Pc watts	h_{FE} min.	Ic amps.	V_{CE} volts	Switching time ton μs	ts μs	tf μs
2SD1066	600	600	450	100	770	100	100	5	4	12	4
2SC2770	600	600	450	100	770	8	60	5	4	8	3

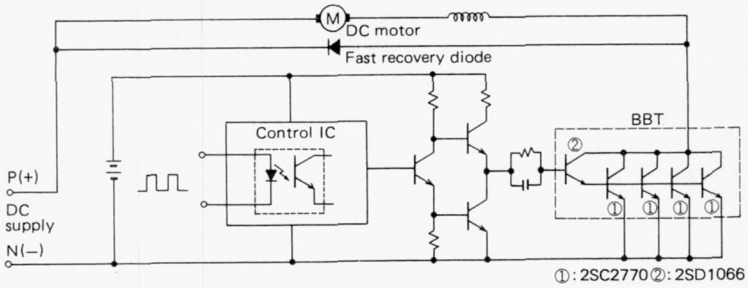

①: 2SC2770 ②: 2SD1066

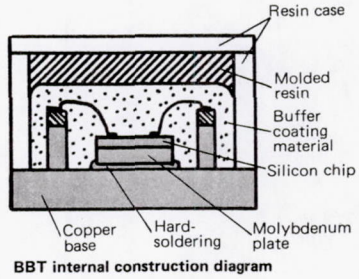

BBT internal construction diagram

Fuji Electric Co.,Ltd.

New Yurakucho Bldg.,
12-1 Yurakucho 1-chome, Chiyoda-ku,
Tokyo, 100 Japan
Phone: Tokyo 211-7111
Telex: J22331 FUJIELEC
Cable Address: DENKIFUJI TOKYO

Figure 5. - Data sheet showing revolutionary new power transistors.

MOTOROLA

SEMICONDUCTORS

P.O. BOX 20912 • PHOENIX, ARIZONA 85036

Designer's Data Sheet

MJ10050

50 AMPERE
NPN SILICON
POWER DARLINGTON
TRANSISTOR
850 VOLTS
500 WATTS

50 KVA SWITCHMODE TRANSISTOR
50-Ampere Operating Current

The MJ10050 Darlington transistor is designed for industrial service under practical operating environments found in switching high power inductive loads off 460-Volt lines.

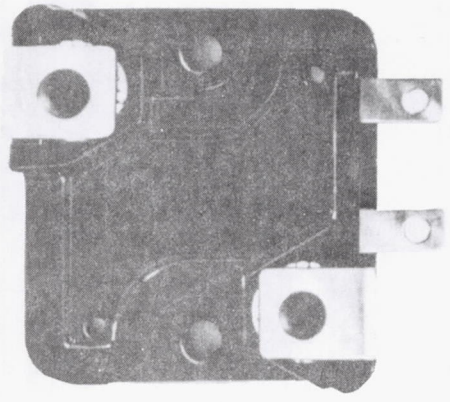

Actual Size

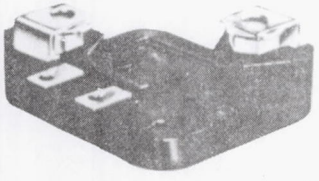

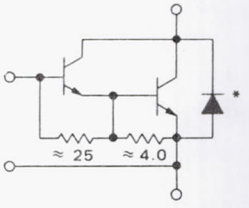

*Emitter-Collector Diode is a high power diode.

Designer's Data for
"Worst-Case" Conditions

The Designer's Data Sheet permits the design of most circuits entirely from the information presented. Limit data—representing device characteristics boundaries—are given to facilitate "worst-case" design.

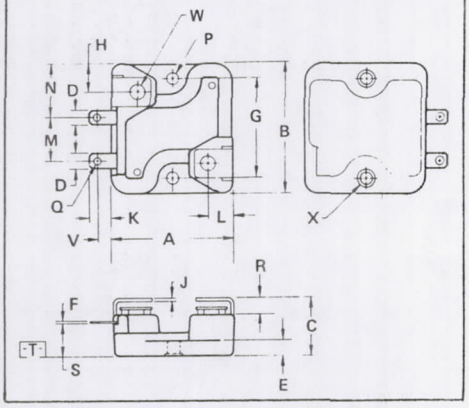

Figure 6. - Data sheet showing Darlington power transistor.

POWERLITHIC™ MODULE

PPM series

ELECTRICAL SPECIFICATIONS

	I_C MAX Note 1	I_C CONT Note 2	I_C SAT Note 3	I_B MAX	V_{CEO} (SUS)	MAX. OPER. FREQ.	Without Antisaturation Diode			With Antisaturation Diode (See Figure 1)		
							t_r	t_s	t_f	t_r	t_s	t_f
PPM30015A	300A	175A	150A	4A	150V	10KHZ	1 μs	5 μs	1 μs	1 μs	2 μs	1 μs
PPM40015A	400A	250A	200A	4A	150V	10KHz	1 μs	5 μs	1 μs	1 μs	2 μs	1 μs
PPM60015A	600A	375A	300A	4A	150V	10KHz	1 μs	5 μs	1 μs	1 μs	2 μs	1 μs
PPM12040A	120A	75A	60A	4A	400V	10KHz	1 μs	10 μs	2 μs	1 μs	4 μs	2 μs
PPM20040A	200A	125A	100A	4A	400V	10KHz	1 μs	10 μs	2 μs	1 μs	4 μs	2 μs
PPM30040A	300A	185A	150A	4A	400V	10KHz	1 μs	10 μs	2 μs	1 μs	4 μs	2 μs
PPM4090A	40A	30A	20A	4A	900V	10KHz	1 μs	20 μs	4 μs	1 μs	8 μs	4 μs
PPM6090A	60A	45A	30A	4A	900V	10KHz	1 μs	20 μs	4 μs	1 μs	8 μs	4 μs
PPM8090A	80A	60A	40A	4A	900V	10KHz	1 μs	20 μs	4 μs	1 μs	8 μs	4 μs

NOTE 1: I_C MAX measured at $V_{CE}=[V_{CEO}$ (sus)].
I_B with Base Drive is $[I_B=I_{B1}=I_{B2}=I_B$ MAX]
at V_{EB}=5v for duration (t=10 μs single pulse)

NOTE 2: $I_{C\,CONT}$ is defined as the continued current obtained
at V_{CE}=10v when Maximum Base Current
$I_{B1}=I_B$ MAX is applied at the Base.

NOTE 3: Saturation Current $I_{C\,SAT}$ is obtained when
$I_B=I_B$ MAX and V_{CE}=2.5V. Duty cycle=2% (@300 μs pulse width)
measured by using a KELVIN Bridge.

MECHANICAL SPECIFICATIONS (Dimensions in inches)

$R_{\theta JC}$: Non-isolated copper base plate, 0.12°C/W. Isolated black anodized aluminum base plate, 0.30°C/W.

HIGH POT: 1500 Volts minimum between collectors and heat-sink mounting of isolated case (black anodized alum, case).

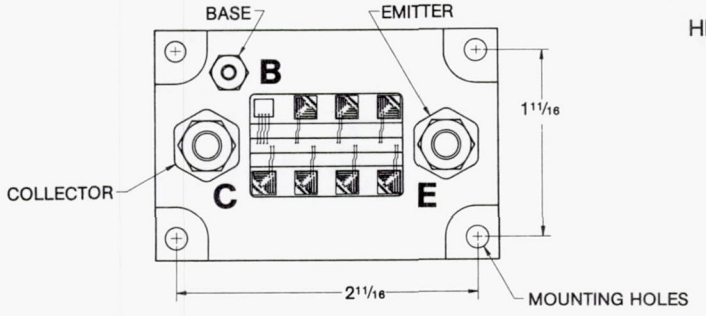

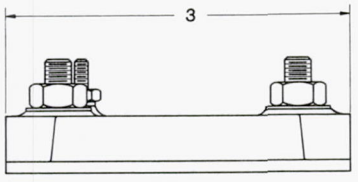

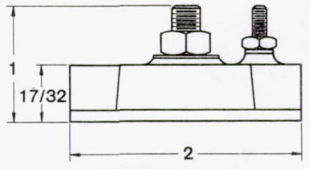

POWER TRANSISTOR COMPANY

800 W. CARSON ST., TORRANCE, CA 90502 (213) 320-1190

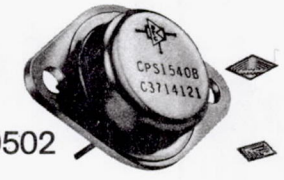

Figure 7. - Data sheet showing electrical specifications of power transistors.

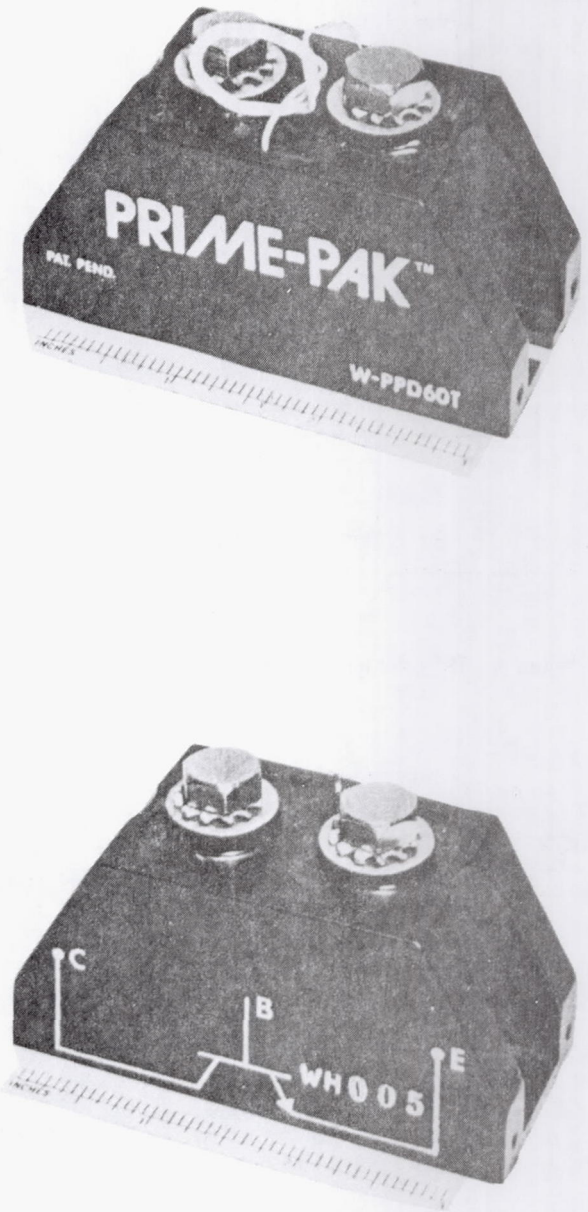

Figure 8. - Thermal Associates' "Prime-Pak."

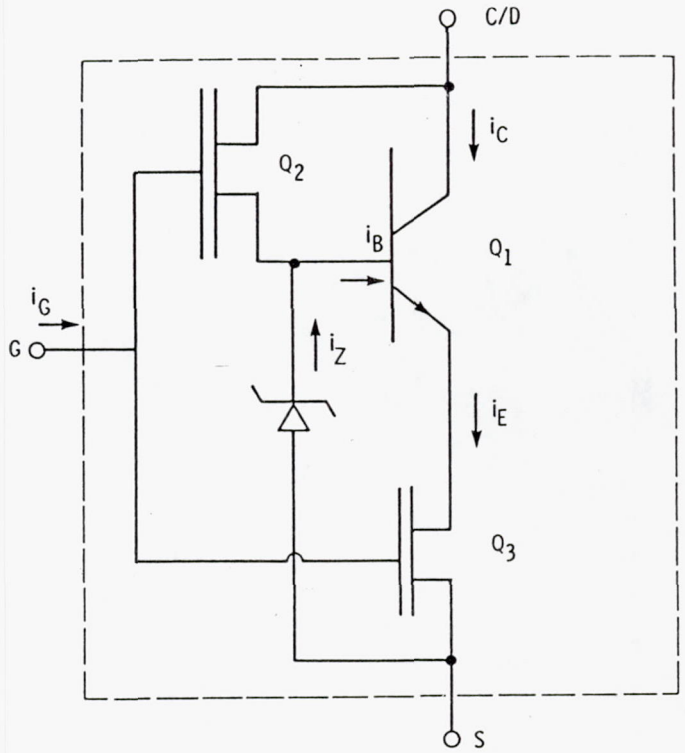

Figure 9. - FET-gated bipolar power transistors (FGT).

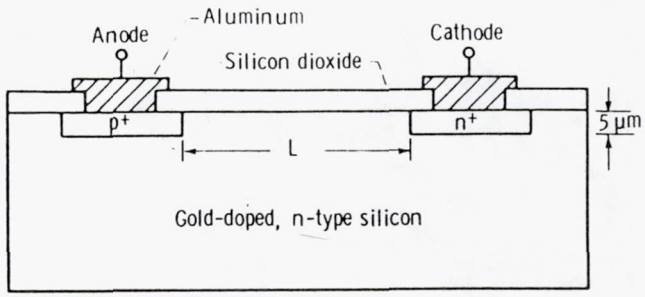

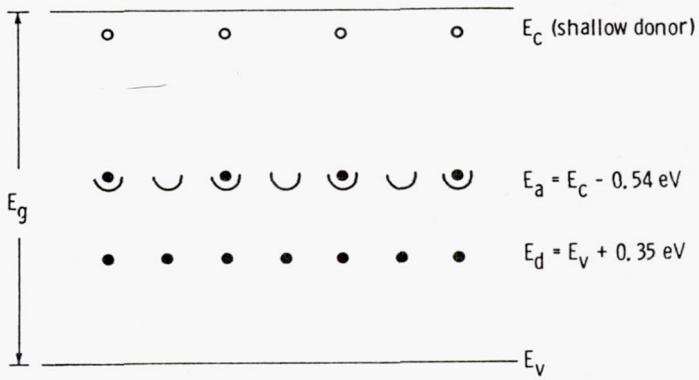

Figure 10. - Cross section and energy level diagram of double-injection deep-impurity switch.

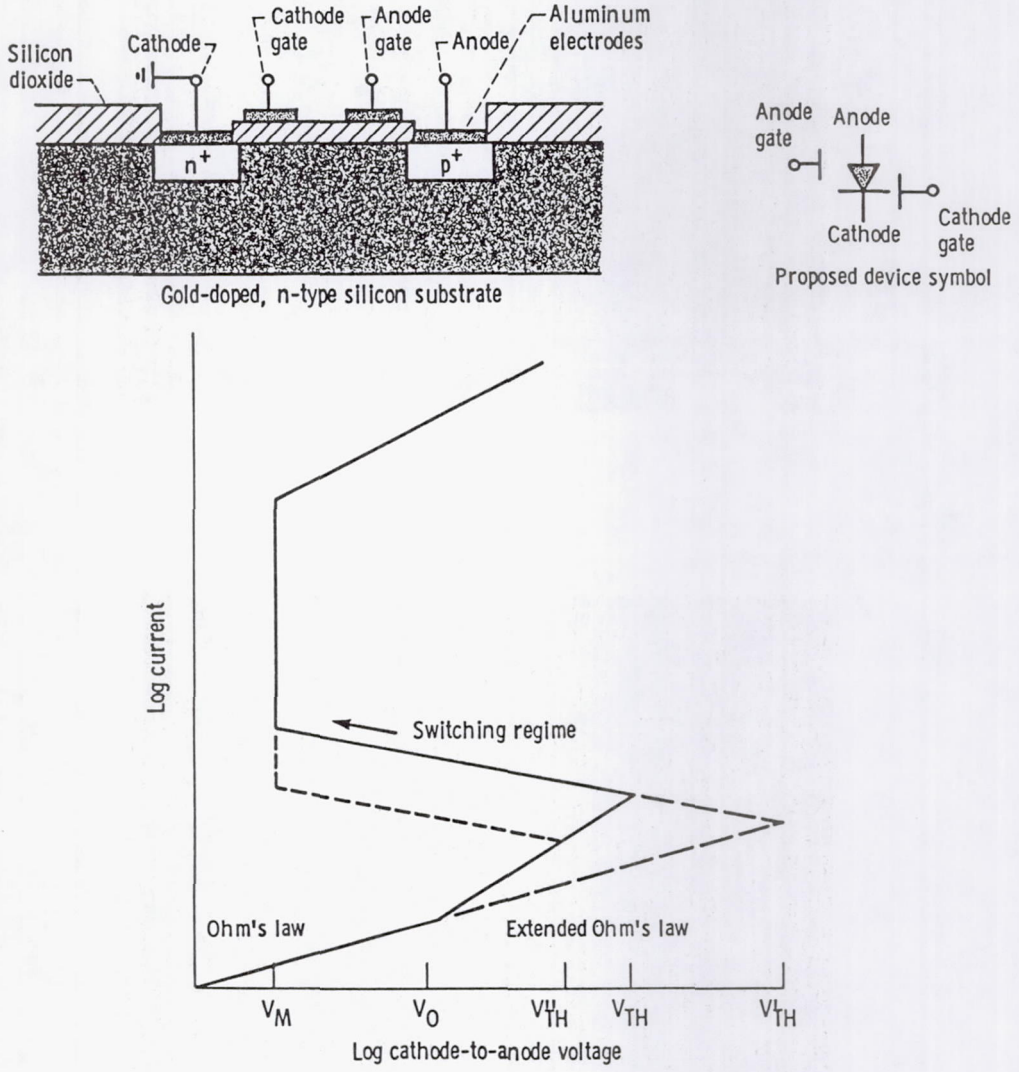

Figure 11. - Volt-ampere characteristic showing voltage gating.

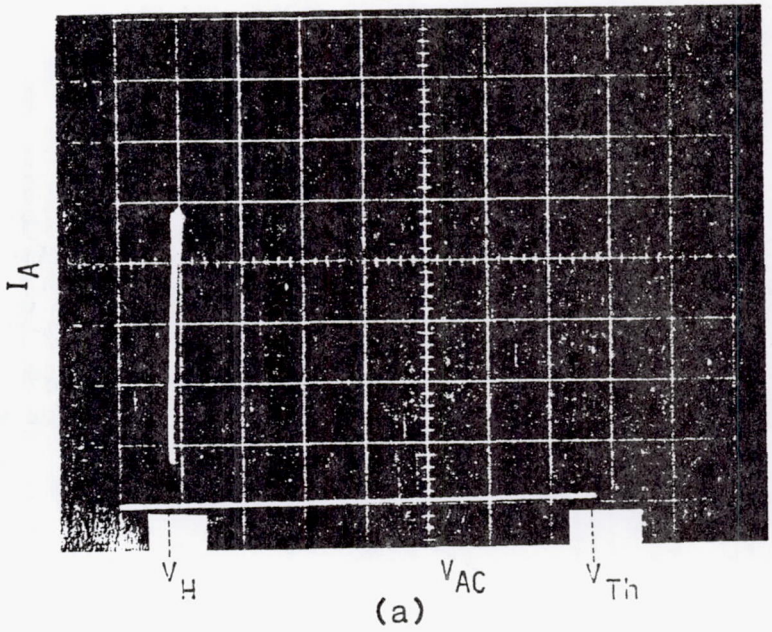

(a)

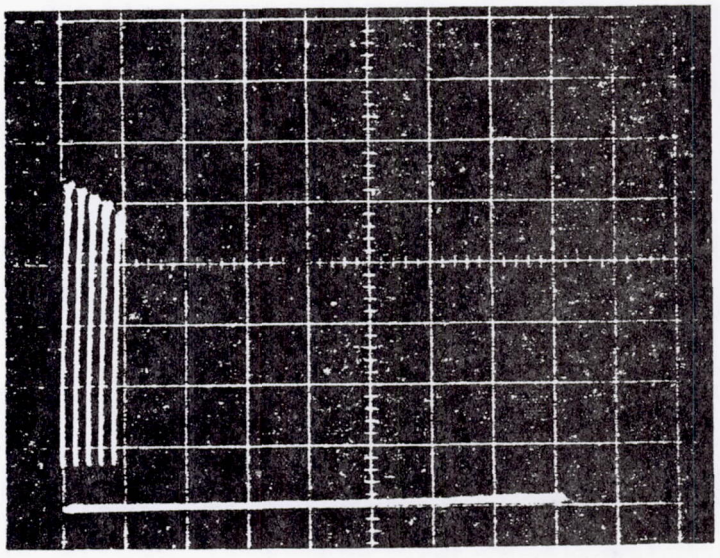

(b)

Figure 12. - Oscilloscope traces showing switching characteristics of injection-gated device.

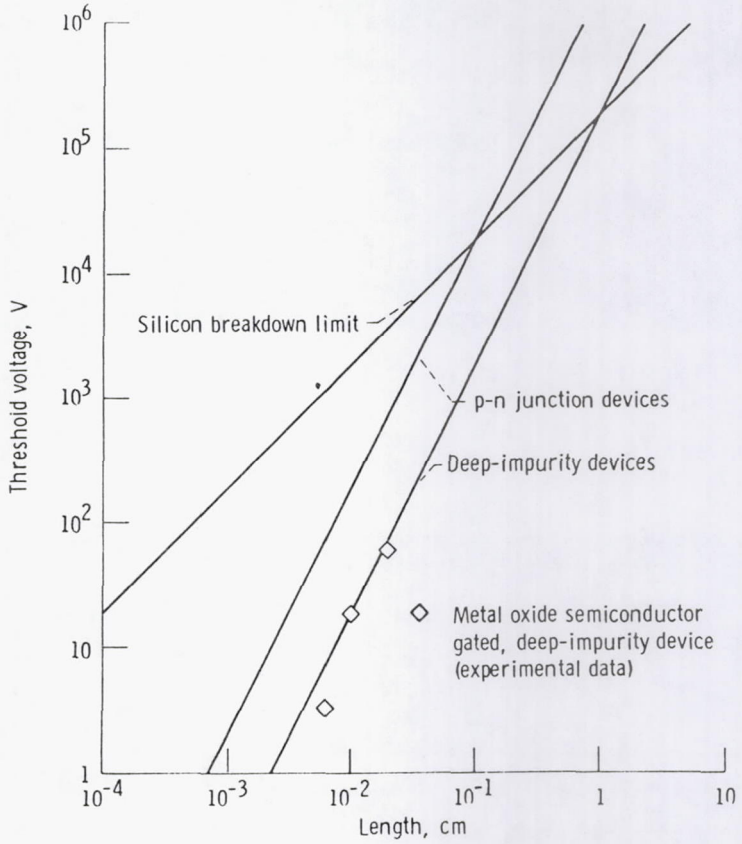

Figure 13. - Voltage limitations in silicon.

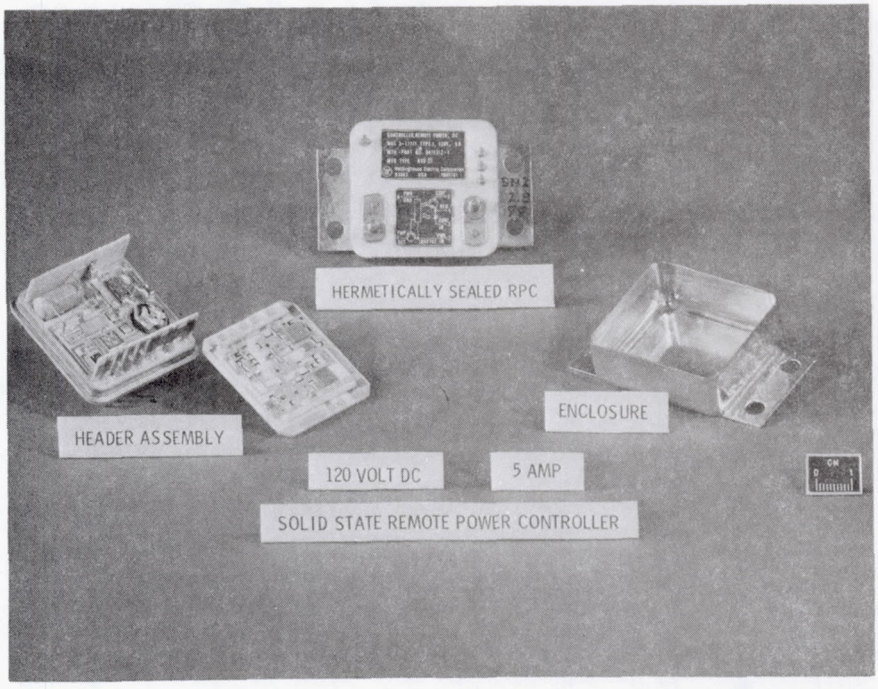

Figure 14. - 120-V, 5-A solid-state remote power controller.

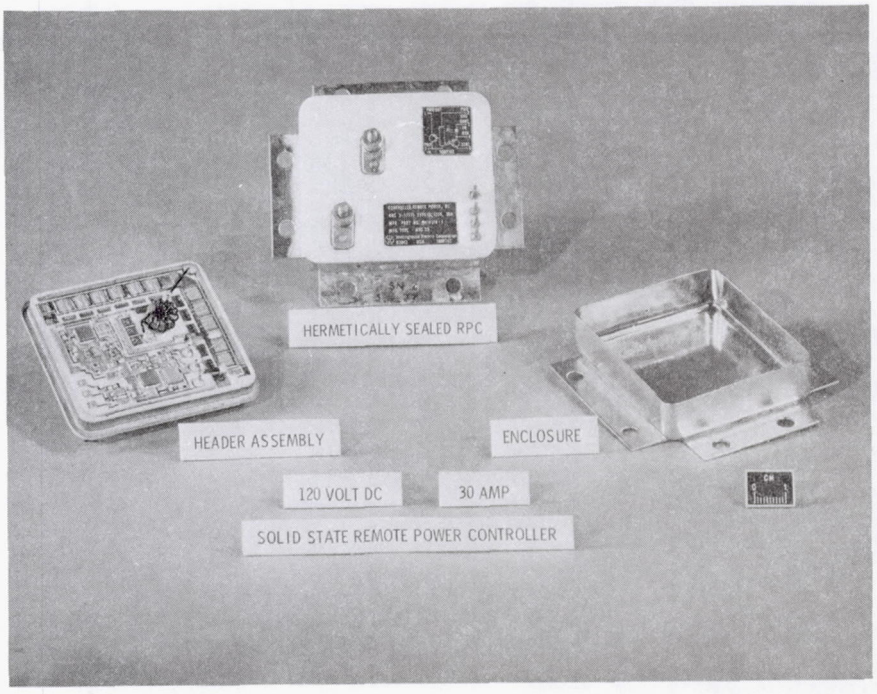

Figure 15. - 120-V, 30-A solid-state remote power controller.

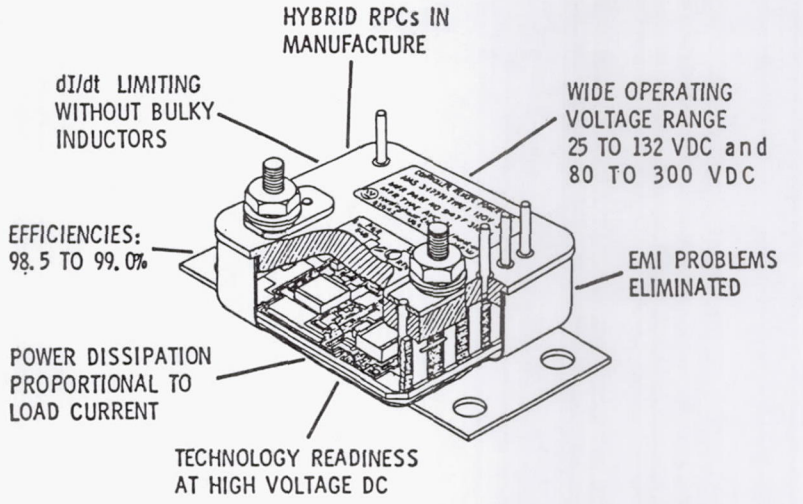

Figure 16. - Advantages of solid-state remote power controller.

LIGHTWEIGHT, HIGH-FREQUENCY TRANSFORMERS

Gene E. Schwarze
National Aeronautics and Space Administration
Lewis Research Center
Cleveland, Ohio 44135

The weight of a power electronic transformer can be reduced in three ways. One way is to increase frequency. As frequency is increased, the cross-sectional area of the core can decrease. The kilovolt-amperage rating of a transformer is proportional to frequency, flux density, and current density. The second way is to use high current density in the windings. When the kilovolt-amperage rating is held constant, increasing the frequency has to decrease the cross-sectional area. Also, increasing current density must decrease the cross-sectional area of a conductor for a given current. This causes a decrease in the window area and reduces the size and weight of the transformer.

The third and perhaps the major way is thermal management or thermal control. Maximum use must be made of good heat transfer techniques. Of course, in the space environment, conduction is the method of thermal management. Another, but minor, method is radiation. You attempt to build as many thermal paths as possible in your device and also to use high-thermal-conductivity materials. That is not just restricted to the insulation systems but applies even to such things as the core material. To dissipate the heat from the core losses, you must also use a high-thermal-conductivity material.

Figure 1 compares space and commercial transformers. The 25-kVA space transformer was developed under contract by Thermal Technology Laboratory, Buffalo, N. Y.

The NASA Lewis transformer technology program attempted to develop the baseline technology. We chose to start at the 25-kVA level. Future projections are for megawatt transformers. For the 25-kVA transformer the input voltage was chosen as 200 V, the output voltage as 1500 V, the input voltage waveform as square wave, the duty cycle as continuous, the frequency range (within certain constraints) as 10 to 40 kHz, the operating temperatures as 85° and 130° C, the baseplate temperature as 50° C, the equivalent leakage inductance as less than 10 μH, the operating environment as space, and the life expectancy as 10 years. Such a transformer can also be used for aircraft, ship, and terrestrial applications.

Figure 2 shows the mechanical structure of the 25-kVA transformer. Basically the mechanical structure consists of three parts: the plates, the clamps, and the baseplate. The plates provide the conduction cooling for the windings. There are eight plates; each plate is approximately 1/10th inch thick. The plates are slit from the top of the core tube to the top of the plate to prevent the plate from acting as a shorted turn. The plates then conduct the heat down to the baseplate. Each plate has a foot that is mechanically fastened to the baseplate. We use a double "C" core arrangement. The material used in this particular application was 80Ni-20Fe, known as Supermalloy. The clamps and supports mechanically are fastened to the baseplate. For good thermal transfer the underside of the core is ground smooth to give good contact.

Figure 3 shows the finished product. Kapton sheets are bonded to the cooling plates, and then the windings are bonded to the Kapton. The windings are pie or pancake type with the primary winding on one side of a plate and

the secondary winding on the other side. The primary windings are connected in parallel by the two large bus bars on the top of the transformer. The primary current is fed from both ends of the bus bars. The secondary windings are connected in series, and the output terminals are shown on the right side of the transformer extending at a 45° angle.

The primary and secondary resistances were measured by a four-terminal Kelvin bridge, and the temperature correction was applied. The primary had a resistance of 4.7 mΩ. The equivalent leakage inductance was measured with an impedance bridge. Since we wanted to reflect the leakage inductance to the primary, the secondary was short circuited. As a result the inductance was less than 2 μH. The goal was an inductance of less than 10 μH.

The two components of loss are the primary and secondary I^2R loss and the core loss (table I). The primary loss is 74 W, or approximately 38 percent of the total loss. The secondary loss is somewhat lower, 62 W, or about 32 percent of the total. The total I^2R loss is 36 W, or 69 percent of the total. The core loss is 60 W, or about 31 percent of the total. There is almost an equal division of loss between the primary, secondary, and core losses. Total loss is 196 W. Calculating the transformer efficiency from the total loss results in a value of 99.2 percent.

The weight breakdown (table II) shows the lightweight features of the transformer. The magnetic core weighs 1.53 lb, or 22 percent of the total weight. The coils and bus bar assembly are 1.92 lb, or 28 percent. The structural components, which include the mounting plates, the core supports and brackets, and the baseplate, weigh 2.5 lb, or 36 percent of the total. The insulators weigh 0.47 lb, or 6.8 percent. The fasteners weigh 0.53 lb, or 7.6 percent. The magnetic core and the coils and bus bar assembly weights, the active part of the transformer, add up to 50 percent. The structural components, insulator, and fastener weights also add up to 50 percent. However, in parametric studies, many times the last three weights are ignored.

Total weight is 6.95 lb. Specific weight is 0.28 lb/kVA. Specific power is 3.6 kVA/lb.

The lightweight, high-frequency transformer was a space-program development but can be used for aircraft, shipboard, and terrestrial applications in lightweight, high-frequency dc converters or high-frequency ac distribution systems. The technology developed in this program certainly should be transferable to other power-magnetic components.

TABLE I. - 25-kVA TRANSFORMER LOSS AND EFFICIENCY

DESCRIPTION	LOSS (WATTS)	% OF TOTAL
PRI. WDG I^2R	74	37.8%
SEC. WDG I^2R	62	31.6%
TOTAL I^2R	136	69.4%
CORE	60	30.6%

- TOTAL TRANSFORMER LOSS - 196 WATTS
- TRANSFORMER EFFICIENCY: 99.2%

TABLE II. - 25-kVA TRANSFORMER WEIGHT BREAKDOWN

DESCRIPTION	WEIGHT (LBS)	% TOTAL WEIGHT
MAGNETIC CORE	1.53	22.0%
COILS & BUS BAR ASSY	1.92	27.6%
STRUCTURAL COMPONENTS	2.50	36.0%
INSULATORS	0.47	6.8%
MECHANICAL FASTENERS	0.53	7.6%

- TOTAL WEIGHT - 6.95 LBS
- SPECIFIC WEIGHT- 0.28 LB/KVA (0.13 Kg/KVA)
- SPECIFIC POWER - 3.6 KVA/LB (7.92 KVA/Kg)

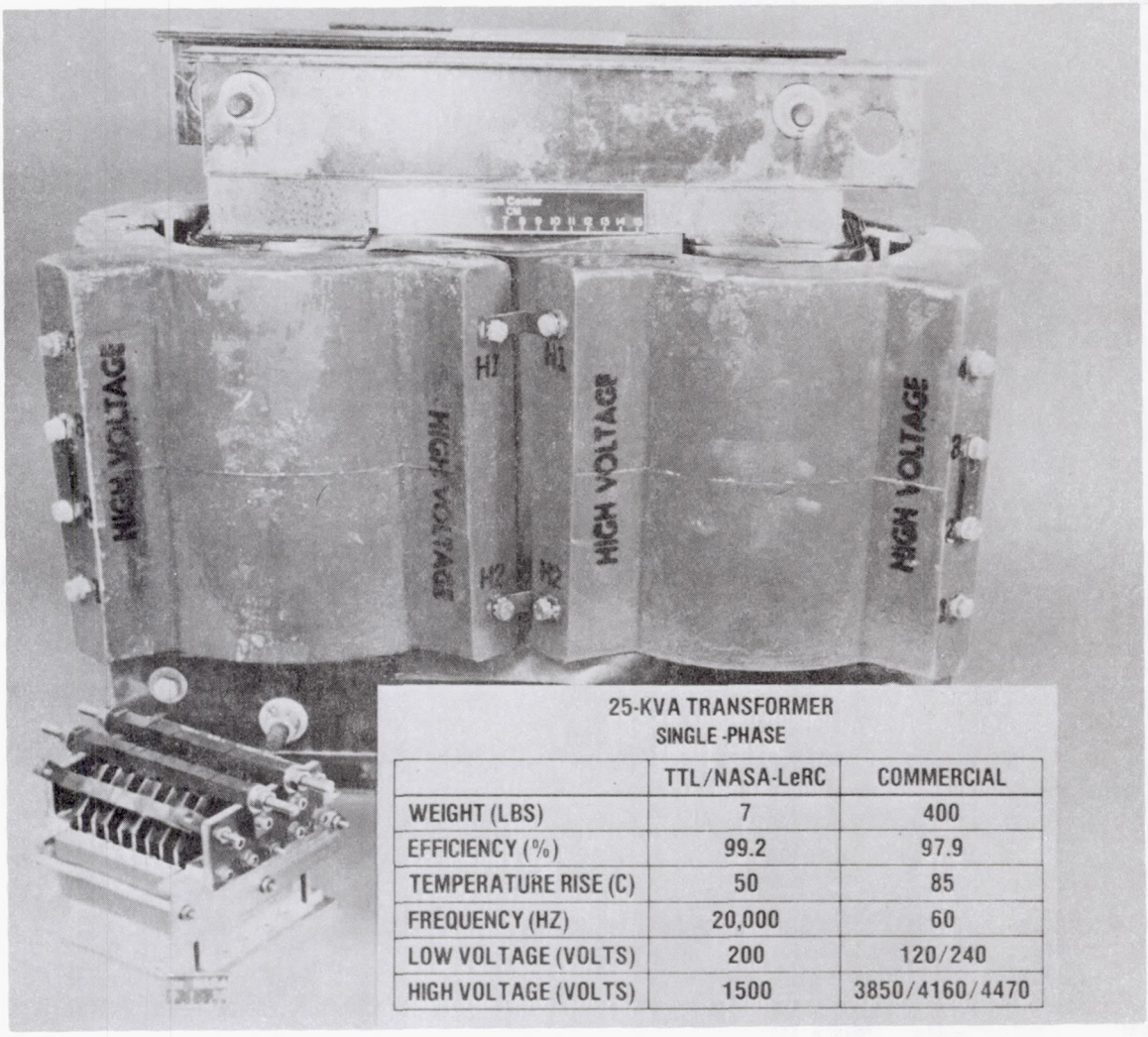

25-KVA TRANSFORMER
SINGLE -PHASE

	TTL/NASA-LeRC	COMMERCIAL
WEIGHT (LBS)	7	400
EFFICIENCY (%)	99.2	97.9
TEMPERATURE RISE (C)	50	85
FREQUENCY (HZ)	20,000	60
LOW VOLTAGE (VOLTS)	200	120/240
HIGH VOLTAGE (VOLTS)	1500	3850/4160/4470

Figure 1. - Comparison of space and commercial 25-kVA single-phase transformers.

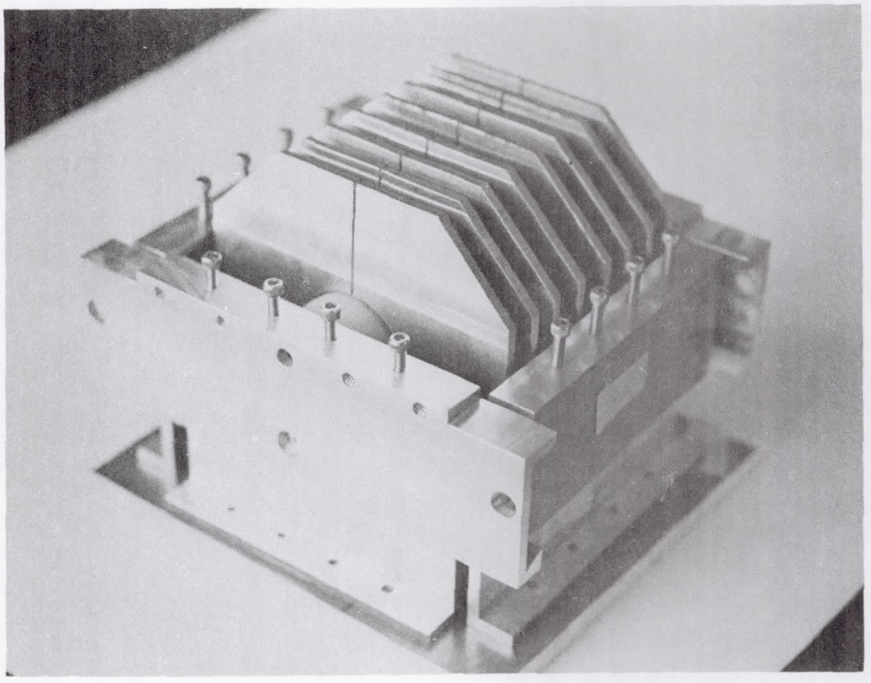

Figure 2. - Mechanical structure of 25-kVA transformer.

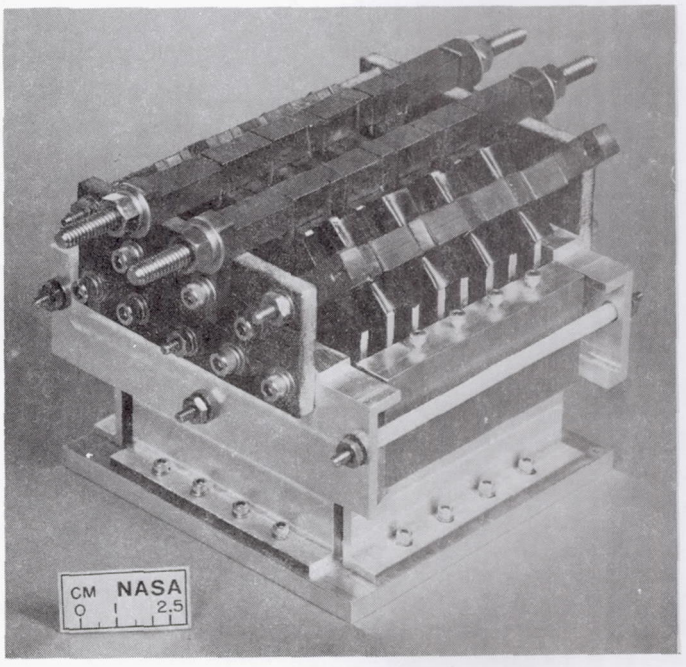

Figure 3. - 25-kVA transformer.

HIGH-CURRENT, HIGH-FREQUENCY CAPACITORS

David D. Renz
National Aeronautics and Space Administration
Lewis Research Center
Cleveland, Ohio 44135

The NASA Lewis high-current, high-frequency capacitor development program was conducted under a contract with Maxwell Laboratories, Inc., San Diego, California. The program was started to develop power components for space power systems. One of the components lacking was a high-power, high-frequency capacitor. Some of the technology developed in this program may be directly usable in an all-electric airplane.

The materials used in the capacitor included the following: the film is polypropylene, the impregnant is monoisopropyl biphenyl, the conductive epoxy is Emerson and Cuming Stycast 2850 KT, the foil is aluminum, the case is stainless steel (304), and the electrode is a modified copper-ceramic.

POLYPROPYLENE FILM

The physical makeup of the various polymer films is vital to the performance of the films as a capacitor dielectric, and particularly so when the longevity of the capacitor in service is so important.

Therefore the contractor was requested to analyze six films. The results are listed in table I. The film that rated the highest was polypropylene, which is the one Lewis chose. The scoring was arbitrary, but everything was scored equally. For the parameters of interest - frequency, voltage, and dielectric breakdown - it is evident that polypropylene film exhibits significant superiority for the application:

(1) Polypropylene films have lower density than the other films being considered, thus resulting in reduced capacitor weight and higher power density.

(2) Polypropylene films wet better than the other films and absorb oil to a greater degree, thus reducing the chance of damage from partial discharges during operation.

(3) Polypropylene polymer has greater crystallinity and is inherently more stable during service than the other films.

(4) Polypropylene's unique combination of temperature coefficient of dielectric constant and dissipation factor result in natural self-stabilization at a temperature just above that of the plate.

(5) The film quality of polypropylene has been raised to a very high order by the film manufacturers because of the competitive situation in the industry and because the capacitor industry is so important to the electric power industry. None of the other films tested had the uniform quality and low level of contamination of polypropylene.

(6) The superior dissipation factor of polypropylene film permits significantly greater power transfer without thermal runaway. This factor alone is so dominant in the selection process as to relegate all other films to lower status.

IMPREGNANT

The impregnant monoisopropyl biphenyl (MIPB) has extreme resistance to gamma radiation, low dielectric loss, and high corona resistance. It was absorbed well by the polypropylene (which was one of the tests that all of the films were subjected to), and it has good wetting characteristics. A good point was that the source of MIPB is in this country whereas some of the other impregnants are only available from foreign sources.

CAPACITIVE ELEMENTS

The design of the capacitor is shown in figure 1. There are two layers of polypropylene film between a split roll of aluminum foil and a floating foil. In each element this puts two capacitors in series, that is, from one connected foil to the floating foil in series with the other connected foil to the floating foil. This construction technique reduces the potential across the dielectric to half what it would be in a conventional capacitor. Using this technique reduces the potential gradient across the dielectric film and thus enhances life. One basic flaw in this thin film is the pinholes. Using two sheets of dielectric protects against pinhole short circuits.

To reduce the interfoil voltage of each element to a value that would provide the highest degree of performance reliability but could still be efficiently accommodated by the thicknesses of available dielectric materials, each capacitor element - or pad - is designed with two series-capacitor sections. To decrease the voltage yet further, two elements are then connected in series, thus reducing the ac voltage to 150 V rms. At this point there should be no partial discharges at the full capacitor operating voltage of 600 V rms plus 600 V dc bias.

The formidable rms current consistent with operating at maximum applied voltage and maximum frequency is to be dealt with by paralleling two series-connected element assemblies. This divides the current and reduces the 125 A to 62.5 A/pad, which can be handled by extended foil design of the elements.

CONDUCTOR-ELEMENT ASSEMBLY

Although the type of capacitor element assembly shown in figures 2 and 3 obviously leaves something to be desired in space utilization, the inefficiency is more apparent than real and the design gains more than it loses. The element assembly must be inherently very stable mechanically and must be extremely secure to withstand the vibration and shock associated with space vehicles. This element assembly will pass a Class III vibration test and will be safe from damage due to acceleration and shock. Electrical integrity will be maintained over the service life stipulated for this component.

The assembly of four elements is secured to the capacitor base in a layer of special epoxy resin that has the dual function of transferring heat from the bottom exposed foils directly to the capacitor base and then to the lower mounting bracket. The epoxy is Emerson and Cuming Stycast 2850KT, a material of exceptional thermal conductivity, low shrinkage, high-temperature resistance, and low-temperature coefficient of expansion.

TERMINATION

A modified bushing design (fig. 4) was employed to bring a terminal (stud) of sufficient size through the bushing to handle the highest rms current. By this means resistive losses of the terminals were reduced to less than 4 W under maximum operating conditions. A low-profile bushing configuration would be even better, but such an insulator was not available. A layer of epoxy similar to that used internally to secure the elements was poured into the reentrant cover, around the terminals, and over the seal-off plug after the capacitor was fully impregnated and seal tested. This material helps transfer heat from the bushings to the mounting bracket and from the case to the lower mounting bracket; it also provides a redundant oil seal around the bushing flanges and over the seal-off plug.

The characteristics of the capacitor Lewis has built and tested are shown in figure 5. The capacitor operates at 600 V rms while biased at +600 V dc. The size is 0.83 μF, and the frequency is 40 kHz. It tested at 40 and 10 kHz. The design loss is less than 30 W. The temperature range is -40° C to +88° C and the volt-ampere rating is 75 kVAR. The capacitor weighs 7.9 lb.

CAPACITOR CASE

Although not immediately apparent from figure 5, this capacitor is inherently very rugged, and the hermetic seal will be maintained over the operational life. The case material, 20-g 304L stainless steel, was chosen for its strength, stability, and weldability and to provide minimum eddy current losses at the maximum operating frequency. Both cover and base are of "reentrant" configuration, to assure minimum heat damage to the interior materials during the welding operation after assembly. The only welding done after assembly of the elements into the case was the weld around the periphery of the cover.

The design loss in the four elements for the 75-kVAR unit is 15 W. There will be 2 W in the foil and 4 W going from the copper bus bars up to the terminals. So the total design loss is 21 W, which is low when compared with the amount of power flowing through the capacitor, 600 V at 125 A.

CORONA TESTING

Another test that was done was to take the split foil, build a parallel pad, and perform corona testing. When the foil was dry (no impregnant), the inception voltage was 1400 V and the extinction voltage was 1250 V. With the impregnant the inception voltage went up to 3200 V and the extinction voltage to 2800 V. Maximum peak operating voltage would probably be 1200 V or less. Therefore the capitator should not fail due to corona.

It is worthwhile to explain here the concern with the values of corona inception voltage (CIV) and corona extinction voltage (CEV) on the capacitor windings (pads) to be installed in the capacitors being prepared for vacuum endurance testing. It is generally accepted that electrical failure of a capacitor operated on alternating current is preceded by increasing partial electrical discharges (corona) in the capacitive elements. The locally generated extremely high temperatures cause deterioration of the insulating materials, both solid and liquid; and the gaseous byproducts of this deterioration either remain in the area of high electrical stress or are dissolved in the impregnant. In either event the result is progressive damage to the

insulation, and the partial discharges increase to an avalanche condition, resulting in electrical failure.

If the CIV value measured on a given capacitor is at least twice the normal operating voltage, it is considered safe to assume that capacitor failure, when it inevitably comes, must result from progressive electrochemical changes in the elements. Such a condition will normally occur beyond the design life of the unit.

The CEV is the voltage at which partial discharges no longer occur, after inception has been brought about. The CEV is usually determined by increasing the applied ac voltage until CIV is obtained and then lowering the applied voltage until corona is no longer detectable. The significance of CEV lies in the fact that an ac capacitor is subjected to electrical transient stresses that are beyond the normal working stresses. If these transients are severe to the point that CIV is reached, no permanent harm will result if the CEV value is above the voltage applied after the transient condition is no longer present. For this reason, it is necessary that the CEV measured on the capacitor be greater than the normal operating voltage. However, it will be obvious that some safety factor must be present to allow for changes in capacitor characteristics over the operating life.

Model windings of the capacitor to be vacuum endurance tested have been prepared and the CIV and CEV measured at 60 Hz with no impregnant and after vacuum drying and impregnation with monisopropyl biphenyl.

The capacitors were tested at the two sets of conditions shown in table II. Condition A was the full power test; however, it was performed in air rather than vacuum because of induction heating in the vacuum tank.

500-HOUR VACUUM ENDURANCE TEST

The baseplate contained 10 capacitors, 5 on each side, as shown in figure 6.

Examination of the temperature rise values of the various areas of the capacitors (fig. 7) indicated that the fuses being connected directly to the stud of a capacitor bushing distorted the temperature conditions of the capacitor. The average temperature rise of the nearby thermocouples was 19.7 deg F; the average temperature rise of areas near unfused bushings was 8.3 deg F. Later calculation of the resistance of the 50-A fuses and determination of the heat loss in the fuses explained the temperature rise of the fused bushings. Needless to say, the 300-A fuses were located away from the capacitors during the 40-kHz vacuum endurance test.

Thermocouples 5 and 10 (fig. 6) represent center-of-cover temperature values of two capacitors in completely different locations on the temperature plate. Even so, the temperature rise values are the same - a modest 16 deg F in what would normally be the highest temperature point on a capacitor. Thermocouple 6 is the only one uniquely located, and it is on the front of the temperature plate. This is fortunate, since the rise of 26 deg F would otherwise have been difficult to explain. Although T6 is located in a normally low-rise area of a capacitor, the temperature rise in this case is the greatest of all points. The reason is that T6 is located at the confluence of four heavy cables, an area of the plate where one could expect maximum temperature.

Thermocouples 4 and 16 are identical points on capacitors on opposite sides of the temperature plate and would be expected to exhibit low values of temperature rise if the epoxy temperature transfer material was properly transferring the local interior heat collected by the bottom extended foils to the

bracket and then to the plate. There is a cable in proximity to T4, which may account for the slightly higher value than shown for T16. T16 was located on S/N 140355, near no cable, and should be expected to have the lowest temperature rise.

Figure 8 shows how the capacitors were crowded into the vacuum tank. Running this setup with 40 kHz caused ground loops in the tank. The tank heated up and two thermocouple cables completely melted. At 40 kHz and 600 V there was a lot of induction heating. Although we tried to modify the vacuum tank, finally the test had to be run in air.

The development program is completed. Capacitors have been tested under load, but we have not had the final design review. The capacitor is sturdy because it was overdesigned. It probably can be made 30 percent smaller.

TABLE I. - RESULTS OF FILM ANALYSES

1. Mylar
2. Polycarbonate
3. Kapton
4. Polypropylene
5. Polysulfone
6. Teflon

	Material					
	1	2	3	4	5	6
Dielectric Strength (Major) x 2	14	14	14	18	14	14
Dielectric Constant (Minor)	5	4	5	3	4	3
Dissipation Factor * (Major) x 2	4	10	6	18	12	14
Insulation Resistance (Minor)	7	9	10	9	6	9
Temp Coeff. of Diel. Constant * (Minor)	1	8	8	7	9	8
Temp Coeff. of Diss. Factor * (Major) x 2	2	16	6	20	10	18
Freq. Coeff of Diss. Factor * (Major) x 2	4	16	8	20	10	18
Chemical Stability (Major) x 2	14	14	18	12	14	16
Density * (Major) x 2	10	14	10	18	14	6
Impregnant Absorption (Major) x 2	4	6	4	14	6	2
Corona Resistance (Major) x 2	16	14	18	16	16	6
Radiation Resistance (Minor)	7	7	8	6	5	8
Thin Film Availability (Major) x 2	18	14	8	14	10	14
Specific Heat (Minor)	5	4	5	7	4	3
Cost * (Minor)	6	5	1	8	5	3
Total	117	155	129	190	139	142

* Parameters marked with asterisk are negative coefficients; ie, a high numerical value yields a low rating.

TABLE II. - TEST CONDITIONS

	Condition A	Condition B
Number of test samples	10	10
Temperature (±5° C), °C	25	25
Barometric pressure, torr	Air	10^{-3}
Applied voltage (±2 percent), V rms	600	600
Wave shape	Sine wave	Sine wave
Frequency (±1 kHz), kHz	40	10
dc bias (±2 percent), V dc	600	0
rms current (sample, ±5 percent), A	125	30

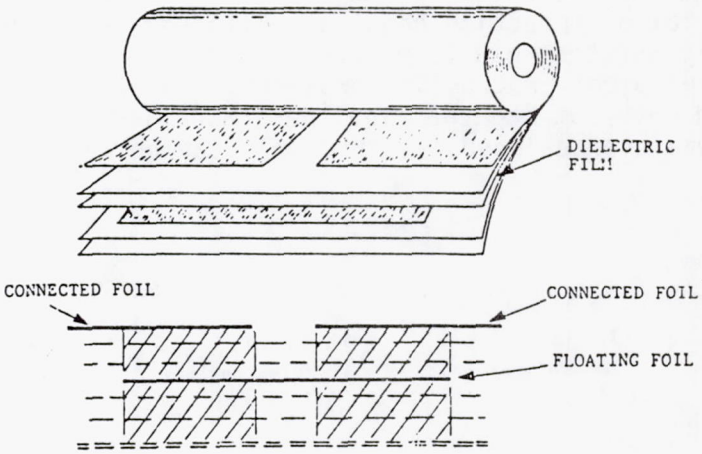

Figure 1. - Details of capacitor element.

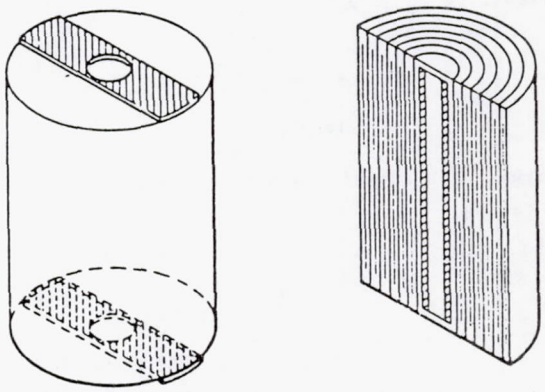

Figure 2. - Capacitor element.

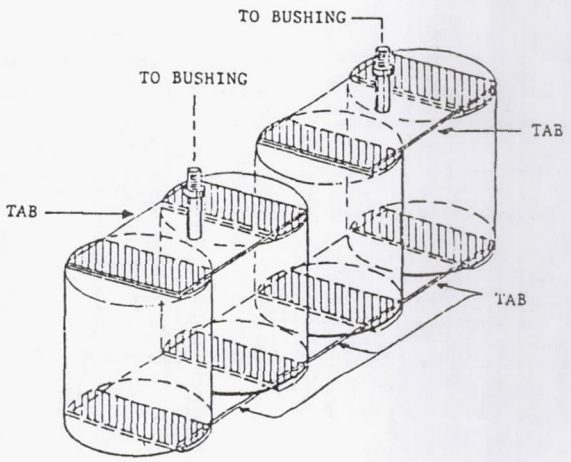

- INITIAL SOLDER SWAGING TO EXTENDED FOILS ACCOMPLISHED WITH J22 SOLDER
- TINNED COPPER TABS SOFT SOLDERED TO SWAGED PATTERN WITH 60/40 T-L SOLDER

Figure 3. - Capacitor element assembly.

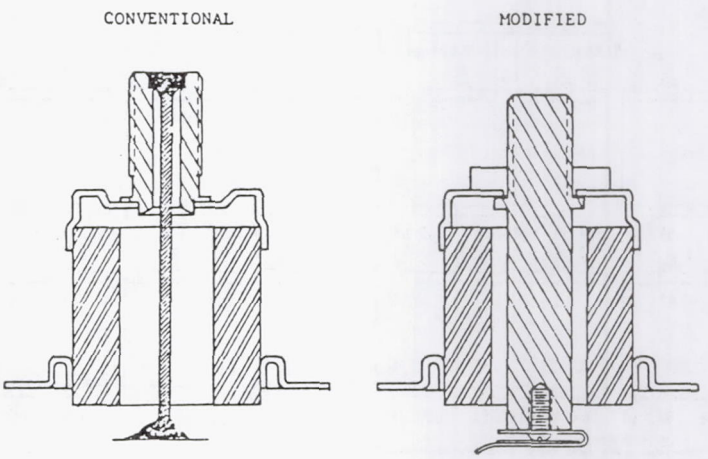

Figure 4. - Electrodes and insulator assemblies.

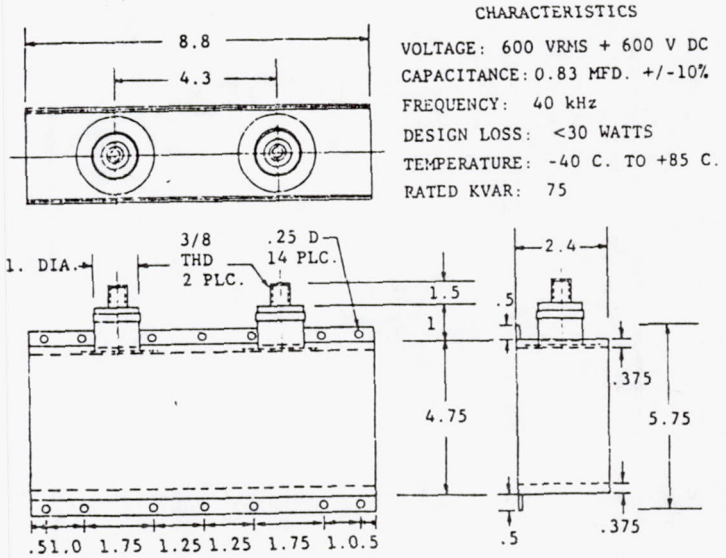

Figure 5. - Characteristics of 400-Hz capacitor.

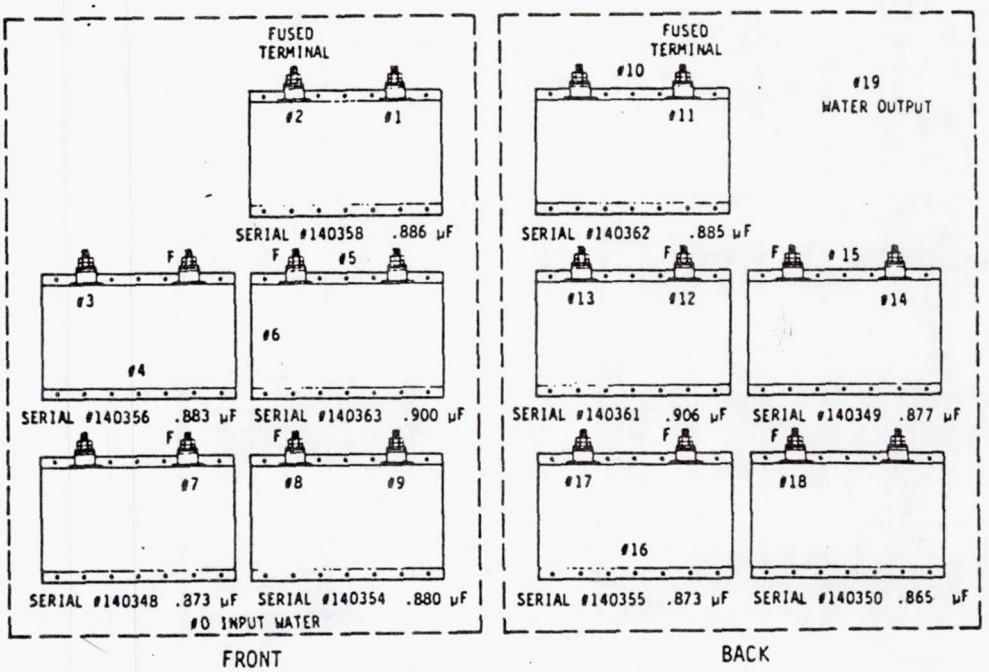

8.828 µF TOTAL 600 V ac 10 kHz
200 kVar 333 AMPS

Figure 6. - Thermocouple locations for 500-hr vacuum endurance test.

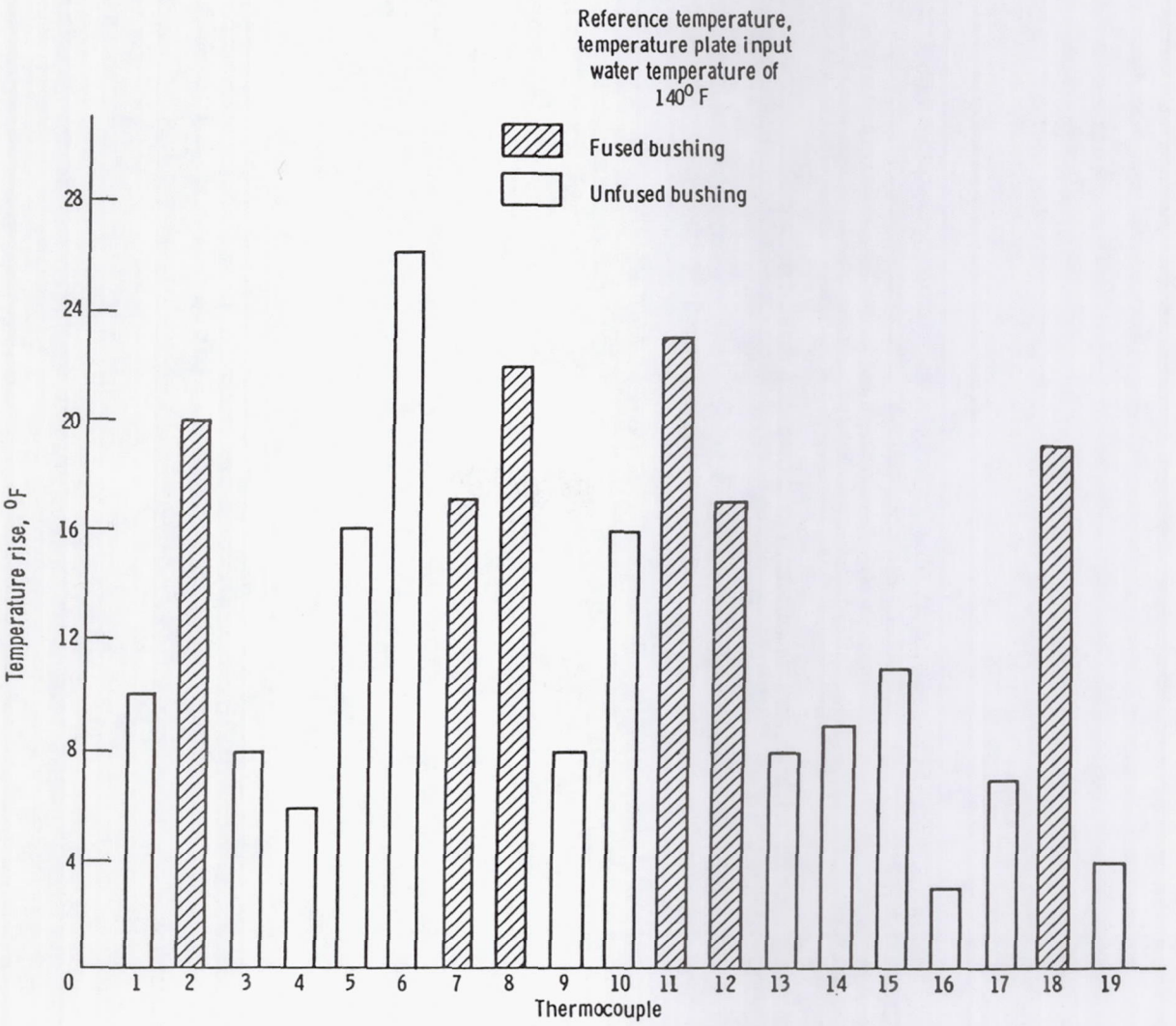

Figure 7. - Vacuum endurance test temperature rise after 503 hrs at 10 kHz.

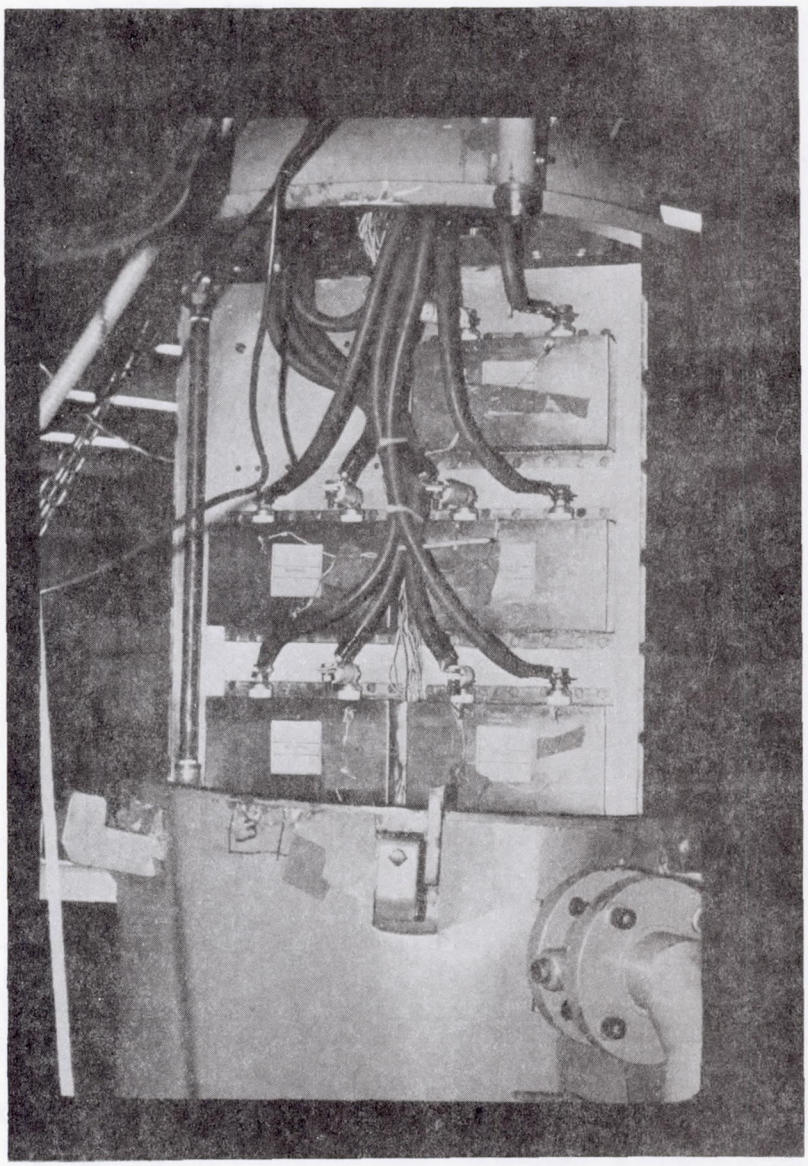

Figure 8. - Capacitor locations for 500-hr vacuum endurance test.

DC-LINK APPROACH TO CONSTANT-FREQUENCY AIRCRAFT POWER

Daniel S. Yorksie
Westinghouse Electric Corporation
Lima, Ohio 45802

This paper discusses a hybrid high-power aircraft electrical system that has very difficult and complex operating requirements. Many issues raised in selecting an approach for this application are similar to those that must eventually be addressed for a large all-electric aircraft. The requirements for this specific system are reviewed, a solution for those requirements is proposed, and some explanation is provided for the choice. Because the system requires a substantial amount of 400-Hz power, a dc-link system was selected to provide that power. The highlights of the power system are

(1) Load requirements of 13.2 kV dc, 400 Hz ac, and 28 V dc (pulsed)
(2) Four channels
(3) Outputs paralleled to feed total load
(4) Load requirements satisfied by three of four channels
(5) Single generator for each channel
(6) Power conditioning remotely located (100 ft) from generator

The load profile (fig. 1) shows that the large power requirements associated with the 13-kV output are only required above 83-percent engine speed. The 28-V pulsed output is a very small part of the overall system requirements on a percentage basis. In going through the selection process and adopting the priority of power level, we will cover the 13-kV requirements first, then cover the 400-Hz requirements, and then lightly touch on the 28-V dc supply considerations. The simple system line diagram for the single-channel configuration is shown in figure 2. The power system contains four identical channels. The loads are now sized for each particular output for the single channel. In figure 2 the approximate distances between generator, power conditioning equipment, and loads are given because they are significant in the overall system considerations and affect which conversion schemes are selected. The evaluation criteria are electrical performance and risk, weight, efficiency, volume, cost, and reliability. Obviously with any airborne system, size and weight are very important selection criteria. However, in a new and complex system such as this, electrical performance and risk must be an important part of the selection process.

The preliminary ground rules for system evaluation are as follows:

(1) Six-phase generator (minimum filtering requirements)
(2) High speed and high frequency
    (a) Minimum generator weight
    (b) Minimum filtering
    (c) Maximum speed, ~25 000 rpm
    (d) Minimum frequency, ~1200 Hz
    (e) Acceptable transmission losses
(3) High transmission voltage
    (a) Minimum transmission losses
    (b) Generator corona considerations, ~ 250 V rms nominal maximum
    (c) Minimum voltage at 53-percent speed, > 120 V rms
(4) Major impact of 13-kV, 270-kW output in determining overall system configuration and parameters

(5) 28-V dc output (4-percent system rating) addressed after 13-kV dc and 400-Hz outputs satisfied

Obviously, in power conversion apparatus, maximizing the pulse number minimizes the filtering requirements. This points in the direction of a six-phase system rather than a three-phase system for the generator. There is obviously a range of practical frequencies bounded, say, on the lower end by minimum frequencies required by certain power conversion schemes and limited at the upper end by losses in high-power rectifiers, transformers, and other such equipment. Minimum voltage requirements are imposed on the generator by various power conversion schemes, and of course maximum voltages are imposed on the system from consideration of corona and other such parameters. Again, power output tends to influence strongly the design priorities. So with this sort of groundwork layed, these ground rules allow us to establish the following set of conversion options:

(1) Starting system parameters
  (a) Six-phase generator-feeders
  (b) Generator voltage L-N, 264 V rms at 100-percent speed
  (c) Generator frequency, 2500 Hz at 110-percent speed
(2) Ripple considerations
  (a) Ripple requirement of 0.26 kV, 2 percent
  (b) Six-pulse rectified voltage with 9.3-percent ripple
  (c) 12-pulse rectified voltage with 2.3-percent ripple
(3) Option 1 - single transformer with delta/wye secondaries
(4) Option 2 - two identical transformers with six-phase supply

The power system will probably be a six-phase system with a generator voltage of about 260 V and a frequency of 1000 to 2000 Hz. The relationship between pulse number and ripple voltage leads to the conclusion that only 12-pulse conversion processes are really practical in meeting the 13-kV ripple requirement. Going through all of this you come to two options for the 13-kV system. Option 1 (fig. 3) is a single transformer with delta/wye secondaries to give a 12-pulse ripple in the output frequency and to minimize filtering. Option 2 (fig. 4) is two identical transformers. This implies a six-phase generator, where the phase displacement for the 12-pulse requirement comes from the phase displacement between the two groups of three feeders in a six-phase supply.

Comparing the advantages and disadvantages of these two approaches to 13-kV conversion shows that

(1) Option 1 (the single transformer) will be somewhat lighter in weight and smaller in volume
(2) Option 1 has more complex insulation requirements with twin secondaries and higher voltage in delta-connected windings (5000 V rms vs. 2900 V rms for wye)
(3) Option 2 will require less filtering for the same level of ripple and distortion
(4) Option 2 requires twin three-phase breakers
(5) Option 2 provides improved heat transfer

Considering the complete conversion stage including transformer, rectifier, filter, and cooling system, option 2 (two transformers with six-phase supply) was chosen.

In selecting control options the operating considerations of steady-state voltage regulation (12 to 13.7 kV dc), current limiting at 1.2 per unit load, and load sharing under paralleling point toward maintaining constant transformer primary voltage. This would allow the natural droop of the paralleled transformer-rectifier units to provide current sharing. Current limiting would also be implemented on the primary (low) voltage side. This leaves three options for voltage and current control:

(1) Voltage control (VC) and current limiting (CL) via generator excitation control (fig. 5)
(2) Voltage control and current limiting via reverse parallel-connected thyristors (fig. 6)
(3) Voltage control via field control and current limiting via thyristor control (fig. 7)

The first option (fig. 5) will impose some constraints on the other power conditioning subsystems, but as later analysis showed, this option does not impose a severe burden on the design requirements for those systems. Overall it has significiant system appeal. As for the second option (fig. 6) a trade-off between the primary and secondary would quickly show that it is preferable to put the phase-controlled arrangement on the primary side rather than on the high-voltage side. The unfortunate aspect of this approach is that the primary electronics now have to be rated for the full system throughput and there is an additional filtering burden imposed on the secondary filter with this type of arrangement. Obviously there is a compromise (option 3, fig. 7) where voltage control would be used during normal operating modes with field control maintaining the phase-controlled rectifier in a full-on condition. This would not impose a severe requirement on the filtering and, if the load could tolerate it, phase control could be used just for current limiting. Unfortunately, the problem of the high rating required for the electronics portion of this process still exists.

In the final analysis we recommend the most simple and straightforward method - option 1, using the process of field control for voltage control and current limiting. Our analysis indicates that this method of control is compatible with actual load requirements, does not unduly penalize the design of the 400-Hz output, and provides a very efficient and highly reliable power conditioning subsystem.

Selection of a 400-Hz conversion option was based on the following considerations:

(1) Kilovolt-amperage management
(2) Neutral forming
(3) Feeder and generator utilization
(4) Interaction with the 13-kV supply

The state of the art for the conversion of bulk, variable-frequency ac power to constant-frequency ac power (VSCF) by solid-state means offers two general solutions: direct ac-to-ac conversion systems and ac-to-dc-to-ac conversion systems. System parameters chosen thus far (i.e., voltage and frequency) leave open the consideration of these two options:

Option 1 - cycloconverter
Option 2 - dc-link inverter

Figure 8 is a rough diagram of option 1, cycloconverter power stage - repeated three times for each of the three output phases. It gives an idea of the complexity and brings out some significant points - especially that with this scheme the neutral must be brought out from the generator.

Option 2, the dc-link inverter (fig. 9), does have to have a neutral forming transformer to provide the fourth wire; however, it does not require the fourth wire, or the neutral, to be brought out from the generator. The scheme that we recommend for operating the inverter stage is a fixed pattern controlling the bridge switches - say the transistors - that would then determine output frequency and distortion factors. Voltage traditionally is controlled by regulating the link voltage. In this case, because of the choices already made on the 13-kV system, a preregulator stage is needed for the dc-link system to compensate for the generator voltage variation over the speed range.

Table I summarizes some of the critical differences between the two systems. Some of the important points are the neutral currents, the filter currents in fault, the weight of the feeder cables, and the weight of the neutral feeder as compared to the neutral forming transformer. The table implies a bias, considering weight only, toward the dc-link option. In other words, the power stages are about equivalent for this comparison between the two approaches, so a trade-off results between the neutral coming from the generator and the neutral former in the dc-link option. On a weight basis the dc-link is favored. However, weight is not the only consideration. First, the cycloconverter circulates reactive power through the feeder system and the generator. In contrast, the dc-link system constrains the reactive current flow to the output stage of the inverter. That is significant. Second, under unbalanced conditions, an undesirable 800-Hz modulation effect is imposed on the generator terminals. The modulation is reflected into the 13-kV supply. Obviously the filter - for a 12-pulse output - is not designed for 800-Hz disturbances. That imposes a severe penalty on the filtering in the 13-kV supply and also creates a problem with the feeding of faults - where significant reactive power is circulated through 110 ft of feeder. There is also the other constraint of maintaining minimum voltages on the generator output so that the supply can meet its other output requirements, such as the 28-V dc system.

If all of these constraints are taken into consideration, for this particular application a dc-link system offers some significant advantages. The input stage does have additional complexity: it is not a rectifier; it now becomes a phase-controlled bridge; it requires some additional filtering on the link. However, on an overall system basis, considering weight, reliability, and efficiency the trade-off works in favor of the dc-link system. Now that we have made that determination, we can briefly review the kind of control strategies that would be applicable (figs. 10 and 11). Some of these have almost been discounted but are included for the sake of completeness.

The first option (fig. 10) is to use field control on the generator. That is a viable option and is obviously the simplest. The same statements hold true here as for the 13-kV system. However, having chosen field control for the 13-kV system implies a separate generator to feed the dc-link system. In the ground rules established by the application requirements, there was a specific requirement of a single generator and that meant a single, physical generator, not necessarily a single generator designed within that physical envelope.

The second option for voltage control is the use of gate-controlled thyristors shown in figure 11. The input stage is in error. The input stage really has to be a phase-controlled bridge. When considering interactions

between the systems, the phase-controlled front end does provide a one-way buffer between the 13-kV system and the 400-Hz system. There is also the question of transient response. The faster response time of option 2 and its effect on transient response at the output of the 400-Hz system more than compensates for the increased complexity. Option 2 also provides buffering of the 400-Hz output due to sudden load changes in the 13-kV output. Although there will be some interaction between the 13-kV and 400-Hz outputs, the controlled rectifier will help to minimize these effects. Option 2 was selected as the preferred approach for the overall system.

In the preceding discussion a selection of the generator configuration has been implied. However, for the sake of completeness, I will briefly cover various generator feeder options. A consideration is that the generator and feeder configurations are interrelated. Also single physical generator requirements constrain dedicated generators to a single shaft. System interaction is an important criterion when evaluating feeder configurations. And generator rating and phase currents must be established to size feeders. The following options will be considered:

(1) Separate electromagnetic design with dedicated feeders
(2) Single generator with dedicated feeders
(3) Single generator with common feeders

Figure 12 is the result of a rating analysis derived from figure 1. Basically it shows that from 0 to 83-percent speed the high-power output is not on. If you control the output in a linear fashion, constant voltage over frequency, the requirements on the electromagnetic devices, like the 13-kV transformers, will be maintained. Sufficient voltage will be produced to power the 400-Hz output. The design rating point after further calculations for the generator turns out to be the 83-percent speed point. Considering different feeder configurations and load requirements results in the set of currents shown at the bottom of the figure.

One of the approaches (option 1, fig. 13) is to have two isolated electromagnetic generators on a common shaft. This is a very simple scheme for voltage regulation. A highly desirable aspect of option 1, from the standpoint of the power conversion equipment, is that it provides the maximum independence and isolation between the 13-kV and 400-Hz outputs. Of course this would be compatible with a simple scheme of field control for both outputs.

Another approach (option 2, fig. 14) is a single generator, which obviously will be less complex and lighter in weight, with dedicated feeders. The figure shows currents and nominal voltages. The distance to the feeders is normally 100 ft. The feeders are all the same size, are tightly bundled, and are a fairly sizable weight consideration in the overall system tradeoff.

The last approach (option 3, fig. 15) would be to run a single set of feeders down to the branch point and then branch off to the two different power conditioning subsystems. This, obviously, is the lightest weight approach.

Table II shows an approximate calculation which reveals that feeder weight, approximately 43 lb, is more important than the kilovolt-amperage of the generator. However, weight alone cannot be used to make the choice. The other aspects that need to be considered between these three options are as follows:

(1) Option 1 offers maximum isolation of the 13-kV and 400-Hz outputs and a simple, reliable method of voltage control.

(2) Option 1 generator has a reactive power penalty and a weight penalty, added mechanical complexity, and a possible 43-lb feeder penalty.

(3) Options 2 and 3 offer a lighter, simpler generator.

(4) The 43-lb weight saving of option 2 over option 3 is obtained at the penalty of isolation between the two outputs.

(5) Option 2 represents a compromise solution between options 1 and 3 in that the 13-kV and 400-Hz units can interact only through the generator's subtransient inductance but not through feeder inductance.

Making a choice is a trade-off among complexity, reliability, weight, and isolation or interdependence between the two supplies: the 400 Hz and the 13 kV. Choosing a single feeder to the branch point results in interactions between the 13-kV and 400-Hz subsystems, which occur not only through the generator subtransient reactance, but also, through the reactance of the feeder cables. And that can be quite significant. The choice then is between an interaction criterion and a weight criterion. At this point, we recommend option 2, probably because of a risk consideration. We would start by limiting the interaction to just the generator subtransient reactance, using the feeder cables as a buffer between the two supplies. Hardware tests may be needed to finally determine which is the better trade-off - the 43 lb or the final weight of the control circuits - to get these two supplies to operate reliably off the same generator. So tentatively we would select option 2 and carry the 43 lb as a potential weight saving after further analysis and tests.

In conclusion, the 28-V dc system, even though it is a pulse system, represents only about 4 percent of the total system, or channel, rating. There are two obvious design approaches: to design the power stage configuration for peak power throughput or to design a system that provides for energy storage. Cost and weight considerations come into play here and tend to bias toward an energy storage approach. The average power on the supply system is only of the order of 600 W because of the very low duty cycle in the output of the 28-V dc system. Also it might be determined that the three-phase supply is satisfactory and that a six-phase supply is not needed for this power level.

Westinghouse finally selected an energy storage approach fed by a very simple current source power-conditioning subsystem (fig. 16). The control options for this type of system with a large capacitor and three or four parallel systems is not as simple as it might seem at first. How natural unbalances in capacitor values and leakage currents are accounted for is fairly significant consideration but beyond the scope of this discussion. Figure 17 shows the final system configuration. The design approach discussed in this paper should be applicable to a variety of aircraft including a large transport with all-electric secondary power.

TABLE I. - 400-Hz CONVERSION OPTIONS

Load Condition	Option 1 Cycloconverter		Option 2 DC-Link Inverter	
	Steady State	Sh. Ckt.	Steady State	Sh. Ckt.
Load KVA	120	NA	120	NA
Load Power Factor	1	NA	1	NA
Load Current, Amp	348	NA	348	NA
Filter Current, Amp	174	~0	162	~0
Converter Output, Amp	389	1,044	384	1,044
DC-Link Current, Amp	NA	NA	456	~0
Input Phase Current, Amp	220	591	186	~0
Neutral Current at 1/3 Load Imbalance, Amp	116		116	
110 Ft. Feeder Wt., Lb. at .27 Lb./A/Phase/100 Ft.	392		331	
110 Ft. Neutral Feeder Wt., Lb.	35		NA	
Neutral Forming Transformer, Wt., Lb.	NA		18	
Total Feeder + Neutral Forming Wt., Lb.	427		349	

For purposes of this comparison, the weight of the two converters is assumed to be comparable. In addition to the above tabulated net feeder weight penalty of 78 lbs./channel, there is a further weight penalty to the cycloconverter generator.

TABLE II. - GENERATOR-FEEDER OPTIONS

Option	1	2	3
Approximate Feeder Weight, Lb.*	367	367	324
Approximate Generator KVA (Extrapolated to 100% Speed)	588	574	574

*Copper Wire (Aluminum wire weight is ≈50% less)

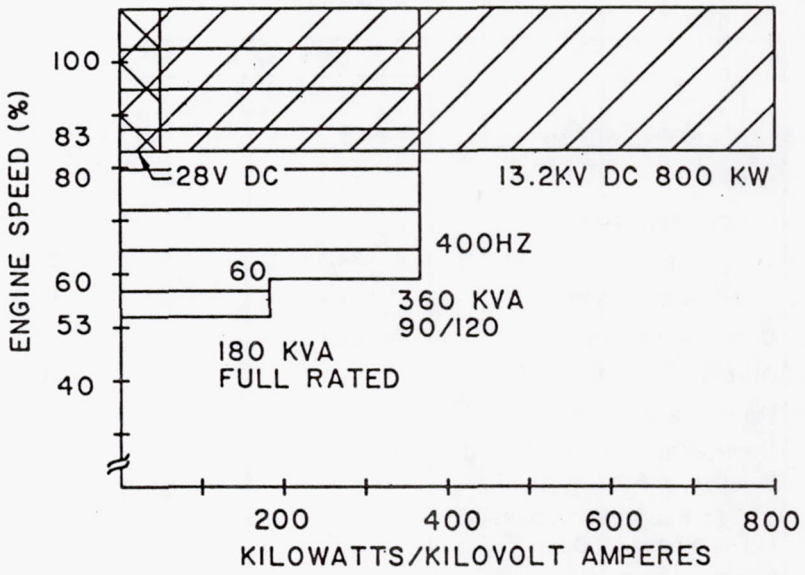

Notes: 1) 28 VDC and 13 KVDC operate only above 83% speed
2) 400 Hz. channel rating is 60 KVA at 53% speed, 120 KVA at 60% speed and above

Figure 1. - Utilization equipment - total load profile.

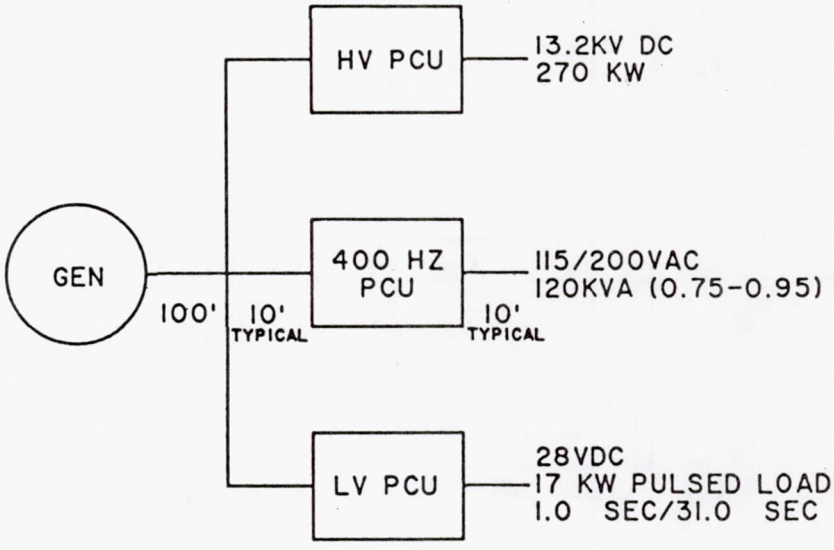

Figure 2. - Single-channel configuration.

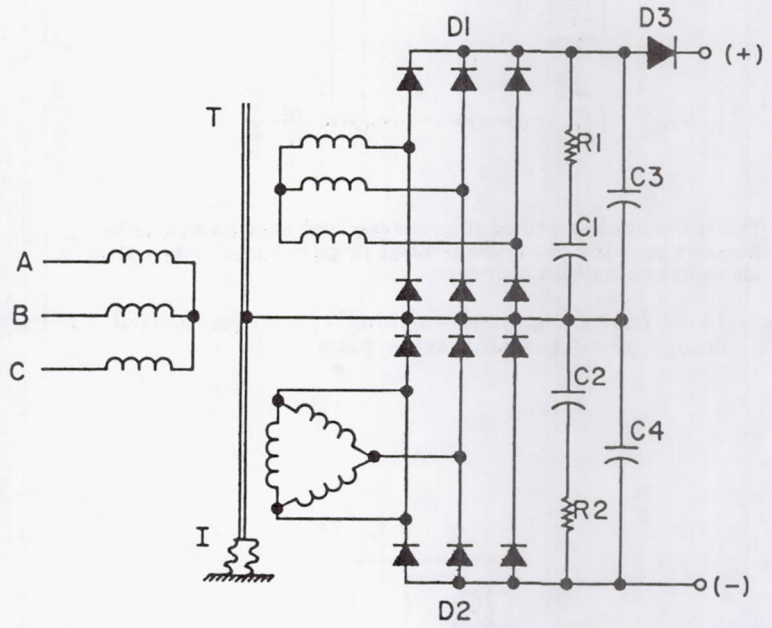

Figure 3. - 13-kV conversion options - option 0, single transformer with delta/wye secondaries.

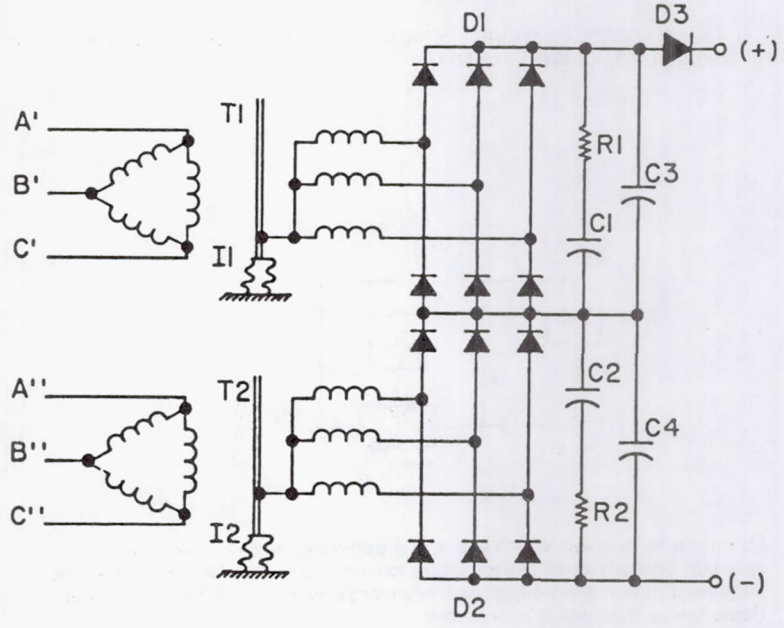

Figure 4. - 13-kV conversion options - option 2, two identical transformers and six-phase supply.

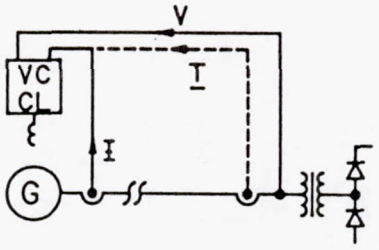

This is the simplest method of control requiring no extra electronics. Requires generator of sufficient voltage range to supply other system elements or constrains their design.

Figure 5. - 13-kV control options - option 1, voltage control and current limiting through generator excitation control.

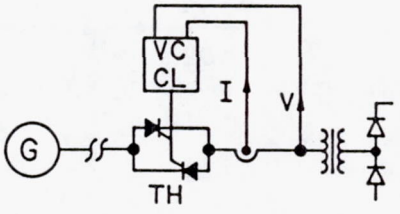

Provides maximum independence of elements fed from a common generator at the expense of additional power electronics rated for total throughput. Requires additional filtering and damping.

Figure 6. - 13-kV control options - option 2, voltage control and current limiting through thyristor control.

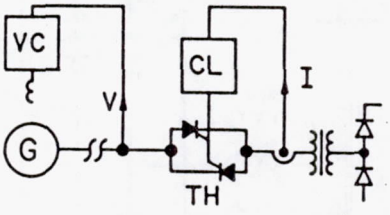

Compromise solution which maintains generator voltage reasonably constant and avoids chopping action except under overload. Still requires additional power electronics. Has advantage over Option 2 only if higher ripple under overload is acceptable.

Figure 7. - 13-kV control options - option 3, voltage control through field control and current limiting through thyristor control.

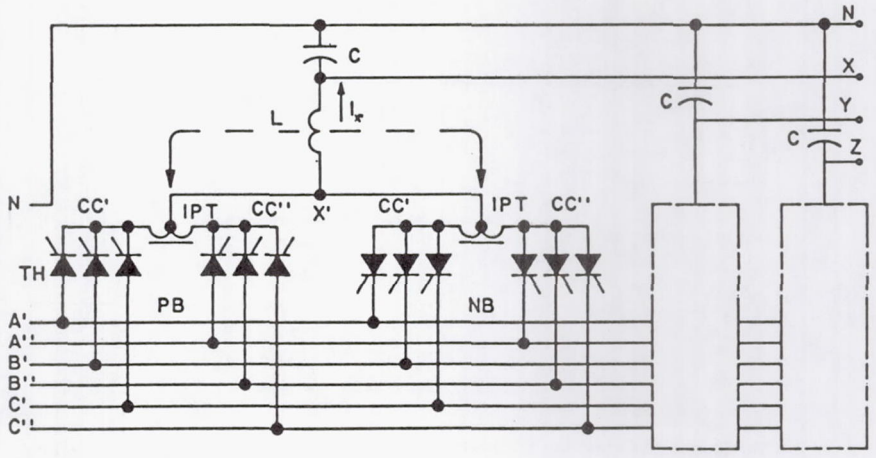

Output voltage quality and steady state and transient regulating accuracy depend to a large extent on the performance of a complex control circuit detecting critical timing of 36 thyristors and selection of six thyristor banks. Cycloconverter has a fixed ratio of net converter output current and input phase current (feeders and generator) of 0.566 and requires a generator neutral feeder cable rated for 33-1/3% nominal output current.

Figure 8. - 400-Hz conversion options - option 1, cycloconverter.

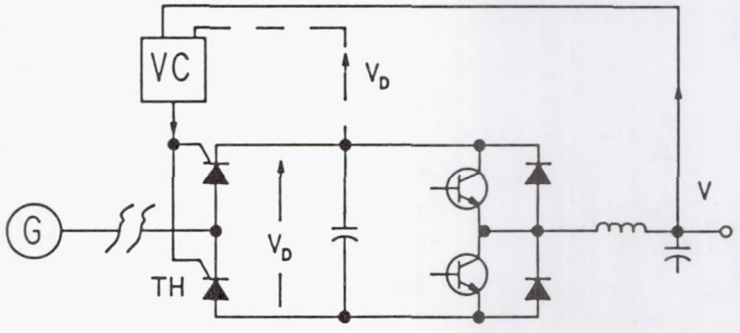

Using a fixed PWM digitally derived waveform pattern, the steady state and transient accuracy of the output voltages depend on the accuracy and speed of the link voltage control. A DC Link system has a ratio of 1.31 (real component of net inverter output current and DC Link current) and 0.41 (DC-Link current and input phase current) and requires a neutral forming transformer.

Figure 9. - 400-Hz conversion options - option 2, dc link.

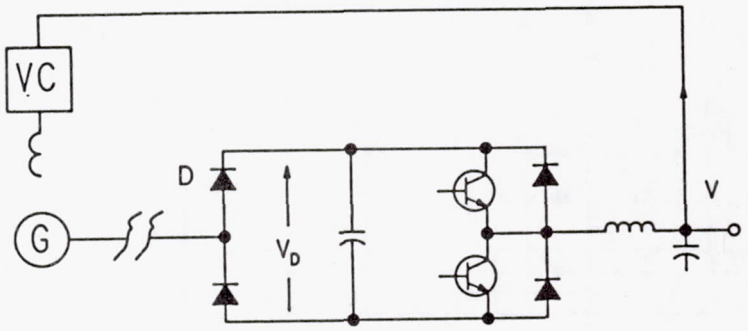

This is the simplest method of control but requires a dedicated generator or a change in the 13 KV output design approach (i.e., thyristor control). It also fixes the generator voltage at approximately 130 VRMS causing a feeder weight and loss penalty.

Figure 10. - 400-Hz control options - option 1, voltage control through field control.

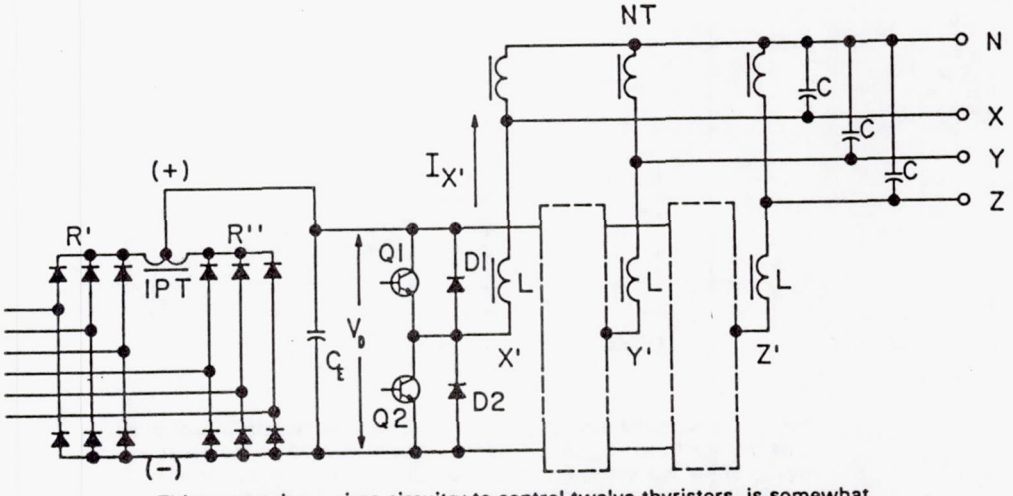

This approach requires circuitry to control twelve thyristors, is somewhat more lossy in the rectifier stage and requires relatively more filtering of the link voltage. However, it does not have the disadvantages of Option 1 and provides twenty times the response time of Option 1.

Figure 11. - 400-Hz control options - option 2, voltage control through gate control of thyristor rectifiers.

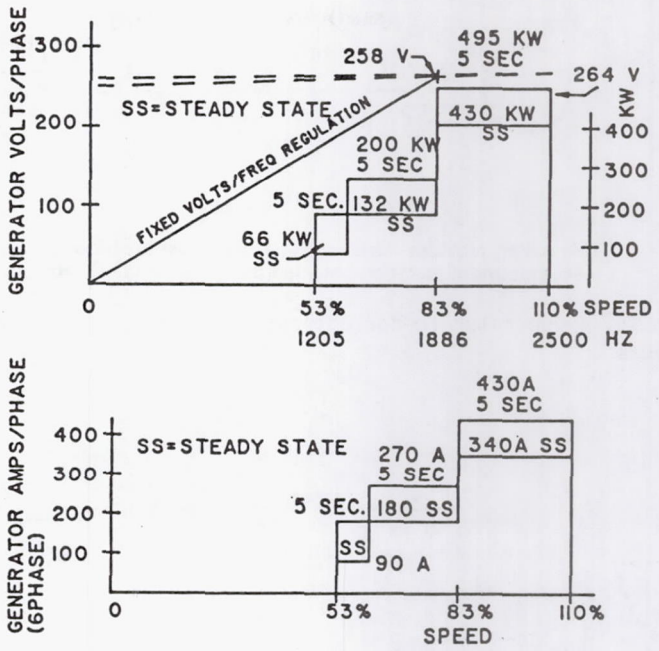

Figure 12. - Generator rating analysis.

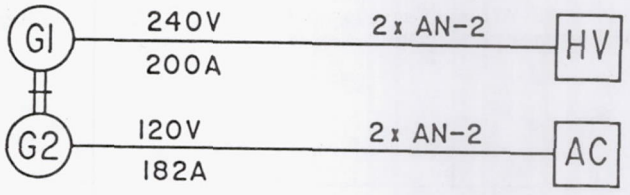

This option provides for the maximum isolation between the 13 KV and 400 Hz. outputs. However, it does require a more complex and heavier generator.

Figure 13. - Generator feeder options - option 1, separate electromagnetic design with dedicated feeders.

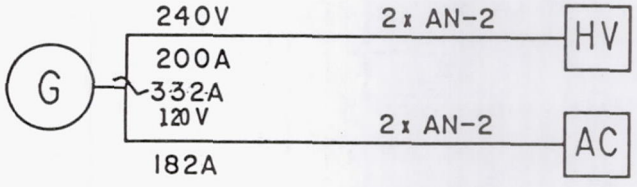

Figure 14 - Generator-feeder option 2 - single generator and dedicated feeders. (This option provides for the lightest and simplest generator configuration. It does not provide the degree of isolation that option 1 provides.)

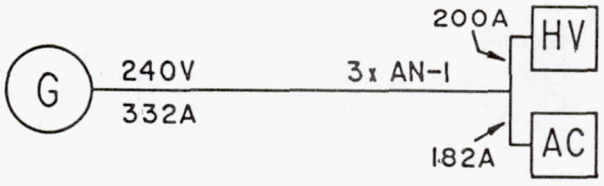

This option provides the simplest and lightest feeder configuration but the least amount of isolation between the 13 KV and 400 Hz. outputs.

Figure 15. - Generator-feeder options - option 3, single generator and common feeders.

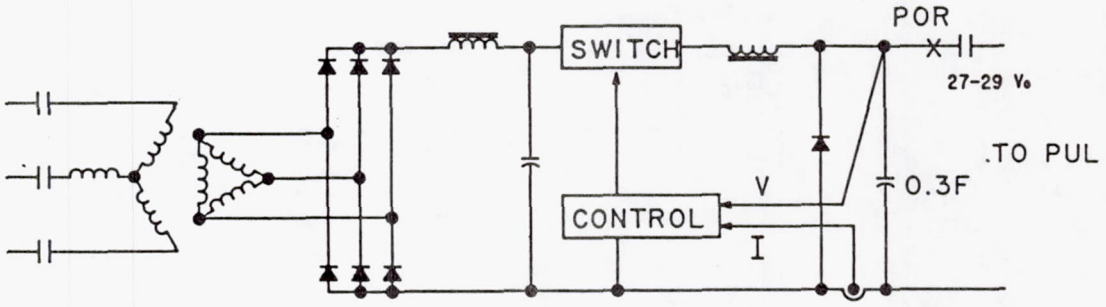

Figure 16. - 28-Vdc system approach - controlled current source with capacitive energy storage.

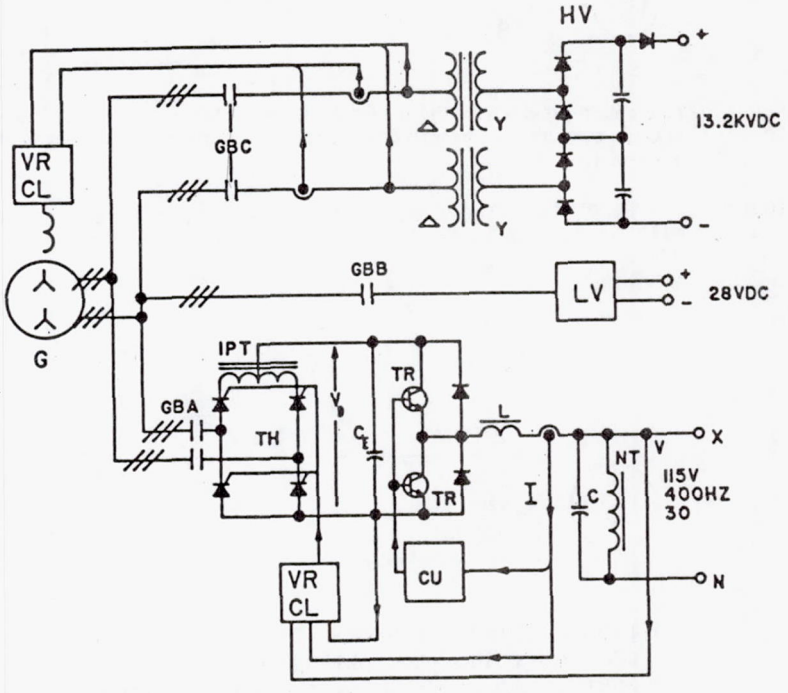

Figure 17. - Final system configuration.

CYCLOCONVERTER ON THE ALL-ELECTRIC AIRPLANE

Robert C. Webb
General Electric Company
Binghampton, New York 13902

This paper discusses the application of a cycloconverter to a permanent-magnet generator. Recent developments, advanced concepts, and advanced technology systems will be covered. Recent developments include permanent magnets, permanent-magnet motors and generators, and power semiconductors.

Figure 1 compares the coercive force as a function of induction for three magnets. In the 1970's a revolutionary breakthrough was made in magnet development that allowed them to be applied to high-power motors and generators.

When the permanent magnet is used in a high-power generator, the control permanent-magnet generator and exciter can be removed, as shown in figure 2. The generator is significantly simplified and its efficiency increased. Figure 3 compares two 60-kVA-rated generator rotors of comparable speed range. A current wire-wound system and a permanent-magnet system are essentially equal in weight, but the advances in magnet technology indicate that the energy product will increase. This will allow the use of smaller magnets; it will minimize the containment, and it will increase speed. The result will be a lighter weight motor or generator. Current rotor technology is based on blocks of permanent-magnet material made into disks or wheels as shown in figure 4. (It will probably not change much.) This allows some flexibility in changing ratings by changing the number of wheels or disks.

For the last 15 years of cycloconverter work variously rated generators have used stud-mounted silicon-controlled rectifiers (SCR) (shown in fig. 5) mounted on a heat plate. This is a fairly common technology, but it has created a cooling penalty. The bases on all of these SCR's were hot and also had to be electrically isolated. Conducting the heat through the electrical isolation is difficult and inefficient.

On the left of figure 6 is an SCR power module that GE developed, built, and tested under a program sponsored by the Wright Patterson Aeropropulsion Laboratory. We took the C158 SCR and put it in a module with a dry interface. Typically, dry interfaces tend to create a problem because of the differential expansion rates. Therefore we used structured copper in a hermetically sealed case and beryllium; so the base of the unit is electrically isolated but has an excellent thermal path as judged by existing technology. On the right in figure 6 is an SCR developed in the last few years. Until very recently transistors with sufficient power range in an individual device were not readily available to apply in power conditioning for aircraft electrical systems. The device is a 450-V, 200-A device.

GE has spent some time working on package development. Figure 7 shows a very small package - about an 1-1/2 in. long and 1/2 in. wide - containing a 450-V, 200-A device. This package has the same type of construction as the power module shown in the previous figure, and it provides the same benefits.

GE's advanced concepts for future aircraft electrical systems are shown in figure 8. The generator could be either integrated with the engine or mounted on the accessory gearbox. We expect that military aircraft generators would be more likely to be integrated and commercial aircraft generators more likely to be accessory gearbox mounted. We have shown an unconditioned, or wild, frequency and voltage bus to be used for distribution and for some loads such as electric deicing. However, conditioned power (115 V, three phase,

400 Hz) will probably always be required and could be provided with either a cycloconverter or a dc link. Direct-current loads could be provided from the wild frequency and voltage bus through transformer rectifier supplies. Some of the larger loads such as actuators, fuel pumps, and environmental control systems (ECS) could be driven by electric motors. We expect that they would use permanent-magnet motors with a cycloconverter or dc link for speed control. In selecting either cycloconverters or dc link, an ac distribution system would seem to favor the cycloconverter and a dc distribution system would favor the dc link.

Figure 9 shows the installation of an integral starter-generator on the TF-34 engine. The study that developed this installation was limited to existing engines. Although the results were quite reasonable, they probably could have been even better had a new engine design been used. If an engine is to be equipped with an integral starter-generator, the best approach would be to design the engine and the starter-generator together.

Three GE programs touched on briefly are the 60-kVA variable-speed, constant-frequency VSCF starter-generator program, which is ongoing; the 150-kVA VSCF starter-generator program, which has been completed, and the 140-hp PM brushless motor, which has been developed. The Wright Patterson Aeropropulsion Laboratory is sponsoring a program to take the permanent-magnet technology developed by GE and flight test it on two A-10's over a 1-year period (fig. 10). This is the next step in the evolution of a permanent-magnet starter-generator system on an airplane. The large housing on the right end of the generator contains a gearbox to match the generator speed to a starter pad on the engine. The actual generator is quite small. The package to the right of the generator contains the cycloconverter which controls the generator during its use as a starter and also allows the two generators to be paralleled. The cycloconverter package is not a final flight design.

Figure 11 is an artist's rendering of a cross section of the 60-kVA permanent-magnet generator. It is a high-speed design with a dry-cavity construction. This eliminates the problem of oil getting into the air gap and of trying to design effective bore seals and slingers. This construction does require that the stator end turns depend on conduction for cooling. We used a contained oil system for cooling, which is similar to the cooling systems on other types of generators.

The cycloconverter has the inherent capability of bidirectional power flow (fig. 12). Thus combining it with a permanent-magnet generator that does not have an exitation problem at standstill results in the ideal system for an ac starter-generator. Only a minimal change in the cycloconverter is required for rotor position sensing during standstill. The change in system weight is insignificant. There is approximately a 7-percent system part-count increase and only a 4-percent decrease in reliability.

Figure 13 shows drag torque plotted against input drive shaft speed for the TF-34 engine. It also shows the starter-generator output torque. When GE originally started this program, it was planned to have a 60-kVA system to go on the A-10. The A-10 has a 30/40-kVA system. It was originally conceived that it would require 60 kVA to start the engine. With some of the circuit and system improvements we have been able to employ, the TF-34 can be started at 40 to 45 kVA. Now let me present some differences between the permanent-magnet system and an air-start system. An air-start system has a high impact torque and a real decaying curve, so that at high speeds there would be minimal torque. The electric starter-generator concept gives a much higher torque at high speed. From lightoff to idle the starter-generator is faster than the air starter, but from initial rollover to lightoff the reverse is true. For

the TF-34 engine the electric starter-generator was a couple of seconds faster than the air starter.

The A-10 program will have both engines dedicated to the 60-kVA system, but the air-starter system will be left on as a backup. The auxiliary power unit (APU) will serve as a backup for electric power in case something goes wrong with the generators because these are not flight test airplanes. They are tactical airplanes that will be used in their common training mission. The configuration is shown in figure 14.

In 1981 we conducted an A-10 engine start test at the Air Guard open-air test facility in Syracuse, New York. We have done numerous laboratory tests where we simulate the engine drag-torque curve. We have tested it with equivalent generators on a ground power cart, but we still did not know what would happen in the flight test program. The Air Guard test was a way of minimizing risks and finding out how well the system works. We used the standard Air Force ground power cart, A/M32A-60, on an actual TF-34 engine. The test setup is shown in figures 15 and 16.

We did three motorings before turning on the fuel and ignition to find out how the system worked. Each time the system performed as had been anticipated; then we did a total of three starts. I was initially concerned that the start times were so high. It turned out that the engine had a dead set of ignitors and it was taking 11 to 12 sec for the fuel to ignite. The start times were still 2 to 3 sec faster than with the air starter.

In February 1982, we set up and ran a test at GE Lynn, where the TF-34 is manufactured. We worked out an arrangement to do starting and generating as part of their component improvement test (CIT) on a new turbine section (fig. 17). A diagram of the Lynn engine test cell is shown in figure 18. We mounteda generator on the engine. The converter was on the catwalk above the engine. We wired the start switch and the disconnect switch into the engine control console and fabricated a load bank with 30 kVA and a 0.7 power factor. The choice of 30 kVA was based only on the availability of resistors and inductors to make that load bank.

Figure 16 shows AMT-IIIR, a factory test cycle used for accelerated life testing. During this cycle the throttle goes from maximum to minimum power nine times. This is followed by a slow deceleration, a return to idle, and a 5-min shutdown. Then the cycle is repeated. We thought - based on our laboratory tests - that we could run the motoring in a continuous mode. The present air-starter system has an overheating problem if run continuously. There is sufficient oil circulation in the idle position to cool the generator. The cycloconverter is a fan-cooled device: whenever it operates in the start mode, the fans are on. Thus there was no limitation on cooling and we could use extended motoring.

In a typical CIT program with the air-starter system, four or five failures occur during accelerated testing. We performed 434 electrical starts and operated the converter for 432 hours with no failures and no unsuccessful starts. The system operated so smoothly that we were able to leave after the first week and a half and allow the regular test personnel to conduct the remainder of the testing.

Figure 20 shows the 150-kVA VSCF starter-generator system. On the basis of the drag-torque data available for the E^3 engine, this starter-generator could provide acceptable start times for that engine. The E^3 engine is very difficult to start because of its high cycle pressure ratio. The 150-kVA starter-generator was built as a potential starter for the F-101 engine used on the B-1 bomber. Figure 21 shows the cycloconverter used with the 150-kVA starter-generator. The package is a laboratory design and therefore is larger than a flight system would be.

We applied this technology to a brushless, high-speed, permanent-magnet motor, shown in figure 22. The motor, which was designed for a torpedo propulsion program, won the 1981 IR-100 award. The motor produced 5 hp/lb for a 0.2-lb/hp specific weight. The 504 power transistor was controlled off a battery, so it employed essentially the dc-link approach.

The trend is toward more electrical loads on airplanes. The electrical systems on the airplanes in inventory today are not of sufficient size to start many of these engines. On most new airplanes -- particularly the new military airplanes -- it appears that the electrical load will exceed the starting load. Permanent magnets will continue to be a real consideration. Energy products are indicated to be rising. The only unfortunate factor there is that all of the significant research in magnets is being done in Japan and the Peoples Republic of China. Very little significant work is being done in the United States in my opinion. Large brushless motors will take on a more and more active role in fuel pumps, environmental control systems, other pumps, and actuators. The future of hybrid electric power generating systems is not clear cut. Evolution of a generator integral with the engine will remain peculiar to military aircraft.

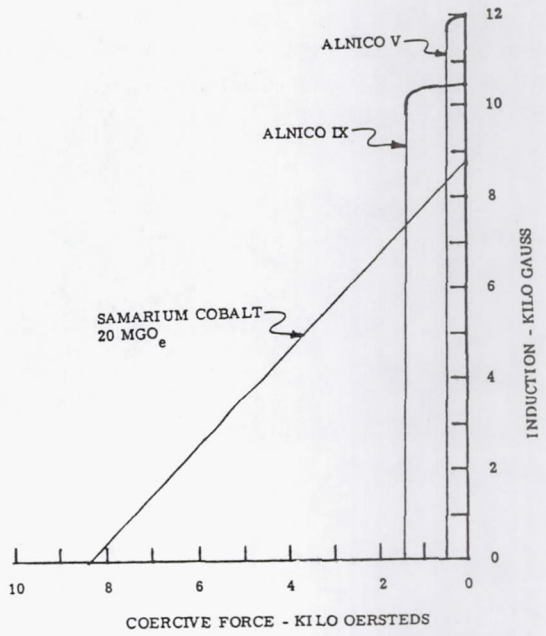

Figure 1. - Comparison of magnets.

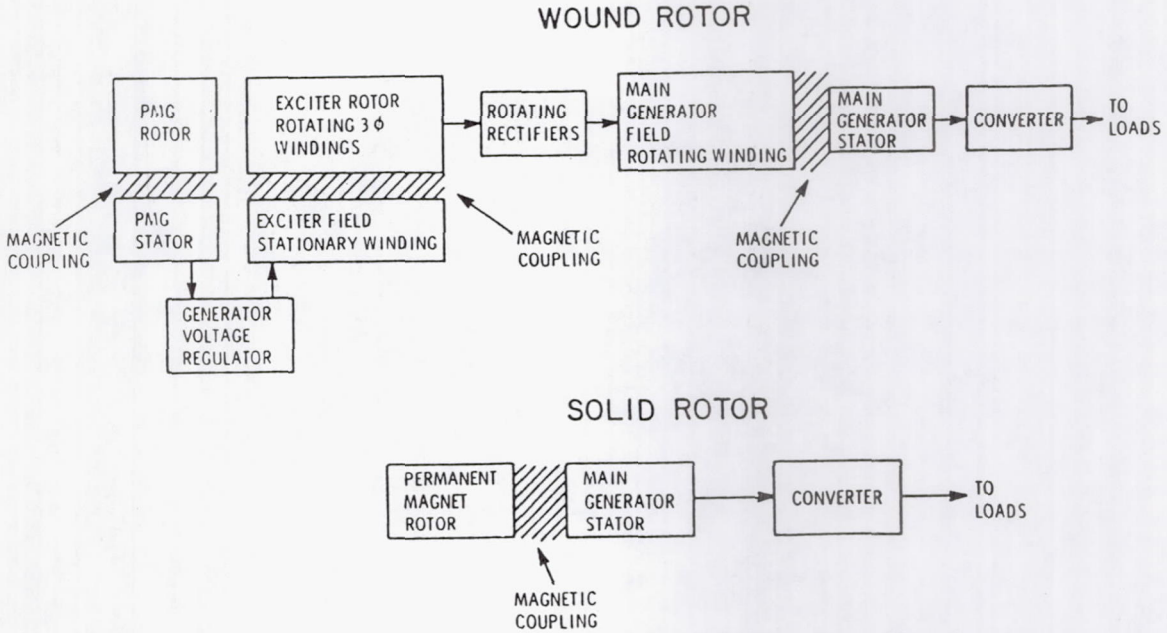

Figure 2. - Comparison of wound and permanent-magnet (solid) VSCF systems.

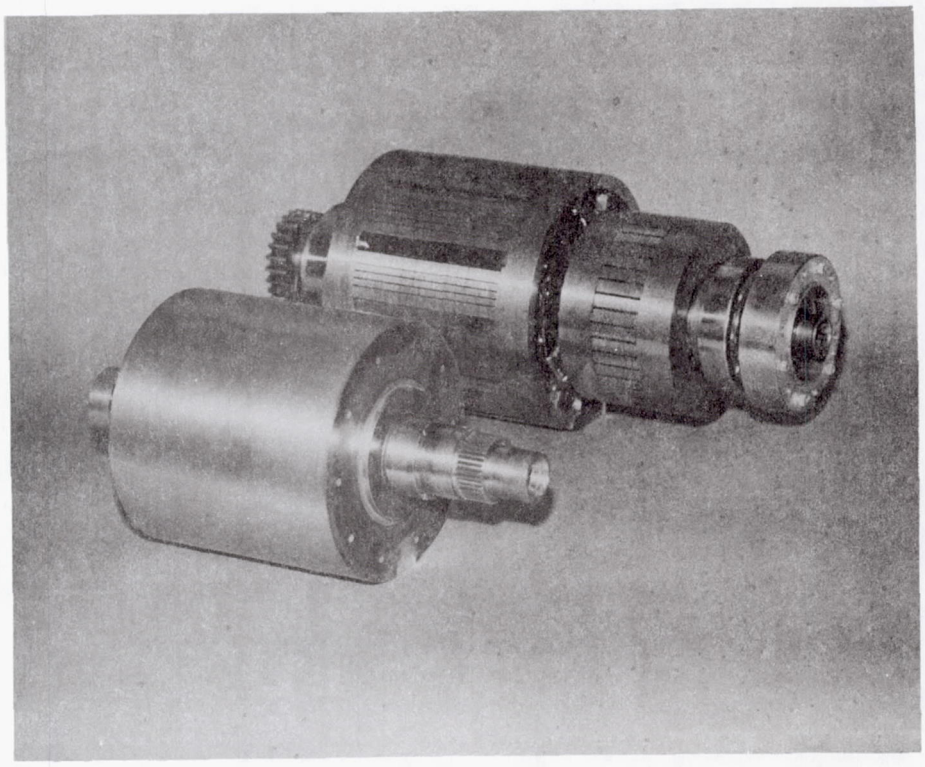

Figure 3. - 60-kVA generator rotors.

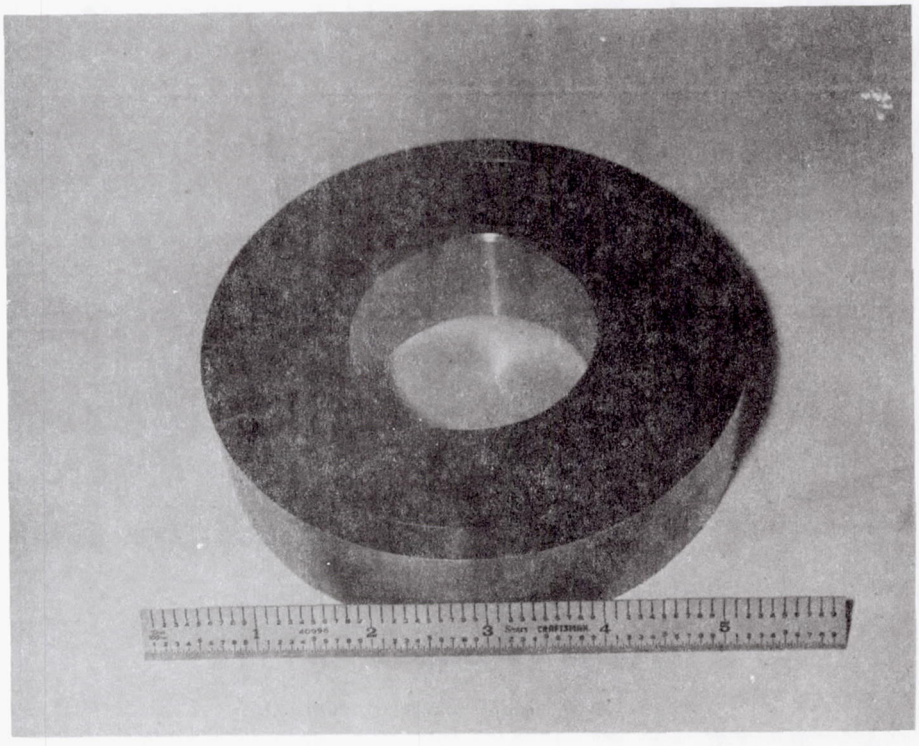

Figure 4. - Disk of permanent-magnet material.

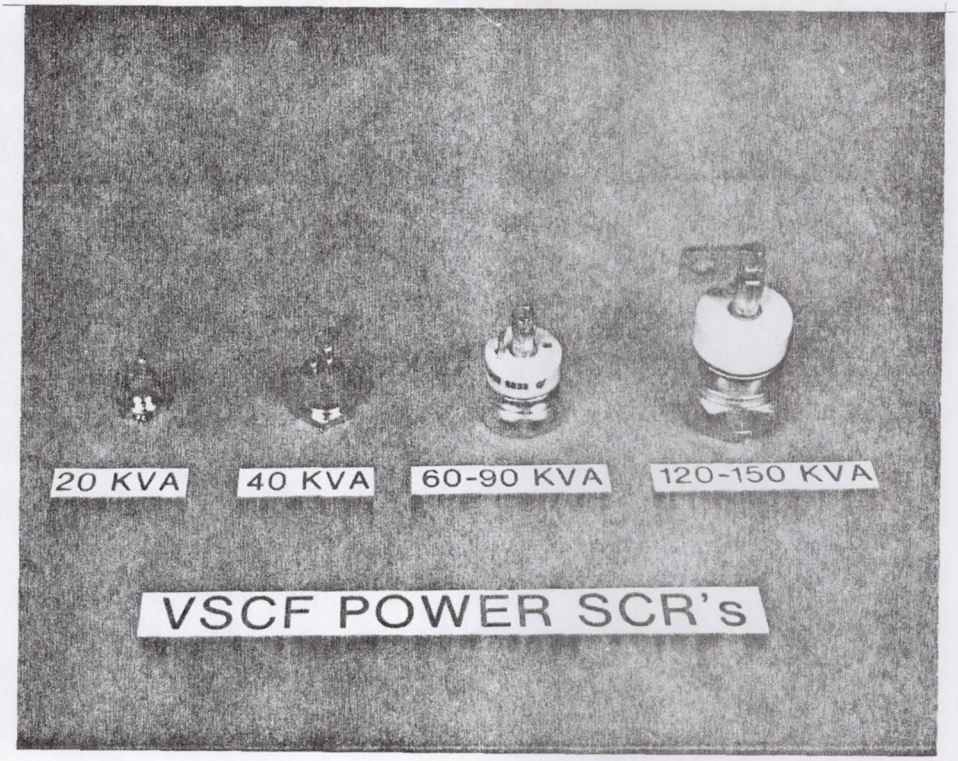

Figure 5. - Stud-mounted silicon-controlled rectifiers.

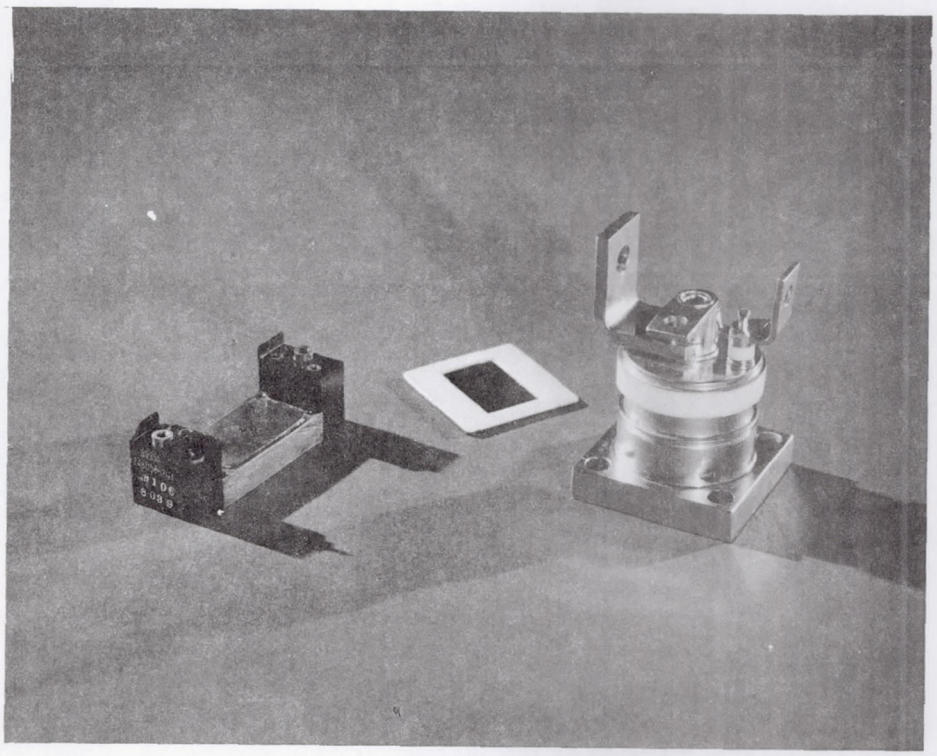

Figure 6. - Two GE SCR power modules.

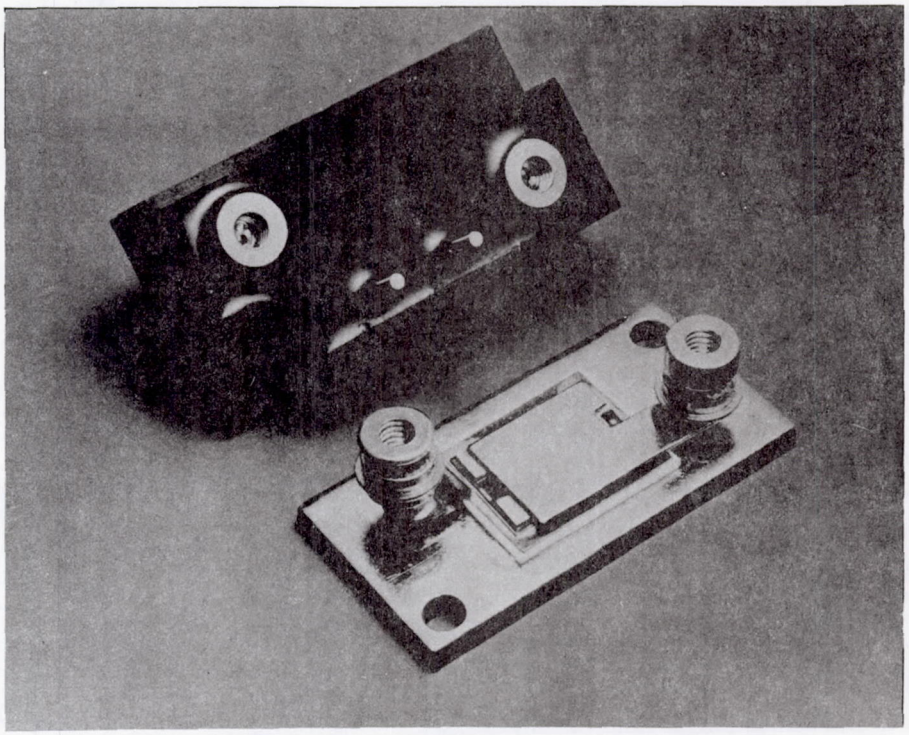

Figure 7. - Small transistor package.

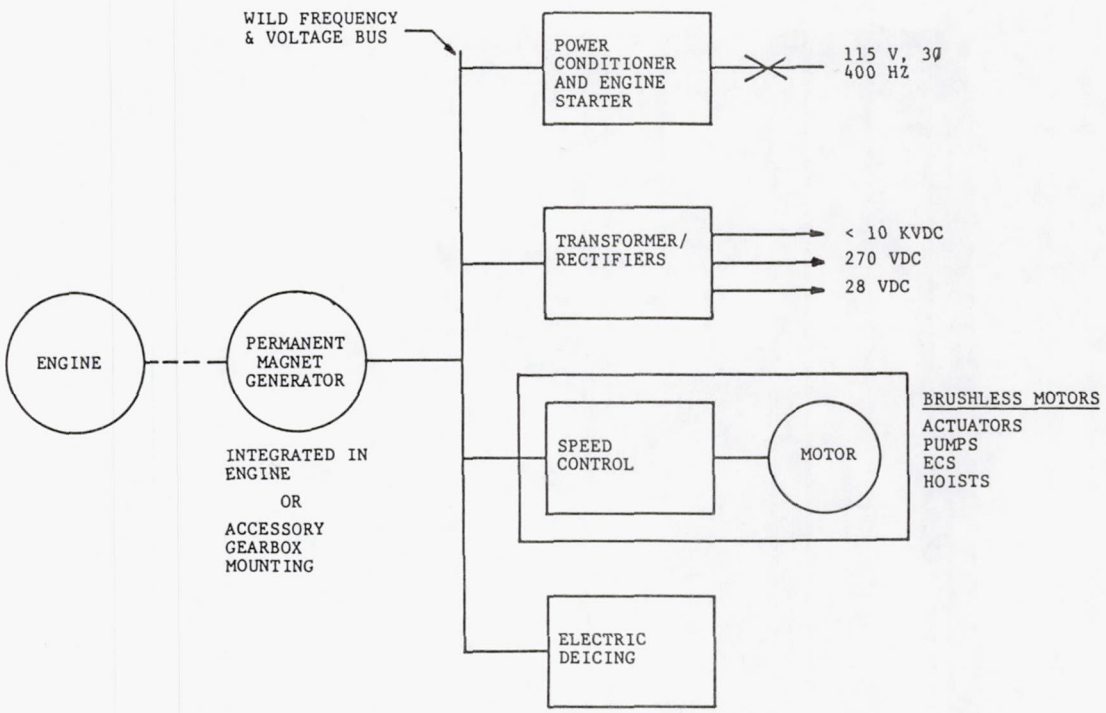

Figure 8. - Future aircraft electrical systems - GE concept.

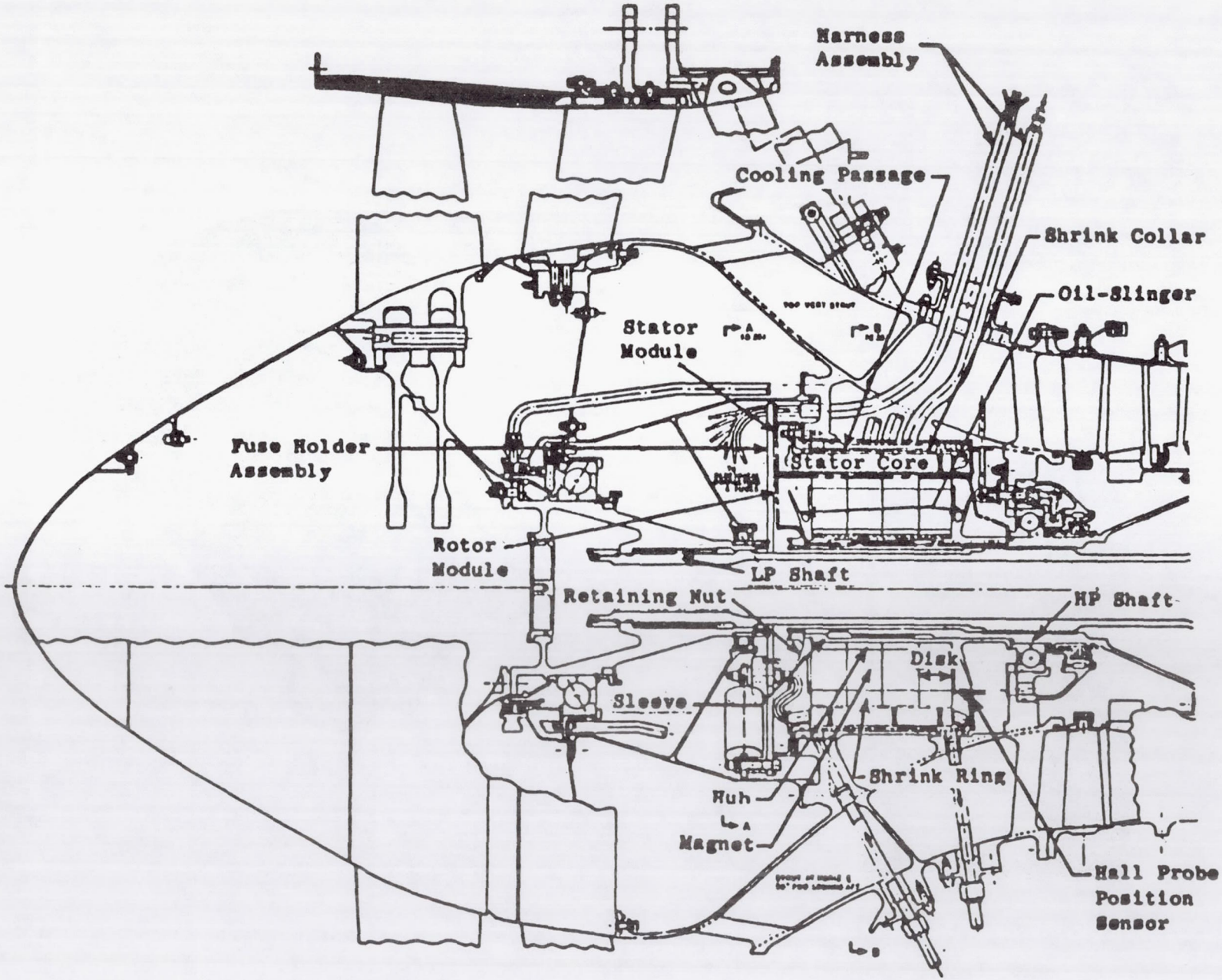

Figure 9. - High-pressure-shaft-mounted, permanent-magnet integral engine starter-generator for TF-34 engine.

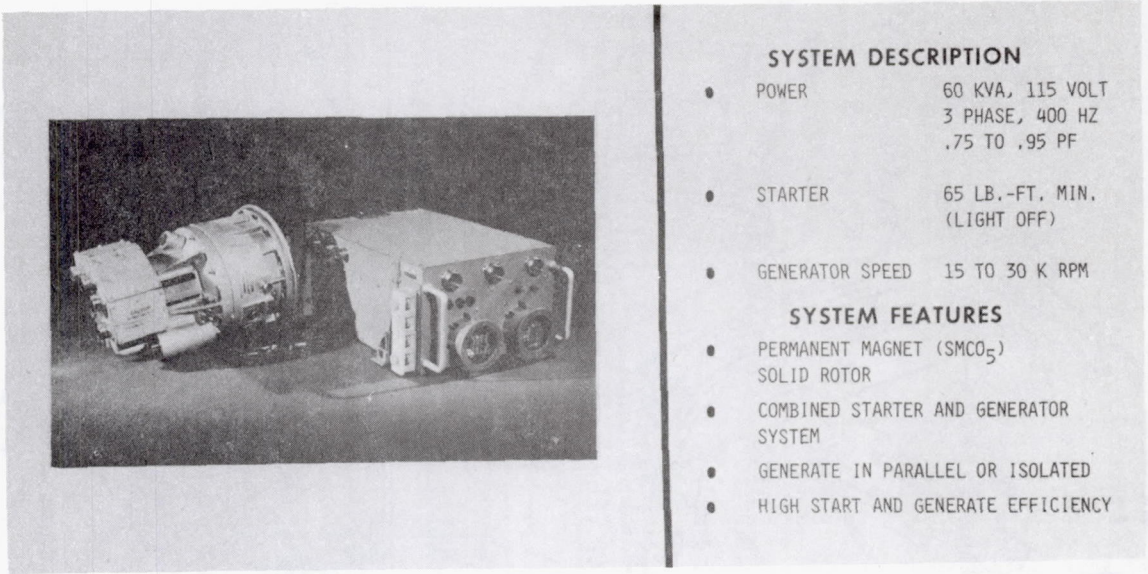

Figure 10. - 60-kVA VSCF starter-generator.

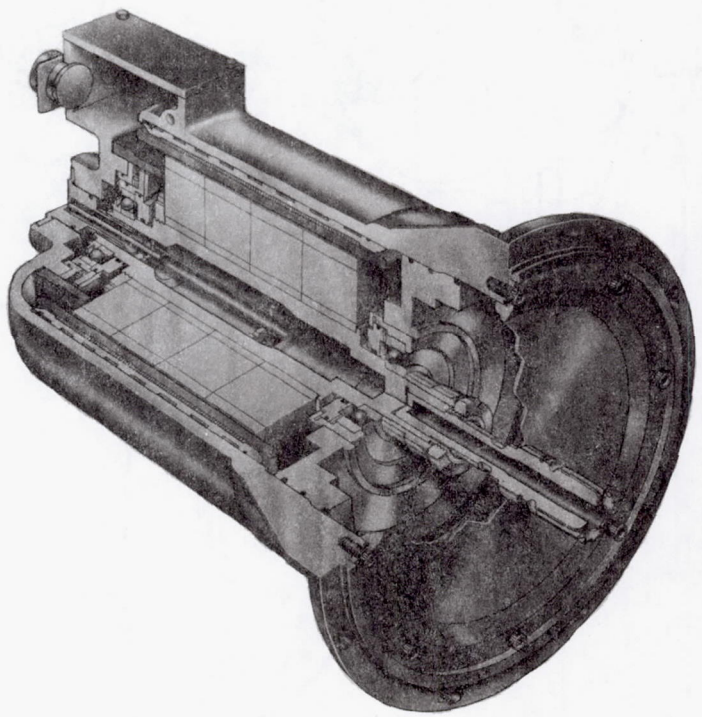

Figure 11. - Cross section of 60-kVA starter-generator.

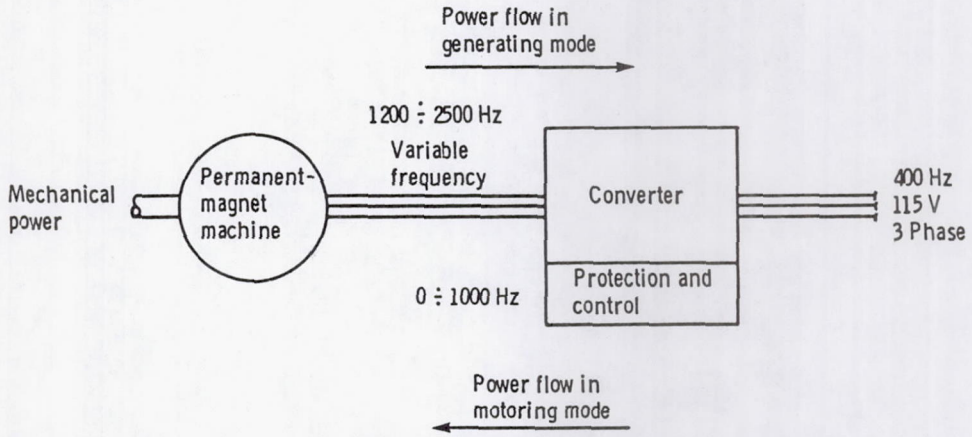

Figure 12. - Permanent-magnet VSCF system concept - bidirectional power flow.

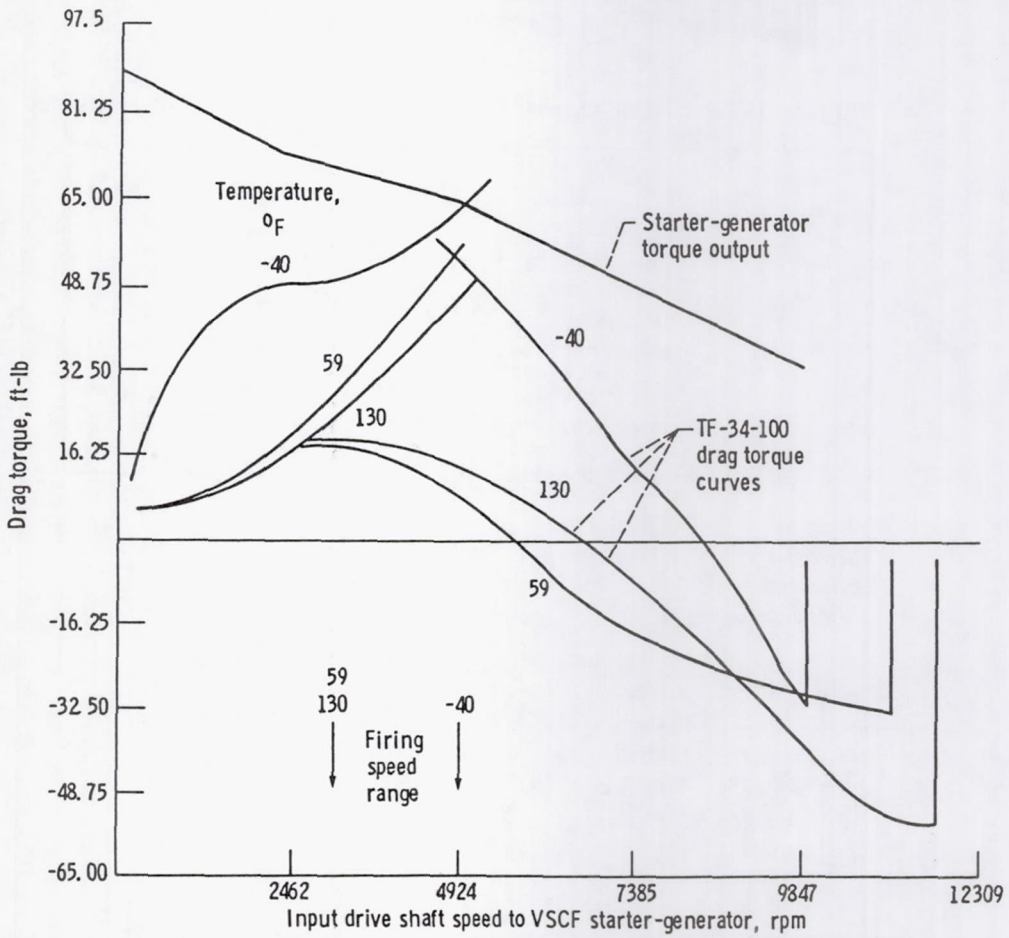

Figure 13. - 60-kVA starter-generator output torque. Starter-generator cutout speed: minimum, 9350 rpm; maximum, 9350 rpm.

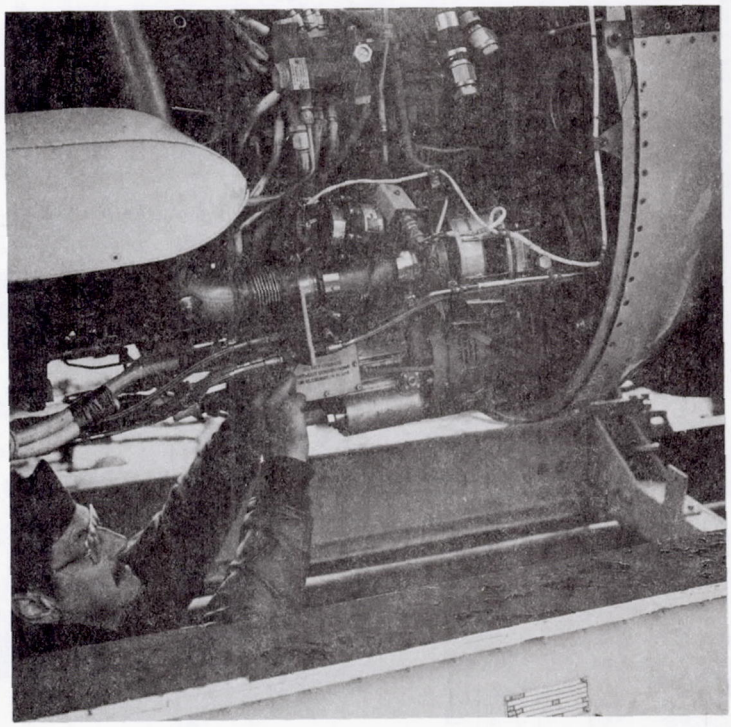

Figure 14. - 60-kVA starter-generator installed in A-10 airplane.

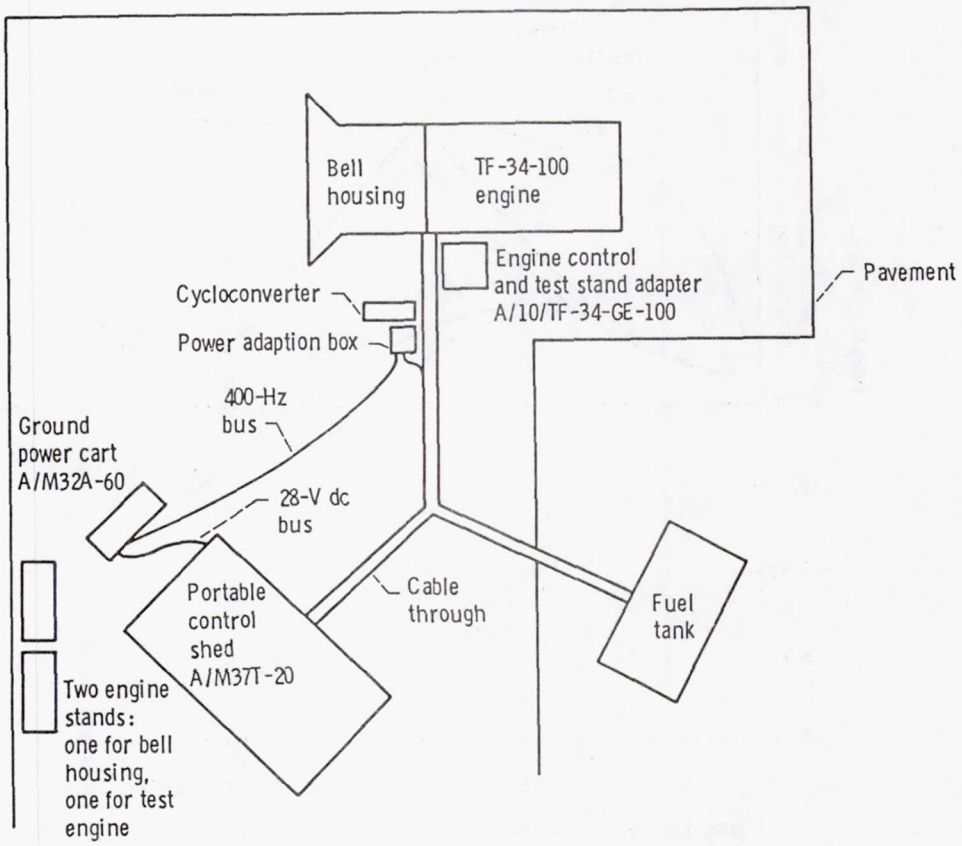

Figure 15. - Syracuse engine test cell.

Figure 16. - Syracuse open-air test facility.

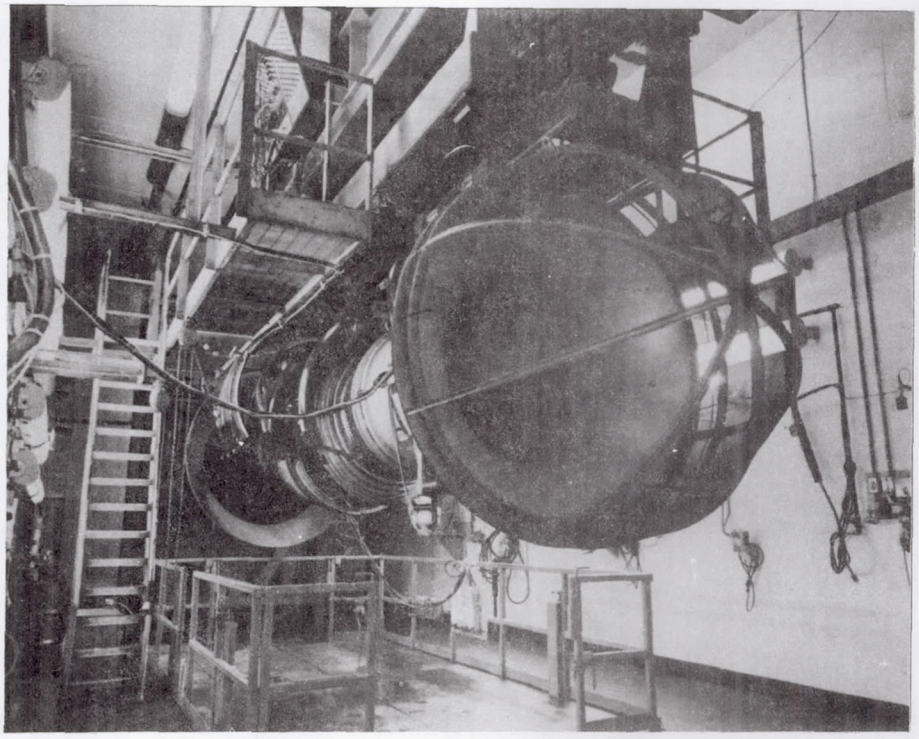

Figure 17. - Lynn test facility.

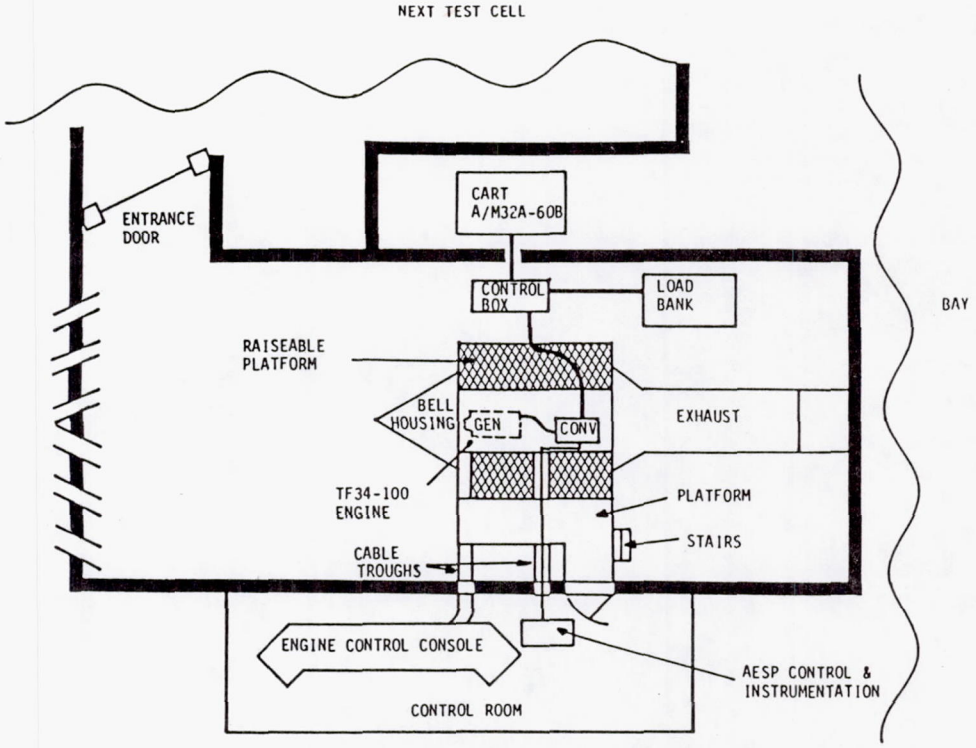

Figure 18. - Diagram of Lynn engine test cell.

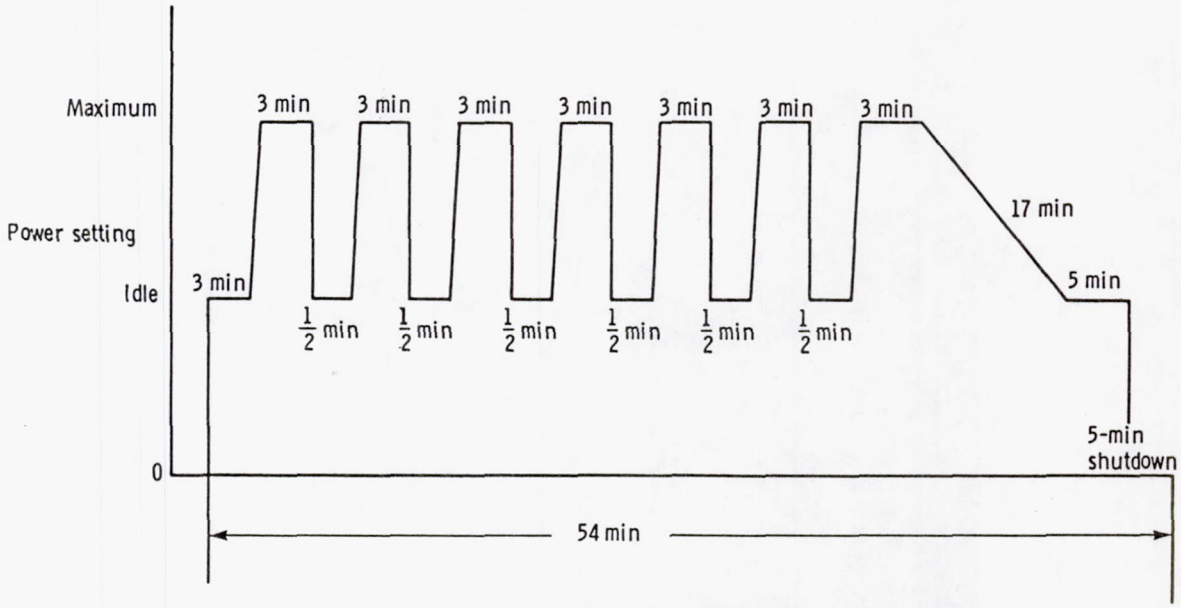

Figure 19. - TF-34-100 proposed AMT III R factory test cycle.

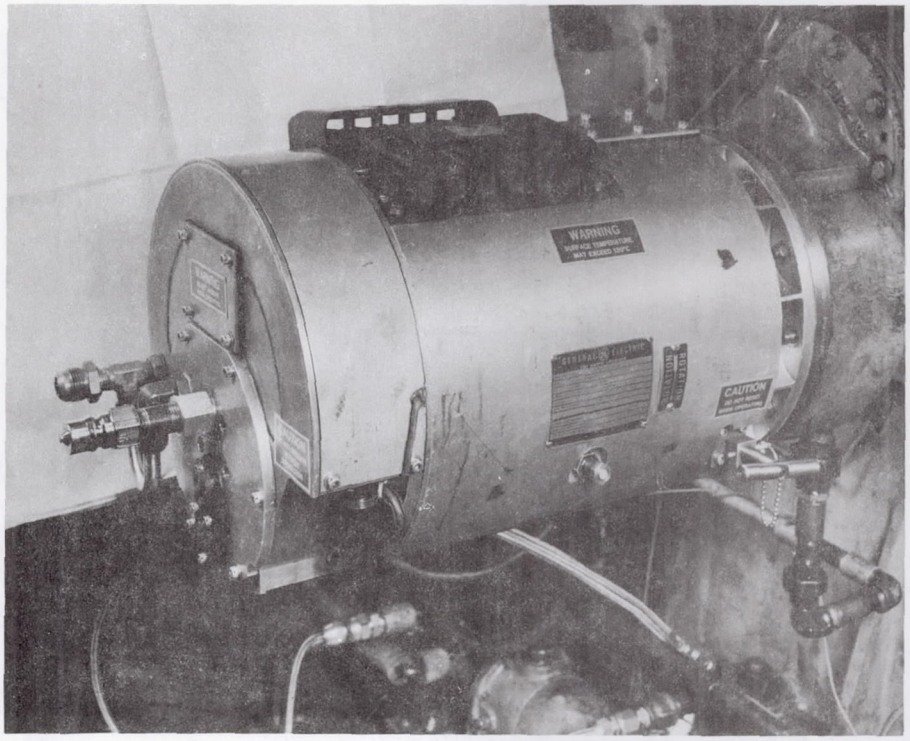

Figure 20. - 150-kVA VSCF starter-generator.

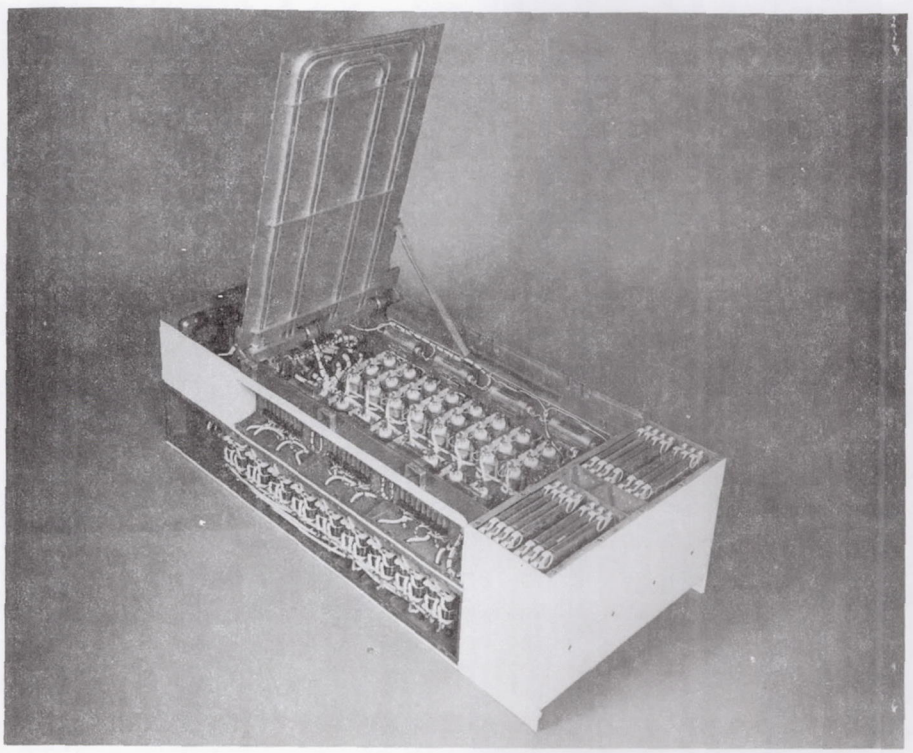

Figure 21. - Cycloconverter for 150-kVA starter-generator.

Description	
Horsepower	141
Speed	20 K RPM
Weight	31 lbs
Rotor Dia.	3.8 inches
Stack	2.8 inches

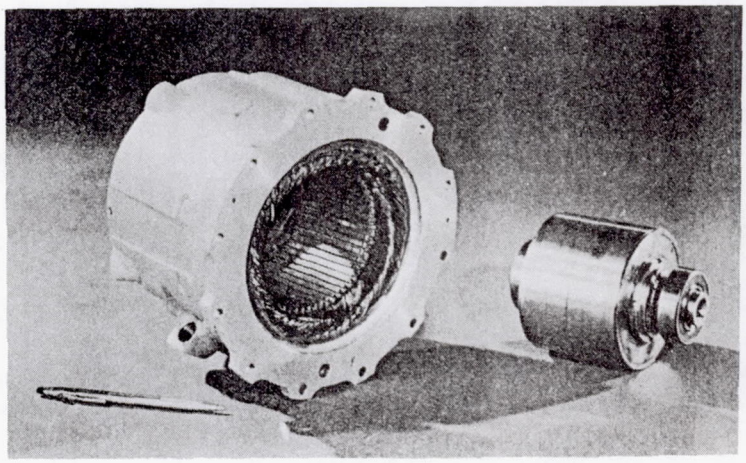

Figure 22. - Brushless, high-speed permanent-magnet motor.

ALL-PURPOSE BIDIRECTIONAL FOUR-QUADRANT CONTROLLER

Irving G. Hansen
National Aeronautics and Space Administration
Lewis Research Center
Cleveland, Ohio 44135

The basic conventions for defining power flow are illustrated in figure 1. The circuit in the upper left of figure 1 defines a positive voltage source and positive current flow. When the current and voltage are plotted as on the upper right, they define positive power flow to the load and fall in the first quadrant. With a negative voltage source and a negative current flow, as shown in the lower left of figure 1, the power flow to the load is still positive, but it falls in the third quadrant as shown in the lower right. Thus positive power, or power flowing to the load, falls in either the first or third quadrant. The other two quadrants are obviously negative power (+I x -E or -I x +E) and represent power flowing from the load. In the second and fourth quadrants the load is acting as a power source.

Figure 2 shows an example of a bidirectional load. With the switch in the position shown, the battery is powering the motor, which in turn is driving a flywheel. When the switch connects the motor to the resistor, the only source of energy in the circuit is the rotating motor and flywheel. Assuming an ideal motor with no inductance and proper excitation, the motor would act as a capacitor. The voltage would remain constant, but the current would reverse and flow from the motor, now in a generating mode, to the resistor. This is illustrated on the plot in the lower half of figure 2 by the arrows pointing downward from the point in the first quadrant to the point in the fourth quadrant. Since with actual motors inductance would be present, the trajectory would be more like the other path of arrows with the current remaining constant and the voltage decreasing and even going negative before reaching the point in the fourth quadrant. In this example the energy flow is bidirectional and several quadrants are involved in the transition of energy from one point to the other. The purpose of the bidirectional four-quadrant controller is to control the flow of energy between the various quadrants.

Figure 3 is a Lissajous pattern showing the locus of operating points for a load. With a sinusoidal voltage and current, and with some phase angle between them, the locus of operating points forms an ellipse as plotted in the figure. If the load were purely resistive, the ellipse would collapse into a line lying in the first and third quadrants only. That is because a pure resistance operates only as a load and not as a source. However, with a load containing both resistance and reactance, energy is stored and released as well as dissipated and the locus extends into all four quadrants. Again, reviewing the basic definition, the load is dissipative in the first and third quadrants and is a source in the second and fourth quadrants.

A resonant circuit, since it has both resistance and reactance, operates in all four quadrants. This means that it can either deliver or accept power; hence it is bidirectional. There will be limits on the voltage and current as shown in figure 4. The circuit will not support a voltage above the line labeled voltage limit nor accept a current above the line labeled current limit. If the resonant circuit is connected to a source each time the locus occupies the first quadrant (or the third quadrant with inversion), the load presented to the source will be a steady dc load. The load voltage and current will always be the same value each time the switch is closed. This

illustrates how a resonant circuit can accept dc power. If a point on the locus were chosen in the second or fourth quadrant, the resonant circuit would act as a dc source instead of a load. Alternating-current operation is a bit more complicated since the switch must be closed and inverted at different times rather than for one fixed quadrant. However, if the switch closure is controlled, frequencies lower than the resonant frequency can be synthesized either for loads or sources. Therefore, through the proper use of resonant circuits and connecting switches, bidirectional four-quadrant ac and/or dc power controllers can be implemented.

Figure 5 shows a bidirectional controller with associated plots for both terminal sets. The plot shown for terminal set 1 indicates that it is accepting power, in this case a dc input. This is the same as the example discussed previously, where the controller is acting as a dc load. The dashed lines on the terminal 2 plot indicate the constant power limit at the output. Because of the law of conservation of energy the output power cannot be greater than the input. However, the output can operate in either the second or fourth quadrants and can provide either dc or ac. The controller can also be operated in an ac-to-ac mode. In that case the controller can be used to provide power factor correction. However, the amount of correction possible is limited by the available reactive power.

The upper half of figure 6 shows a half-bridge transistorized series-resonant dc-to-ac converter. When one transistor is switched on, the current from the dc source flows through the inductor, the transformer, and one capacitor. The current is initially limited by the inductance, gradually increases, and then starts to be limited by the capacitor charging. The result is a quasi sine wave. The transistor is opened when the current goes through zero, and some current flows in the opposite direction through the bypass diode (causing the small bump in the waveform). The second transistor is then turned on, and the current flows in a direction opposite to that of the first transistor (causing an ac output). One very important point is that the transistors are switched off when the current passes through zero. This eliminates second breakdown, which is one of the major causes of transistor failure in converter and inverter circuits. As a result, the series-resonant converter is considerably more reliable than conventional converters, and the transistors can be operated at both high power levels and higher frequencies. The output of this converter is a high-frequency sinusoid that has lower harmonics and slower risetimes than conventional square-wave converters. As a result, the electromagnetic interference (EMI) is much less for this design. The particular circuit configuration shown in figure 6 acts as a current source at the output. This can be very desirable for operating loads such as motors, particularly during startup. When a current-limited source is used, only the frequency needs to be controlled instead of having to maintain a constant voltage-to-frequency V/F ratio as is done with voltage sources. This circuit can also be reconfigured to act as a voltage source by taking the output from the capacitors. Both types of configurations have been demonstrated.

To provide the final controlled output, the high-frequency sinusoidal power of the resonant converter is fed into the circuit shown on the bottom of figure 6. The switches are closed in pairs (synchronous rectification) to connect the transformer to the output momentarily. The synthesized waveform illustrated is a sinusoidal ac of much lower frequency than the carrier. Direct current of either polarity can be synthesized by closing the switches to maintain one output terminal at the same polarity.

Figure 7 shows a fully bidirectional resonant controller with resonant bridges on both ends. This arrangement allows either port to be used as the input accepting either ac or dc power. With this circuit arrangement one full wave bridge is at the source end, the other is at the load end, and the transmission line between operates at the carrier frequency. The capacitance of the line is made a part of the resonant circuit. This reduces the parts count and makes use of the line capacitance that would be present in any case. Systems of this configuration have been tested at 20 kHz with line lengths of 50 m, which is typical of the line length in a large transport aircraft. The line loss was quite small.

Figure 8 illustrates an ac distribution system configured for bidirectional resonant power conversion. The distribution bus at the top of the figure is the high-frequency transmission line as shown on the previous figure. However, instead of just having an input/output circuit at either end of the line, several loads or sources are paralleled on the line. The first bidirectional converter on the left provides dc power to a storage device such as a battery. If the power failed on the main ac bus, the storage device would feed power back to the bus. The second converter is shown as an interface for ground power. Any appropriate type of power (dc, 60 Hz, or 400 Hz) could be used to power other equipment connected to the main bus or even to start the engines. Power could also be fed from the airplane to perform such tasks as starting the engines of another aircraft. The next power converter shown is provided to power various loads on the aircraft. An aircraft system would have a number of these dedicated converters.

The basic purpose of this paper is to provide some information regarding bidirectional four-quadrant resonant power conversion and describe possible applications to aircraft electrical systems. As this technology has been developed sufficiently to demonstrate its feasibility, this is an appropriate time to evaluate the benefits of its application to aircraft electrical systems.

REFERENCES

1. Mapham, N.: An SCR Inverter with Good Regulation and Sine Wave Output, IEEE Trans. Ind. Gen. Appl., vol IGA-3, no. 2, Mar./Apr 1967, pp. 176-187.
2. Schwarz, F. C.: An Improved Method of Resonant Current Pulse Modulation for Power Converters. IEEE Trans. Ind. Electron. Control Instrum., vol. IECI-23, no. 2, May 1976, pp. 133-141.
3. Myers, R.; and Peck, R. D.: 200 kHz Power FET Technology in New Modular Power Supplies. Hewlett-Packard Journal, vol. 32, no. 8, Aug. 1981, pp. 3-11.
4. Babu, S. R.: A Practical Resonant Converter Using High Speed Power Darlington Transistors. PCI '82, Intertec Communications, Inc., 1982, pp. 122-141.
5. Biess, J. J.; Inouye, L.Y.; and Shank, J. H.: High Voltage Series Resonant Inverter Ion Engine Screen Supply. Power Electronics Specialists Conference, IEEE, 1974, pp. 97-105.
6. Biess, J. J.; and Frye, R. J.: Electrical Prototype Power Processer for 30-cm Mercury Electric Propulsion Engine. AIAA Paper 78-684, Apr. 1978.
7. Robson, R.; and Hancock, D.: A 10-kW Series Resonant Converter Design, Transistor Characterization, and Base-Drive Optimation. NASA CR-165546, 1981.

8. Schwarz, F.C.: Bi-Directional Four Quadrant (BDQ4) Power Converter Development. NASA CR-159660, 1979.

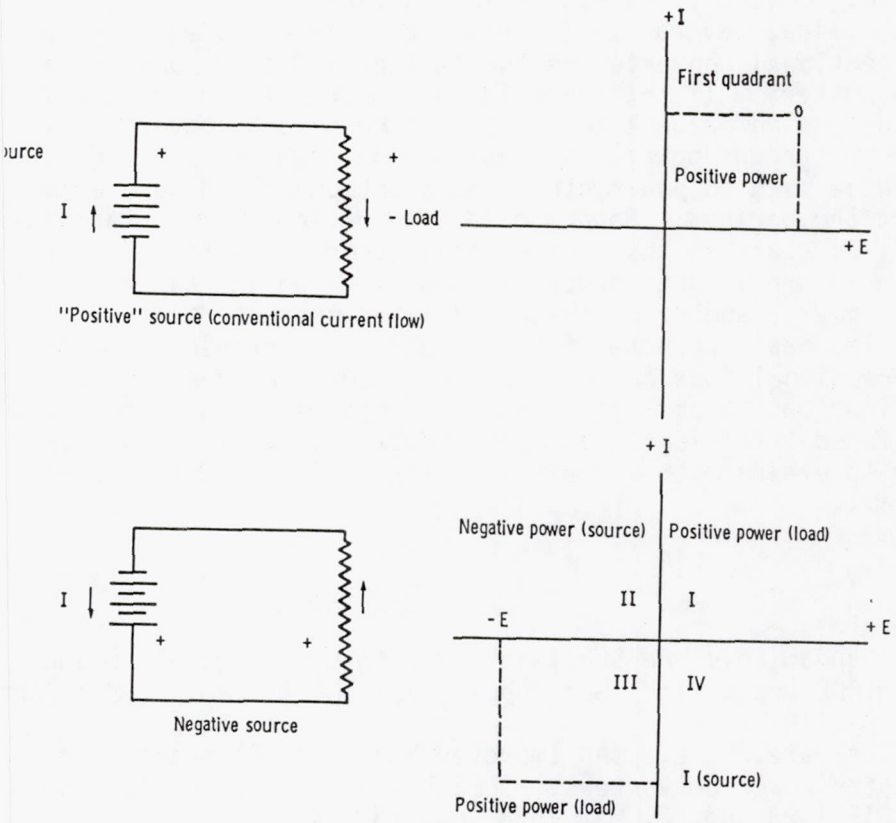

Figure 1. - Basic definitions of four-quadrant controller.

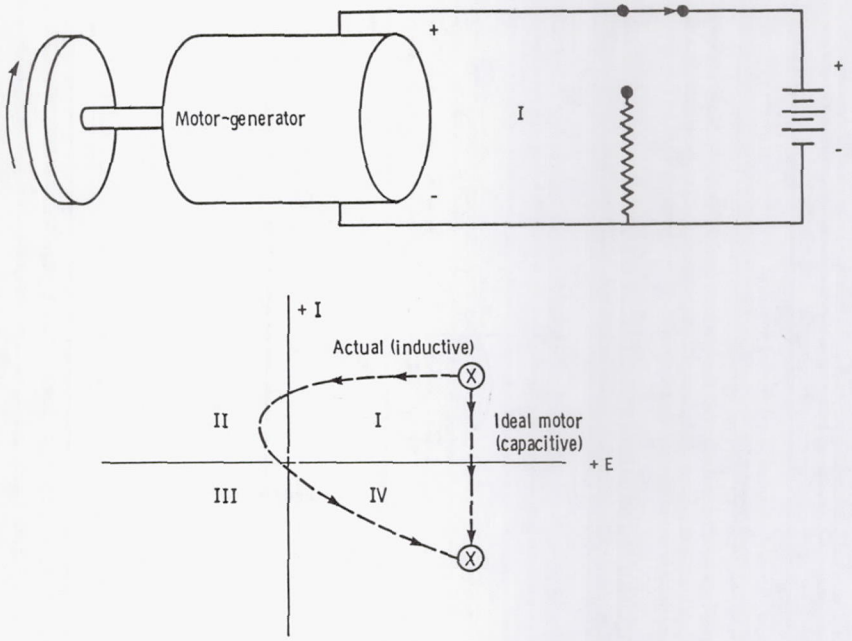

Figure 2. - Bidirectional energy flow.

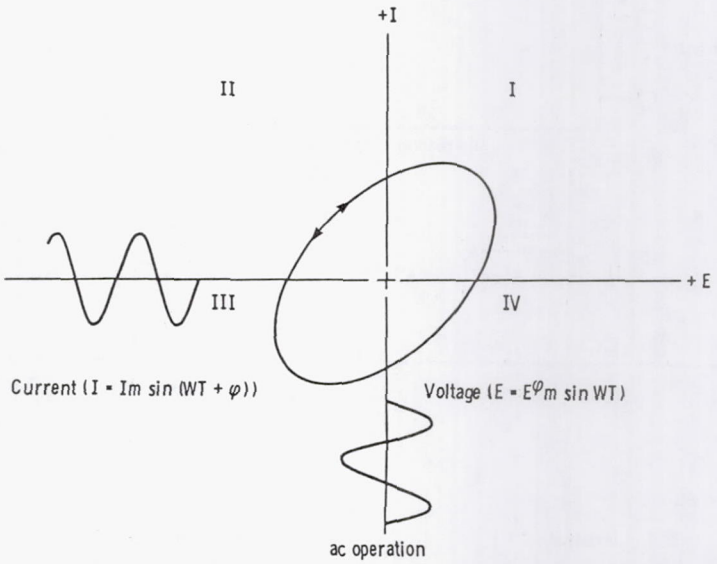

Figure 3. - Loci of operation points depending on magnitude and phase of load (Lissajous pattern).

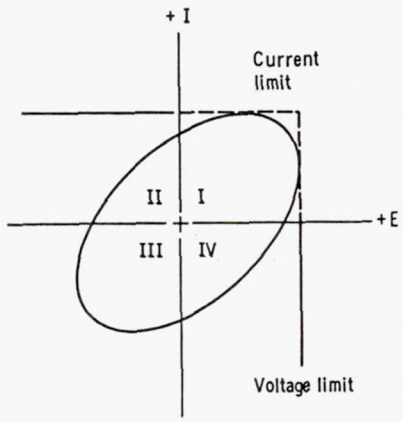

Figure 4. - Resonant circuit.

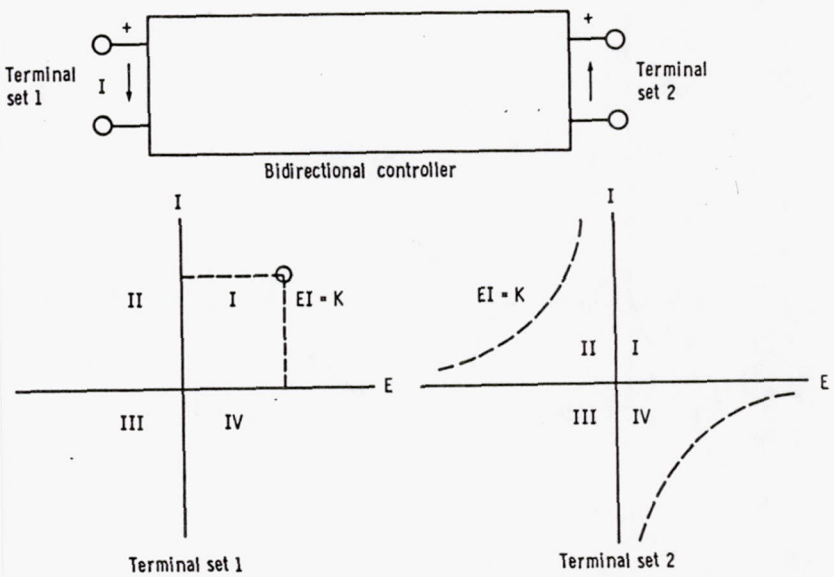

Figure 5. - Conservation of energy - a problem with bidirectional converters.

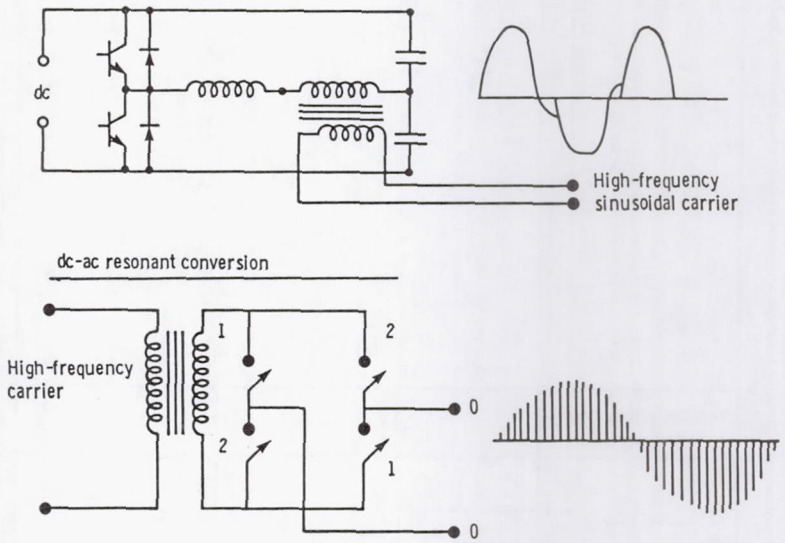

Figure 6. - Low-frequency synthesis (including bipolar dc).

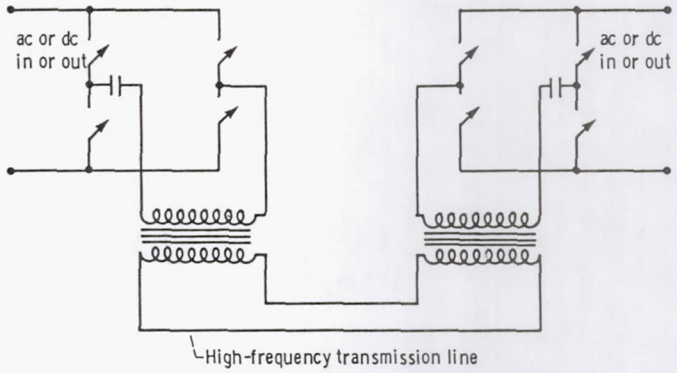

Figure 7. - Bidirectional resonant controller.

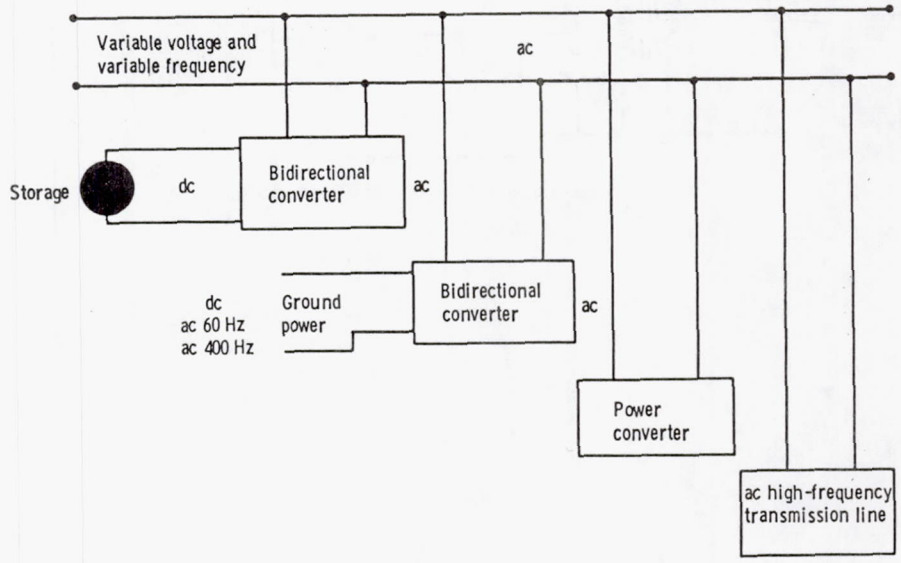

Figure 8. - Distribution system. (Power converter is dc (fixed or variable frequency), ac (variable voltage), or bidirectional if required.)

RESULTS OF DISCUSSION SESSIONS

The workshop attendees separated into four groups to participate in informal discussions on the following topics: machine technology, component technology, systems, and controllers. A standard set of questions was provided to the groups as an aid to their discussion. Those questions are as follows:

(1) Is there a clear best direction or technology in your area? If so what is it?

(2) If there is not a single clear direction, why is that so and what needs to be done to arrive at a single direction (or technology)?

(3) What are the effects of other aircraft systems and components on the power system and its components? What needs to be done to accommodate these effects?

(4) What are your comments regarding the various technologies that Lewis personnel discussed during the presentation? Are there any concerns regarding the application of these technologies?

(5) Are there any specific efforts that the group feels are important and should be addressed?

The groups modified these questions to some extent to fit their particular topics. The results from each of the groups are discussed in the following sections.

Machine Technology Discussion Results

The best direction for machine technology is to improve the materials used in rotating machinery. The concensus of those involved in machine design and fabrication was that if better materials are available, better motors and generators can be built.

A number of areas were suggested where improved materials are desirable. The first was permanent-magnet materials. An improvement in the characteristics of permanent-magnet materials, such as higher flux density, will result in machines that are smaller, lighter, and more efficient. An improvement in the manufacturing process that provides lower cost magnets will result in less expensive machines. This would increase the number of applications where permanent-magnet machines are practical.

The second area suggested for materials improvement was lubricating grease for machine bearings. Current lubricating greases have upper temperature limits well below the maximum temperature limits of the rest of the materials in a motor or generator. As a result, the machine cannot be operated at its maximum capability. A higher temperature bearing grease would correct this problem. Another problem is that a grease that works well at high temperatures does not work well at low temperatures and vice versa. A bearing grease with a wider operating temperature range would solve this problem.

The third area of material technology development covered the advanced technologies that Lewis is currently supporting, particularly intercalated graphite and Metglas. These materials would contribute to more efficient and lighter weight motors and generators, and they should be developed to the point where they can be used.

The group also suggested some other areas that should be investigated. The first area was thermal design, particularly the thermal design of an electromechanical actuator for a flight control surface. These actuators are mounted in the flight surfaces of an aircraft, with no control on their

environment nor any active temperature controls. As a result, the temperature excursions may be substantial.

The second area suggested for study was the packaging of power semiconductors. The weight of power semiconductor packages is so large as to be an appreciable portion of the weight of a controller. Lighter weight packages that still provide adequate thermal control would be very desirable.

The third area concerned the bonding between magnetic and nonmagnetic materials. This bonding is used in the construction of the rotors of permanent-magnet machines, where high strength is very important. Although techniques are available to provide good bonds, they tend to be very expensive and as a result are not always used. What is needed is a good inexpensive method of bonding.

Component Technology Discussion Results

In the component area, no single direction was selected, rather a number of component types were discussed and the suggested need for that type of component presented. One important point made by the group was that any component development work needs to be accomplished early in a program so that the devices are available for use when the system design effort begins.

The first area discussed concerned transistor current ratings. It was felt that the current capability of 500-V transistors is not large enough for the power levels expected in aircraft. The suggested ratings for power transistors to be used in aircraft systems was 500 V and 400 A (gain of 20).

The second area of discussion concerned transistor surge currents, particularly in the higher voltage transistors. Transistors are currently available with 1000-V, 100-A ratings. However, their surge current capability is not well defined. The suggestion was to evaluate the surge current ratings of existing transistors. The desired ratings are 900-A surge current for an 800-V, 100-A (gain of 20) transistor.

The third area covered transformers, particularly with regard to their packaging. The basic transformer electrical designs are probably adequate to power levels of 100 kW. However, improvements in the packaging design could provide substantial weight reductions, greater reliability, and better efficiency.

The next area discussed was capacitors. The advanced-technology capacitors discussed at this workshop met most of the requirements. However, the group felt that higher temperature capability was definitely needed. Use of fuel for cooling electronics on an aircraft requires a capacitor operating temperature of about 100° C.

Switchgear was also discussed, but it was felt that an operating range was more appropriate than a specific rating. The operating voltage range was selected at 115 to 300 V. This level was felt to be sufficiently high for weight and efficiency benefits but not so high as to cause corona problems. The frequencies selected were dc and 400 to 3000 Hz. The ac range covers the currently used 400 Hz to 3000 Hz, which is about as high as the group expected to see in the near future. Direct current has already been selected for some applications. The expected current range is from 1 A for small loads to 300 A for a main circuit.

The final area of discussion covered high-temperature electronics. Electronics could be used on the engines of aircraft much more easily and reliably if their operating temperature was around 300° C. One of the applications would be a controller for an electric fuel pump. High-temperature electronics also has benefit when used elsewhere on the aircraft since the cooling problem is much reduced.

Systems Technology Discussion Results

The system technology group quickly came to the conclusions that there is no one best power system for all applications and that there probably never will be. Instead of trying to select a number of acceptable systems, they tried to define what the characteristics of a power system should be for an aircraft with all-electric secondary power. The first characteristics defined were that all secondary power for the aircraft is supplied by the electrical generators and that these generators serve as starter motors for the engine. The second characteristic addressed was the types of power requirements. These were defined as flight critical, mission critical, and noncritical. The flight-critical power is required to maintain control of the aircraft and includes power to the primary flight control surfaces. This is a new level of criticality for aircraft electrical systems since most aircraft can fly with the electrical system inoperative. Mission critical is that level of power necessary to complete the planned mission. Noncritical power may cause some inconvenience but has no effect on the safety of the mission.

An aircraft with all of its secondary power supplied electrically will require an electrical system substantially larger than those on current aircraft. As a result, energy management becomes more important. Three characteristics of energy management were defined as follows: transmission efficiency, load management, and thermal management. The delivery of large quantities of power requires efficient transmission to keep the losses small. Some of the loads, such as the environmental control system, are very large and they must be switched on and off the bus in a controlled fashion so they do not affect the power quality. Even with a very efficient system the losses will be large since the system itself is large. Effective means must be established to dissipate these losses to prevent excessive component temperatures.

An aircraft with all-electric secondary power will also probably have a digital fly-by-wire control system. The power management control system will also be digital, and it must be compatible with the flight control system. This generation of aircraft could also have composite structures. The power system architecture must be designed with the nonconductivity of composite structures considered.

The next area that the systems group addressed was the state of the technologies for aircraft power systems. The technologies were categorized as to readiness date as follows: existing, near term (1990), and far term (2000 and beyond). Table I shows technologies associated with power generation and the group's assessment of the readiness dates. Table II shows the dates for data handling and electromechanical actuators. Table III shows the readiness assessment for power distribution and control technologies. These figures indicate that much of the technology appropriate for aircraft electric power systems needs some development effort. Most of the readiness dates fall into the near-term (1990) category. This indicates that the technology necessary for a viable all-electric airplane can be available in the near term. However, the development effort must start now if that technology readiness date is to be met.

The group expressed a concern that there is no power systems program currently in progress at Lewis. They felt that such a program should begin soon. This program is needed to integrate the various technology areas and to evaluate the risks associated with each of these areas. In addition, the far-term technologies should be evaluated as to their payoff. If it is sufficient, these technologies should be accelerated to meet the near-term date.

Controller Technology Discussion Results

The members of this discussion group decided that the bidirectional resonant controller is clearly the best direction for control of power in an all-electric airplane. The primary reason for this selection was the versatility of this type of controller. Its bidirectional capability allows it to control the power for engine starting as well as during the generating mode. Because of its variable-frequency output it can provide speed control for motor loads such as actuators or environmental control system drives. The output is adjustable to form sine waves, square waves, and dc and any reasonable shape in between. Since the logic circuits of the various controllers are identical, they can be used to provide redundancy. Besides this versatility, the resonant controller is very efficient, with values in the 95 percent range. Also, because of the high frequency of operation (20 kHz) they are lightweight.

The primary effect of the resonant controller on the rest of the power system and on other systems is its rapid response to failures. The controller output can be turned off twice every cycle of operation. Since the resonant circuit oscillates at 20 kHz, it can be turned off only a few microseconds after a failure is detected. In many instances the current could be interrupted before the fault fully developed. Also, the energy stored in the resonant circuit of a typical controller is only about 1 joule. This limits the energy that can flow into a fault before it is interrupted. The basic message is that faults can be isolated rapidly and with minimum damage to the rest of the system.

The group made a number of comments regarding technologies associated with controllers. The first was directed toward semiconductors and their limited temperature capability. The group felt that semiconductors are forced to operate near their temperature limits because of the environment they are placed in. A higher temperature semiconductor such as gallium arsenide would be very effective in improving the reliability of controllers. If higher temperature semiconductors are not forthcoming, the thermal design using current semiconductors needs careful attention. The reliability of the other components used in controllers needs to be evaluated. This is particularly true for transformers, which to date have been one-of-a-kind designs. The group felt that redundancy management should be a part of any systems study. The physiology of high-frequency power needs to be investigated, both physical contact as well as audio reception.

The group made a number of recommendations. First, they suggested an early standardization of control logic interfaces. This would reduce duplication of design efforts, provide more sources for hardware, and insure compatibility between manufacturers. Second, they recommend that the stability of the resonant controller be evaluated, particularly under transient conditions. And third, they suggested that the electromagnetic interference of a high-frequency controller needs study. There do not appear to be any technical inpediments to the resonant controller approach, but it is not a mature technology and much work needs to be done.

TABLE I. - POWER GENERATION TECHNOLOGIES

Technology	Potential technology readiness date		
	Existing	Near term (1990)	Far term
Integrated starter-generator		o	
Gearbox generator	o		
Permanent magnet	o		
Wound rotor	o		
Superconducting			o
300-hp/ft^3 APU		o	

TABLE II. - DATA HANDLING AND ELECTROMECHANICAL ACTUATOR TECHNOLOGIES

Technology	Potential technology readiness date		
	Existing	Near term (1990)	Far term
Standard data bus	o		
Fiber optics		o	
Autonomous power system		o	
Central processing unit		o	
Heat-pipe cooling		o	
Cryogenics			o
EMA:			
Flight control		o	
Engine control		o	
Integral actuator package	o		

TABLE III. - POWER DISTRIBUTION AND CONTROL TECHNOLOGIES

Technology	Potential technology readiness date		
	Existing	Near term (1990)	Far term
High-power motor controller	o		
High-power bus control			
ac	o		
dc		o	
Solid state		o	
Solid state/electromechanical		o	
Low-forward-drop solid state			o
Lightweight conductors			o
Flat cable and terminator		o	
Central load management	o		
Distributed load management		o	
Integrated load management/avionics			o

1. Report No.	2. Government Accession No.	3. Recipient's Catalog No.
NASA CP-2282		

4. Title and Subtitle	5. Report Date
AIRCRAFT ELECTRIC SECONDARY POWER	June 1983
	6. Performing Organization Code: 534-02-22
7. Author(s)	8. Performing Organization Report No.: E-1632
	10. Work Unit No.
9. Performing Organization Name and Address: National Aeronautics and Space Administration, Lewis Research Center, Cleveland, Ohio 44135	11. Contract or Grant No.
	13. Type of Report and Period Covered: Conference Publication
12. Sponsoring Agency Name and Address: National Aeronautics and Space Administration, Washington, D.C. 20546	14. Sponsoring Agency Code

15. Supplementary Notes

16. Abstract

A workshop on aircraft electric secondary power was held at the Lewis Research Center of the National Aeronautics and Space Administration on September 14 and 15, 1982. The purpose was to discuss technologies related to aircraft power systems for an all-electric aircraft. The proceedings contains 15 papers on power systems, machine technology, components, and controllers plus the results of the discussion sessions.

17. Key Words (Suggested by Author(s))	18. Distribution Statement
Electric power; Aircraft; Power systems; Machine technology; Components; Controllers	Unclassified - unlimited STAR Category 07

19. Security Classif. (of this report)	20. Security Classif. (of this page)	21. No. of pages	22. Price*
Unclassified	Unclassified	205	A10

*For sale by the National Technical Information Service, Springfield, Virginia 22161

*USGPO: 1983-659-094-507